



GENERAL ATOMIC

GA-A14311

LARGE CLOSED-CYCLE GAS TURBINE PLANT

by
COLIN F. McDONALD

NOTICE

This report was prepared as an account of work sponsored by the United States Government. Neither the United States nor the United States Energy Research and Development Administration, nor any of their employees, nor any of their contractors, subcontractors, or their employees, makes any warranty, express or implied, or assumes any legal liability or responsibility for the accuracy, completeness or usefulness of any information, apparatus, product or process disclosed, or represents that its use would not infringe privately owned rights.

This is a preprint of a paper presented at the AGARD Lecture Series on Closed-Cycle Gas Turbines held at the Von Karman Institute for Fluid Dynamics, May 9-13, 1977, Brussels, Belgium, and printed in the Series Proceedings.

Work supported in part by the U.S. Energy Research and Development Administration, Contract EY-76-C-03-0167, Project Agreement No. 46, and also in part by a group of electric generating utilities, with work participation by industrial firms.

MASTER

GENERAL ATOMIC PROJECTS 2095, 4351, and 3227

MAY 1977

DISCLAIMER

This report was prepared as an account of work sponsored by an agency of the United States Government. Neither the United States Government nor any agency thereof, nor any of their employees, makes any warranty, express or implied, or assumes any legal liability or responsibility for the accuracy, completeness, or usefulness of any information, apparatus, product, or process disclosed, or represents that its use would not infringe privately owned rights. Reference herein to any specific commercial product, process, or service by trade name, trademark, manufacturer, or otherwise does not necessarily constitute or imply its endorsement, recommendation, or favoring by the United States Government or any agency thereof. The views and opinions of authors expressed herein do not necessarily state or reflect those of the United States Government or any agency thereof.

DISCLAIMER

Portions of this document may be illegible in electronic image products. Images are produced from the best available original document.

LARGE CLOSED-CYCLE GAS TURBINE PLANT

by

Colin F. McDonald
Manager, Component Design Branch
Advanced Concepts Division
General Atomic Company
San Diego, California

ABSTRACT

A most challenging and interesting application of the closed-cycle gas turbine for electrical power generation is a plant with a high temperature gas cooled reactor (HTGR) as the heat source, and this paper presents the design studies for a 1200 MWe plant. The closed-cycle gas turbine experience in Europe together with the HTGR experience in the United States and Europe provide the basis for a direct cycle nuclear gas turbine plant. The GT-HTGR plant combines the existing HTGR core with a closed-cycle helium gas turbine power conversion system which operates on the same helium used as the reactor coolant.

In this series of lectures a summary is given of the design evolution for a large nuclear closed-cycle gas turbine power plant study by the General Atomic Company for U.S. utility central stations.⁽¹⁾ The presentation includes a background on closed-cycle gas turbines, the incentives for the GT-HTGR, cycle selection, plant configuration studies, performance, selection of a reference plant design, component design activities, and a description of the waste heat binary power plant. Included also are development and testing alternatives, and related international programs in the closed-cycle gas turbine field.

(1) Studies carried out since 1971 have been sponsored by the U.S. Energy Research and Development Administration, with support by a group of electric generating utilities, and work participation by industrial firms.

CONTENTS

1.0	INTRODUCTION	1
2.0	RELATED CLOSED-CYCLE GAS TURBINE BACKGROUND	3
2.1.	Closed-Cycle Gas Turbine Operating Experience	4
2.2.	Closed-Cycle Gas Turbines with Air as Working Fluid	4
2.2.1.	Escher Wyss Plant	4
2.2.2.	2.3 MWe Ravensburg Plant	4
2.2.3.	6.6 MWe Coburg Plant	7
2.2.4.	13.75 MWe Oberhausen I Plant	7
2.2.5.	6.4 MWe Haus Aden Plant	11
2.2.6.	17.25 MWe Gelsenkirchen Plant	11
2.2.7.	30 MWe Spittelau Plant	14
2.3.	Closed-Cycle Gas Turbines with Helium as the Working Fluid	14
2.3.1.	The La Fleur Helium Turbine Process Plant	14
2.3.2.	Escher Wyss Helium Gas Turbine for La Fleur Process	16
2.3.3.	50 MWe Oberhausen II Helium Turbine Plant	21
2.4.	Activities in Support of Nuclear Gas Turbine Development	23
2.4.1.	High Temperature Helium Test Facility (HHV)	23
2.4.2.	Steam Cycle HTGR Helium Component Development	24
2.4.2.1.	Helium Axial Flow Circulator	24
2.4.2.2.	Steam Generator for HTGR Plant	28
2.5.	Summary	28
	References	32
3.0	NUCLEAR GAS TURBINE INCENTIVES AND BENEFITS	38
3.1.	Incentives and Motivation	38
3.2.	GT-HTGR Plant Benefits	43
3.2.1.	Low Power-Generation Cost	43
3.2.2.	High Reliability and Availability	47
3.2.3.	Flexibility in Plant Siting	47
3.2.4.	Inherent Safety	47
3.2.5.	Minimum Environmental Impact	50
3.2.6.	Conservation of Resources and High Cost Benefit	50
3.2.7.	Application of Reject Heat	50
3.2.8.	Flexibility in Plant Rating	51
	References	55
4.0	BACKGROUND OF GT-HTGR DESIGN STUDIES	56
4.1.	Thermodynamic Cycle and Performance	56
4.1.1.	Thermodynamic Cycle	58
4.1.2.	Major Cycle Parameters	64
4.1.3.	Plant Performance	65
4.1.4.	Performance Potential	68
4.2.	GT-HTGR Plant Configuration Studies	76
4.2.1.	Plant Configurations with Vertical Turbomachinery	79
4.2.2.	Plant Configurations with Horizontal Turbomachinery	89
4.2.2.1.	Initial Configuration with Horizontal Turbine	91
4.2.2.2.	Selected Configuration with Horizontal Turbine	91
	References	114

5.0	GT-HTGR REFERENCE PLANT DESIGN	115
5.1.	Optimization Studies	115
5.2.	Thermodynamic Cycle and Performance	115
5.3.	Primary System Design	119
5.4.	Prestressed Concrete Reactor Vessel (PCRV)	129
5.5.	Component Design	135
5.5.1.	Turbomachinery	135
5.5.2.	Heat Exchanger Design	138
5.6.	Maintenance Considerations	145
5.7.	Overall Plant Configurations	147
5.8.	Summary	151
	References	152
6.0	COMPONENT DESIGN CONSIDERATIONS	153
6.1.	Turbomachine Design	153
6.1.1.	Compressor Aerodynamic Design Considerations	153
6.1.2.	Turbine Aerodynamic Design	164
6.1.3.	Turbomachine Mechanical Design	166
6.1.4.	Turbomachine Installation and Removal	175
6.1.5.	Rating Potential for 60 Hz Turbomachine	175
6.1.5.1.	Blade Stresses	175
6.1.5.2.	Material Properties	177
6.1.5.3.	Turbomachine Size Limits	179
6.1.5.3.1.	Nickel-Base Blade Material	179
6.1.5.3.2.	Refractory Blade Material	179
6.2.	Heat Exchanger Design Considerations	179
6.2.1.	Recuperator Design	185
6.2.2.	Precooler Design	190
6.2.3.	Heat Exchanger Fabrication Considerations	199
6.2.4.	Heat Exchanger Installation, Handling, & Maintenance	202
6.2.5.	Heat Exchanger Economic Considerations	204
6.2.6.	Heat Exchanger Design Summary	204
6.3.	Control Valve Design	206
6.4.	Materials Testing Program	211
	References	215
7.0	SECONDARY POWER CYCLE (BINARY PLANT)	216
7.1.	Working Fluid Selection	216
7.2.	Secondary Power Cycle Conditions	219
7.3.	Component Design Considerations	222
7.3.1.	Ammonia Turbine Design	222
7.3.2.	Turbine-Driven Ammonia Feedpump	232
7.3.3.	Condenser Conceptual Design	237
7.4.	Secondary Power Cycle Building Layout	242
7.5.	Summary of Secondary Power Cycle Design Studies	242
	References	245

8.0	DEVELOPMENT AND TESTING ALTERNATIVES	247
8.1.	Helium Component Test Facility (HCTF)	247
8.2.	Nuclear PCL Testing in a Demonstration Plant	247
8.3.	Temporary Helium Heater Approach	253
8.4.	Subcomponent Test Approach	253
8.5.	Development Needs Common to Fossil-Fired and Nuclear Closed-Cycle Gas Turbines	254
9.0	RELATED INTERNATIONAL NUCLEAR CLOSED-CYCLE GAS TURBINE PROGRAMS	254
10.0	SUMMARY	257
	ACKNOWLEDGEMENTS	258

ABBREVIATIONS

BBC	Brown, Boveri & Cie, Mannheim, Germany and Baden, Switzerland
BOP	Balance of Plant
EVO	Energie-Versorgung-Oberhausen - a 50 MWe Closed-Cycle Helium Turbine Power Plant
GCFR	Gas Cooled Fast Reactor
GHH	Gutehoffnungshutte Sterkrade AG
GT-HTGR	Nuclear Closed-Cycle Gas Turbine Plant
HCTF	Helium Component Test Facility
HHT	Hochtemperaturreaktor mit Helium Turbine - High Temperature Reactor with Helium Turbine
HHV	Hochtemperatur-Helium-Versuchsanlage - a large scale power conversion loop component facility.
HTGR	High-Temperature Gas-Cooled Reactor
KFA	Kernforschungsanlage, Julich, Germany
LWR	Light Water Reactor
PCL	Power Conversion Loop
PCRV	Prestressed Concrete Reactor Vessel
PWR	Pressurized Water Reactor
ROT	Reactor Outlet Temperature
RTS	Reactor-Turbine System
UTC	United Technologies Corporation

1.0 INTRODUCTION

Until recent years the availability and abundance of low cost and clean gaseous and liquid fuels in the U.S.A. has stimulated the development of open cycle gas turbines with little emphasis placed on the utilization of the waste heat. With the exception of small Brayton cycle power conversion systems for space application, the closed-cycle gas turbine has not received much attention in the U.S.A. until the early 1970's when fuel conservation became increasingly important.

In Europe, particularly Germany and Switzerland, the merits of the closed-cycle gas turbine have long been recognized for combined electrical power and the utilization of the waste heat for industrial and urban district heating. During the last 30 years several plants, with electrical power levels up to about 20 MWe (and approximately equivalent heat rejection thermal energy) have operated very successfully, and with some of these units in operation for over 100,000 hours, creditable plant availabilities of over 90 percent have been realized. Initially, pulverized coal was used as the fuel for these plants, but later, in accordance with the fuel supply situation in Europe, changes were made in some of these plants to gaseous and liquid fossil fuels.

Of the many advantages of the closed-cycle gas turbine, perhaps the most significant are: (1) high potential efficiency, hence fuel conservation and minimum environmental impact, (2) adaptability to a wide range of heat inputs including fossil, nuclear (fission and fusion), and solar, (3) heat rejection characteristics well suited to either dry-cooling, wet-dry cooling, district heating, utilization of a secondary power cycle, or LNG vaporization, (4) compact power conversion system giving lower capital cost, (5) high availability, good reliability, and low maintenance associated with the clean closed-cycle working fluid, and (6) relatively short development period to get utility size machines into service.

Following a comprehensive survey of related closed-cycle gas turbine background, the main incentives for the design and development of the GT-HTGR plant are discussed. The bulk of the presentation consists of essentially four major design related areas for the nuclear gas turbine power plant as outlined below:

- 1) Background of GT-HTGR design studies, including aspects of cycle selection, plant configuration studies, and component preliminary design
- 2) Reference plant design description, including optimization study, performance considerations, power conversion loop details, and balance-of-plant design
- 3) Component design considerations, including descriptions of the turbomachinery, heat exchangers and control valves
- 4) Secondary Power Cycle description for an advanced version of the GT-HTGR, including working fluid selection, performance, and component design description

Development and testing alternatives are briefly discussed for the nuclear closed-cycle gas turbine plant. The presentation on large closed-cycle gas turbines closes with a brief review of the cooperative international program (U.S. - Germany/Switzerland) which is underway in the nuclear gas turbine field. The objective of this joint investigation study is to establish, to the highest degree possible, commonality in plant configuration, which would be of benefit to both the U.S. and European programs.

2.0 RELATED CLOSED-CYCLE GAS TURBINE BACKGROUND

J. Ackeret and C. Keller's ingenius idea of the closed-cycle gas turbine was first published in 1939 (Ref. 2.1). Because of the war and the post-war economic situation it took more than 15 years before the first commercial operating plant using a closed-cycle was ordered by a European community utility. Since then, some fourteen plants have been built in Europe, Britain, Russia, and Japan. Many of these plants have now operated for over 100,000 hours and have demonstrated high degrees of reliability and availability, and have made money for their owner operators. Some of the early experiences in the closed-cycle gas turbine field are outlined in References 2.2 through 2.6. A recent survey of the operational status and current trends in gas turbines for European utility applications (funded by the Fossil Energy Organization of ERDA) includes a comprehensive coverage of current closed-cycle gas turbine experience (Ref. 2.7).

Regardless of the initial success of closed-cycle gas turbines (as will be outlined in Section 2.1), European utilities have been reluctant to purchase and install this type of plant on a broad basis, yet amongst engineers it has always seemed that closed-cycle systems have been on the verge of acceptance. Some of the reluctance is related to the unfamiliarity of the utilities with a seemingly new non-steam system. Perhaps the most significant reason for slow acceptance is that the best way to exploit the full capabilities of closed-cycle systems is to use them in applications where both electrical power and heat are required. The power industry (particularly in the U.S.) is structured so that most utilities sell only electricity, other companies or organizations sell thermal energy (i.e., steam or hot water). Observations of the market trends in Europe indicate that more integrated approaches are now being developed. Numerous heat-power systems have been installed, and more are under consideration particularly those using fossil-fired closed-cycle gas turbine systems with electrical power levels up to 25 MW(e) and approximately equivalent thermal energy.

Based on the good technical and financial experience of the European plant to date, and the current trends in market requirements (energy conservation, alternate low grade fuels such as coal, need for heat as well as electric energy for industrial processes and urban district heating, and the potential advantages of the direct cycle nuclear power plant with a helium turbine) the extensive utilization of closed-cycle gas turbines may be realized in the near future.

2.1 CLOSED-CYCLE GAS TURBINE OPERATING EXPERIENCE

All of the known closed-cycle gas turbine plants are identified in Table 2.1 which is taken from Ref. 2.7. Details of these various plants are given in Refs. 2.8 through 2.27. Experience gained with these 17 plants over the period from 1940 to date covers a wide range of sizes, applications, and fuels. Most important, many of these plants now have over 100,000 hours of operation (in many cases with availabilities of over 90 percent); much of this operation has been with various types of pulverized coal, coke oven gas and heavy oil. Many of the early problems in these plants were systematically identified and resolved, and all of the industrial plants met or exceeded performance guarantees. As it turns out this long operating experience is directly applicable to the requirements and trends emerging from the current energy crisis and concern for the environment mentioned above.

Early plants had relatively small capacity, more recent plants are in the 30-50 MWe range (still very small relative to the normal utility requirements). With the exception of the Oberhausen II plant all of the early European plants used air as the closed-cycle working fluid, which is well suited to plants of small power output. Of the closed-cycle air plants referred to in Table 2.1, five are still in operation and these, together with plants of historical significance are discussed in Section 2.2. Operating plants and component experience, with helium as the working fluid are discussed in Section 2.3, and this leads to a brief introduction of activities underway in support of nuclear closed-cycle gas turbine studies as summarized in Section 2.4.

2.2 Closed-Cycle Gas Turbines with Air as the Working Fluid

2.2.1 Escher-Wyss Plant

The first experimental closed-cycle plant was built by Escher Wyss in Zurich. This 2000 kw, oil-fired plant, was built in 1939 and first run in 1940 (Refs. 2.2 and 2.3). An overall view of this pioneer plant is shown on Fig. 2.1 (from Ref. 2.8). The acceptance tests for this plant were run in December 1944, and all of the expectations were fulfilled and a plant efficiency of 32.6% was demonstrated. During the war this plant produced the necessary power and electricity for the Escher Wyss works during more than 6000 hours of operation. This pioneer plant proved the viability of the closed-cycle concept, and formed the technological base for future fossil-fired CCGT.

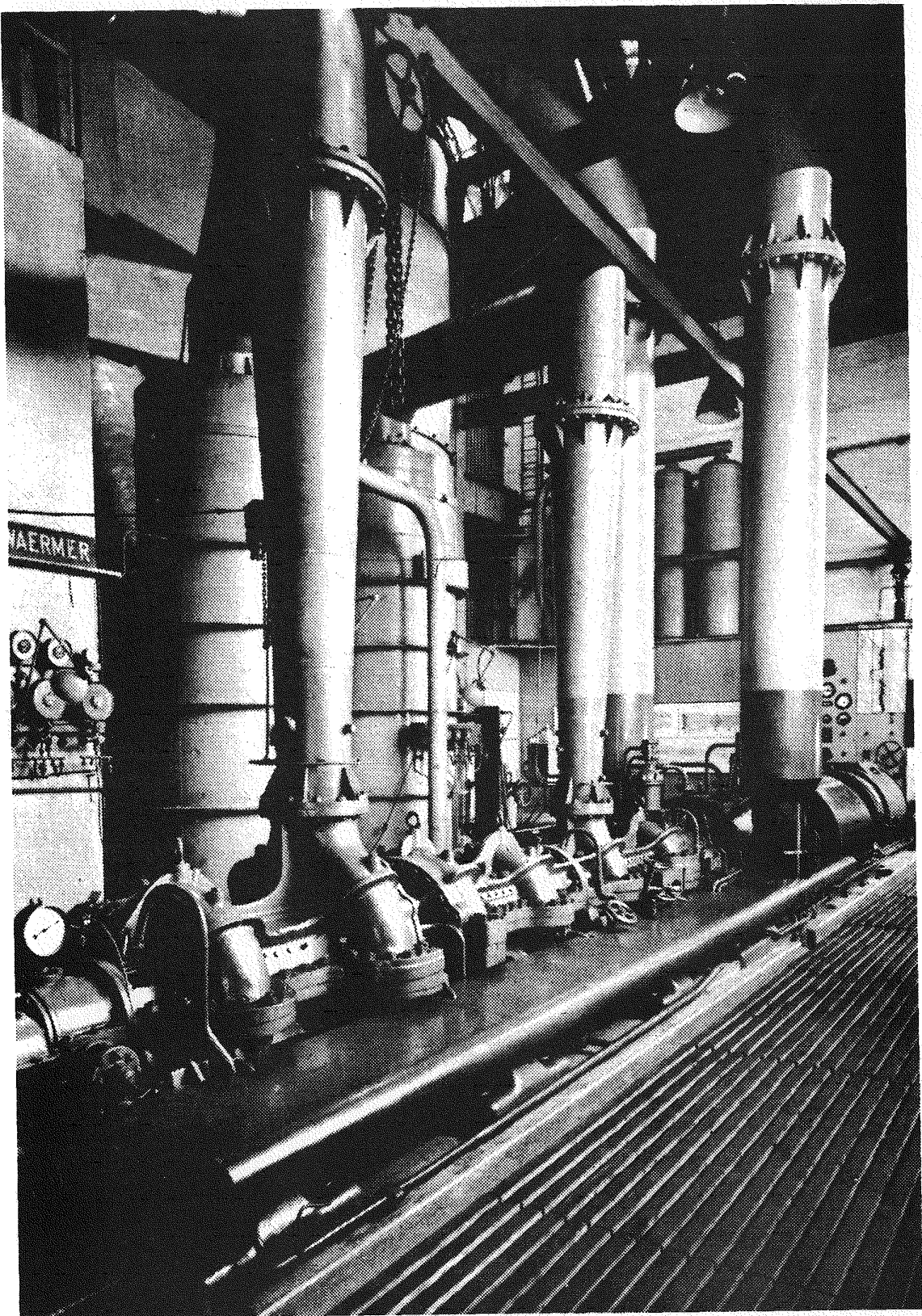
2.2.2 2.3 MWe Ravensburg Plant

The first pulverized coal fired industrial gas turbine in the world, the 2.3 MWe Ravensburg plant, started operation in 1956. (Refs. 2.6, 2.8, 2.10, and 2.15).

Units	Manufacturer	Application	Continuous	Heat	Plant	Commission-	Running	Fuel	Turbine	Comp.	Inlet	Remarks
			Output						Temp.			
			MWe	MW	%		Hours		°C	Bars		
Escher-Wyss Zurich, Switzerland	Escher-Wyss	Power	2	-	32.6	1940	6000	Oil	700	-		First Test Plant Retired
Ravensburg, Germany	E-W + GHH	Power & Heat	2.3	2.3-4.1	25	1956	120,000 to 6-76	Coal or Oil	660	7.2		
Coburg, Germany	GHH	Power & Heat	6.6	8-16	28	1961	100,000 to 6-75	Coal	680	7.3		
Oberhausen I Germany	GHH	Power & Heat	13.75	18.5-28	29.5	1960	100,000 to 6-76	Coal/Coke Oven Gas	710	8		
Oberhausen II Germany	GHH + EVO	Power & Heat	50	53	31.3	1975	3,000 to 5-76	Coke Oven Gas	750	10.5		First Use of Helium as Working Fluid Elect. Power Plant
Haus Aden, Germany	GHH	Power & Heat Comp. Drive	6.4	7.8	29.5	1963	100,000 to 6-75	Mine Gas+Coal	680	9.3		
Gelsenkirchen Germany	GHH	Power & Heat	17.25	20-29	30	1967	75,000 to 6-76	Bl. Furn. Gas & Oil	711	10.2		
St. Denis Paris, France	-	Power	12.5	-	-	1951	5,000 since '56	Oil	660	-		First Big Plant/ Double Pressurized Heater
Toyotomi, Japan	Fuji Elect. & E-W	Power	2.0	-	26	1957	90,000	Nat. Gas	660	7.2		
Nippon Kokan Japan	Fuji Elect.	Power	12	-	29	1961	85,000 to 12-70	Bl. Furn. Gas	680	6.7		
Rothes Great Britain	-	Power	2.0	-	-	1960	~1,000	Coal Slurry	660	-		Stopped Due to Mine Closure
Altnabrekk Great Britain	-	Power	2.2	-	-	1959	~1,000	Peat	660	-		Stopped Due to Mine Closure
Kashira Russia	E-W	Power & Heat	12	9-12	28	1961	-	Brown Coal	680	7		Achieved Guarant.
Spittelau Austria	BBC/E-W	Power & Heat	30-22	29-58	31-24	1972	-	Oil or Gas	720	-		Achieved Guarant. Dismantled
Die Oxygene Phoenix	E-W & LaFleur	Cryogenic Gas Production	2	-	-	1966	5,000	Nat. Gas	680	-		Helium Fluid; Dismantled
Adv. Power Conv. Exp. Test Facilities Ft. Belvoir, VA	Corps of Engineers (Stratos Et Al)	Army Power Requirements	0.5	-	18.6	1959	-	Oil	650	8.1		Experimental (Fluid, N ₂)
Adv. Power Conv. Skid Experiment San Ramon, Calif.	Corps of Engineers (Stratos Et Al)	Army Power Requirements	0.500	-	16.7	1964	-	Oil	650	8.1		Experimental (Fluid, N ₂)

GA-A14311

Table 2.1 Summary of Existing Closed-Cycle Gas Turbine Plants (from Ref. 2.7)



GA-A14311

Fig. 2.1 First Closed-Cycle Gas Turbine Plant (by Courtesy Escher Wyss)

This plant supplies the combined heat and power requirements of the works and office buildings of the Escher Wyss AG, Ravensburg. Although the plant is shutdown during the weekends an impressive 120,000 hours of operation (up until June 1976) have been accumulated since its commissioning at the beginning of 1956. To date, the plant has been shut down and started about 1200 times. Availability is now over 87 percent. Even although this plant is quite small (2.3 MWe) as shown from the overall view on Fig. 2.2 (from Ref. 2.8) it is very economical compared with the grid prices from the nearby utilities. The main users of the electrical power are the electric furnaces in the foundry and forging works, the welding machines, and the normal current supply for the fabrication buildings. Two thirds of the factory and the office buildings are supplied with heat.

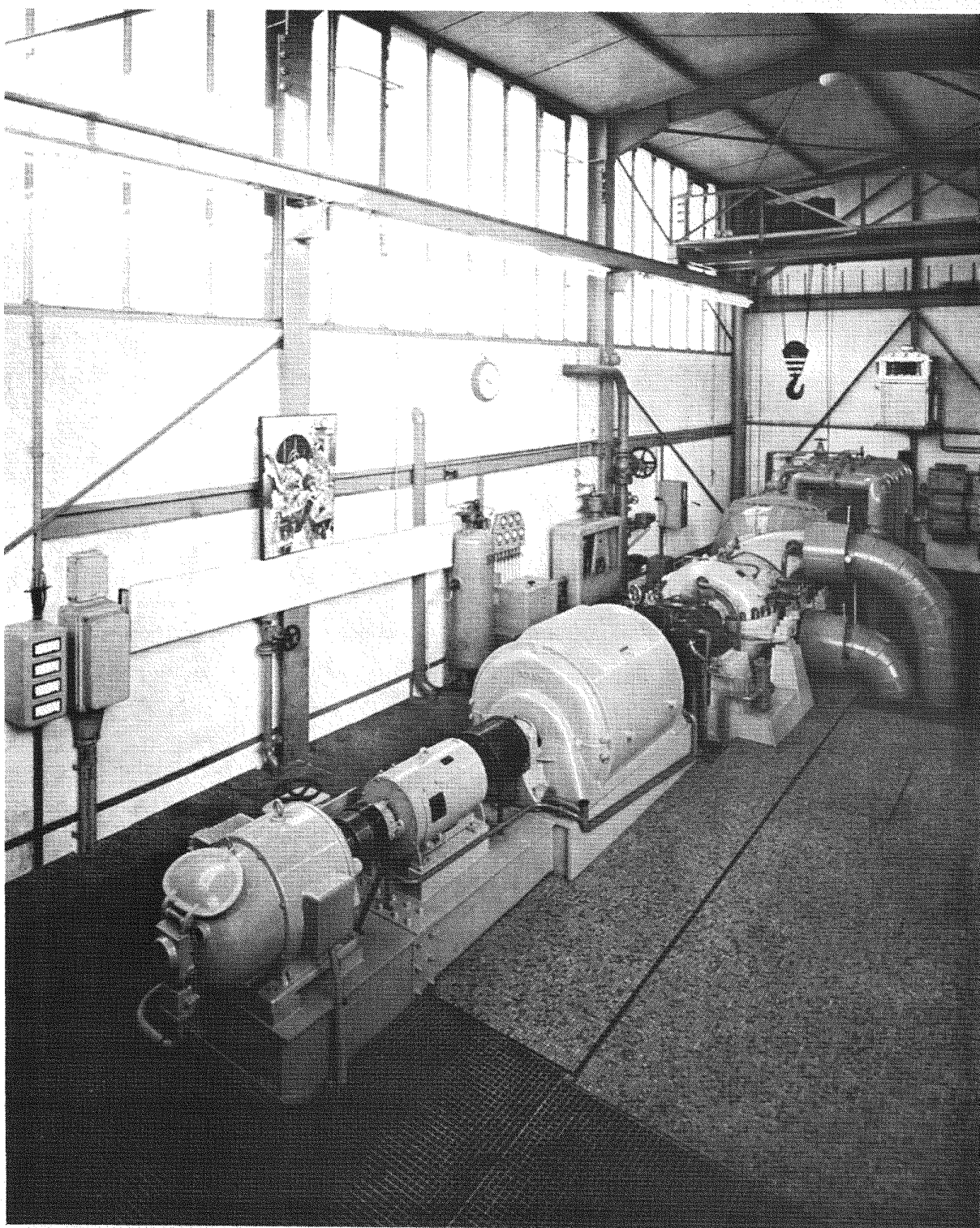
This closed-cycle plant, which was designed for pulverized coal firing, has also been running on heavy and light fuel oil, thus taking advantage of the lowest price of the different fuels on the market, and demonstrating the versitility of the CCGT.

2.2.3 6.6 MWe Coburg Plant

The closed-cycle plant for the city of Coburg in Germany also utilizes the combined electrical power and heat supply. The plant was commissioned in 1961 and until June 1975 had an operating time of 100,000 hrs. As outlined in Ref. 2.15 the availability of this plant is 83 percent, and ratio of heating to electrical power generation of 1.5 has been realized over the total operating period. The compact nature of the turbomachinery for this 6.6 MWe plant is shown in Fig. 2.3 (from Ref. 2.27). This plant was designed for pulverized coal firing. For ignition and to improve the stability of the flame, especially in part load operation, 10 percent of the total heat input is supplied by natural gas.

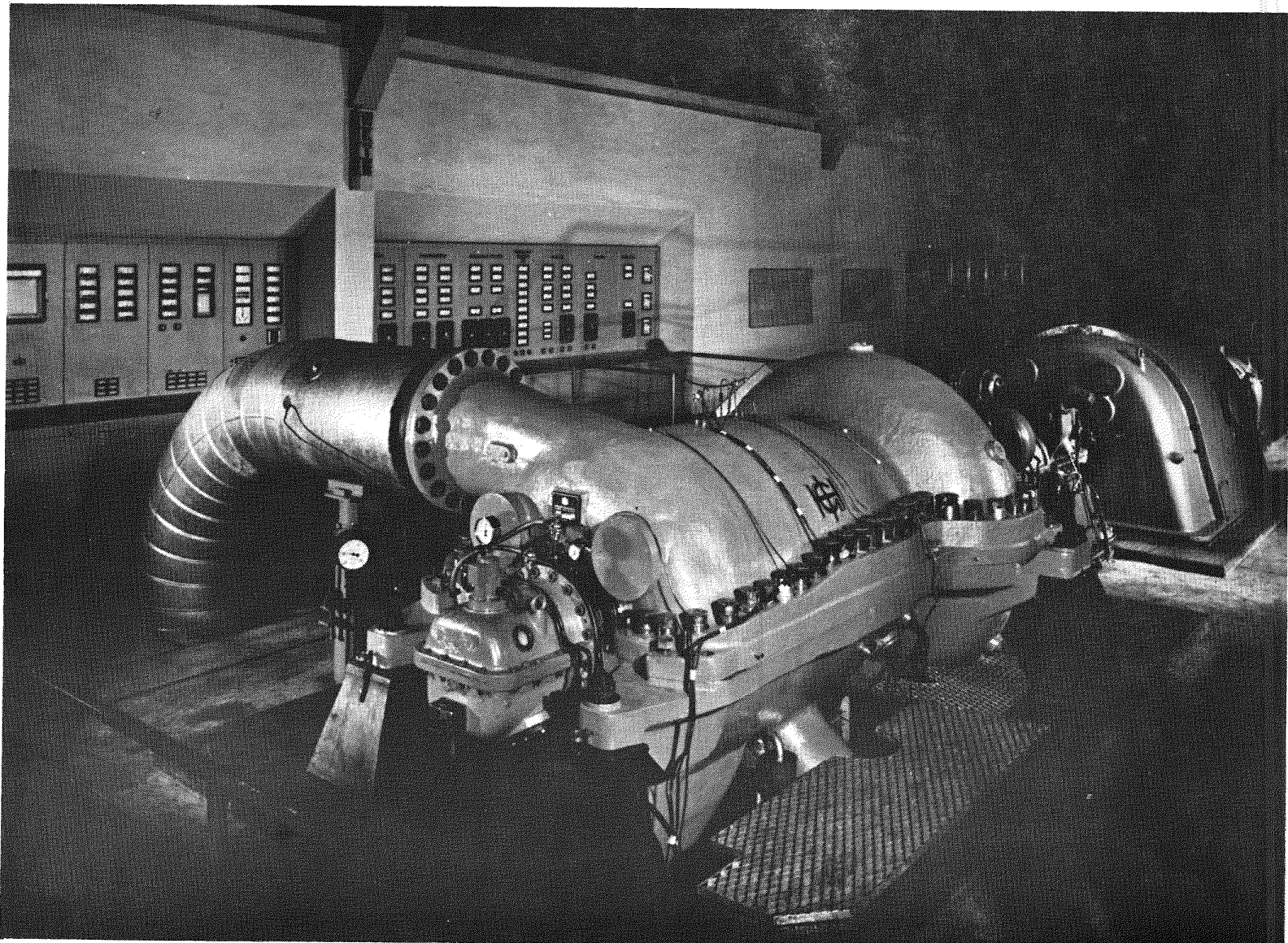
2.2.4 13.75 MWe Oberhausen I Plant

It is noteworthy that this plant represents a milestone in that it was the first time a major German utility (RWE) agreed to collaborate with a district heating organization (EVO) on a combined heat power system. It is rated for an electrical output of 13.75 MWe and a heating power of 18.5 - 28 MW, depending on compressor inlet temperature. Since commissioning in August 1960 the plant had an operating time of 100,000 hours (up until June 1976) and as outlined in Ref. 2.15, has had an availability of over 73 percent. Details of this plant are given in Refs. 2.13 and 2.14, and an overall view of the turbo set is shown on Fig. 2.4 (from Ref. 2.27). Until the beginning of 1965 this plant was fired with a high-grade nut coal and



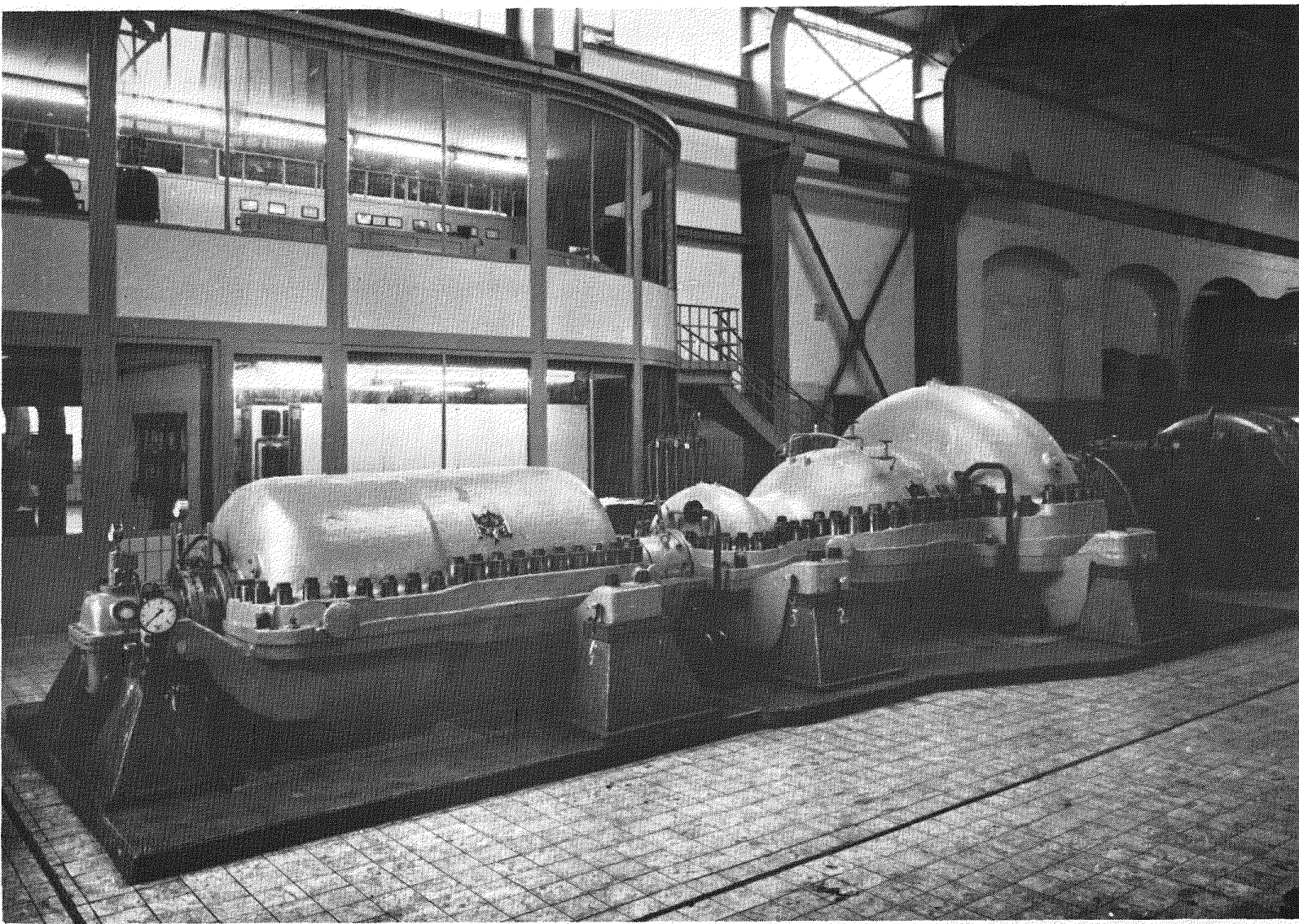
GA-A14311

Fig. 2.2 2.3 MW(e) Ravensburg Plant (by Courtesy GHH)



GA-A14311

Fig. 2.3 6.6 MW(e) Coburg Plant (by Courtesy GHH)



GA-A14311

Fig. 2.4 13.75 MW(e) Oberhausen I Plant (by Courtesy GHH)

afterwards with coke fines with a higher ash content. The Oberhausen area makes coke for the steel industry, and low Btu coke oven gas is a by-product which is bought by the local utility from the mining company. Since 1971 the heater for this plant has been fired with coke-oven gas, with supplementary light fuel-oil firing if there is not enough gas available.

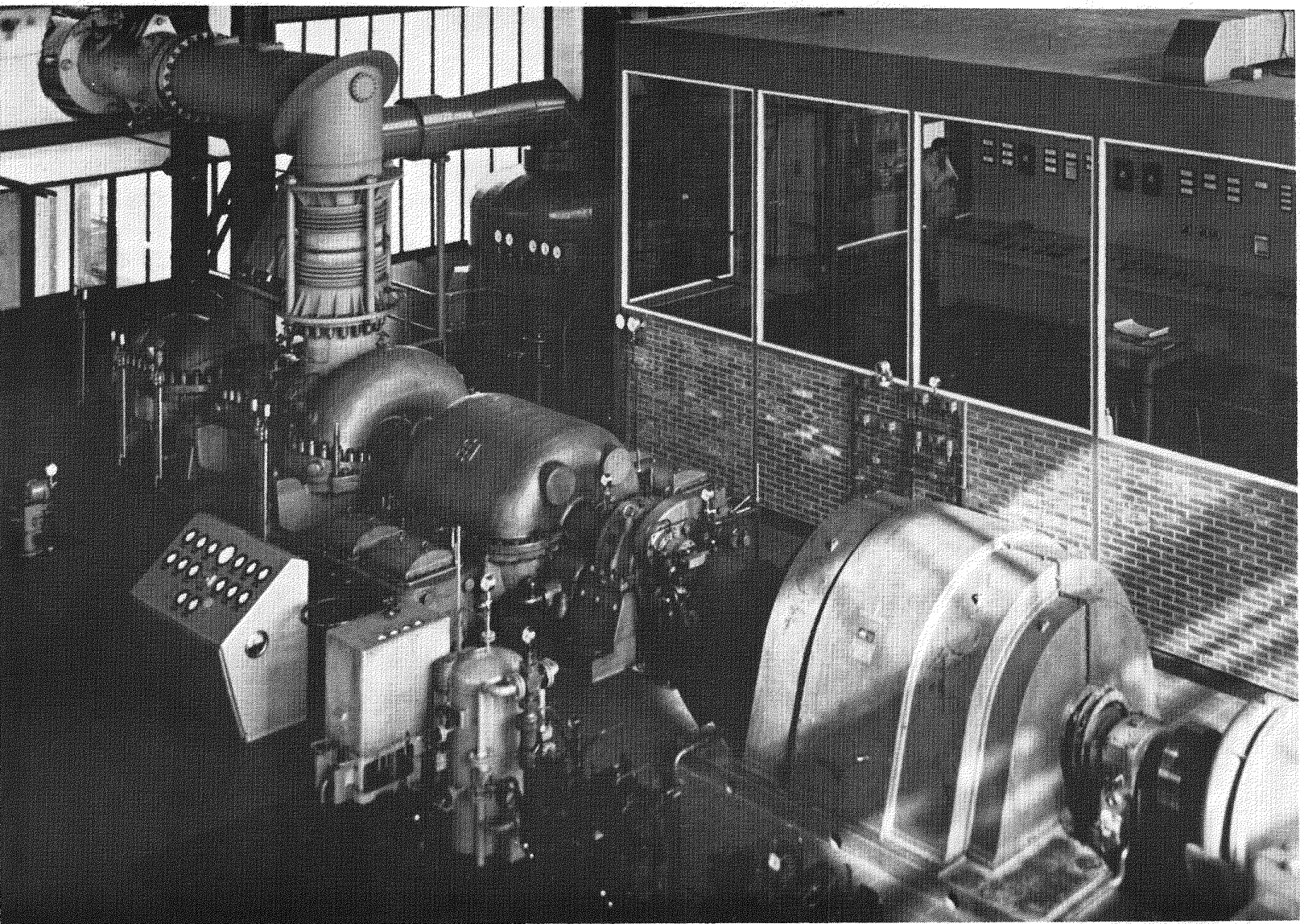
Because of the good results with this plant a number of similar projects are under consideration, and as mentioned in Ref. 2.7 the plant for the town of St. Gallen in Switzerland is now in the planning stages.

2.2.5 6.4 MWe Haus Aden Plant

This closed-cycle gas turbine was erected for the Haus Aden coal mine in the Ruhr area of Germany. It is rated at an electrical output of 6.4 MWe and a heating power of 7.6 MW. This plant was primarily built for supplying the mine with compressed air for ventilation. The compressor is arranged on the same shaft as the turboset and the alternator, and its power input is about 3 MW. About 70 percent of the heating power is used for the hot water supply of the mine itself, with the remainder being used for central heating of neighboring houses. The heater is fired with mine gas and pulverized coal and details of the plant are given in Refs. 2.10, 2.14, and 2.15. An overall view of the Haus Aden plant turboset is shown on Fig. 2.5 (from Ref. 2.27). From commissioning in April 1963 up to July 1975 the plant had reached an operating time of 94,000 hours, which corresponds to an extremely high availability of 91 percent. The turboset in this plant is still running with its original blading, and has proved to be very reliable.

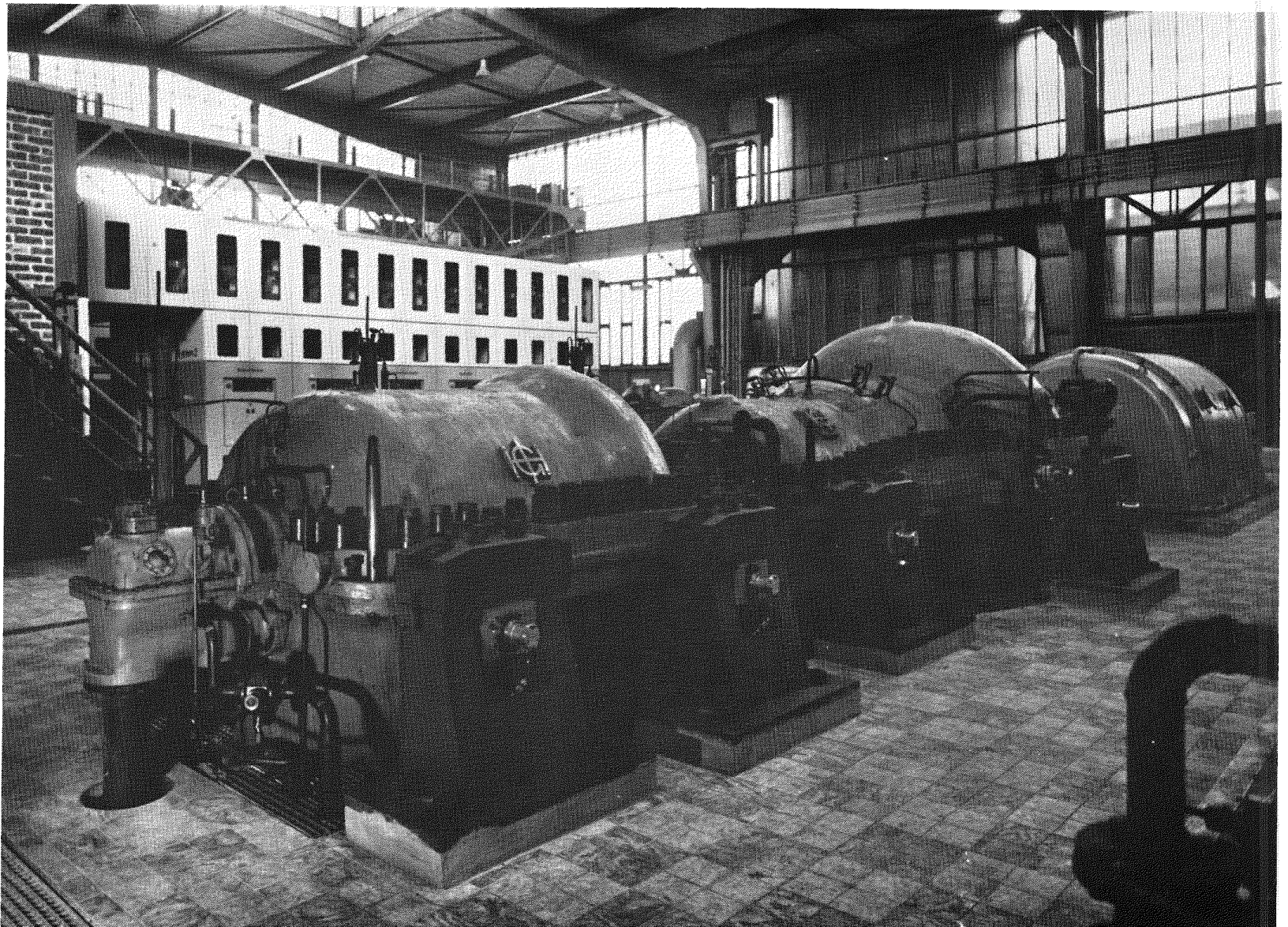
2.2.6 17.25 MWe Gelsenkirchen Plant

The Gelsenkirchen plant is the largest closed-cycle gas turbine plant in operation with an electrical output of 17.25 MWe and a heat supply of 20-29 MW. The plant operates in a steel works at Gelsenkirchen in Germany, and has been running since 1967. Up until June 1976 the plant has achieved an operating time of 75,000 hours and has demonstrated an availability of over 75%. The fuel for this plant consists of a mixture of blast furnace gas and oil. The percentage of the two fuels can be varied between 0 percent and 100 percent for each. Details of the plant are given in Refs. 2.14 and 2.15, and an overall view of the turboset is shown in Fig. 2.6 (from Ref. 2.27).



GA-A14311

Fig. 2.5 6.4 MW(e) Haus Aden Plant (by Courtesy GHH)



GA0A14311

Fig. 2.6 17.25 MW(e) Gelsenkirchen Plant (by Courtesy GHH)

Details of the turboset are shown on Fig. 2.7 (from Ref. 2.15) and exhibit typical characteristics of an intercooled, single-shaft machine for a non-integrated fossil-fired plant. This figure is included, because later in this report, comparisons will be made with a machine concept for an integrated nuclear plant where constraints on the turbomachinery envelope have a strong influence on the design of the compressor and turbine inlet and outlet scrolls and volutes.

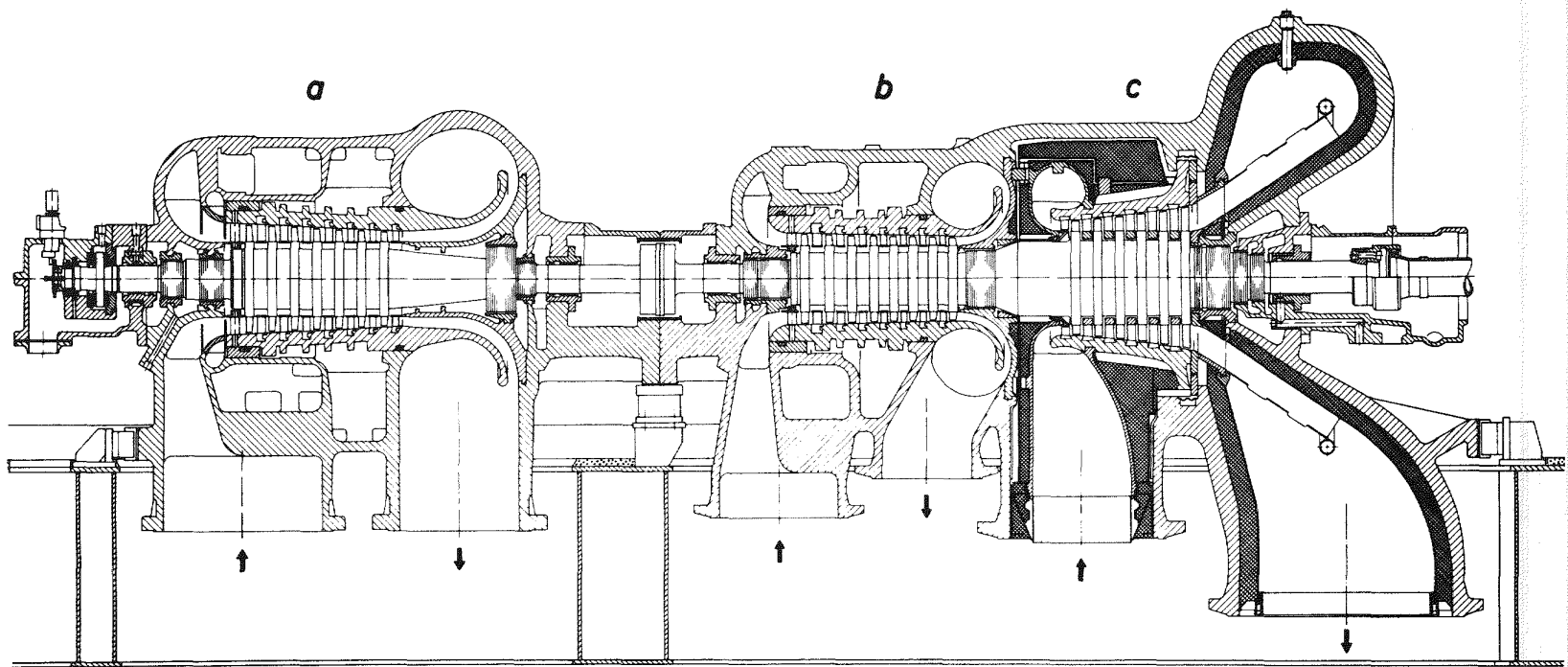
2.2.7 30 MWe Spittelau Plant

This plant represented the latest, most modern design of a combined heat-power plant of the closed-cycle type using air as a working fluid. With a nominal electrical output of 30 MWe and a heat production of 57 MW the plant was designed for operation in Vienna. The system provided 300°F (149°C) water to heat private homes and offices. With the waste heat recovery the total energy usage, or efficiency was 85 percent. The total efficiency was 31 percent without heat recovery.

The plant was built and tested, and after initial problems were resolved, all guarantees were ultimately satisfied. Unfortunately other, non-technical problems developed between the electric power organization and the organization for district heating. As a result of local legal and political maneuvers, and over the objections of many key technical and engineering leaders in Europe, it was decided at the end of 1975 to dismantle the plant.

2.3 Closed-Cycle Gas Turbines with Helium as the Working Fluid

Considerable attention has been given to the selection of working fluids for closed-cycle gas turbines. Air, helium, nitrogen, carbon dioxide and various mixtures of gases have received extensive attention (Refs. 2.28-2.34) and it is not proposed to elaborate on these in this presentation. There seems to be general agreement that, based on power level, air should be the working fluid at the lower power levels up to about 50 MWe. Above 50 MWe, and of course for nuclear direct cycle plants, helium is clearly the correct choice. The following sections briefly outline the helium gas turbine experience to date.



GA-A14311

Fig. 2.7 Turbomachine for Gelsenkirchen Plant (by Courtesy GHH)

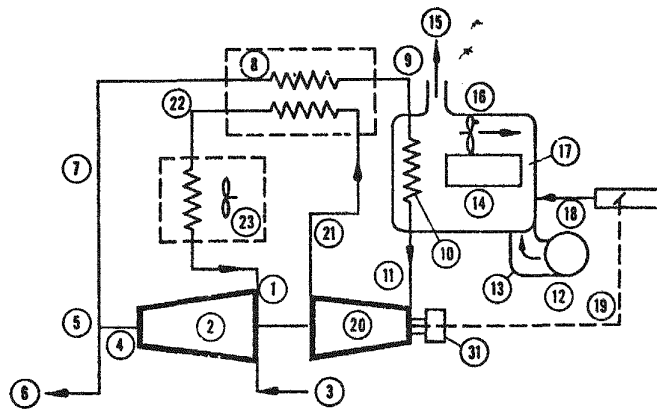
2.3.1 The La Fleur Helium Turbine Process Plant

It is not widely recognized that the first helium gas turbine in the world was in fact designed, built, and operated in the United States. As outlined in Refs. 2.17-2.19 La Fleur Enterprises in May 1960 undertook the design of a closed-cycle gas turbine utilizing helium as the working fluid. The useful output of this machine was in the form of a stream of helium bled from the last stage of the compressor. As shown in the cycle diagram on Fig. 2.8 this stream was used in a low temperature refrigeration cycle and returned to the compressor inlet at approximately ambient temperature. The design of this plant was completed at the end of 1960 and construction initiated immediately. The overall plant, shown on Fig. 2.9 (from Ref. 2.19), underwent initial testing in the Spring of 1962.

This plant was strictly prototype, and with a turbine inlet temperature of 1200°F (650°C) the compressor pressure ratio was 1.48, and the total helium mass flow rate was 16 lb/sec (7.26 kg/sec). The noteworthy aspect of this project was that essentially of all the design work, including that for the 16 stage compressor and 4 stage turbine, was done by two persons, and that the initial test runs in which the machine first became self-sustaining were accomplished 18 months after the decision to build a helium gas turbine had been made. The experience from this small prototype plant led to the design and construction of a larger helium turbine for a liquified gas cryogenic plant as outlined below.

2.3.2 Escher Wyss Helium Gas Turbine Plant for La Fleur Process

A free running helium turbomachine set was built by Escher Wyss in Switzerland around 1966 as outlined in Refs. 2.8 and 2.12. The turbine power (6 MW) for this industrial type was used to compress helium in an intercooled axial compressor. Sixty two percent of the compressor delivery produced the turbine power and 38%, corresponding to 2 MW useful power output was bled off in the cryogenic cycle for the liquefaction of 90 tons/day of nitrogen. The turbine inlet temperature was 1220°F (660°C), the total helium flow rate 24.2 lb/sec (11 kg/sec), the compressor pressure ratio 2.0, and the rotational speed was 18,000 rpm. A view of the rotor for this helium gas turbine is shown on Fig. 2.10 (from Ref. 2.8). An overall view of the helium turbomachine assembly embodying the LP and HP compressors and turbine in an all welded casing is shown on Fig. 2.11.

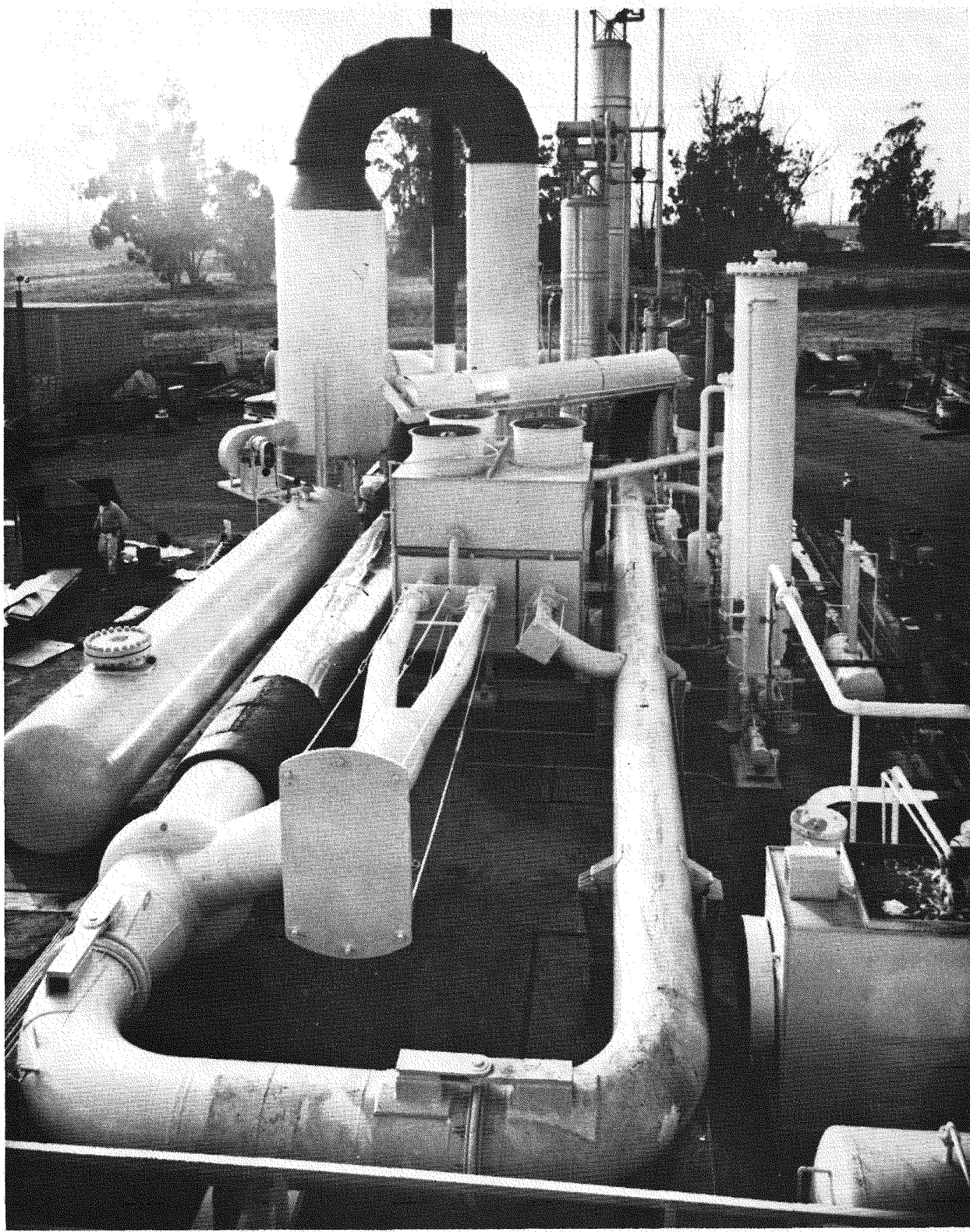


Gas Turbine Components

1. Helium to compressor from cooler 23, front end of compressor
2. Compressor in pipe
3. Low pressure into compressor from process
4. Outlet end of compressor
5. End of 14' diffuser
6. High pressure to process
7. Helium to 8
8. Regenerator
9. Pipe to heating coil behind cooler
10. Heating coil for helium behind cooler
11. Heated helium into turbine, behind crossover pipe 21
12. Combustion air inlet and fan
13. Pipe to combustor
14. Combustor
15. Exhaust
16. Recirculating fan behind cooler
17. Pipe to 14
18. Fuel in
19. Speed regulator
20. Turbine behind cross over pipe 21
21. Pipe to regenerator behind cooler
22. Pipe to cooler
23. Cooler
24. Helium storage tank
25. Cooling tower
26. Dryer
27. Tank for removing CO_2 from air
28. Argon distillation tower
29. Oxygen distillation tower
30. Four regenerative heat exchanges
31. Refrigeration turbine on same shaft as main turbine.

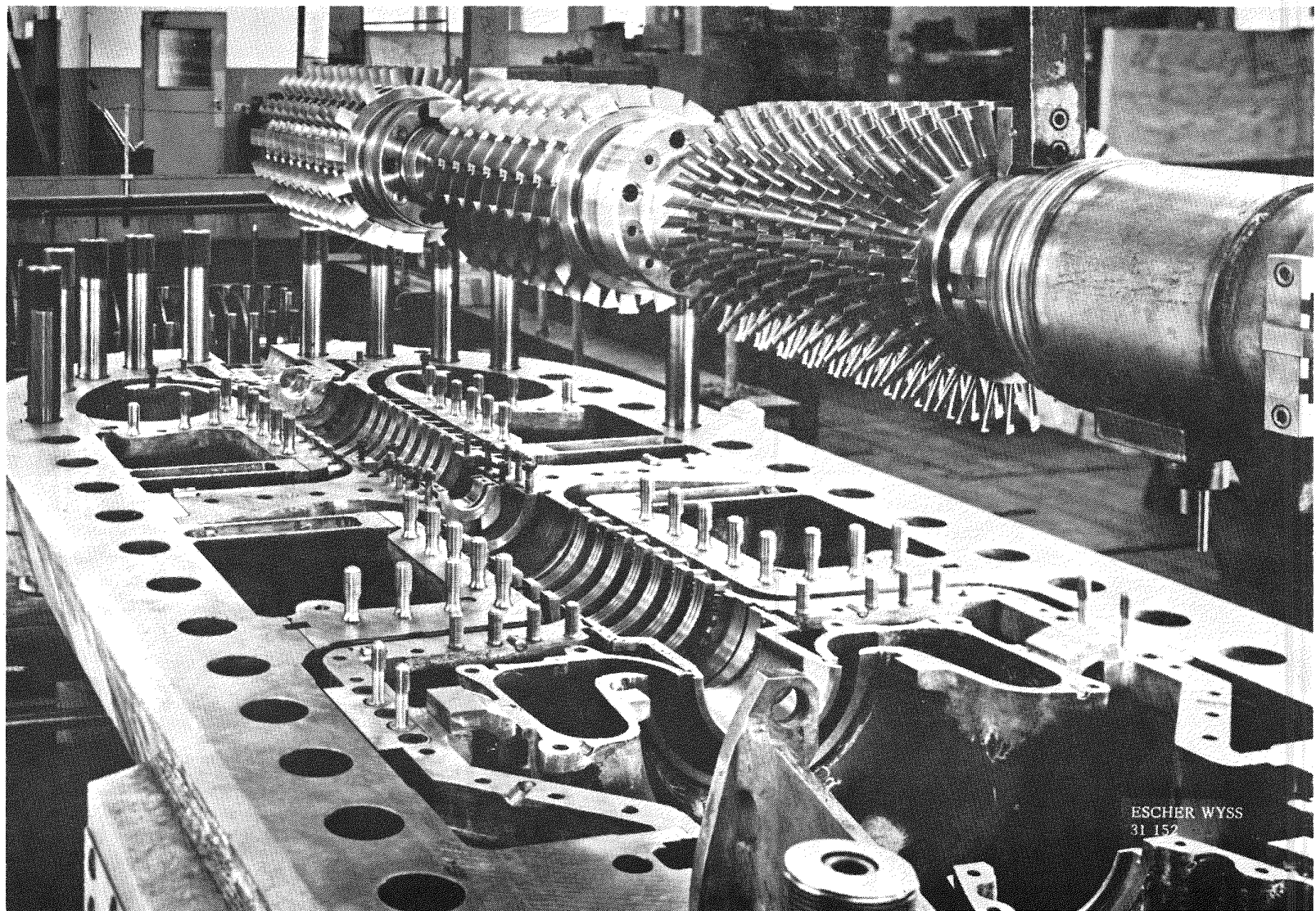
GA-A14311

Fig. 2.8 Cycle Diagram for La Fleur Closed-Cycle Plant



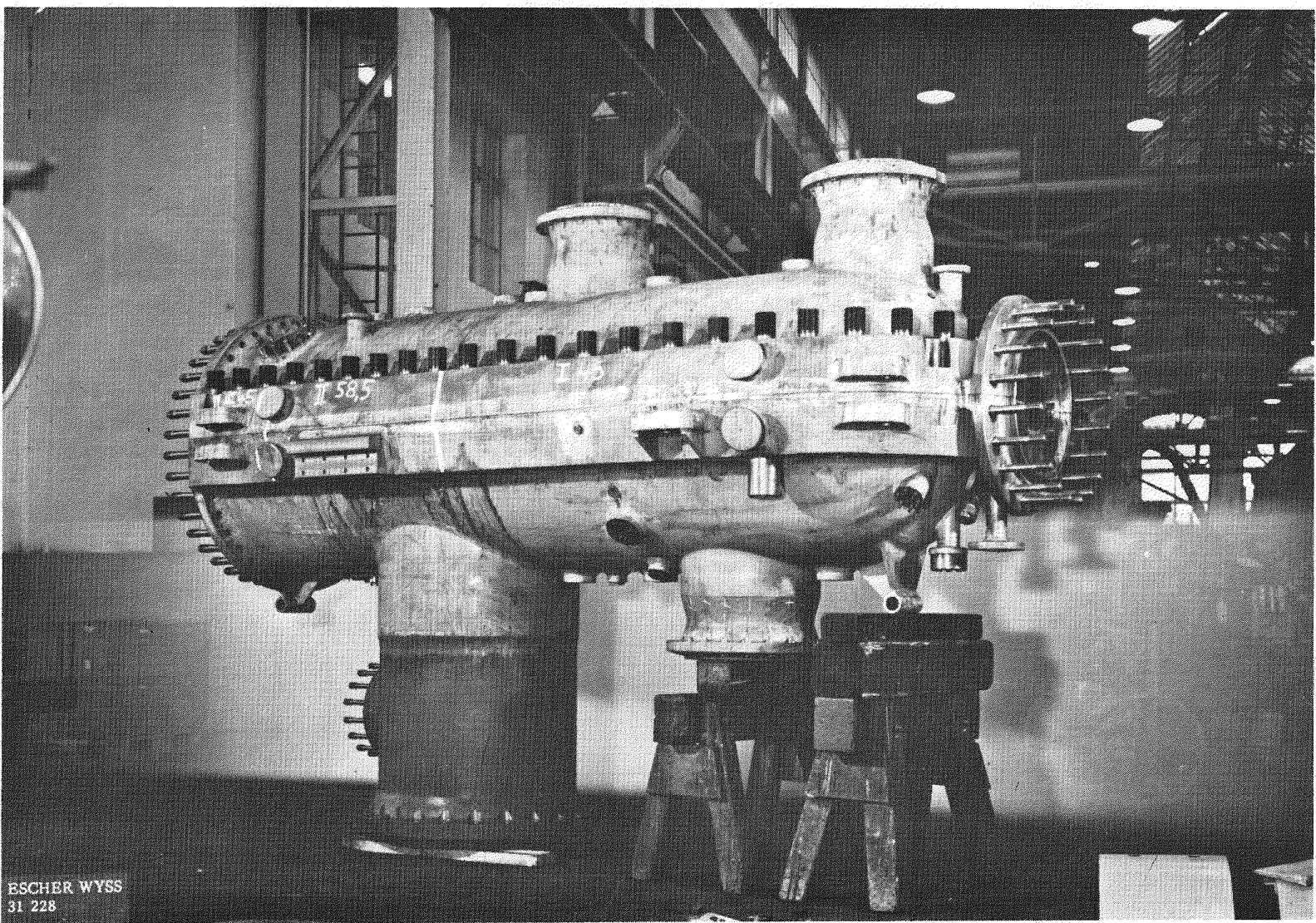
GA-A14311

Fig. 2.9 Overall View of Initial La Fleur Plant with Helium Turbine
(by Courtesy Jim La Fleur)



GA-A14311

Fig. 2.10 Rotor Assembly for La Fleur Process Plant (by Courtesy Escher Wyss)



ESCHER WYSS
31 228

GA-A14311

Fig. 2.11 Overall View of Helium Turbomachine (by Courtesy Escher Wyss)

This La Fleur cryogenic plant with the helium gas turbine operated for over 5000 hours in the United States. This very specialized plant proved to be too expensive to manufacture for the limited market for cryogenic liquids. Anticipated market growth did not materialize, and while the machinery performed satisfactory, the plant was withdrawn from service. As far as the helium power conversion system was concerned, the plant represented a significant milestone since the technology generated was applied to follow-on helium turbine projects, initially fossil-fired, but always with the long term goal of a nuclear heat source.

2.3.3 50 MWe Oberhausen II Helium Turbine Plant

The first heating power plant employing a helium turbine was built by Energieversorgung Oberhausen AG (EVO) from 1972 to 1974. Many reports and papers have been written on this important plant and aspects of the design, construction and erection have been covered in Refs. 2.14, 2.15, 2.16, 2.20-2.24.

This plant is of particular significance since it is not only intended to serve the power and heating needs of Oberhausen, but it also represents a small scale pilot plant for future large nuclear closed-cycle helium gas turbine plant. With a system pressure less than in the projected nuclear plant, the components (turbo-machinery and heat exchangers) in the Oberhausen plant are equivalent in size to a plant with a power rating of about 300 MWe. An overall view of this plant is shown on Fig. 2.12 (from Ref. 2.27). This fossil-fired plant, with a net electrical output of 50 MWe and a heat rating of 53 MW for district heating, is part of the 4th Atomic Energy Program of the Federal Republic of Germany. An essential part of the project is the High Temperature Reactor with a Helium Turbine of Large Output (HHT). In this plant the behavior of the turbo-unit, the heat exchangers with piping and auxiliary facilities are being investigated in connection with all operating flows, such as startup, shutdown, load changes, loss of load, etc. For this purpose the plant has been provided with comprehensive instrumentation. Experience with the Oberhausen II plant will contribute to the design and construction and operation of large helium turbine power plants.

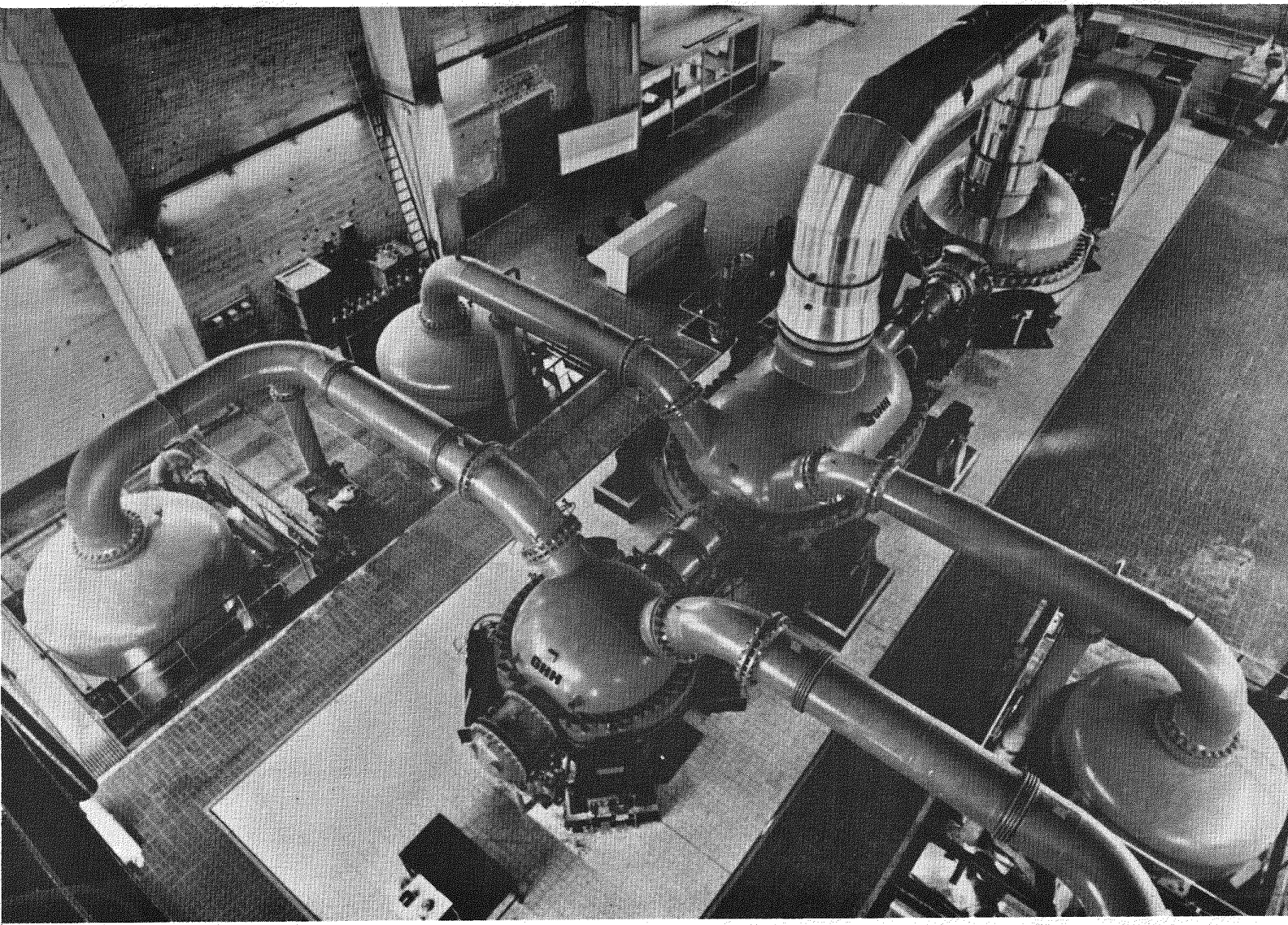


Fig. 2.12 50 MW(e) Oberhausen II Helium Turbine Plant (by Courtesy of GHH)

Construction of the plant was completed in the autumn of 1974, and initial operation started in December 1974. Some initial problems, considered somewhat inevitable in a new plant of this type, were encountered but in November 1975 the helium turbine was synchronized with the grid and district heating was supplied to the city of Oberhausen. With a turbine inlet temperature of 660°C the electrical output has been increased to 15 MWe. Within the period of approximately 3000 hours (until May 1976), main interest has focused on accumulating knowledge of the operating behavior of the plant and thereby to test the various component parts of the plant at moderate loads. Work continues towards commissioning on this pioneer helium turbine power-heating plant.

2.4 Activities in Support of Nuclear Gas Turbine Development

Ever since the onset of the development of nuclear reactors for energy production, especially reactors using a gaseous coolant, the idea of the use of a closed-cycle gas turbine to provide the power conversion function for a gas cooled reactor has appeared attractive to many engineers. Suggestions for the development of the direct cycle nuclear reactor appeared around the end of the second world war (Ref. 2.35) and have been proposed by Dr. Peter Fortescue of General Atomic and others with increasing frequency in subsequent years (Refs. 2.36-2.54). Together with the above mentioned closed-cycle gas turbine activities, planned helium component test rig operation, and HTGR plant component experience as briefly discussed below, will play an important role towards the ultimate goal of introduction of large nuclear gas turbine power stations.

2.4.1 High Temperature Helium Test Facility (HHV), Julich, Germany

The HHV system, at the KFA in Julich, is an experimental plant only and is designed for testing specific components which can be investigated in the test array of the HHV system under conditions similar to that expected in a nuclear gas turbine plant. In addition to the possibility of integrating trial components into the system, the operation of the system in itself presents the possibility of demonstrating and securing decisive data about the turbo unit, hot-gas conduction, fittings, and monitoring instruments. The instrumentation is such as to enable

data to be obtained on flow characteristics of the turbo-unit blading, efficiency of blade cooling, as well as the behavior of the various seals. Details of this facility are given in Refs. 2.47 and 2.53.

A cycle diagram and details of the turbomachine are given on Fig. 2.13, and a view of HHV turboset is shown on Fig. 2.14 (from Ref. 2.47). The two turbine stages produce about 45 MW while the eight compressor stages absorb about 86 MW. The difference in power is supplied by a synchronous motor. The pressures and temperatures are such that essential components of a 700 MWe turbomachine can be tested under conditions very close to the actual operating conditions in the reactor. The HHV facility does not require a helium heater or a recuperator. A cooler is required to remove the heat which is continuously put into the cycle by the electric motor. Start-up for this facility is scheduled for 1977. A model of the HHV test facility is shown on Fig. 2.15

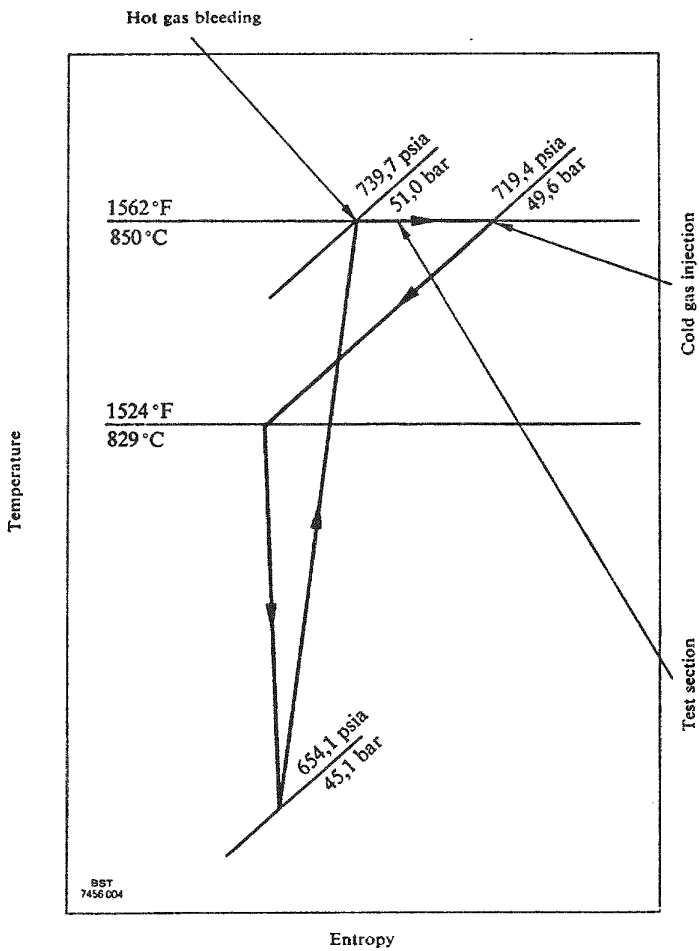
2.4.2 Steam Cycle HTGR Helium Component Development

Another source of technology from which the nuclear gas turbine can strongly benefit is the steam cycle HTGR plant. While there is substantial commonality in the area of the PCRV, the discussion here will be limited to the major helium components; namely, the circulator and high temperature heat exchangers (steam generators). Brief discussions on these are given below.

2.4.2.1 Helium Axial Flow Circulator

Experience at General Atomic in the design, development and fabrication of circulators for gas-cooled reactors has provided a technical base for the design of rotating machinery for closed-cycle gas turbines. Based on early gas cooled reactor circulator design and operating experience the series steam turbine helium circulator was conceived and developed by General Atomic. The circulator consists of a single stage axial-flow compressor driven by a single stage steam turbine. Initial design studies led to an arrangement where the compressor and drive turbine are integrally attached to a single vertical shaft and overhang from a central bearing and seal housing. This type of circulator is used in the 330 MWe Fort St. Vrain nuclear generating station in Colorado. This plant has four circulators,

Units		
Rotational speed	(rev/min)	3000
Hub diameter	(in)	63.0
	(mm)	1600
Length of bladed section	(in)	91.7
	(mm)	2330
Distance between thrust bearing and bearing on compressor exit side	(in)	297.6
	(mm)	7560
Outer diameter of housing	(in)	144.1
	(mm)	3660
Diameter of shaft seal, turbine inlet side	(in)	18.7
	(mm)	475
Compressor exit side	(in)	22.0
	(mm)	560
Diameter of inlet and exit duct	(in)	39.4
	(mm)	1000
Number of stages, turbine compressor	(-)	2
	(-)	8
Compressor exit pressure	(psia)	739.7
	(bar)	51.0
Compressor exit temperature	(°F)	1562
	(°C)	850
Turbine inlet pressure	(psia)	719.4
	(bar)	49.6
Turbine inlet temperature	(°F)	1524
	(°C)	829
Relative pressure difference between compressor exit and turbine inlet	(%)	3
		3
Mass flow rate at compressor exit	(lb/s)	467
	(kg/s)	212
Difference between compressor and turbine power	(MW)	40.8
		37.0
Nominal power of electric motor	(MW)	45.0



GA-A14311

Fig. 2.13 Parameters and Details of HHV Test Facility (by Courtesy BBC)

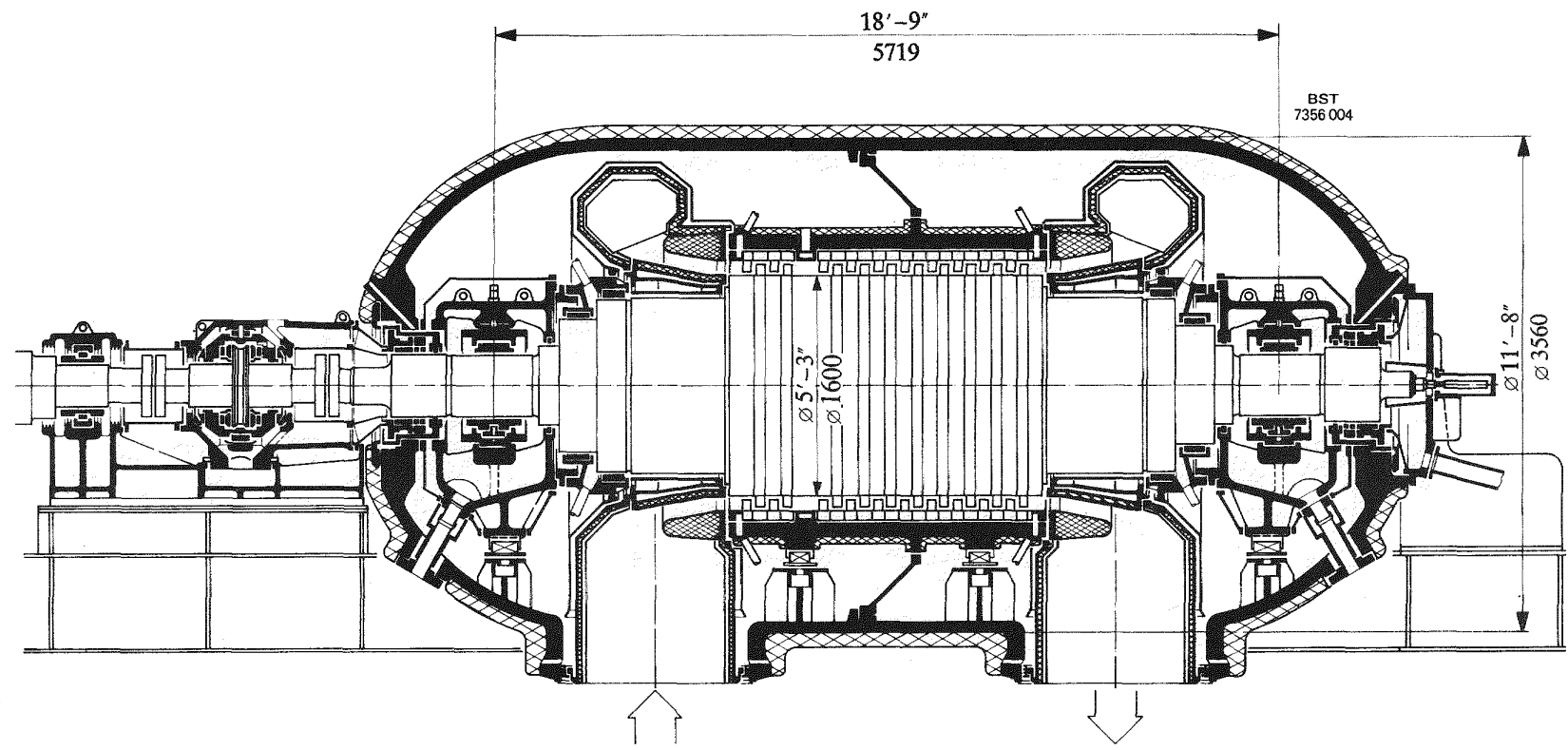
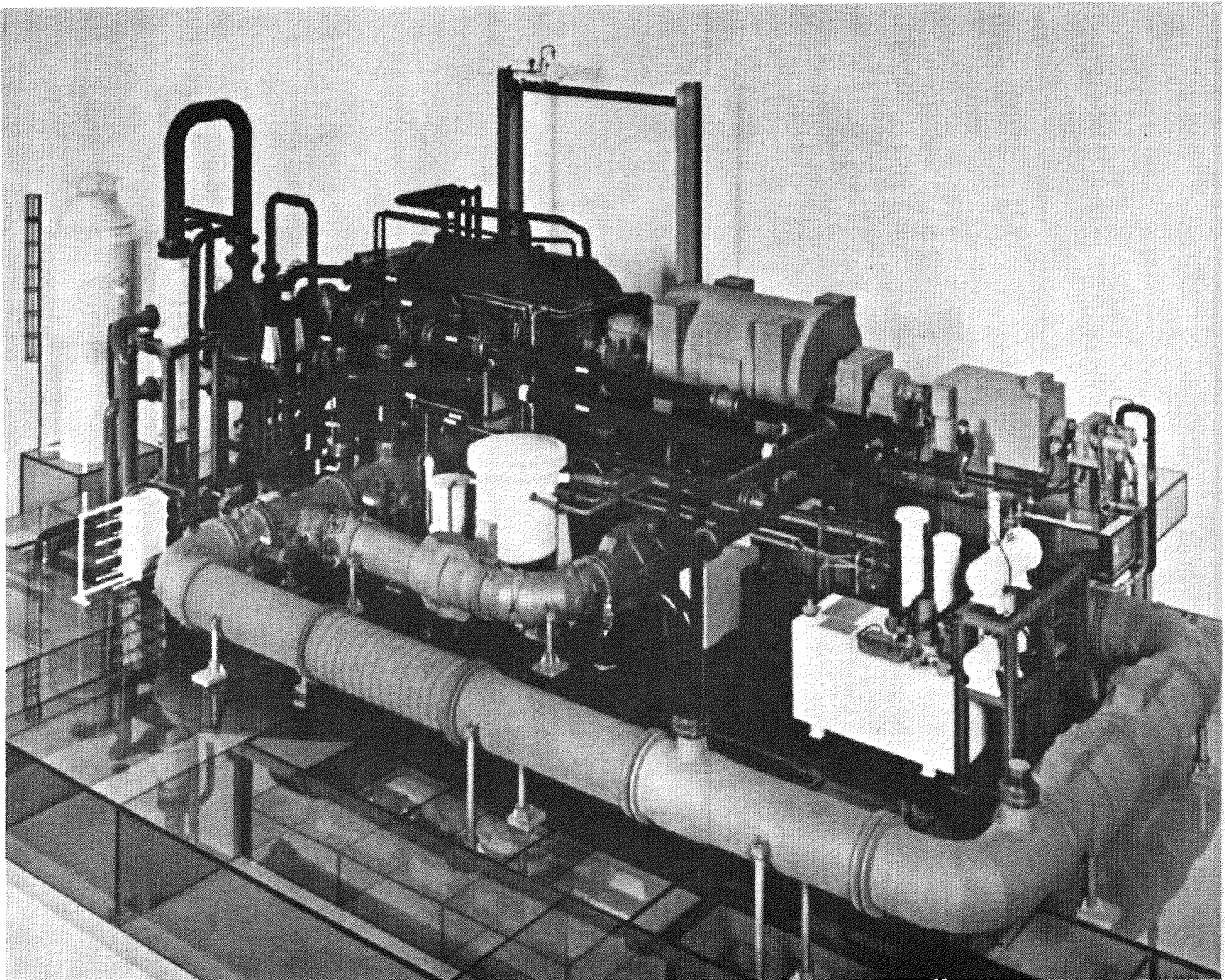


Fig. 2.14 Turboset for HHV
(by Courtesy BBC)



GA-A14311

Fig. 2.15 HHV Test Facility Model
(by Courtesy BBC)

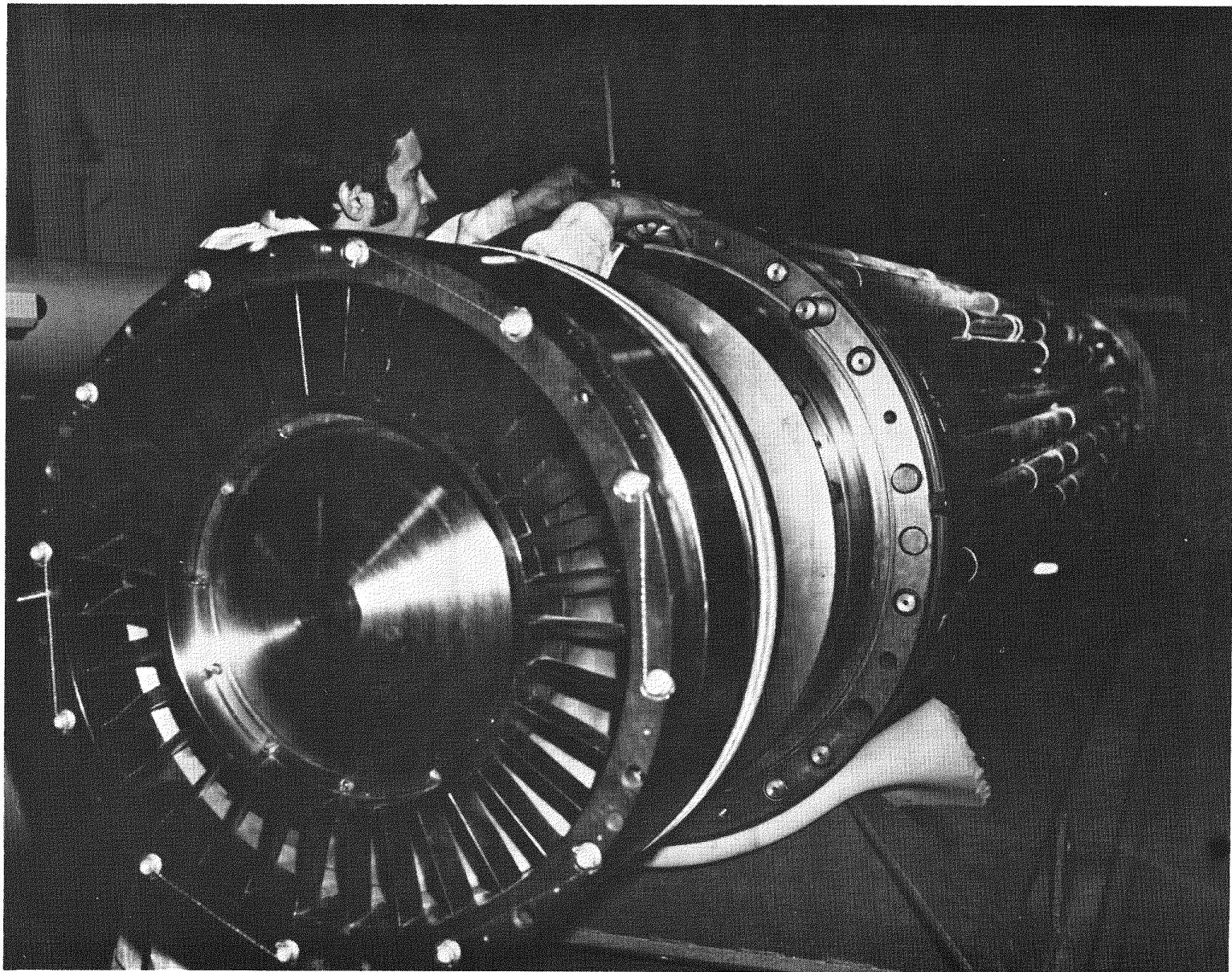
two of each primary coolant loop. The design of these circulators was done by General Atomic, and details of the subsequent comprehensive development program in the areas of aerodynamics, performance, rotor dynamics and bearing technology are given in Refs. 2.55 - 2.58. An overall view of the Fort St. Vrain plant circulator, which has a power rating of 5500 hp (4.1 MWe) is given on Fig. 2.16. Details of the circulator design for the large HTGR and GCFR plants are given in Ref. 2.59.

2.4.2.2 Steam Generators for HTGR Plant

While the role of the heat exchangers in the steam cycle and gas turbine HTGR plants are different, they have commonality as regards thermal and structural analysis, materials development, and fabrication methods. General Atomic Co. had developed a high level of technical expertise in the field of high temperature heat exchangers designed for extended life operation in a helium environment. Steam generator experience (Refs. 2.60, 2.61, and 2.62). The helically-coiled, once-through steam generators for the 330 MWe Fort St. Vrain plant are described in Refs. 2.63, 2.64, and 2.65. An overall view of the steam generator (12 of which are required for the Fort St. Vrain Plant) is shown on Fig. 2.17. The steam generators, like the heat exchangers for the nuclear gas turbine plant, require detailed expertise in the identification of structural design criteria and allowable stresses, in addition to a highly sophisticated thermal stress and vibration analysis capability. For the HTGR steam generators the analyses have been verified by comprehensive development programs encompassing heat transfer, fluid flow, flow stability, material, vibration, and fabrication development testing. The bulk of the analytical procedures and computer code thus confirmed are broadly applicable for the GT-HTGR plant heat exchangers.

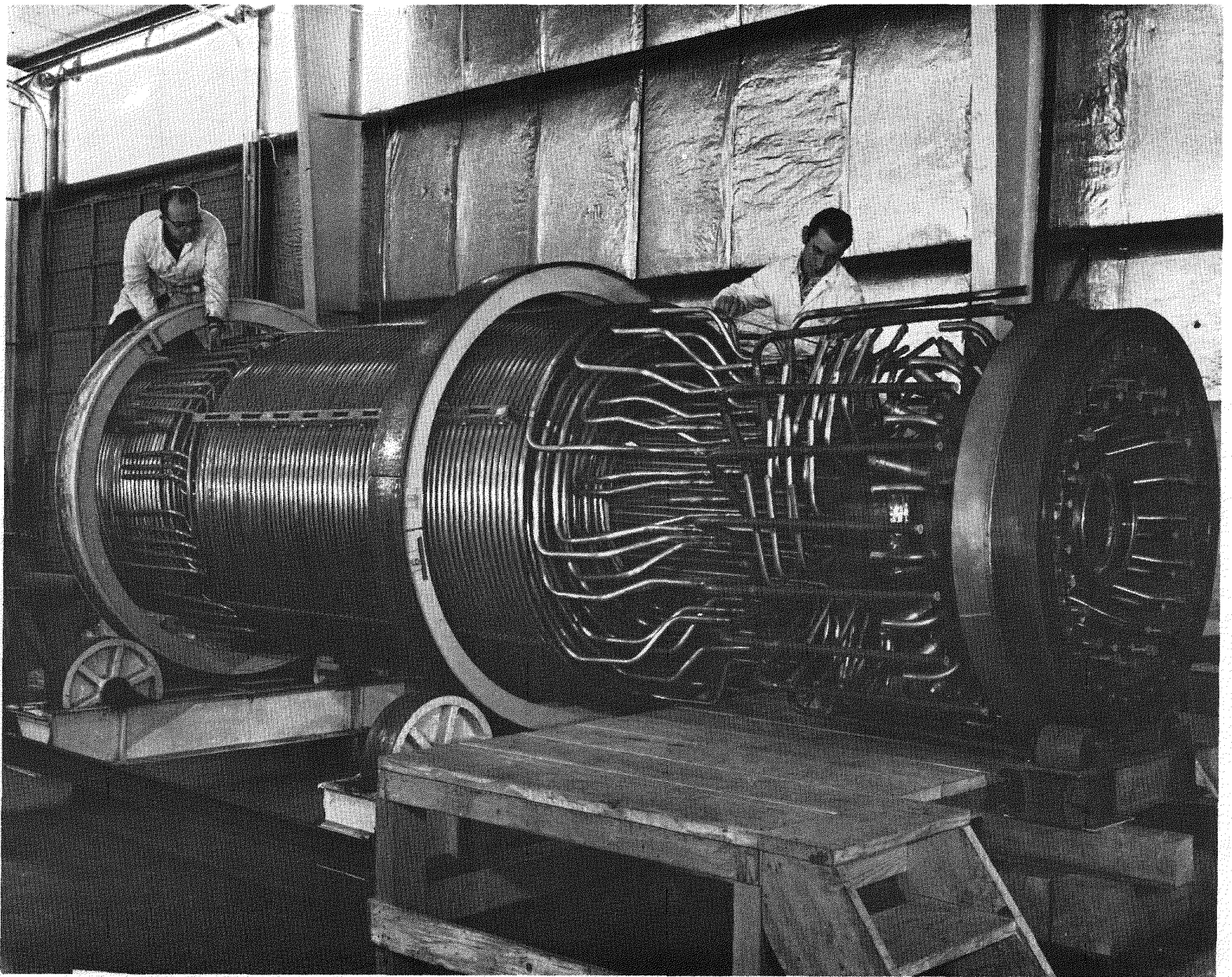
2.5 Summary

When a new power conversion system is proposed for large scale utility power generation its successful introduction depends to a large extent on economics



GA-A14311

Fig. 2.16 Overall View of Helium Circulator for Fort St. Vrain HTGR Plant



GA-A14311

Fig. 2.17 Steam Generator Assembly for Fort St. Vrain HTGR Plant

of operation, development effort required, and its technology base. In the case of the nuclear gas turbine, the established technologies in the areas of gas cooled reactors and closed-cycle gas turbines should result in successful introduction of this power conversion concept with a minimum development effort, i.e., essentially no new technology required. This section on related closed-cycle gas turbine experience includes a comprehensive bibliography to emphasize the depth to which closed-cycle gas turbine activities have been pursued, predominantly in Europe. The proven versatility of the CCGT to be operated with a variety of fossil fuels, and to be modified quickly as the fuel availability situation changes (coal, oil, gas, etc.), makes it an attractive power conversion system for today's market place.

The emphasis in this lecture, is of course, on large closed-cycle gas turbines, and this is meant to imply the nuclear gas turbine. To complete the background in the field of closed-cycle gas turbines other applications should be mentioned. Possible future application of the CCGT for fast breeder and fusion reactor plants are discussed in Refs. 2.66-2.69, space power systems (Ref. 2.70-2.72), solar plant (Ref. 2.73), marine power plants (Refs. 2.74-2.77), vehicular use (Ref. 2.78), and a new emerging application that of LNG vaporization (Ref. 2.79). A further application of small CCGT (utilizing a fluidized bed coal combustor) for residential complexe's total energy systems has been discussed in Ref. 2.80.

REFERENCES

- 2.1 Ackeret, J., and C. Keller, "An Aerodynamic Power Plant," Revue Polytechnique Suisse, 1939, p 229
- 2.2 Keller, C., "The Esher Wyss - AK Closed-Cycle Turbine, Its Actual Development and Future Prospects," Transactions of the ASME, November 1946.
- 2.3 Keller, C., "Closed-Cycle Gas Turbine, Esher Wyss - AK Development, 1945-1950, Transactions of the ASME, August 1950.
- 2.4 Keller, C., "Operating Experience and Design Features of Closed-Cycle Gas Turbine Power Plants," ASME Paper Number 56-GTP-15.
- 2.5 Robinson, S. T., "The Closed-Cycle Gas Turbine Power Plant," ASME Paper Number 52-A-137.
- 2.6 Keller, C., and W. Gaehler, "The Coal-Burning Closed-Cycle Gas Turbine," ASME Paper No. 61-GTP-2
- 2.7 Harmon, R. A., "Operational Status and Current Trends in Gas Turbines for Utility Applications in Europe," Report prepared for Fossil Energy Organization of U. S. Energy Research and Development Administration, Division of Coal Conversion and Utilization Advanced Power Systems, August 16, 1976.
- 2.8 "Closed-Cycle Gas Turbines for all Fuels: Coal, Oil, Gas, Nuclear," Esher Wyss News, Vol. 39, No. 1, 1966.
- 2.9 Keller, C., and M. Frutschi, "Closed-Cycle Plants - Conventional and Nuclear - Design, Application Operation," Gas Turbine Engineering Handbook, Second Edition, Vol. II, 1972, p265.
- 2.10 Haas, W., and H. Frutschi, "Operating Closed-Cycle Plants," Gas Turbine International, March-April, 1972.
- 2.11 Keller, C., and D. Schmidt, "Industrial Closed-Cycle Gas Turbines for Conventional and Nuclear Fuel," ASME Paper Number 67-GT-10.
- 2.12 Spillman, W., "The Closed-Cycle Gas Turbine for Non-Conventional Applications," ASME Paper No. 66-GT/CLC-8.
- 2.13 Deuster, G., "Long-Time Operating Experience with Oberhausen I Closed-Cycle Gas Turbine Plant," ASME Paper Number 70-GT-73.
- 2.14 Bamment, K., J. Rurik, and H. Griepentrog, "Highlights and Future Development of Closed-Cycle Gas Turbines," ASME Paper Number, 74-GT-7.

2.15 Bammert, K., and G. Groschup, "Status Report on Closed-Cycle Power Plants in the Federal Republic of Germany," ASME Paper No. 76-GT-54.

2.16 Bammert, K., "A General Review of Closed-Cycle Gas Turbines Using Fossil, Nuclear and Solar Energy," ISBN 3-521-06101-9, Verlag Karl Thiemig, Munich, Germany, 1975.

2.17 La Fleur, J. K., "The Use of Turbomachinery in the Field of Cryogenics," Gas Turbine Engineering Handbook, Vol. II, 1972, p296.

2.18 La Fleur, J. K., "Description of an Operating Closed-Cycle Helium Gas Turbine," ASME Paper No. 63-AHGT-74.

2.19 "The La Fleur Process Turbine," Gas Turbine July-August, 1963.

2.20 Zenker, P., "The Oberhausen 50 MW Helium Turbine Plant," Combustion, April 1976, p21.

2.21 Bammert, K., and G. Deuster, "Layout and Present Status of the Closed-Cycle Helium Turbine Oberhausen," ASME Paper No. 74-GT-132.

2.22 Griepentrog, H., "First Closed-Cycle Helium Turbine," Diesel and Gas Turbine Progress, March 1975.

2.23 Jeffs, E., "District Heating Plant Tests Future Nuclear System," Energy International, March 1975.

2.24 Bammert, K., G. Krey, and R. Krapp, "Operation and Control of the 50 MWe Closed-Cycle Helium Turbine Oberhausen II," ASME Paper No. 74-GT-13.

2.25 Janis, J. M., G. S. Braun, and R. D. Ryan, "Performance Testing of the Compact APCSE Closed Brayton Cycle System," ASME Paper No. 67-GT-34.

2.26 Bailey, J. A., F. D. Jordan and C. A. Kinney, "Status of the Army Closed Brayton Cycle Gas Turbine Program," ASME Paper No. 67-GT-13.

2.27 Weber, D., "Total Energy Applications for Closed-Cycle Gas Turbines," Paper presented at International Total Energy Congress, Copenhagen, Denmark, October 4, 1976.

2.28 Mason, J. L., "Working Fluid Selection for Closed Brayton Cycle," presented at the Sixth AGARD Combustion and Propulsion Colloquim, Cannes, France, March 1967.

2.29 Bammert, K., and R. Klein, "The Influence of He-Ne, He-N₂, and He-CO₂ Gas Mixtures on Closed-Cycle Gas Turbines," ASME Paper No. 74-GT-124.

2.30 Melese-d'Hospital, and P. Fortescue, "Thermodynamic Comparison of Gas Coolants for Nuclear Reactors," Proc. Instn. Mech Engrg. 1966-1967.

2.31 Senoo, Y., "Gas Medium Selection and Turbomachinery Matching for Closed Brayton Cycle System," ASME Paper Number 63-WA-86.

2.32 Robinson, S. T., "Influence of Working-Fluid Characteristics on the Design of the Closed-Cycle Gas Turbine," ASME Paper No. 57-GTP-13.

2.33 Ainley, D. G., and J. F. Barnes, "An Assessment of the Component Sizes of Nuclear Closed-Cycle Gas Turbines Using Argon and Helium," Proc. Instn. Mech. Engrg., Vol. 181, 1966-67.

2.34 Osterle, F., and K. Teranasthiarphan, "A Thermodynamic Assessment of Carbon Dioxide as a Working Fluid in Closed Gas Turbine Cycles," Paper 759163, Tenth Intersociety Energy Conversion Engineering Conference, Newark, Delaware, August 1975.

2.35 Smith, S. C., A. H. Fox, R. T. Sawyer, and H. R. Austin, "Applied Atomic Energy," Prentice Hall, New York 1946.

2.36 Fortescue, P., "Tomorrow's Plant: Gas Turbine, Nuclear Power, Dry Cooling," Power Engineering, August 1971.

2.37 "Nuclear Gas Turbines," Proceedings of the International Conference organized by The British Nuclear Energy Society in London, April 8-9, 1970.

2.38 Twardziok, W., "Calculation and Design of Closed-Cycle Helium Turbines for High Temperature Reactors," Lecture Series 24, Closed-Cycle Gas Turbines, Von Karman Institute, Brussels, Belgium, May 11-15, 1970.

2.39 Keller, C., "The Use of the Closed-Cycle Helium Gas Turbine in Atomic Power Plants," Esher Wyss News Vol. 39, No. 1, 1966.

2.40 Bammert, K., "Nuclear Power Plants with Closed-Cycle Helium Turbine for Industrial Energy Supply," ASME Paper No. 70-GT-93.

2.41 Bammert, K., H. H. Finckh, and M. O. Trackler, "Nuclear Gas Turbine of Large Output for HHT-Plants," ASME Paper No. 74-GT-140.

2.42 Bammert, K., and E. Bohm, "Nuclear Power Plants with High Temperature Reactor and Helium Turbine," ASME Paper No. 69-GT-43.

2.43 Taygun, F., and H. U. Frutschi, "Conventional and Nuclear Gas Turbines for Combined Power and Heat Production," ASME Paper No. 70-GT-22.

2.44 Burylo, P., "The Main Features of Direct Cycle Helium Gas Turbines Integrated with a High Temperature Reactor," paper presented at International Nuclear Industries Fair, Basel, Switzerland, October 1972.

2.45 Bammert, K., and J. Rehbach, "Gas Turbine for a Nuclear Power Plant," Atomkernenergie (ATKE) Bd. 18 (1971) Lfg. 2.

2.46 Endres, W., "Large Helium Turbines for Nuclear Power Plants," ASME Paper No. 70-GT-99.

2.47 Haselbacher, H., and A. Eiermann, "Development of Helium Gas Turbine Systems in the Nuclear Field," ASME Paper No. 74-GT-123.

2.48 Shepherd, L. R., and G. B. Lockett, "Direct Cycle Application of High Temperature Gas Cooled Reactors," ENEA Symposium on the Technology of Integrated Primary Circuits for Power Reactors, Paper EN-1/40, Paris, May 1968.

2.49 Hurst, J. N., and A. W. T. Mottram, "Integrated Nuclear Gas Turbines," Paper EN-1/41. Ibid.

2.50 Hodzic, A., D. Haferkamp, H. Arndt, and F. Endress, "Reference Design of the (European) HTGR Nuclear Gas Turbine Power Plant," Paper presented at European Nuclear Conference, Paris, April 1975.

2.51 Krase, J. M., J. W. Holland, E. Arndt, H. Kramer, H. V. Schenkler, and B. Sarlos, "The Development of the HTGR Direct Cycle," paper presented at a Symposium on Gas-Cooled Reactors with Emphasis on Advanced Systems, Julich, Germany, October 1975.

2.52 Hodzic, A., D. Haferkamp, and K. U. Schneider, "Design Concept of the 3 x 360 MWe HHT Reference Nuclear Power Plant," Ibid.

2.53 Noack, G., J. Terkessidis, and P. Zenker, "Significance of the Helium Turbine Power Plant at Oberhausen (EVO) and of the High-Temperature Helium Test Facility at Julich (HHV) for the Development of the HTR Direct-Cycle System (HHT)," Ibid.

2.54 Keller, C., "Small Reactors and Helium Turbines Equals Near Term Energy Savings," Mechanical Engineering, September 1976.

2.55 Yampolsky, J., et al, "Steam Turbine Driven Circulators for High-Temperature Gas Cooled Reactors, Part I: Design," ASME Paper Number 72-WA/NE-20.

2.56 Barbat, V.J., et al, "Steam Turbine Driven Circulators for High-Temperature Gas Cooled Reactors, Part II: Development," ASME Paper Number 72-WA/Ne-21.

2.57 Cavallaro, L., and J. Yampolsky, "Design and Development of a Steam Turbine Driven Circulator for High Temperature Gas Cooled Reactors," Nuclear Engineering and Design, 26 (1974) pp135-157.

2.58 Yampolsky, J., "Circulators for Helium Cooled Reactors," Nuclear Engineering International, December 1972.

2.59 Oakes, E., "The Design of Gas Cooled Reactor Circulators," Paper presented at ASME-ANS Conference on Advanced Nuclear Energy Systems, Pittsburgh, March 14, 1976.

2.60 Bomelburg and Schuetzendorf, "Operating Experience with Steam Generators in Gas-Cooled Reactors," Paper presented at ANS Winter Meeting, Washington, D.C. 1974.

2.61 Hunt, P., et al., "Design of Steam Generators for Large HTGR Plant," Sulzer Technical Review "Nuclex 75," Basel, Switzerland.

2.62 Schuetzendorf, W. G., et al., "HTGR Steam Generator Development," Paper presented at ASME/ANS International Conference on Advanced Nuclear Energy Systems, Pittsburgh, 1976.

2.63 Schuetzendorf, W. G., "Design Details of Steam Generator for 330 MWe HTGR Power Plant," Energie, April 1970.

2.64 Quade, R. N., et al., "Design of Fort St. Vrain Steam Generators, Paper presented at ASME Winter Annual Meeting, November 1971.

2.65 Schuetzendorf, W. G., and P. Hunt, "Review of Design Criteria for Steam Generator of HTGR for PSC of Colorado," ASME Paper No. 69-WA/Pwr-5.

2.66 Melese d'Hospital, G., and P. Fortescue, "Fast Breeder Reactors with Direct Gas Turbines," ASME Paper No. 69-WA/NE-17.

2.67 Forster, S., "The Closed Helium Turbine Cycle with a Fusion Reactor as Energy Source," ASME Paper No. 72-WA/Ener-10.

2.68 Fraas, A. P., "Problems in Coupling a Gas Turbine to a Thermonuclear Reactor," ASME Paper 72-GT-98.

2.69 Kuo, S., "A Conceptual Design Study of Closed Brayton Cycle Gas Turbine for Fusion Power Generation," Paper presented at 11th Intersociety Energy Conversion Engineering Conference, Lake Tahoe, Nevada, September, 1976.

2.70 Pietsch, A., "Solar Brayton-Cycle Power System Development" AIAA Paper 64-726.

2.71 Mock, E. A., "Closed-Brayton Cycle System Optimization for Undersea, Terrestrial, and Space Applications," Lecture Series 24, Closed-Cycle Gas Turbines, Von Karman Institute, Brussels, Belgium, May 11-15, 1970.

2.72 Gable, R. D., and H. J. Lloyd, "Space Power Applications of the All Purpose Mini Brayton Rotating Unit," Paper 759161, 10th Intersociety Energy Conversion Engineering Conference, Newark, Delaware, August, 1975.

2.73 Palmer, H. B., "Solar Farms Utilizing Low Pressure Closed-Cycle Gas Turbines," Paper 749006, 9th IECEC Conference, San Francisco, California, August 1974.

2.74 Pietsch, A., "Potential Application for Closed Cycle Gas Turbines," Paper 749087, Ibid.

2.75 Dobler, F. X., and R. A. Rackley, "Closed Gas Turbine Marine Power Systems," Paper 759160, 10th IECEC Conference, Newark, Delaware, August, 1975.

2.76 Gathy, B. S., "A Marine Nuclear Power Plant Design Utilizing the Direct Brayton Cycle," ASME Paper No. 70-GT-3.

2.77 "Closed-Cycle Gas Turbine Engines," Automotive Engineering, November 1975.

2.78 Pietsch, A., and R. A. Rackley, "400 HP Closed Gas Turbine Bus Engine," Paper presented at 8th IECEC, Philadelphia, August 1973.

2.79 Griepentrog, H., and P. Sackarandt, "Vaporization of LNG with Closed-Cycle Gas Turbines," ASME Paper No. 76-GT-129.

2.80 Fraas, A.P., "Small Coal Burning Gas Turbine for Modular Integrated Utility System," Paper 749017 presented at 9th IECEC Conference, San Francisco, Aug. 26, 1974.

3.0 NUCLEAR GAS TURBINE INCENTIVES AND BENEFITS

3.1 Incentives and Motivation

As mentioned in the previous section utilization of a closed-cycle gas turbine power conversion system was recognized at the conception of gas cooled reactor for electrical power generation. However, it was felt that with the gas cooled reactor still in its infancy, it would take an extensive and very costly development program to establish the viability of both a new heat source and power conversion system. Accordingly, gas cooled reactor technology was pursued with a conventional steam cycle plant, and at the time this reached commercialization, studies were initiated to explore the potential of combining an existing HTGR core with a closed-cycle helium gas turbine power conversion system which operates on the same helium used as the reactor coolant. Many publications have documented the merits of the high temperature gas-cooled reactor, and Ref. 3.1 through 3.9 are included to cover the helium-cooled family of reactors. From Fig. 3.1 it can be seen that the closed-cycle gas turbine is adaptable to the HTGR, Gas Cooled Fast Breeder (GCFR), and Fusion nuclear reactors, with helium as the coolant. While this presentation concentrates on the HTGR application, the adaptability of the closed-cycle gas turbine to advanced helium cooled power systems of the future is emphasized, and this can be considered a major incentive for its development. An initiation of activities in the U.S. on the GT-HTGR plant is discussed in Ref. 3.10.

To date the steam turbine system has wholly dominated the field of central station power production, and this of course also includes all nuclear plants thus far built or under construction. Modern steam plants operate with a maximum steam temperature of around 1000°F (538°C) and for both fossil-fired and HTGR plants the overall station efficiency is close to 40 percent. Stress levels and metallurgical considerations in the steam turbine tend to limit temperature growth for the Rankine power conversion system, and higher efficiencies can only be realized with more complex cycles.

In practice the only effective competition for the steam turbine in the large power field is, of course, the gas turbine, and more particularly the closed-cycle gas turbine, for without the aid of pressurization the necessary turbine machinery and duct sizes needed limit the usefulness of the open cycle to about 100 MWe at today's level of turbine inlet temperature for long-life industrial units. Comparisons between the steam cycle and two variants of the closed-cycle gas turbine are shown on Fig. 3.2. In the case of the Rankine cycle the 1000°F (538°C) can be achieved in the HTGR steam plant with helium temperatures of no more than 1300°F

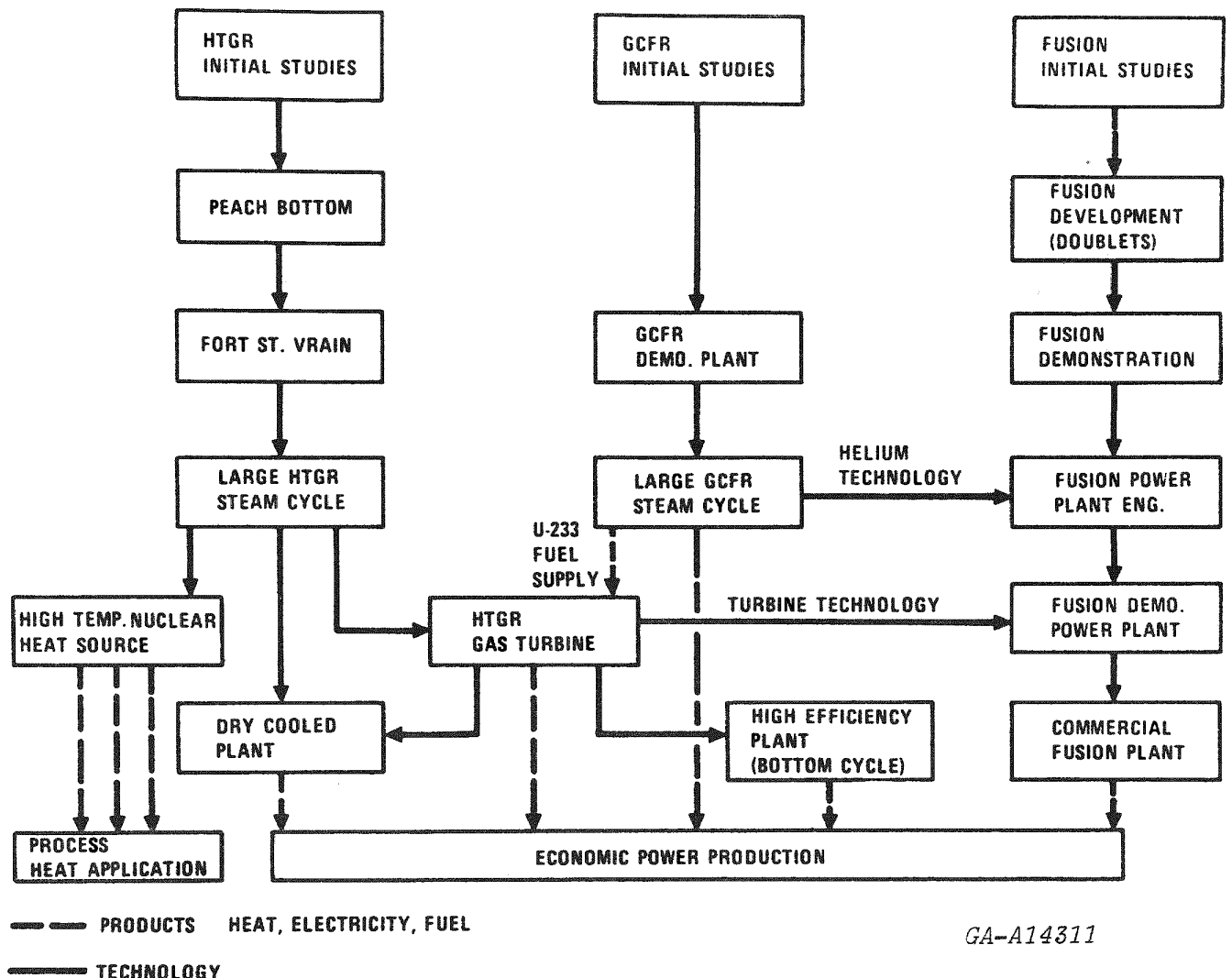


Fig. 3.1. Helium-Cooled-Reactor Economy

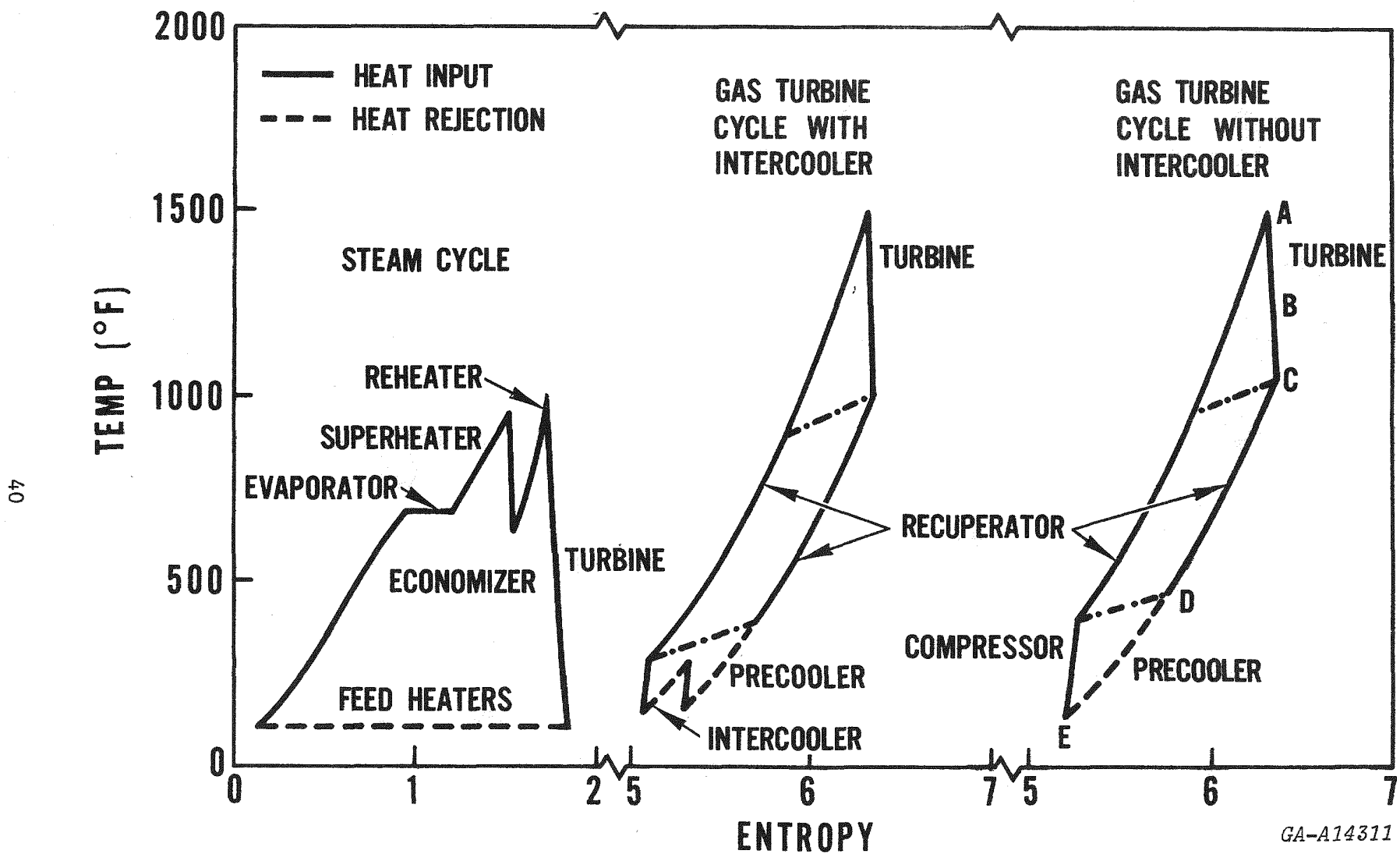


Fig. 3.2 Comparison of Steam and Gas Turbine Plant Cycles

(704°C) to 1400°F (760°C). Further reductions in steam generator surface by utilizing higher helium temperatures would be offset by increased cost for the resulting specialty alloys. The essential point here is that this step far from fully exploits the inherent capabilities of the all-graphite type of core which principally characterizes the HTGR. The interest in the GT-HTGR is rooted, not in the desire to marginally improve and thereby outmode a presently viable steam system, but rather to exploit as yet unrealized capabilities of the HTGR.

The advent of a nuclear reactor capable of direct input of heat at the 1500°F (816°C) to 2000°F (1093°C) level into an inert gas coolant is an event for which the development of the closed-cycle gas turbine has awaited many years, for the problem of the high temperature exchanger needed by fossil fueling has limited the potential of the closed Brayton cycle.

A key feature of the closed-cycle gas turbine is the high density of the working fluid at the turbine exit that is achieved by appropriate pressurization. This is typically at least two orders of magnitude higher than that for a steam turbine, which must exhaust into a vacuum. The important point is that exhaust density largely governs the size of the machinery and associated piping, leading to expectation of cost and space savings for the gas turbine and, incidentally, escape from the maximum unit power limitation that the steam turbine's bulk imposes.

Another striking feature of the gas turbine is the smallness of the necessary expansion ratio involved, this being about 2.5 to 1 (for helium) as opposed to about 2500 to 1 for the steam cycle. The significance here is that the need to provide for the corresponding huge range of volumetric flows that the steam turbine must pass is a design handicap from the standpoints of both efficiency and of economy of material utilization. By avoiding need for extreme range of blade lengths and moisture content effects, the gas turbine can maintain a high stage efficiency throughout the necessary expansion with substantial benefit to overall adiabatic efficiency. Because extremely large exhaust end bulk is not needed a much more compact turbine is possible.

Another merit of the gas turbine sometimes overlooked is the very considerable reduction in needed auxiliary equipment. All the complex hardware represented by the pipes, valves, and instrumentation associated with water treatment, boiler feed pumps, the entire reactor coolant circulation system, is eliminated, affecting not only just cost but also operation, maintenance, and space requirements. This gain in simplicity, it need hardly be said, is of particular welcome in nuclear plants.

An argument often used against the gas turbine cycle, on the other hand, is that the absence of a phase change in the working fluid entails use of very large internal power recirculation, represented by a compressor power far in excess of that for the corresponding feed pumps of the Rankine cycle. In fact, the penalty of providing the large recirculation power is outweighed by the total benefit of the higher top temperatures available to the gas turbine and the high compressor and turbine stage efficiencies that are possible.

A feature of the closed-cycle gas turbine plant, sometimes cited as a thermodynamic disadvantage, is that its heat rejection occurs over a range of temperatures, (as shown in Fig. 3.2) rather than at the one temperature of a condensing vapor. This of course does represent a departure from one of the criteria for the most efficient possible thermodynamic cycle, but in return the higher average temperature of heat rejection can greatly ease the practical problem of reject heat dissipation. Indeed a higher mean rejection temperature can become a valuable asset when a premium is placed on the temperature level of the waste heat, as when there is an industrial use (district heating, for example) or when direct air cooling is contemplated. The well-known merits of the high reject temperature from a closed-cycle gas turbine have been expounded extensively in the open literature and will not be reiterated here.

The use of waste heat, which will be covered in detail later in this presentation, from the GT-HTGR plant is in the form of a secondary power cycle for the further production of electric power, whereby overall plant efficiencies in the range of 50% can be realized without the necessity for the extensive development involved in exploiting still higher initial temperatures, and without departure from traditional electric generation means.

The essential point relating to dry cooling results from the fact that the gas turbine naturally rejects its heat over a wide band of temperatures, for the heat is derived from the sensible, rather than the latent, heat of the single phase working fluid. Thus, when a high effectiveness recuperator is used, without intercooling as presently proposed for the reference plant design, the heat is in fact rejected over a range of temperatures about equal in width to the compressor temperature rise. This is about an order of magnitude higher than permissible condensate temperature use, and it follows then that dry towers for a gas turbine plant could be designed for about a tenth of the airflow needed for the alternative steam plant, with correspondingly some ten times the air circulation heat available from a given natural circulation tower height, or for a given fan power in the case of forced circulation.

Either case would therefore yield as additional bonus a some three fold increase in available air velocity to aid heat transfer and further reduce the size. In practice, it is more economic to apply only some of the advantage to air flow reduction, using the rest to provide larger effective temperature differentials to further reduce necessary cooling surface area.

Fig. 3.3 illustrates a typical overall result in terms of the skyline profile of three alternative nuclear plants of approximately the same power, drawn to the same scale. The one uses a gas turbine and dry air cooling, and the other two use steam turbines, with dry and wet air cooling, respectively. Compared with the gas turbine, the dry-cooled steam system employs about four times the total heat transfer surface area and needs about seven times the total air flow. An appreciation of the tower sizes for the gas turbine and steam cycle HTGR plants can be seen on Fig. 3.4.

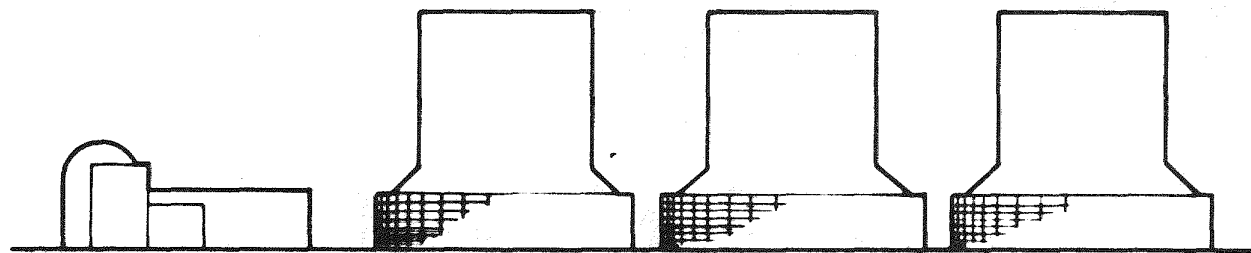
3.2 Gas Turbine HTGR Plant Benefits

The GT-HTGR offers major improvements in plant simplification, capital cost, efficiency, and waste-heat rejection. Heat rejection is either by economical dry-cooling towers or, optionally, by a low-temperature secondary power cycle (GT-HTGR binary-cycle plant) that generates additional power. At 1652°F (850°C) turbine inlet temperature the dry-cooled plant will have 40% efficiency and the binary-cycle plant 48%. For an advanced version of the plant, with further development to 1742°F (950°C) turbine inlet temperature dry-cooled and binary plant efficiencies increase to 43% and 51%, respectively. The GT-HTGR plant benefits are summarized on Table 3.1, and briefly discussed below.

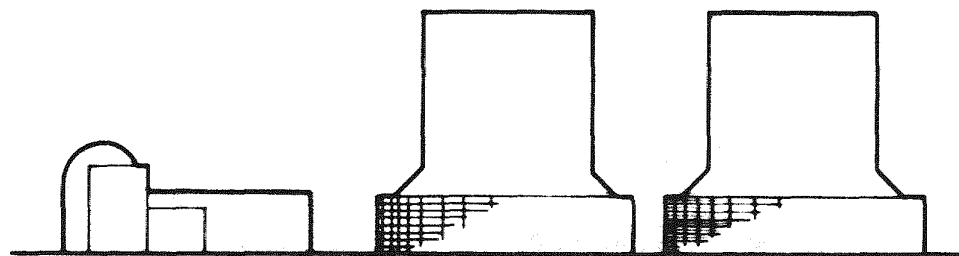
3.2.1 Low Power-Generation Cost

Substantially reduced power generation costs for the GT-HTGR were indicated in the recent ERDA assessment of gas-cooled reactors (Ref. 3.11). Data from this assessment quantifies the advantage as a 12% reduction in capital cost as compared with twin wet-cooled PWRs of the same reactor core thermal power. When the GT-HTGR is compared to the PWR, both dry-cooled and at equal thermal powers, power generation cost of the PWR has been estimated to be 26% greater than that of the GT-HTGR. Advantages are predicted for the GT-HTGR in fuel cost, operating and maintenance cost as well as in capital cost.

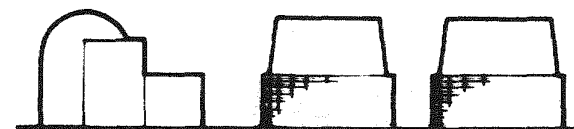
The cost savings projected for the GT-HTGR are due largely to high efficiency and heat rejection temperature plus simplified plant layout. The plant is simpler because the steam turbine plant with its complex auxiliary equipment



STEAM CYCLE
LOW EFFICIENCY (LIGHT WATER REACTOR)



STEAM CYCLE
HIGH EFFICIENCY (HTGR)

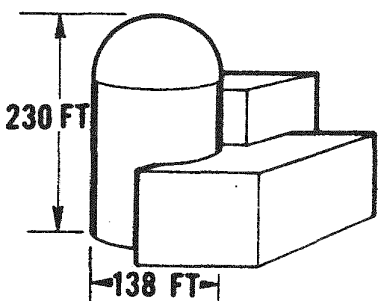


GAS CYCLE
HIGH EFFICIENCY (HTGR)

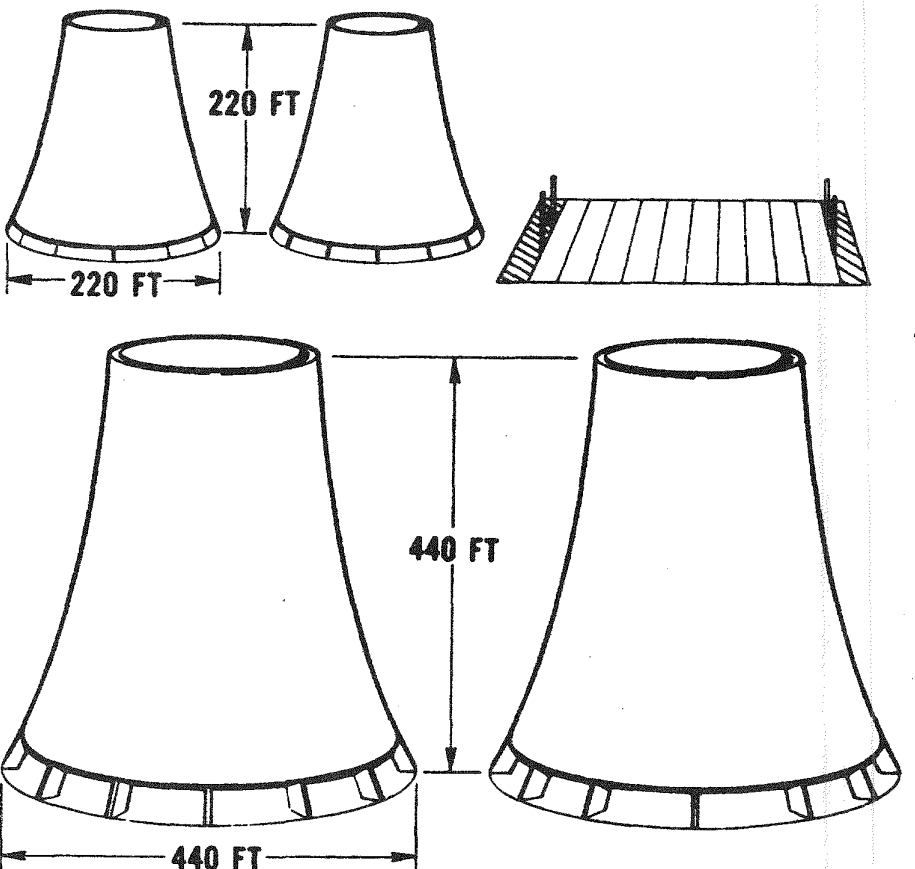
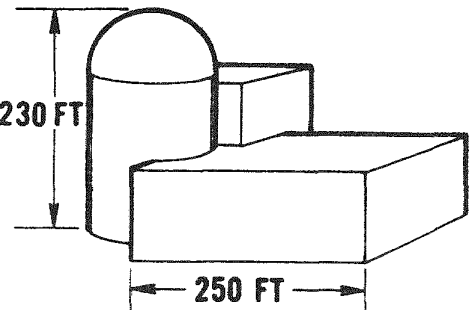
GA-A14311

Fig. 3.3 Simplified Comparison of Steam Cycle and Gas Turbine Plant Skyline Profiles

GAS TURBINE CYCLE



STEAM CYCLE



GA-A14311

Fig. 3.4 1200 MW(e) HTGR Power Plant Size Comparison

TABLE 3.1
GAS TURBINE HTGR BENEFITS

- REDUCED POWER COSTS
- HIGHER RELIABILITY AND AVAILABILITY
- FLEXIBILITY IN PLANT SITING
- MINIMUM ENVIRONMENTAL IMPACT
- INHERENT SAFETY
- CONSERVATION OF RESOURCES
- HIGH COST-BENEFIT
- APPLICATIONS OF REJECT HEAT
- TRANSFER OF TECHNOLOGY

GA-A14311

is completely eliminated. The simplicity of the overall plant arrangement is shown in the artist's conceptual rendition of the GT-HTGR on Fig. 3.5. High optimum heat-rejection temperatures and high efficiency will yield significant cost savings in the dry-cooling tower systems.

3.2.2 High Reliability and Availability

Plant simplicity resulting from the elimination of many systems upon which the steam-cycle plant depends, together with utilization of lower temperature heat exchangers in the power conversion system, engenders the GT-HTGR with improved reliability. The ERDA-109 Report (Ref. 3.12) evaluates the GT-HTGR system above LWRs on the basis of gas-cooled reactor availability records in the United Kingdom (>80%) and the excellent availability record for closed-cycle gas turbines in Europe discussed earlier (>90%).

3.2.3 Flexibility in Plant Siting

A dry-cooled GT-HTGR plant can be sited independent of large sources of water because of economical dry cooling. As mentioned above, this economy is the natural consequence of a closed-cycle helium turbine power conversion system since waste heat is rejected normally at temperatures much higher than in a condensing steam cycle and therefore smaller dry cooling towers are possible.

3.2.4 Inherent Safety

The well-known safety advantages of the HTGR are manifest in the GT-HTGR. A major objective in the development of the HTGR was to attain a high degree of inherent safety, minimizing the need for engineered safety features. Inherent safety features include:

- o The use of thorium mixed with uranium as a fuel, which provides a built-in automatic temperature control. As the temperature increases, the rate of fission promptly decreases.
- o The use of a large mass of graphite as the moderator, ensuring that the effects of any sudden changes in temperature in the core will be slow and readily controllable. The HTGR graphite core can absorb roughly 20 times as much heat per degree of temperature rise as can the LWR cores.
- o The use of helium as the coolant means reactivity does not respond to changes in coolant density. This makes for inherently easier control.
- o Adoption of an integrated plant arrangement as shown on Fig. 3.6 in which the entire reactor coolant system, as well as the power conversion loop, is enclosed within the prestressed concrete reactor vessel (PCRV), eliminating the possibility of a rupture in external coolant piping and of any sudden loss of primary coolant.

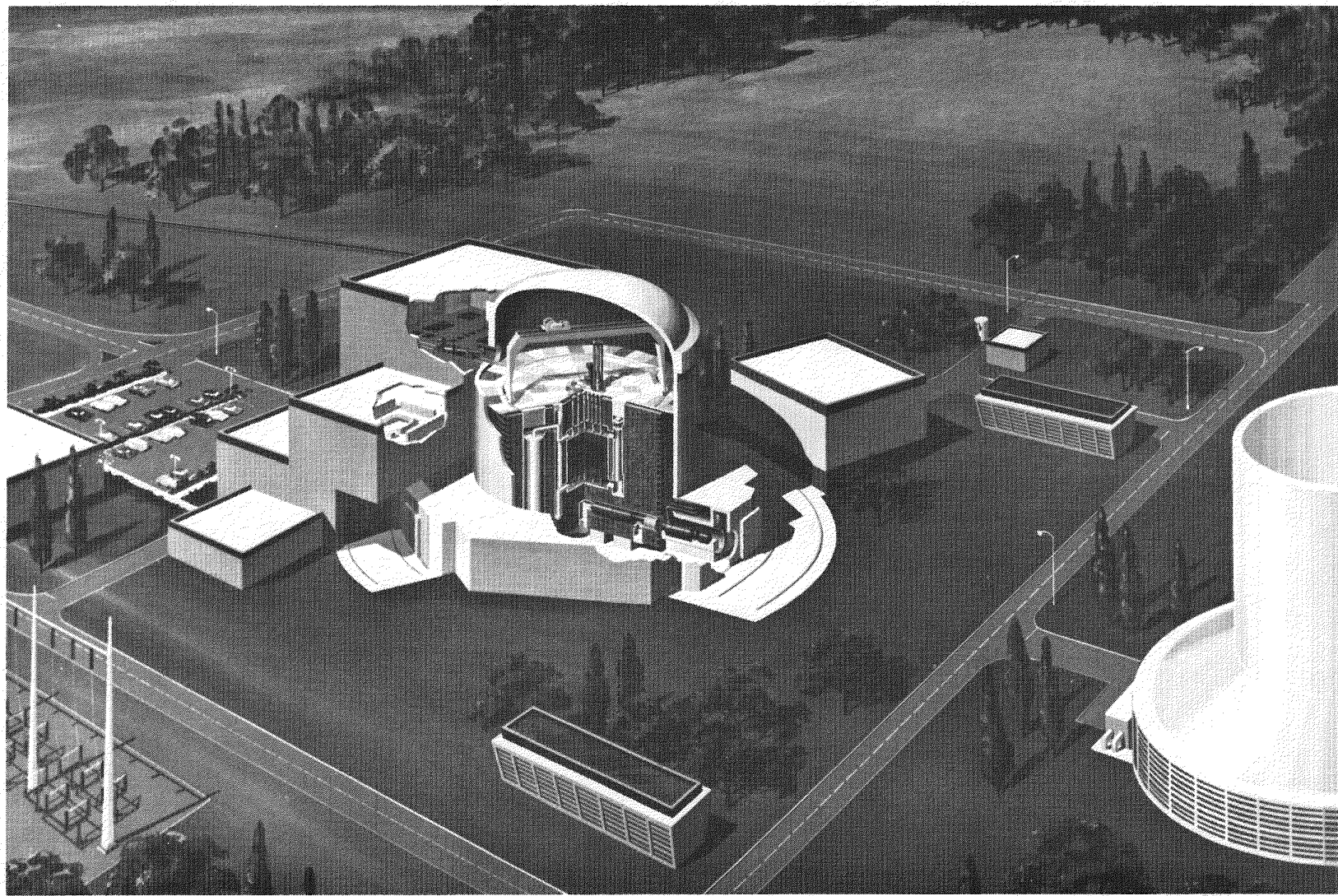


Fig. 3.5 Overall Concept of GT-HTGR Power Plant with Dry-Cooling *GA-A14311*

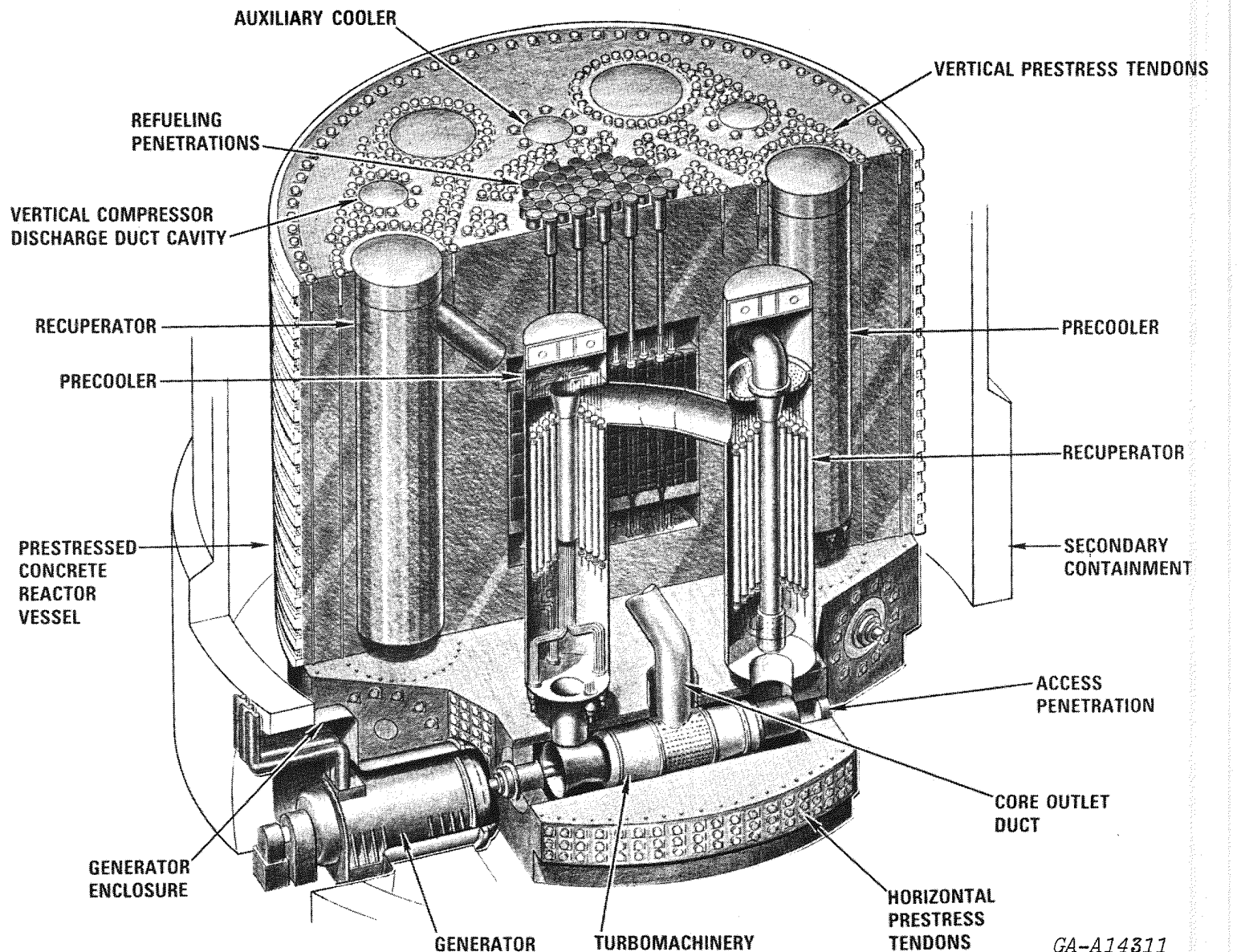


Fig. 3.6 3 Loop 3000 MW(t) GT-HTGR Power Plant

GA-A14311

In addition to the above inherent safety features, the GT-HTGR includes a number of engineered design features including (1) a core auxiliary cooling system (CACS) as an independent back-up, and (2) a reserve shutdown system independent of the normal control rod system.

3.2.5 Minimum Environmental Impact

Because of the GT-HTGR high efficiency the high heat-rejection temperatures, dry-cooling tower size will be minimal and will have less impact on the environment than dry-cooled LWRs. Microclimatic perturbations will be minimized because the amount of heat rejected will be reduced by about one-half. Dry-cooling towers have no moisture plume normally associated with wet-cooling towers. Dry-cooling consumes essentially no water. If water cooling is available, a secondary power cycle can be added to the GT-HTGR to yield efficiencies approaching 50%, while using only about one-half the water an LWR uses. The GT-HTGR's helium coolant, combined with installed trapping devices, results in exceptionally low radioactive releases to the atmosphere. Solid and liquid wastes are also minimal, and these are not released to the environment but are packaged for offsite disposal.

3.2.6 Conservation of Resources and High Cost Benefit

Both the high-fuel conversion ratio and high-net station thermal efficiency of the GT-HTGR offer substantial conservation of U_3O_8 . For example, the GT-HTGR with 48% efficiency that could be commercially introduced in 1995 would conserve one million short-tons of U_3O_8 compared to an all-LWR scenario under the base case assumptions used in ERDA-1535 for power growth and U_3O_8 cost. The U_3O_8 savings plus capital savings translate into a present worth benefit in excess of \$20 billion, using a 7.5% discount rate.

Water, another vitally important natural resource, needs to be conserved. In Northern California two winters with substantially less than average rainfall has resulted in a strain on limited water supply, which points to future dry-cooling of power plants. Although all reactor plants can be dry or wet-cooled, low efficiency and low heat rejection temperature LWRs can be so cooled only with a significant economic penalty.

3.2.7 Application of Reject Heat

The reject heat from the GT-HTGR, being on the order of 350°F (177°C), can be effectively utilized to either increase the electrical efficiency of the plant to values approaching 50% with application of a secondary power cycle mentioned above, or to be used directly as heat for such applications as:

- Water Desalination
- District Heating/Air Conditioning
- Low Temperature Process Heat
- Agriculture

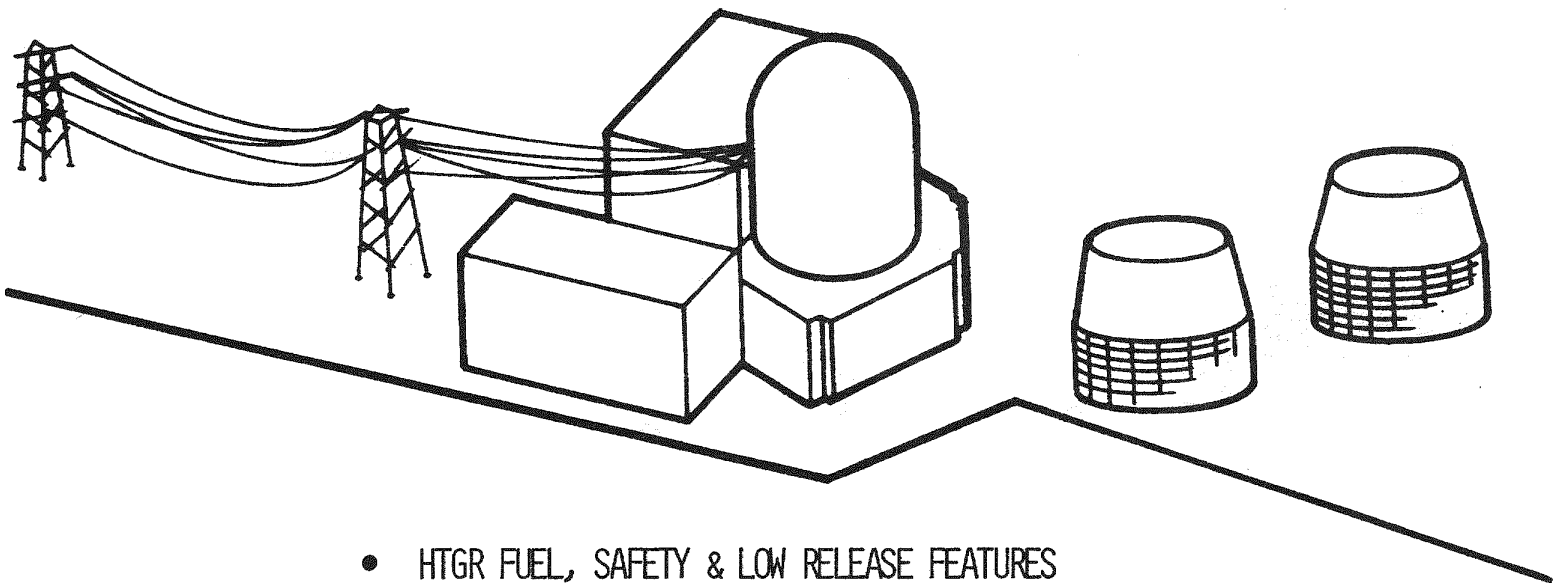
If the waste heat is so utilized, this will subsequently improve still further the overall energy utilization factor and economics of the plant.

3.2.8 Flexibility in Plant Rating

Because a multi-loop primary system approach was selected for the GT-HTGR, variations in plant ratings can be accommodated without additional development. The reference design described in a later section is based on a 3000 MW(t)/1200 MW(e) system containing three power conversion loops each with a rating of 1000 MW(t)/400 MW(e). With a loop rating of 1000 MW(t), plant variants embodying between one and four power conversion loops have been evaluated.

The above benefits for the GT-HTGR plant are summarized in Fig. 3.7 and 3.8 for the dry-cooled and binary plant variants, respectively.

While not strictly classed as a benefit it is worth mentioning that the reference plant design is based on: (1) existing HTGR technology, (2) established industrial gas turbine technology, (3) use of existing materials, and (4) established manufacturing processes. At the beginning of any long-term power generating plant study it is clearly important to be able to project future growth and market needs since these may indeed have a strong influence on the plant design, even at the conceptual stage. Because of the conservative nature of the initial design assumptions for the GT-HTGR, the concept has significant future growth and development potential as outlined on Table 3.2.



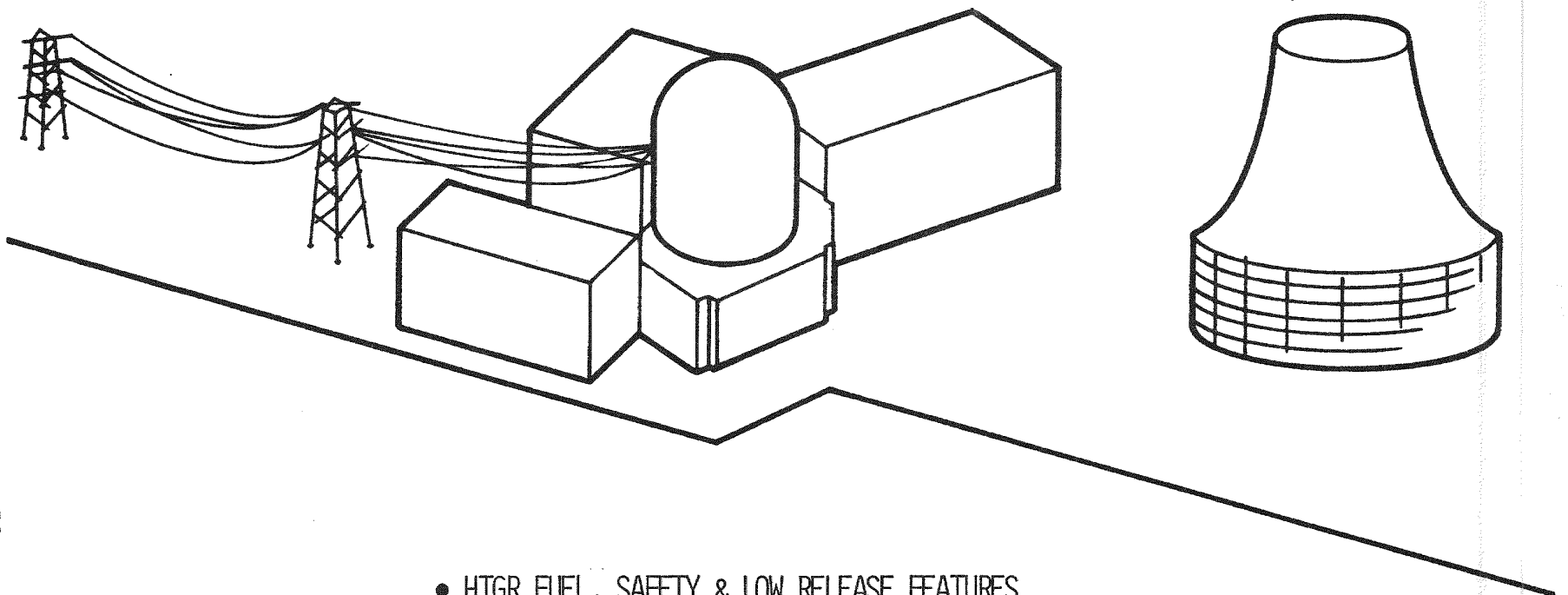
- HTGR FUEL, SAFETY & LOW RELEASE FEATURES
- SIMPLIFIED SYSTEMS BY USE OF GAS TURBINE
- ECONOMICAL DRY COOLED GENERATION
- INCREASED SITING FLEXIBILITY
- ELIMINATES LICENSING & ENVIRONMENTAL PROBLEMS RELATED TO WATER RESOURCES
- CAPACITY

3 LOOP - 1200 MW(E)

4 LOOP - 1600 MW(E)

GA-A14311

Fig. 3.7 GT-HTGR with Dry Cooling



53

- HTGR FUEL, SAFETY & LOW RELEASE FEATURES
- HIGH EFFICIENCY, OUTPUT & ECONOMY
- LESS WATER CONSUMPTION, IMPROVED FUEL UTILIZATION
- CAPACITY

3 LOOP - 1440 MW(E)

4 LOOP - 1920 MW(E)

GA-A14311

Fig. 3.8 GT-HTGR with Binary Cycle

TABLE 3.2

GT-HTGR FUTURE DEVELOPMENT POTENTIAL

- GAS TURBINE HTGR BINARY CYCLE POWER PLANT
- INCREASED TURBINE INLET TEMPERATURE
YIELDING INCREASED PLANT EFFICIENCY
- IMPROVED COMPONENT PERFORMANCE TO
INCREASED PLANT EFFICIENCY
- INTEGRATED INDUSTRIAL/POWER COMPLEX USING
ELECTRICAL AND PROCESS HEAT ENERGY FROM
A GT-HTGR
- GAS TURBINE BREEDER REACTOR (GCFR)
- GAS TURBINE FUSION REACTOR

REFERENCES

- 3.1 Landis, J. W., "The GGA High Temperature Gas-Cooled Reactor: A General Discussion", Journal of the British Nuclear Energy Society, October 1973, Vol. 12, No. 4, p. 367.
- 3.2 Fortescue, P., and H. B. Stewart, "The Role of HTGR's and FBR's in Meeting the Energy Crisis", ASME Paper 72-WA/NE-3.
- 3.3 Fortescue, P., A. J. Goodjohn, and G. Melese-d'Hospital, "Developments of Helium-Cooled Reactor Systems", Paper presented at the ANS topical meeting on Advanced Reactors, Atlanta, Georgia, September 1974.
- 3.4 Simnad, M., and G. Melese-d'Hospital, "Prospects for Helium-Cooled Fission and Fusion Reactors in the Developing Countries", Paper presented at Energy for Developing Countries International Congress, Shiraz, Iran, April 1975.
- 3.5 Melese-d'Hospital, G., "The Role of Helium-Cooled Reactors in Meeting the Energy Crisis and Conserving Resources", Paper 749077, 9th IECEC Conference, San Francisco, California, August 1974.
- 3.6 Fortescue, P., "Tomorrow's Plant: Gas Turbines, Nuclear Power, Dry Cooling", Power Engineering, August 1971.
- 3.7 Fortescue, P., "Gas Turbines and Nuclear Power", Combustion, December 1972.
- 3.8 Goodjohn, A. J., and R. D. Kenyon, "The High Temperature Gas Cooled Reactor - An Advanced Nuclear Power System for the 1980's", ASME Paper No. 73-Pwr-8.
- 3.9 Sager, P. H. "Thermal Power Conversion Systems for Fusion Plants", Paper presented at the 10th IECEC Conference, Newark, Delaware, August 1975.
- 3.10 Krase, J. M., D. C. Morse, and T. W. Schoene, "The Direct-Cycle Nuclear Gas Turbine with Economical Dry Air Cooling", Paper presented at the American Power Conference, Chicago, April 18-20, 1972.
- 3.11 "Gas Cooled Reactor Assessment", A. D. Little, Inc., United Engineers and Constructors and S. M. Stoller Corporation. Report prepared for the U.S. Energy Research and Development Administration, August 1976.
- 3.12 "Technical and Economic Assessment of the Direct Cycle Gas Cooled Reactor Plant", Report ERDA-109, September 1975.

4.0 BACKGROUND OF GT-HTGR DESIGN STUDIES

At the onset of the GT-HTGR plant studies in 1971 the HTGR was developed and commercially accepted for use with modern steam plants. Although gas-cooled reactors have, with a few exceptions, been developed for use with steam turbine power conversion systems, the potential benefits for a closed-cycle gas turbine driven by the reactor coolant gas have long been recognized. The interest in the gas turbine plant is rooted, therefore, not in the desire to improve and thereby outmode a presently viable steam system, but rather in exploiting as yet unrealized capabilities of the HTGR; namely, that of higher temperature. Investigations at General Atomic have been aimed at producing the preliminary design, performance, engineering, and economic data needed for assessment of commercial application of gas turbine HTGR power plants in the 1200 MW(e) class.

It is clear that for a new plant of this type all of the performance, safety, and economic goals are not realized with the first conceptual design, and in fact, many iterations are necessary involving strong interaction between systems analysts, plant and component designers, and economic specialists. This portion of the presentation covers (1) thermodynamic cycle selection and performance, and (2) a brief summary of plant configurations which have been evaluated over the last five years, leading to the current plant reference design which will be discussed comprehensively in Section 5.

4.1 Thermodynamic Cycle and Performance

Design of the gas turbine system begins with thermodynamic cycle studies for these essentially dictate the component duties and indicate and guide assessment of available design trade-offs. The steam cycle HTGR has a plant efficiency of 39.5% when wet cooled, this being reduced to about 36.5% for a dry cooled variant. The initial goal of the GT-HTGR plant was therefore to at least match the 36.5% efficiency level, and realize cost savings from (1) the inherent simplicity of the direct cycle and (2) the economic dry cooling potential from the Brayton cycle power conversion system.

In a phased design program the main features of the plant configurations evaluated are shown on Table 4.1. Apart from the Reference Plant, which will be discussed later, it can be seen that plant efficiency has varied from about 35.5% to 36.5%, and performance aspects have been presented previously in References 4.1 through 4.5. It is not the purpose of this presentation to review the performance aspects of these four plants, but rather to briefly outline the rationale behind the selection of the thermodynamic cycle and the major plant primary system parameters.

TABLE 4.1: GT-HTGR CYCLE PARAMETERS

PLANT DESIGN	PHASE 1	PHASE 2	PHASE 3	PHASE 3A	PLANT REFERENCE
					PHASE 3B*
Design Date	1972-3	1973-4	1974-5	1975-6	1976-7
Reference Source	4.1	4.2	4.3	4.4	4.5
Reactor Core Rating, MWe			3000		
Plant Type			Integrated		
Cycle Type			Non-Intercooled		
Heat Rejection			Dry-Cooled		
Turbomachine Orientation	Vertical	Vertical	Horizontal (Radial)	Horizontal (Radial)	Horizontal (Delta)
Heat Exchanger Position	Recuperator in Separate Cavity	Precooler in Separate Cavity	Concentric Arrangement	Recuperator and Precooler in Separate Cavities	Recuperator & Precooler in Separate Cavities
Number of Loops	4	4	3	3	3
Loop Rating, MWe	750	750	1000	1000	1000
Turbomachine Rating, MWe	275	270	360	370	400
Ambient Air Temp, °F(°C)	75(23.9)	75(23.9)	75(23.9)	59(15)	59(15)
Turbine Inlet Temp, °F(°C)	1500(816)	1500(816)	1500(816)	1500(816)	1562(850)
Compressor Pressure Ratio	2.25	2.35	2.35	2.41	2.50
Compressor Inlet Temp, °F(°C)	105(40.6)	95.5(35.3)	95(35.0)	78(25.6)	79(26)
Maximum Pressure, psia(MPa)	1000(6.89)	1000(6.89)	1000(6.89)	1000(6.89)	1150(7.93)
Compressor Efficiency, %	90.0	88.5	89.0	89.0	89.8
Turbine Efficiency, %	90.0	91.0	91.0	91.5	91.8
Generator Efficiency, %	98.0	98.0	98.4	98.7	98.7
Recuperator Effectiveness	0.87	0.89	0.89	0.89	0.898
Plant Power Output, MWe	1097	1078	1069	1097	1200
Plant Efficiency, %	36.5	35.93	35.62	36.6	40.0

GA-A14311

*Cycle parameters and plant layout optimized for minimum power generating cost.

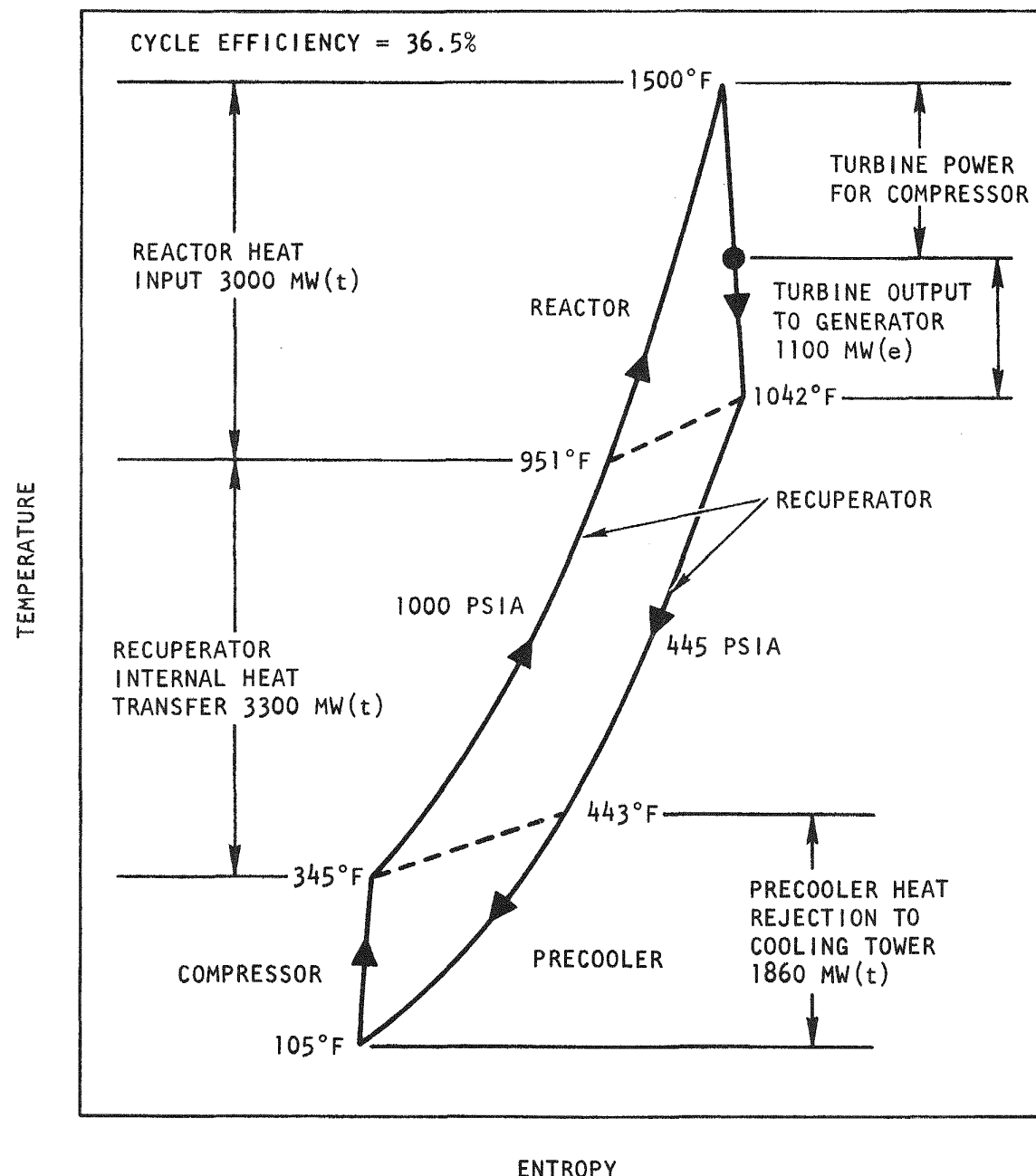
4.1.1 Thermodynamic Cycle

The basic temperature-entropy diagram for the non-intercooled GT-HTGR is shown on Fig. 4.1. Top and Bottom gas temperatures are held fixed, the former by the approximate capability of the HTGR core as presently developed for steam plants, and the latter by the suitability for dry-tower heat rejection. Simplified cycle and loop diagrams for the GT-HTGR are shown on Figs. 4.2 and 4.3, respectively.

The primary fluid heated in the reactor core to 1500°F (816°C) (only slightly higher than temperatures in today's HTGRs) and is then expanded through the turbine. The turbine provides the power necessary to drive the compressor and also drives the electrical generator. At the turbine exit, all useful work has been subtracted from the helium, but it still has a great deal of useful thermal energy. This energy from the turbine exit is transferred via the recuperator to the cooler high-pressure helium before it enters the core. The magnitude of this internal energy transfer within the cycle is of the same order as the reactor thermal input, and this emphasizes the importance of the recuperator in a closed-cycle gas turbine system. At a temperature of over 400°F (205°C) all energy useful to the power cycle has been extracted. The remaining heat to be rejected from the cycle is removed via a water-cooled exchanger (precooler), transported by a circulating water loop, and ultimately rejected to the ambient air through a dry cooling tower. The cooled helium is then compressed back up to the system maximum pressure, becomes the receiver of recuperator heat, and enters the core, thus completing the cycle.

The above discussion is based on the simplest of cycles and precludes utilization of an intercooler. In any operation involving the compression of gases by machines having more than one stage, the efficiency of the process can be increased by cooling the gases between the stages. Non-integrated fossil-fired, closed-cycle gas turbines employ one or more intercoolers between compressor stages, but it was felt that such units would detract from the simplicity and maintainability of an integrated nuclear gas turbine. Studies showed that while the intercooler offers a cycle efficiency advantage of about three percentage points, this advantage appeared to be offset by the added installation complexity of the system. The advantages and disadvantages of intercooling for a nuclear gas turbine are given on Table 4.2.

Diagrams relating pressure ratio and recuperator effectiveness with cycle efficiency (for a given turbine inlet temperature) are shown on Fig. 4.4 for non-intercooled and intercooled variants. Because of the somewhat pessimistic assumptions as regards increased pressure losses (ducts plus intercooler), and the higher compressor inlet temperature associated with an assumed 80% effective intercooler, the increase in efficiency is small. While dependent on an actual plant configuration, it



GA-A14311

Fig. 4.1 GT-HTGR Thermodynamic Cycle

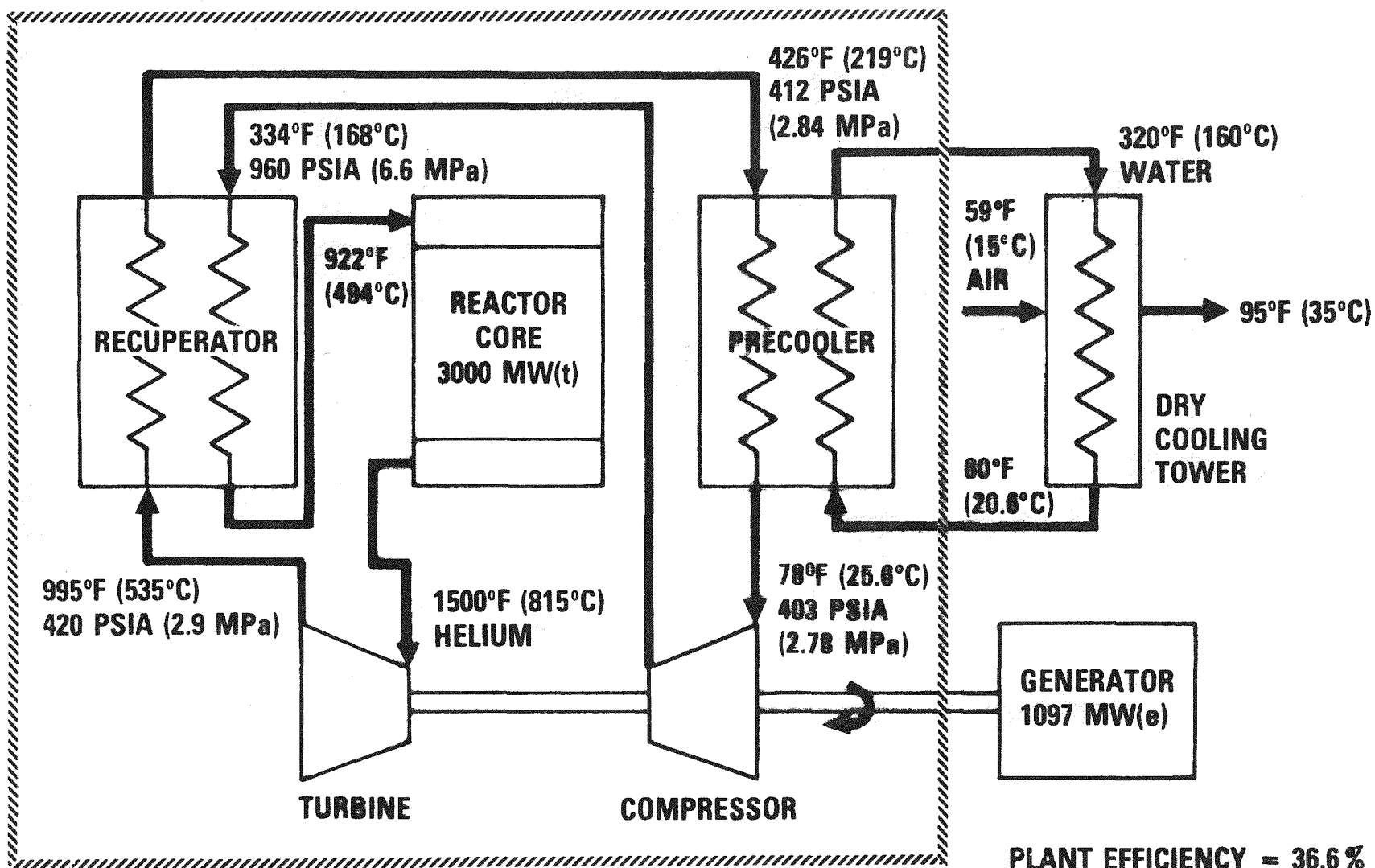


Fig. 4.2 GT-HTGR Cycle Diagram

GA-A14311

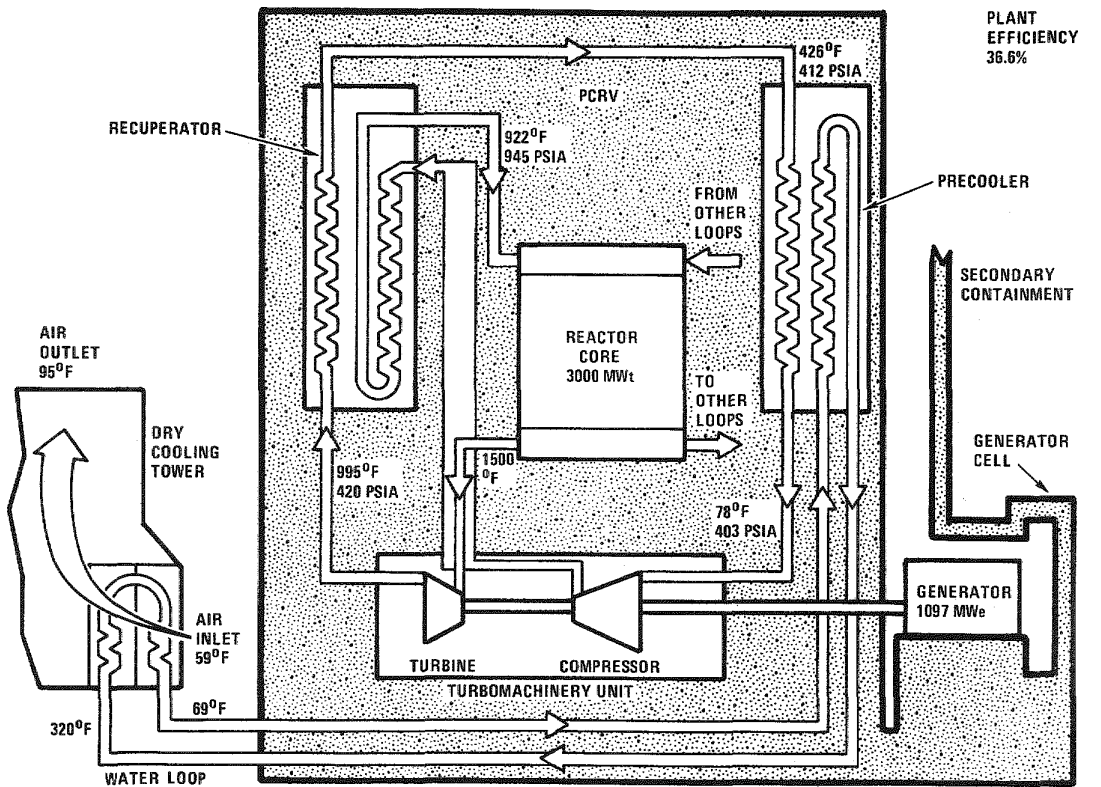


Fig. 4.3 GT-HTGR Loop Cycle Diagram

GA-A14311

TABLE 4.2: INTERCOOLING FOR THE GT-HTGR PLANT

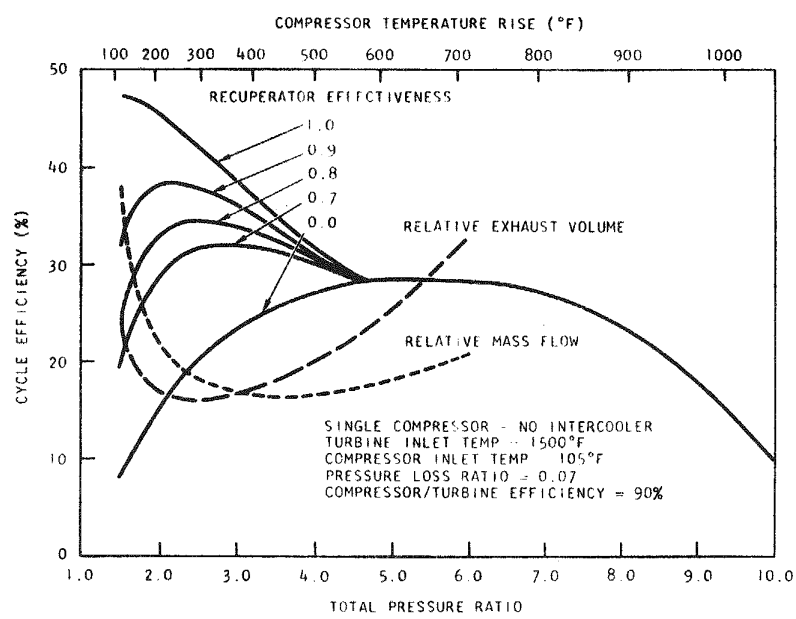
ADVANTAGES

1. Potential increase in Cycle Thermodynamic Efficiency.
2. Reduced helium mass flow rate (smaller components).
3. Cooler high-pressure gas available for cavity liner cooling.
4. Possible use as emergency coolers (decay heat).
5. Reduces precooler thermal duty.
6. Utilizes experience of all of the small (non-integrated) fossil-fired closed-cycle gas turbines in Europe.

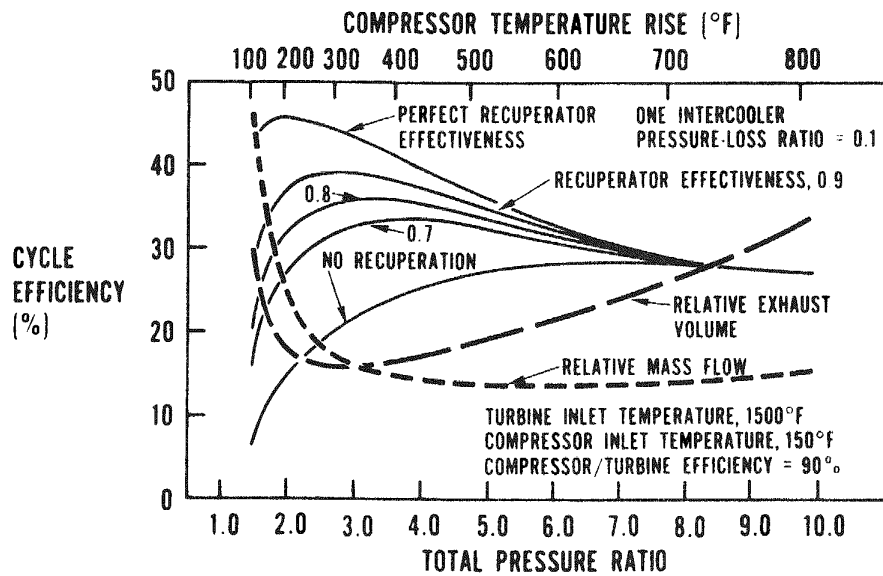
DISADVANTAGES

1. Added complexity to integrated primary system.
2. Added pressure losses tend to negate increased thermodynamic efficiency.
3. More complex turbomachine (added bearings, service systems, and longer shaft).
4. Increased plant maintenance.
5. Not adaptable to binary cycle.
6. Added cooling water systems (pipes, pumps, valves, controls).
7. Additional source of water ingress.
8. Reduced availability and reliability.
9. Higher compressor pressure ratio for maximum efficiency implies increased number of compressor and turbine stages.

GA-A14311



Cycle efficiency vs pressure ratio and recuperator effect



Cycle efficiency vs pressure ratio, with 80% effective intercooler

GA-A14311

Fig. 4.4 Influence of Pressure Ratio and Effectiveness of Cycle Efficiency

is felt that with good design (including pressure loss minimization) that an increase in plant efficiency between two and three percentage points can be realized with inter-cooling. Consistent with one of the major goals of the plant design; namely, keeping the system simple, even at the expense of slight performance penalties, a non-intercooled cycle was selected. Another important consideration in reaching this decision was the value placed on high reject temperature for the secondary power plant option. With an intercooled cycle the reject temperature is too low for additional power recovery.

4.1.2 Major Cycle Parameters

Two of the major parameters which have a significant effect on the cycle; namely, reactor outlet temperature and maximum system pressure, were established at the onset of the program. At that time, in line with the principle of fullest use of existing technology and design for the gas turbine plant, the reactor core design for the 1160 MW(e) HTGR Steam Cycle Plant was utilized. For the 3000 MW(t) core design, a mixed mean reactor outlet gas temperature of 1500°F (816°C) could be provided with the present fuel without exceeding the HTGR maximum fuel temperature limits. This design approach not only minimized the reactor development involved, but also relieved the turbine design from blade cooling requirements, since the 1500°F (850°C) turbine inlet temperature is modest by existing long-life industrial gas turbine standards. The selected maximum system pressure level of 1000 psia (6.89 MPa) was established for consistency in the design of the PCRV with the then 700 psia (4.83 MPa) working pressure of the HTGR steam plants and the 1250 psia (8.62 MPa) pressure of Gas Cooled Fast Reactor design studies.

The influence of compressor pressure ratio and recuperator effectiveness on cycle efficiency is shown in Fig. 4.4. While maximum cycle efficiency is the obvious goal, the choice of pressure ratio and recuperator effectiveness were strongly influenced by turbomachinery design consideration and heat exchanger space availability. It can be seen that for a non-intercooled cycle that a high degree of recuperation is necessary for cycle efficiencies in the range of 35-40%. A design pressure ratio slightly less than optimum has usually been selected to minimize the number of compressor and turbine stages which are strongly influenced by the low molecular weight, high specific heat, helium working fluid. The initial choice of pressure ratio was 2.25, but as can be seen from Table 4.1 there has been a trend to slightly higher values (resulting in higher specific power cycles) as plant design studies have progressed. Similarly, with recuperator effectiveness, values have increased as more efficient heat exchanger configurations were identified with detailed design

attention. Another significant factor is that selected pressure ratios and recuperator effectiveness give a turbine exhaust volume flow rate close to the minimum value. Since the last turbine stage is the largest element of the rotating assembly and tends to determine the overall diameter of the turbomachinery, there is an obvious incentive to select cycle parameters to give minimum exit volumetric flow.

As mentioned earlier the establishment of a plant to satisfy all of the project goals is an evolutionary process, and as the design progresses it may not be possible to satisfy all of the initial assumptions. As component design definition was improved (particularly the turbomachinery) more realistic efficiencies were generated and in turn these were factored into the computation of plant efficiency. It can be seen from Table 4.1 that with about three years of design work the basic parameters were only changed slightly, confirming that the initial values were close to achieving the then goal of 36.5% efficiency. As will be discussed in Section 5, in-depth plant optimization studies (for minimum power generating cost) led to the selection of a new set of major parameters for the reference plant design.

4.1.3 Plant Performance

From Table 4.2 it can be seen that early plant designs were carried out and rated with an ambient air temperature of 75°F (23.9°C). Later, to conform with the power generating industry, the ISO sea level standard atmospheric temperature of 59°F (15°C) was adopted. The ISO sea level standard atmosphere has been adopted for the nominal rating of open-cycle industrial gas turbines and is broadly representative of U. S. geographical and annual average conditions. The plant capability is dependent upon the ambient temperature as shown in Fig. 4.5. To the left of the design point ambient, the plant output is limited by the reactor power rating (3000 MW(t)); to the right the output is limited by the design condition for the turbomachinery. The variant of output with ambient temperature is generally similar to that for a dry-cooled nuclear steam turbine plant.

Performance aspects of the GT-HTGR plant have been covered in detail in Ref. 4.6. Of particular interest to a utility company is the performance of the power plant at part-load. For the GT-HTGR plant part-load operation can be accomplished by using any of three separate control modes or by combinations of control modes as shown on Fig. 4.6. The most efficient control mode is helium inventory control. Ideally, removing helium from the system should act only to reduce helium densities and pressures, while leaving the system temperature unchanged. Inventory control, however, is not expected to be used except for scheduled long-term operation at part-load power. This is because helium transfer from and to the operating inventory is normally

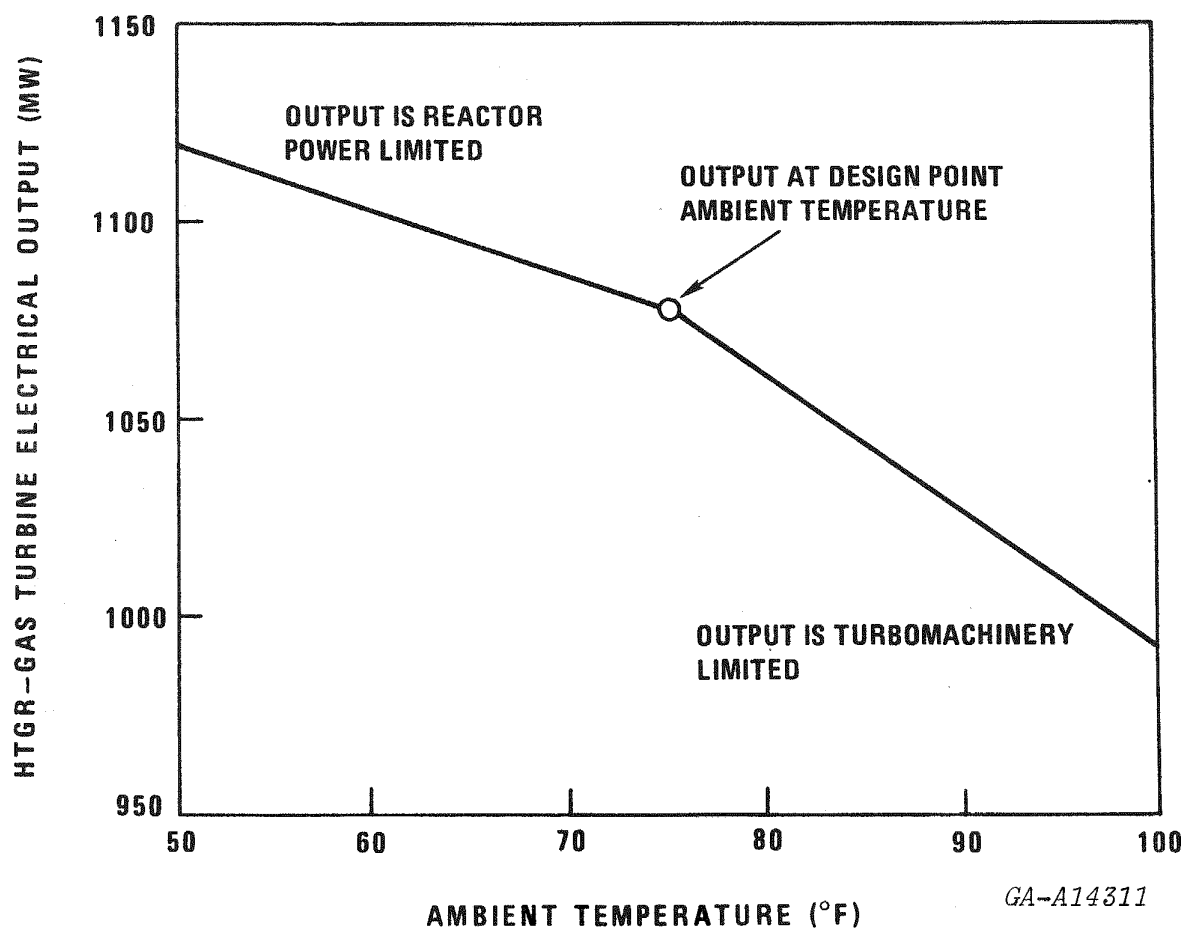


Fig. 4.5 Effect of Ambient Temperature on Plant Output

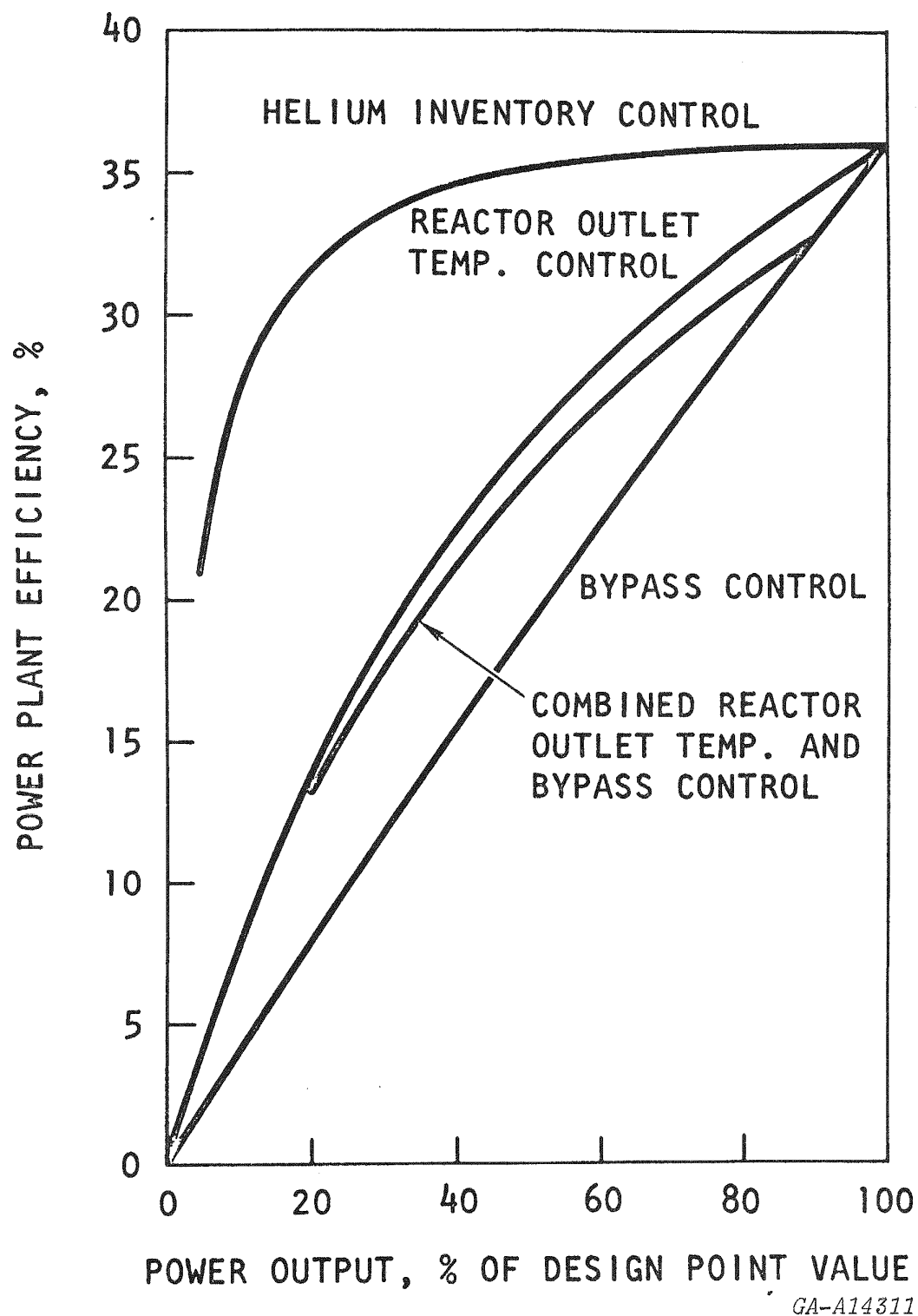


Fig. 4.6 Part-Load Efficiency for Various Control Modes

a very slow process, since the gas must first pass through the purification system before being stored. The second most efficient control mode is reactor outlet temperature (ROT) control. As the ROT is decreased, the temperatures all around the system decrease and system pressures also decrease. Although ROT control cannot be used to make a step change in power output (because of the very large core thermal capacitance), it is fast enough to accommodate a ramp load change acceptable to most utilities (5% per minute). The third separate control mode is bypass control. Bypass control is the most rapid of the three separate control modes and can be used to accomplish a 10% step load change (in approximately one second). This control mode produces the worst part-load efficiency, and therefore its application for extended time periods is to be avoided. A combined control mode has been adopted for load following, but some bypass flow must be maintained to meet the requirement for a step load change of $\pm 10\%$ of full power.

4.1.4 Performance Potential

While the gas turbine offers substantial performance improvements for turbine inlet temperature increases, a 1500°F (816°C) value was initially selected, this later increasing to 1562°F (850°C) as a result of (1) optimization studies and (2) for commonality with the European HHT program. The HTGR's capability of providing much higher outlet temperature have been discussed previously (Refs. 4.7 and 4.8) and values up to 1800°F (982°C) are projected for process heat applications. There are essentially two avenues of approach to increases of reactor outlet temperature: (1) the most readily predictable approach is by means of modifications to existing fuel block cooling arrangement, application of existing fuel particle types, and changing the fuel loading arrangement and (2) using present fuel block cooling and loading arrangements, obtain increased coolant outlet temperature by modifying the fuel particle coating chemistry to make the particles capable of withstanding higher fuel temperatures without increasing fission product release. Table 4.3 (from Ref. 4.8) shows how a combination of the above could be utilized to give an increase in core outlet temperature from 1500°F (816°C) to 1800°F (982°C).

With the foregoing modifications, it is postulated that reactor outlet temperature could be increased to 1800°F (982°C) and, in fact, the reactor outlet temperature is not limited by the core but rather the capabilities of the gas turbine loop. The gas turbine can be designed to accommodate a turbine inlet temperature of 1800°F (982°C) (typical of present day industrial gas turbine practice) by use of advanced refractory turbine blade materials, such as TZM, or the use of present day materials with gas cooling. The effects of increasing the temperature go beyond just the turbine, and necessitate changes in the thermal barrier and heat exchanger materials,

TABLE 4.3: SCOPE FOR INCREASE OF HTGR GAS OUTLET TEMPERATURE
 (Without Increase of Maximum Fuel Temperature)

BASIS	Available Gas Temperature °F (°C)
HTGR Core Loading and Orificing for entry temperature increase 640°F (338°C) to 930°F (500°C) to suit turbine application.	1500(816)
Substitution of Fort St. Vrain-type fuel blocks (210 fuel holes instead of 132).	1680(915)
As above with all TRISO particles (effect of closer allowable fuel stick-block clearance).	1723(940)
As above, 3-year cycle instead of 4-year.	1763(962)
As above, power density reduced from 8.4 to 7 w/cm ³ .	1800(982)

GA-A14311

and while significant increases in cycle efficiency are projected the influence this has on power generating cost needs extensive study.

The effect of increasing reactor outlet temperature, together with compressor pressure ratio, on cycle efficiency is shown on Fig. 4.7. If top temperature is raised and the same recuperator effectiveness is maintained, optimal efficiency rises very rapidly, and very little more compression is needed. However, this inevitably raises the necessary reactor inlet temperature, and this has to be watched since it affects the top control and loading standpipe zones, which must be kept reasonably cool. If this increase in inlet temperature is avoided in the only way open, by reducing the recuperator effectiveness, not only is the efficiency reward of top temperature rising for less, but the necessary compressor ratio must be increased as on Fig. 4.8. The message in all this is that there is indeed a commensurate reward for upgrading reactor temperatures, but more than just turbine inlet temperature must be considered.

Another point regarding projected temperature increases, is that not only does efficiency rapidly improve with temperature, but so also does the power obtainable from a given machine frame size as shown on Fig. 4.9. This results from the reduced specific mass flow and a reduced fraction of power needed for compression, and it is of particular importance because of its influence on plant cost.

While the choice of 1562°F (850°C) as the turbine inlet temperature for the reference plant design gives an acceptable plant efficiency (40% when dry-cooled) it is prudent on the part of the designer to look into the future and see if long-term projected increases in turbine inlet temperature could influence the choice of major cycle parameters selected for the design of the reference plant.

The effect of pressure ratio and turbine inlet temperature on the power obtainable from given loop component sizes is shown in Fig. 4.10. From these curves it can be seen that the turbomachinery and heat exchangers are affected differently. It can be seen that for the same pressure ratio an increase in turbine inlet temperature from 1500°F (816°C) to 1800°F (982°C) gives a power increase of 1.4 for the same machinery use, but this would be restricted to a gain factor of 1.27 for the same heat exchanger and duct sizes. Additional data as a function of turbine inlet temperature is shown on Fig. 4.11. The 27% higher power that would accompany an increase in top temperature to 1800°F (982°C) could be realized with essentially the same turbomachinery if this could accommodate a 13% increase in blade chords, which would be necessary to carry the higher bending stresses.

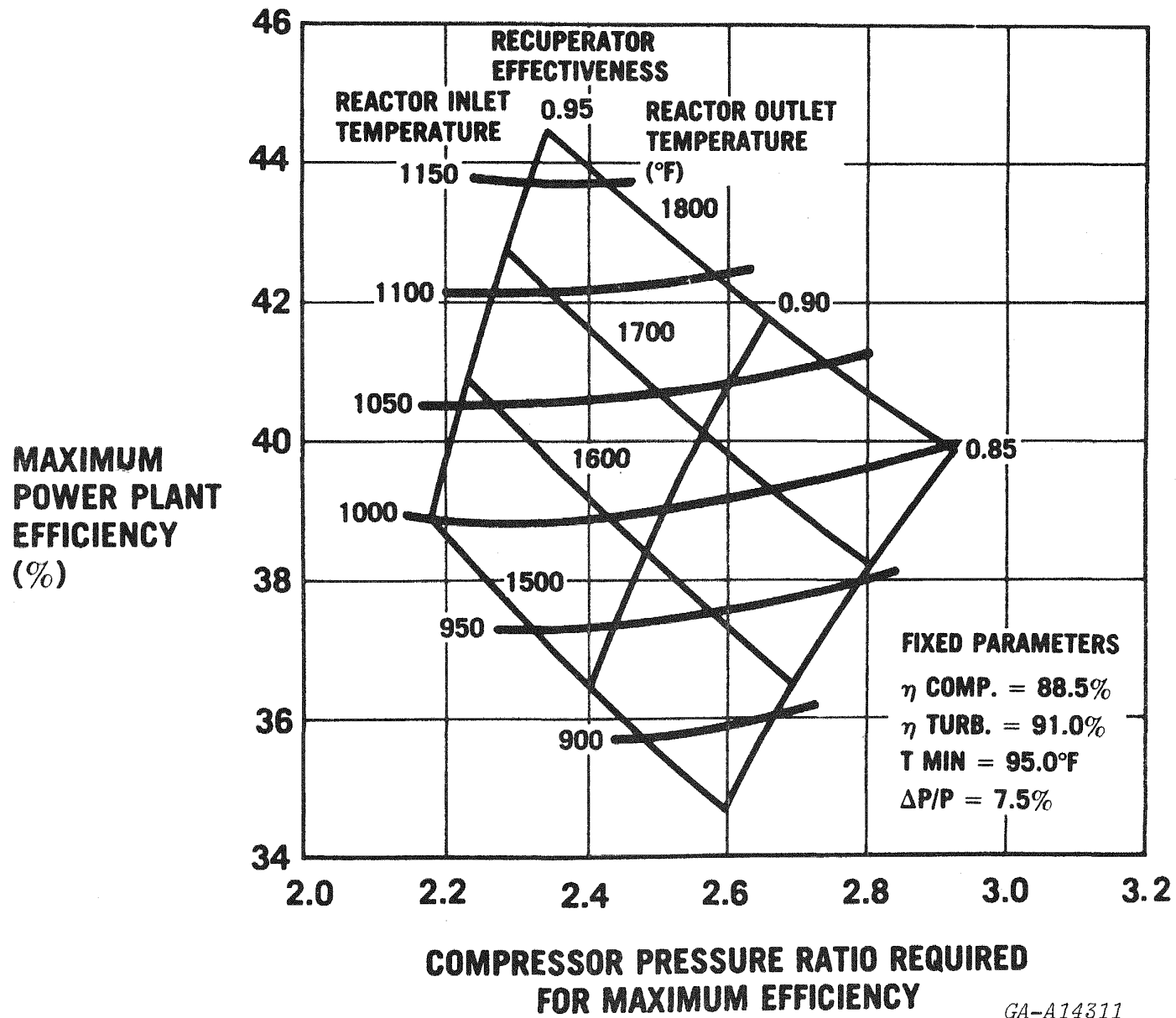
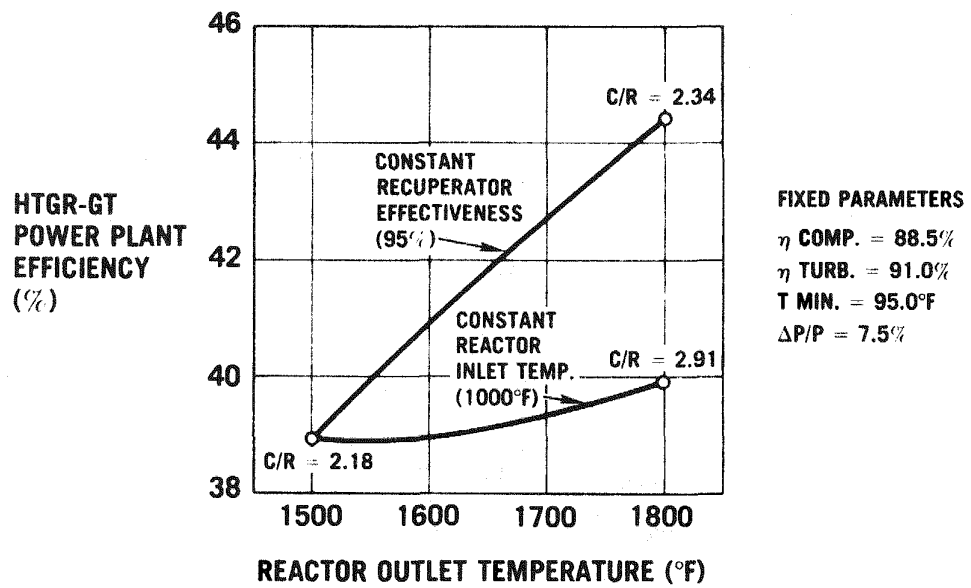


Fig. 4.7 Influence of Temperature and Pressure Ratio on Plant Performance



GA-A14311

Fig. 4.8 Limiting Effects of Reactor Inlet Temperature

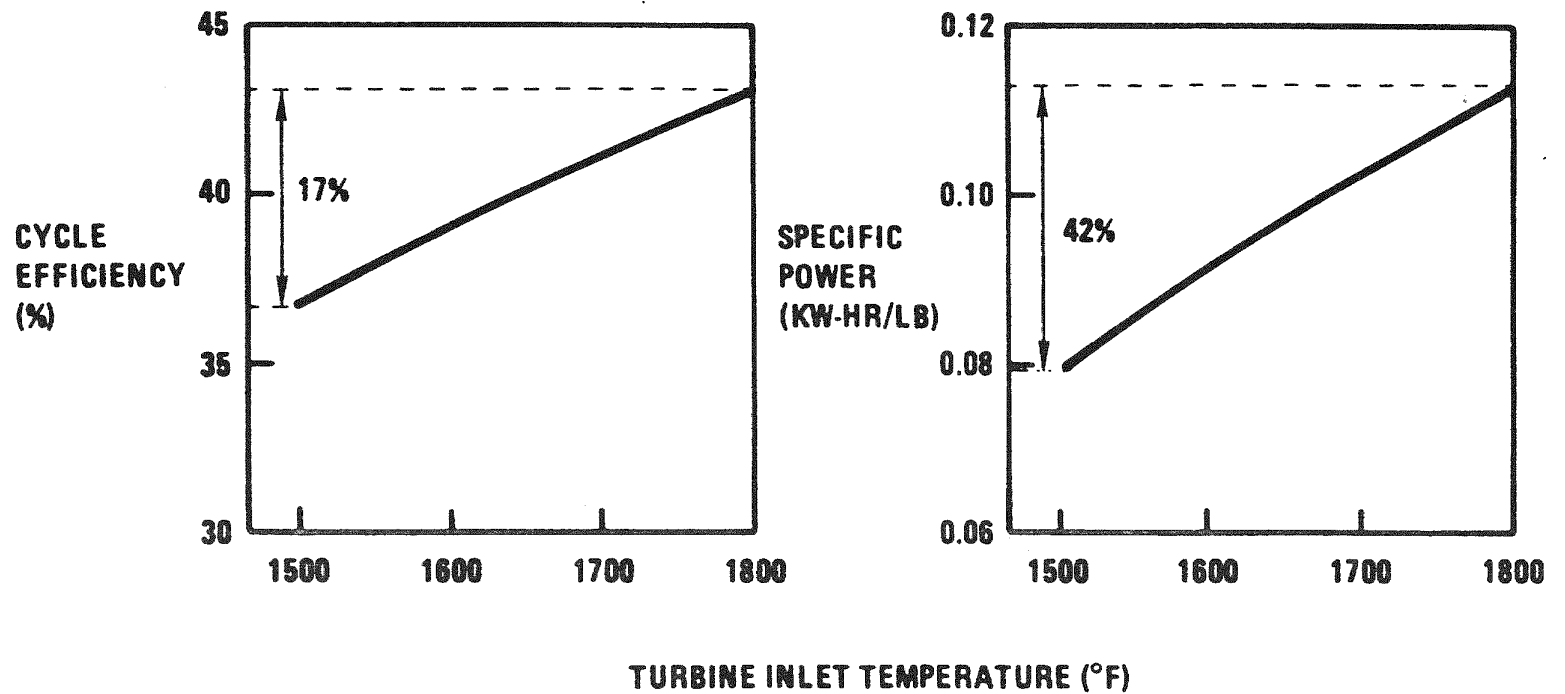
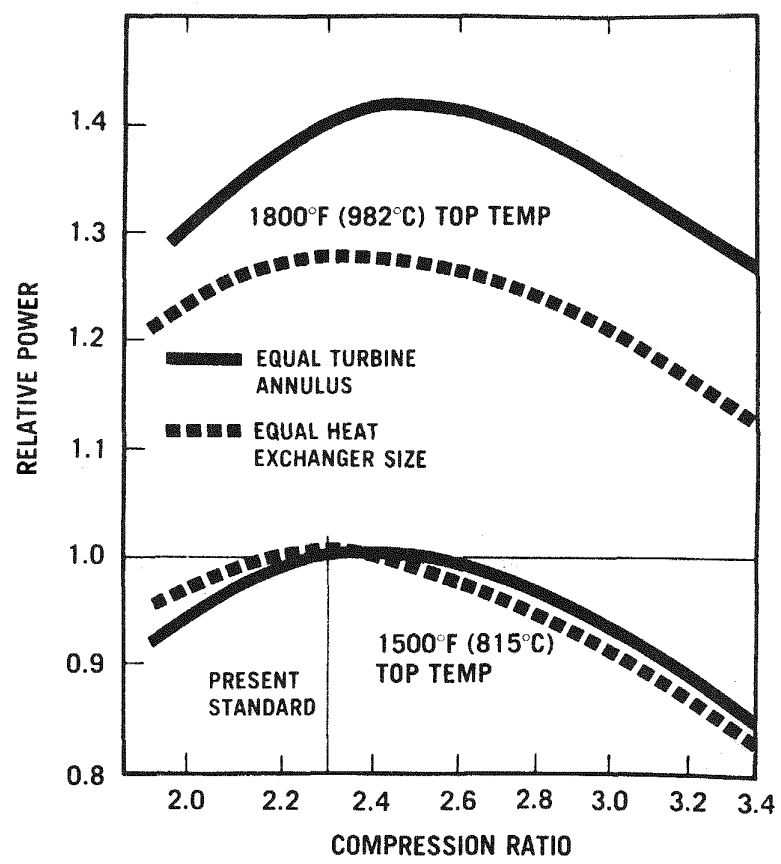


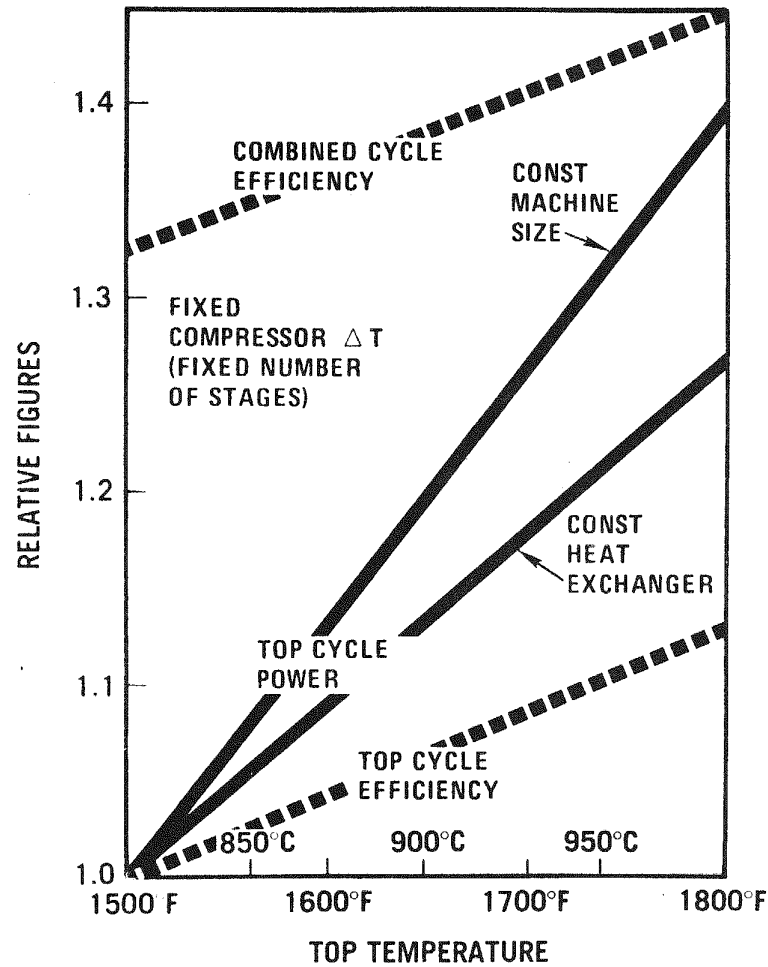
Fig. 4.9 GT-HTGR Performance Improvement Potential

GA-A14311



GA-A14311

Fig. 4.10 GT-HTGR Loop Power Capability



GA-A14311
 Fig. 4.11 Effect of Turbine Inlet Temperature on Power and Efficiency

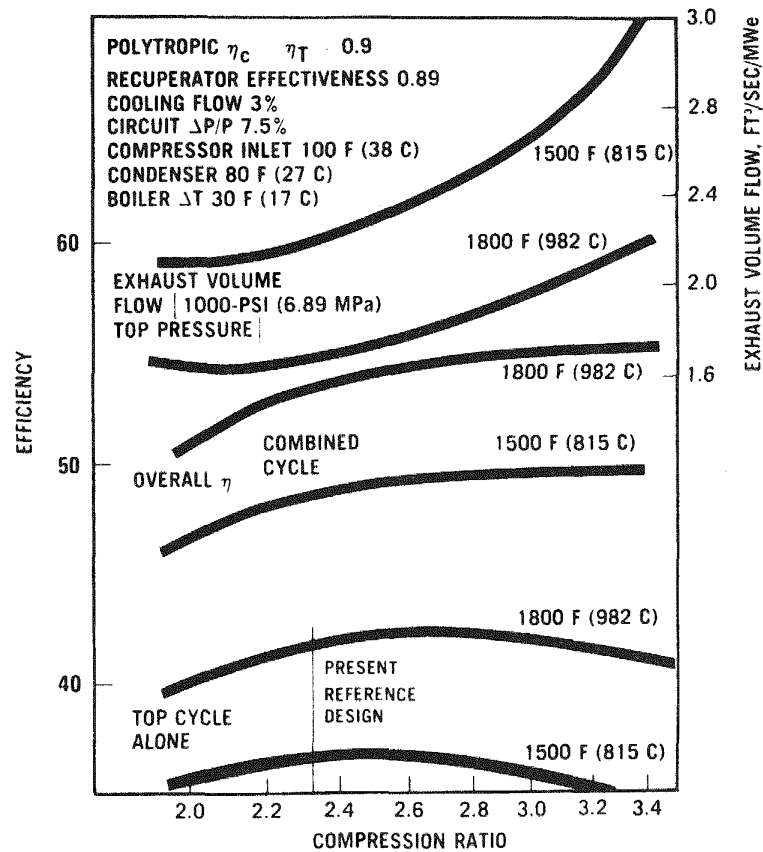
The evaluation of the initial selection of pressure ratio for projected increased performance plant variants was extended to the binary plant option. Again, the effect of increased temperature in the primary system was studied. From Fig. 4.12 it can be seen that raising the system top temperature benefits not only the top cycle but the bottom one also, because the input temperature to the secondary power cycle is increased. The summary of the above discussion from the component standpoint is that it is significant to note that further raising of the compressor pressure ratio (larger number of stages) is not necessary for increased turbine inlet temperature for plant variants with or without a binary cycle, and that the pressure ratio selected for the reference plant (2.5) would also be applicable to advanced plant variants of the future.

4.2 GT-HTGR PLANT CONFIGURATION STUDIES

Since the 1970 meeting in London on nuclear gas turbines (Ref. 4.9) substantial plant conceptual design work has been done in Germany, Switzerland, France, and England on nuclear gas turbine power stations of differing configurations and ratings. It is not the purpose of this presentation to review these designs but rather to outline the configuration studies done by General Atomic for the GT-HTGR plant.

Early in the program many plant configurations were studied and conceptual layouts prepared, but as these were evaluated deficiencies in many areas were identified (i.e., performance, safety, complexity). It would not be meaningful to discuss these early configurations, so this presentation will be limited to arrangements that had merit, but in some cases became obsolete as more in-depth analyses and design work was done. The four configurations presented essentially follow the general descriptions given in Table 4.1, the reference plant being described in detail in Section 5. All four configurations have been fully described in the published literature, so detailed coverage will not be presented in this paper, but rather the salient features will be identified and discussed briefly.

At the onset of the GT-HTGR studies the following points of design philosophy were established as guiding principles to be observed throughout the program: (1) make maximum use of existing HTGR and gas turbine technology; (2) simplify systems even at the expense of slight efficiency penalties; (3) use conservative design parameters, and (4) give major attention to safety, reliability, and maintainability early in the design. Initial studies were directed at the assessment of various configurations, and before discussing these the decisions made in the following areas are discussed:



GA-A14311

Fig. 4.12 Potential Efficiency with Binary Cycle

- 1) Intercooled versus non-intercooled,
- 2) Integrated versus non-integrated circuit,
- 3) Single versus multiple power conversion loops,
- 4) Split-shaft versus single-shaft turbomachinery,
- 5) Horizontal versus vertical machinery.

As mentioned in a previous section the issue of intercooling is somewhat controversial since it is strongly favored by the Europeans. Consistent with one of the above major goals of the plant design, namely keeping the primary system simple, even at the expense of slight performance penalties, a non-intercooled cycle was selected.

For reasons of safety and integrity, the integrated design concept was selected for the GT-HTGR plant with the integrated design concept the reactor, turbomachinery, heat exchangers, and the entire helium inventory are enclosed within the PCRV. The integrity of the PCRV is the result of the highly redundant prestressing tendons and strands which are not subject to neutron embrittlement and thermal cycling. As described in the following sections, integrated concepts embodying a PCRV similar to the type being developed for the then 1160 MW(e) HTGR steam plant were selected so that existing PCRV technology could be utilized.

Factors that have a major influence on the plant design are the number of gas turbine loops per reactor and, in particular, the question of one loop versus multiple loops. At first sight, a single gas turbine loop would appear somewhat simpler and more conventional, but when considering that use of advanced turbine blade materials (or cooling) is necessary, in conjunction with complex helium ducting between the turbomachinery, reactor, and multiplicity of heat exchangers, it was concluded that an integrated multiple-loop configuration came closer to satisfying all of the plant safety, reliability, maintenance, and economic goals. As will be discussed in the component section there is a question regarding the feasibility of a single 1200 MW(e), 60 Hz turbomachine. With multiple loops, the turbomachinery is smaller, and the stresses in the rotating elements are reduced thus eliminating the need for advanced materials or blade cooling. The desirability of non-nuclear testing a complete prototype gas turbine loop favors the selection of multiple loops, since the test facility will be more practical and less expensive. With a multi-loop design, a departure from strictly on-site repair, substituting instead the philosophy of part replacement by spare power conversion modules, is rendered possible by virtue of the relatively small bulk and limited cost of the individual components of the multiple loops and their possible common use in other plants.

The issue of single-shaft or split-shaft turbomachinery was explored in some of the early plant layouts and are discussed in Ref. 4.1. The early merits of a split-shaft arrangement were seen as: (1) decoupling of the gas generator and power turbine gave some flexibility in plant layout (i.e., the former could be vertical and the latter horizontal), (2) 50 Hz - 60 Hz adaptability with changes to the power turbine only, (3) better part-load efficiency, and (4) smaller gas generator section because of optimum rotational speed greater than the electrical generator synchronous speed of 3600 rpm. However, as outlined in Ref. 4.1, the decision in favor of a single-shaft configuration (compressor, turbine, and generator on the same shaft) was based on the conclusion that this arrangement offers the advantage of design simplicity (i.e., less bearings and service systems, etc.) higher reliability, easier control, and lower cost. The control aspect was considered important since it was felt that a single shaft machine overspeed would put less demanding requirements on the control valves (principally because of the response time associated with the increased inertia of the single-shaft machine). The single-shaft machine with its lower rotational speed (3600 rpm), has lower stress levels in the compressor and turbine blading.

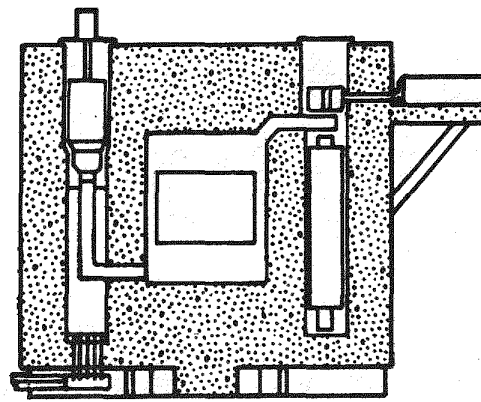
The last of the above five major design influencing features is that concerning the orientation of the power conversion machinery (i.e., vertical or horizontal). This aspect will be discussed in the following sections, since of the four power plant variants shown on Table 4.1 (excluding the reference plant) the two early ones embodied vertical machinery, and the latter two had horizontal turbomachinery.

Simplified view of three configuration alternatives embodying some of the above features, that were evaluated early in the program, are shown on Fig. 4.13.

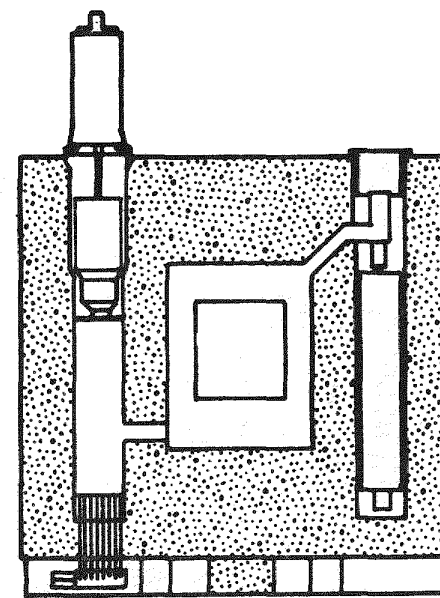
4.2.1 Plant Configurations with Vertical Turbomachinery

Initial plant studies followed the ground rules mentioned earlier, an important one being the utilization, to the maximum degree possible, of existing HTGR steam plant technology. In the area of the PCRV, the design developed for the steam plant (as shown on Fig. 4.14 from Ref. 4.10) had vertical sidewall cavities for the steam generators and circulators, and this type of configuration was favored early in the gas turbine program. The two plants embodying vertical machinery have been fully described in Refs. 4.1 and 4.2 and are briefly discussed below.

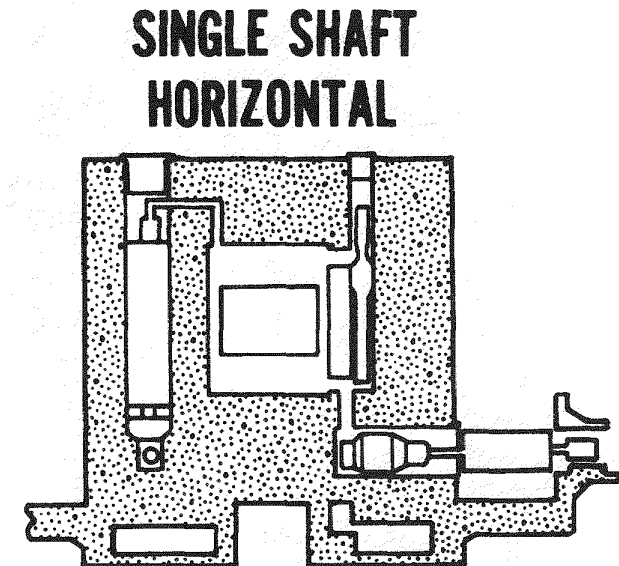
An overall view of the initial vertical configuration is shown on Fig. 4.15, with details of the power conversion components shown on Fig. 4.16. In this plant schematic it can be seen that the complete turbomachinery assembly is mounted above the precooler in one cavity, and the recuperator is installed in the



SPLIT SHAFT

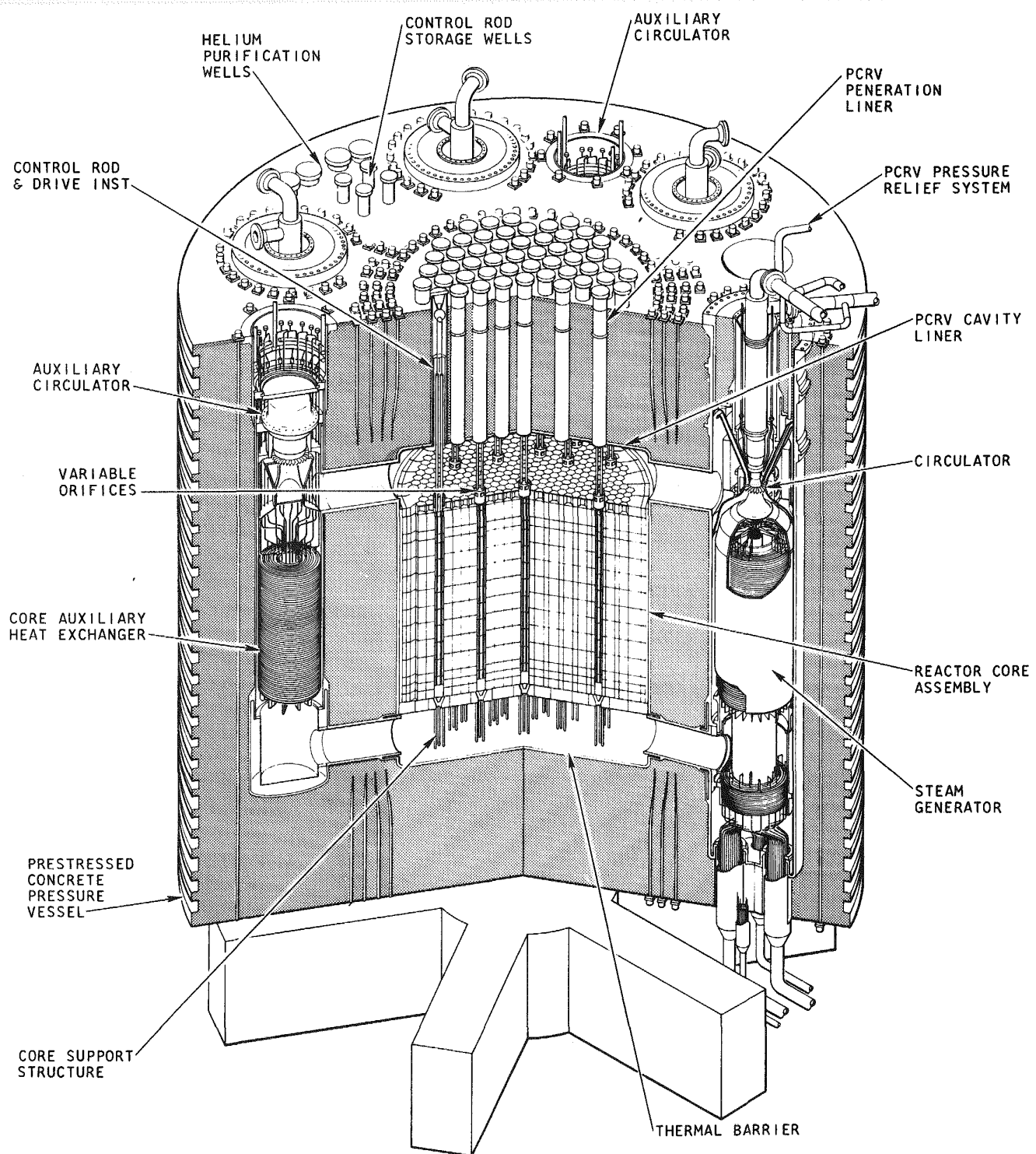


**SINGLE SHAFT
VERTICAL**



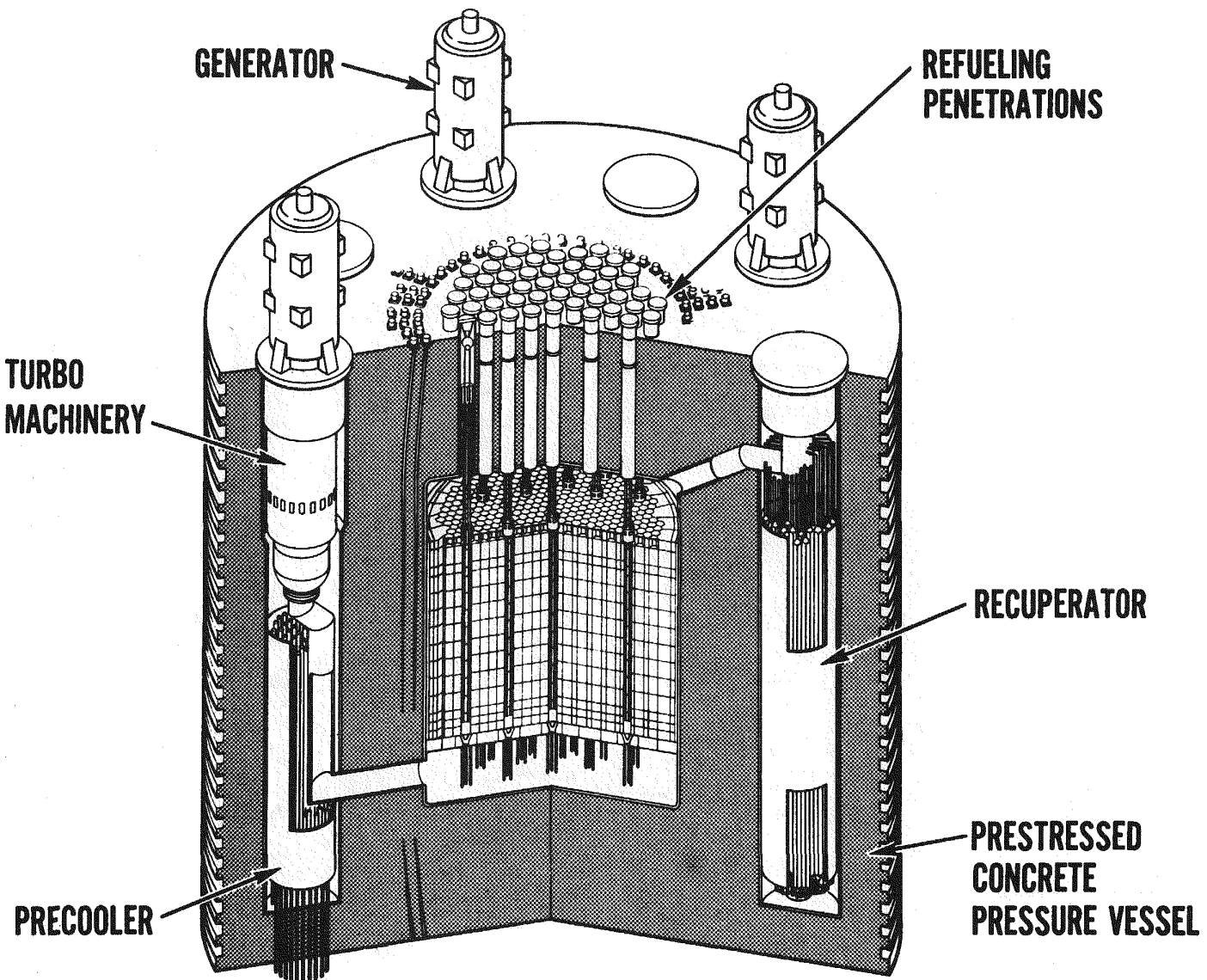
**SINGLE SHAFT
HORIZONTAL**

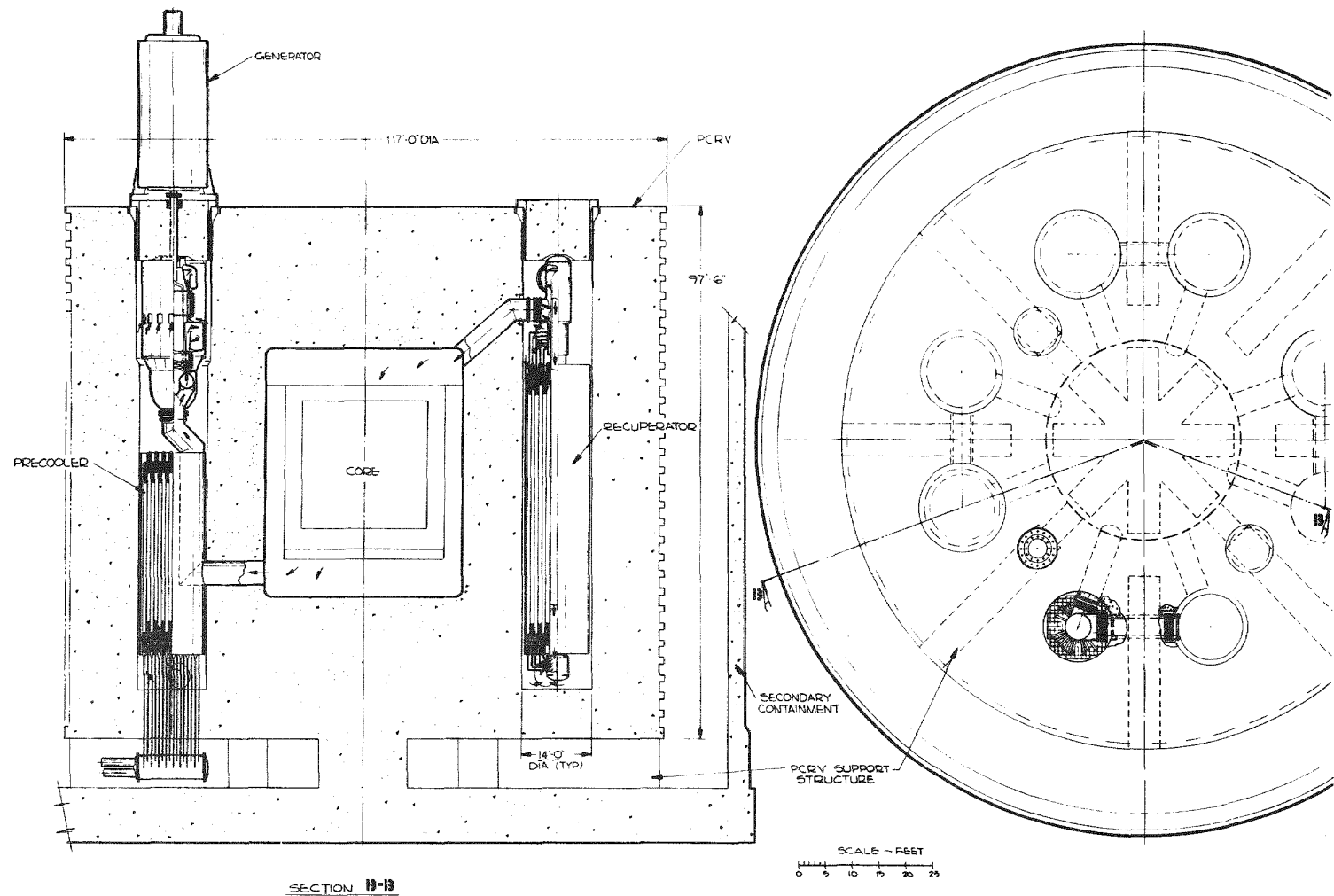
Fig. 4.13 Simplified Views of GT-HTGR Plant Configuration Alternatives



GA-A14311

Fig. 4-14. HTGR Nuclear Steam Plant Core Arrangement





GA-A14311

Fig. 4.16 PCL for Vertical Machine Arrangement

other cavity. The single-shaft turbomachine unit is supported from the underside of the concrete plug of the precooler cavity. The drive shaft penetrating the plug is connected to the vertical generator. The combined end thrust and weight of the generator and turbomachinery are taken on a thrust bearing located outside the PCRV for accessibility and ease of maintenance.

A follow-on version of the plant configuration with vertical turbomachinery involved a re-orientation of the heat exchangers. From Figs. 4.17 and 4.18 it can be seen that the precooler was installed in its own cavity for the following reasons, (1) to avoid interaction with the turbomachinery and the water-cooled exchanger in the event of a failure in the former, and (2) growing interest in the secondary cycle and the realization that the heat source heat exchanger (i.e., precooler) would be larger than for the dry-cooled plant. The much shorter recuperator was achieved by changing the high-pressure fluid to flow outside the tubes, rather than inside as previously, this essentially increasing the number of tubes (i.e., closer pitching) and reducing the flow length.

These vertical arrangements had four turbomachinery loops, and the major component sizes were convenient for factory assembly and straightforward handling and shipping. The helium turbomachinery consists of a vertically mounted compressor-turbine unit as shown on Fig. 4.19. The high-density working fluid used in the helium closed-cycle gas turbine results in a very compact power conversion system. From Fig. 4.20, it can be seen that the 275 MW(e) helium turbomachine is similar in size to a 70 MW(e) open-cycle industrial gas turbine. The vertical orientation of the rotating machinery did not pose insurmountable problems to the turbomachine designer, and the 275 MW(e) helium gas turbine was designed to conventional gas turbine practice. The machine was designed within the imposed diameter constraint of 11.5 ft. (3.5 m). This value was established as part of the maintenance plan of transporting (by rail) a contaminated machine (inside a shielded cask) to a central overhaul facility. The turbomachine utilizes existing nickel-base alloys for the turbine blading, and the design stress levels are commensurate with a life of 280,000 hours (i.e., 40 years with an 80% utilization factor).

In this early phase of the program it was felt that the vertical generator configuration offered substantial cost savings, and use of a more conventional PCRV design (as being used in HTGR steam plant) outweighed the moderate development effort associated with the vertical generator. Since detailed structural calculations of a PCRV embodying both vertical and horizontal cavities had not been done, there was concern regarding its feasibility. The vertical generator, however, did

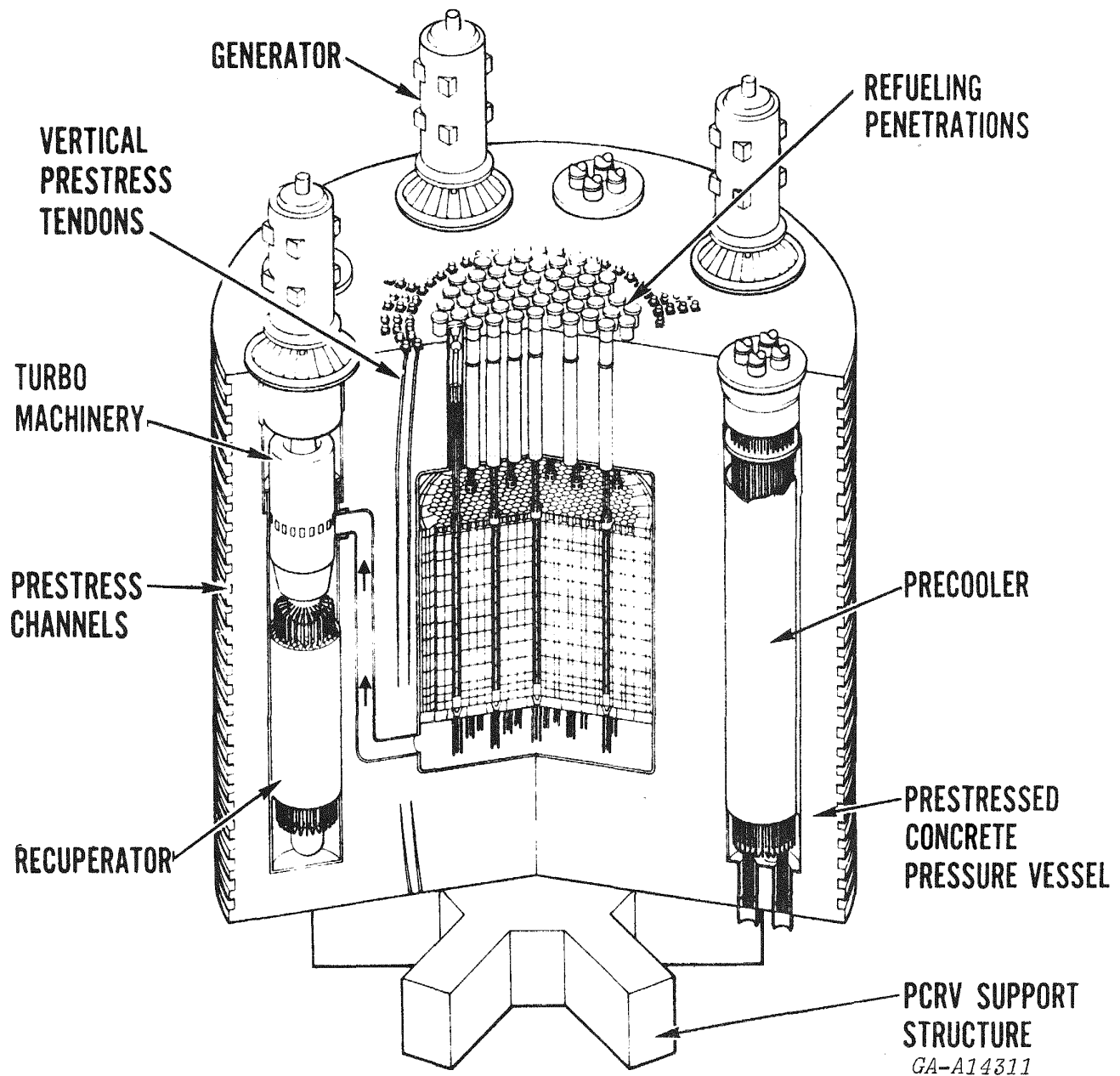


Fig. 4.17 Alternate Vertical Generator Configuration

GA-A14311

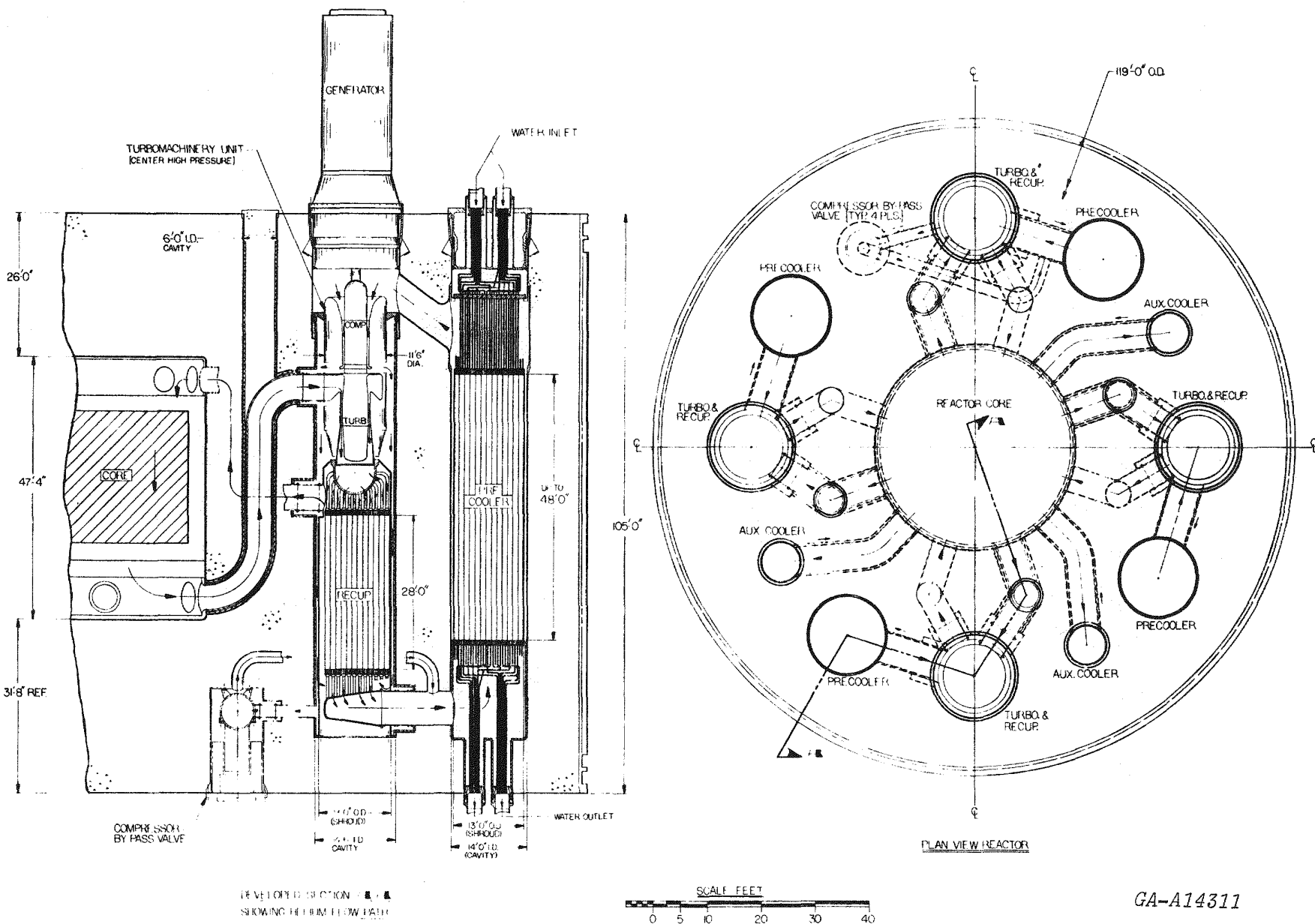
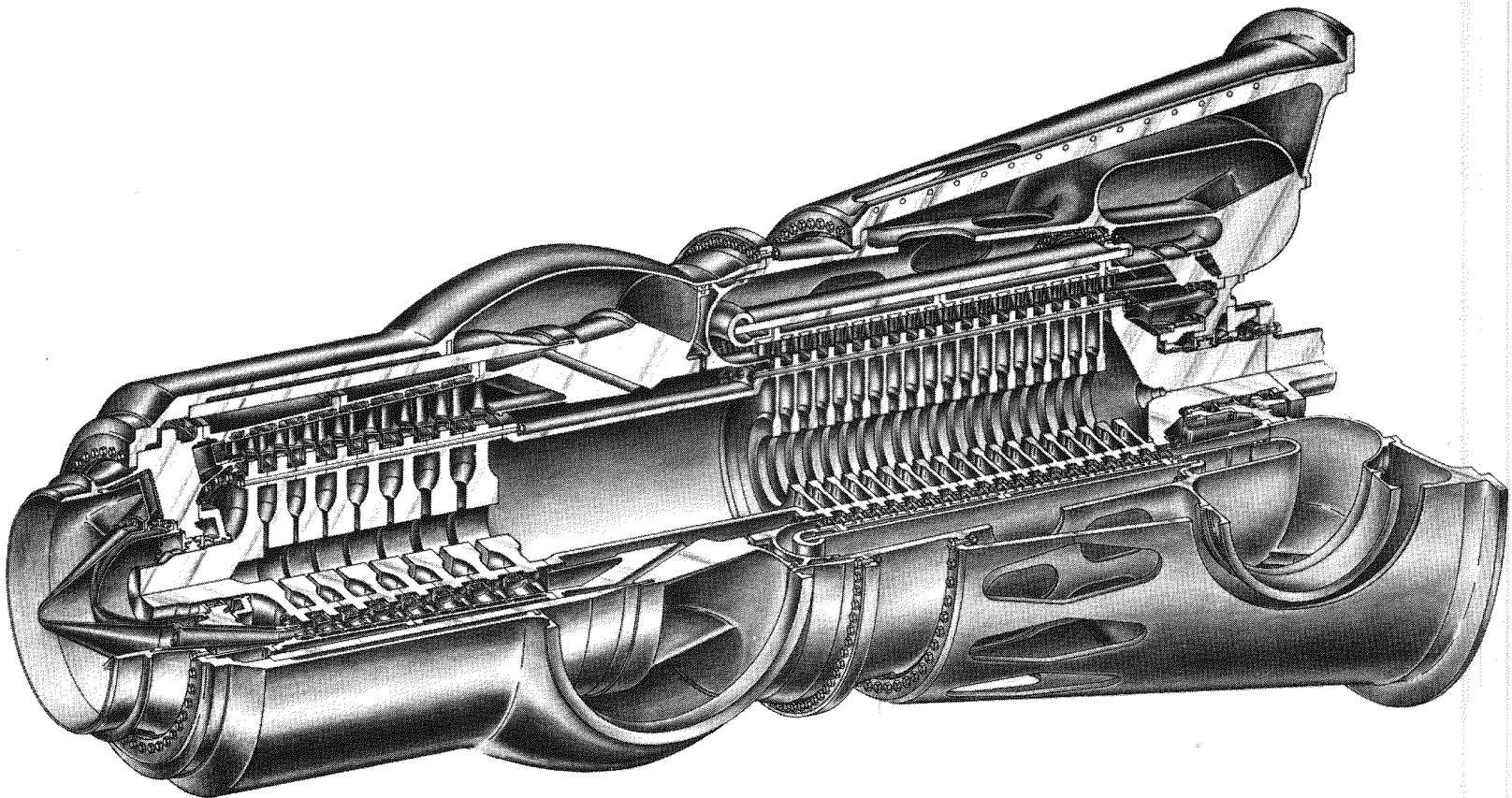


Fig. 4.18 PCL for Alternate Vertical Machine Arrangement

87



Pratt &
Whitney
Aircraft

DIVISION OF UNITED AIRCRAFT CORPORATION

U
A.

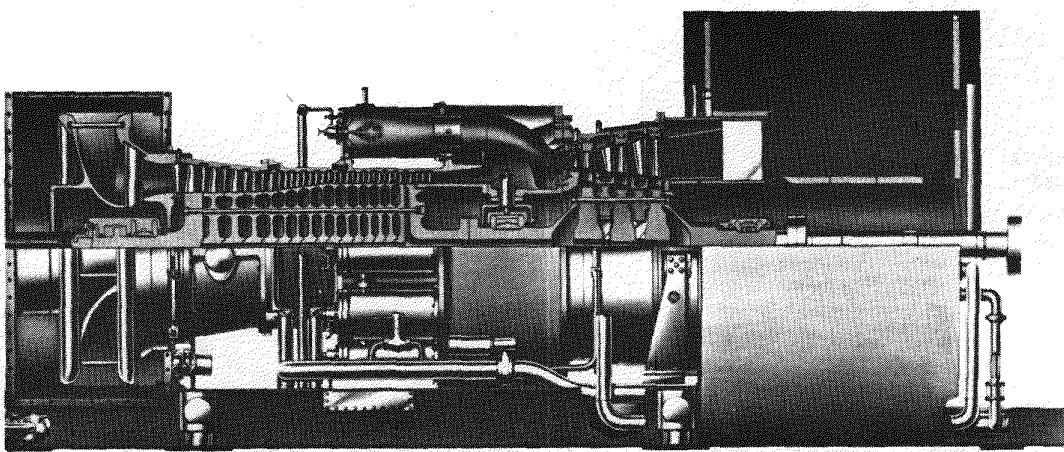
J6877-2
731805

GA-A14311

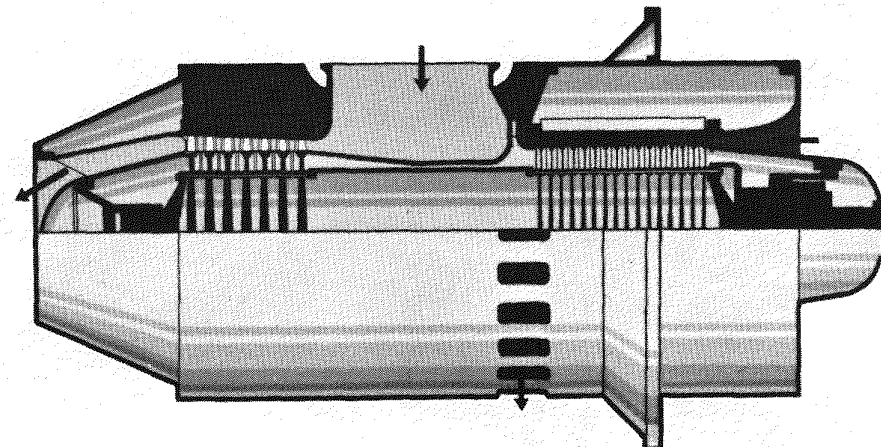
Fig. 4.19 Isometric of Vertical 275 MW(e) Helium Turbomachine (by Courtesy Pratt & Whitney)

88

**70 MWe
GENERAL ELECTRIC
MODEL 7000
OPEN CYCLE
GAS TURBINE**



**275 MWe
HTGR HELIUM
TURBOMACHINERY**



GA-A14311

Fig. 4.20 Turbomachine Size Comparison

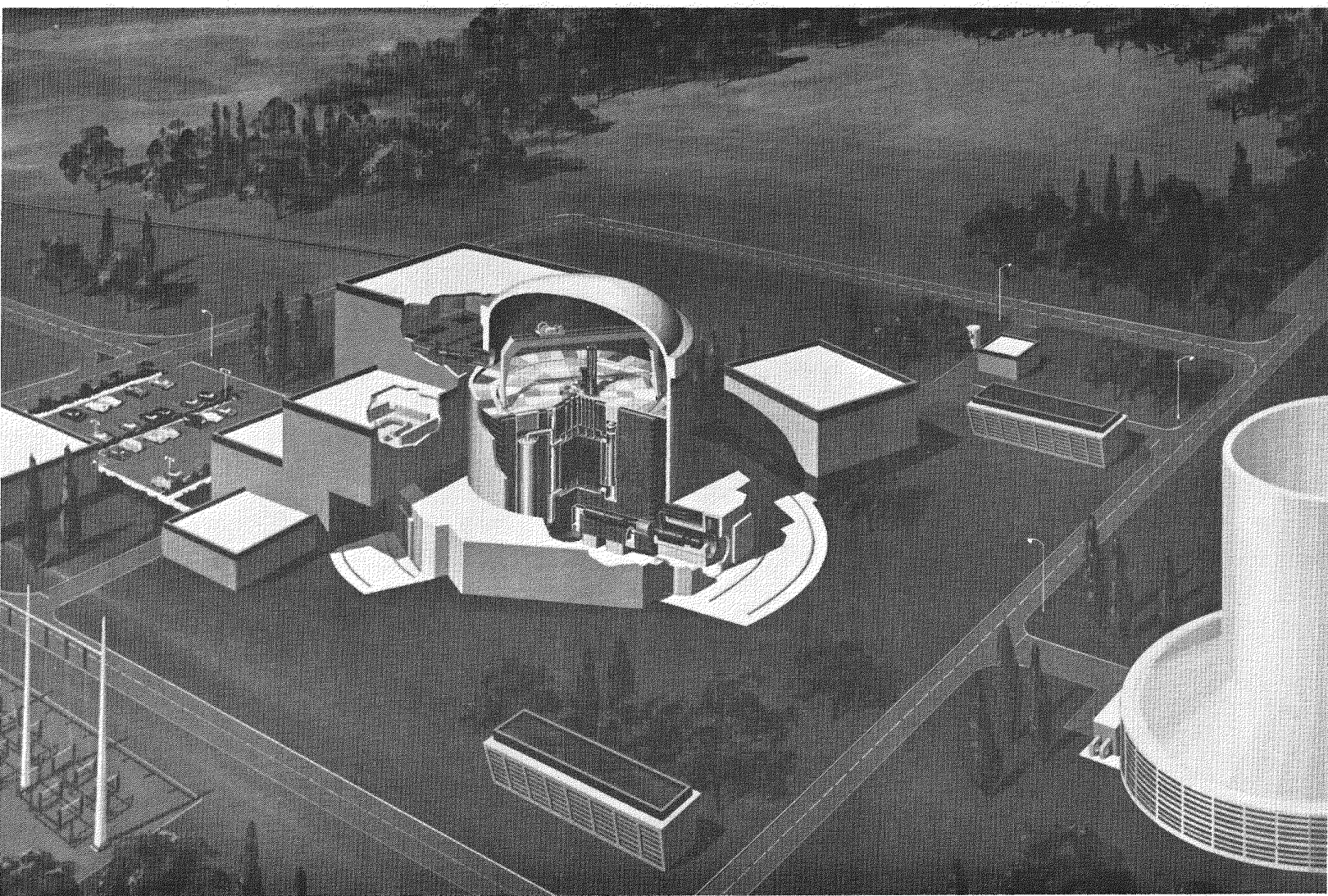
represent a significant departure from steam plant practice, but the three turbo-machinery and generator companies participating in the initial phase of the program with General Atomic independently established the feasibility of the vertical generator. The electrical portion of the generator was basically the same as a horizontal turbogenerator with revised cooler and casing and mounting structural design for the vertical orientation.

The four-loop vertical configurations established in the early phases of the program were designed with the established ground rules mentioned earlier and exhibited overall plant efficiencies in the 36%-36.5% range. Balance of plant design work was carried out and economic evaluations completed. A conceptual overall view of a GT-HTGR plant embodying vertical rotating machinery is shown in Fig. 4.21. As outlined below, in 1974 design studies were initiated on a plant with horizontal turbomachines, following PCRV structural analyses (done both in the U.S. and Europe) that showed the feasibility of this vessel concept.

4.2.2 Plant Configurations with Horizontal Turbomachinery

In 1974-75 preliminary design studies were performed for horizontal machinery orientations as well as higher power capacity loops, with emphasis being placed on the solution of problems and difficulties encountered in the earlier assessments of the horizontal design. PCRV engineering design studies and detailed three-dimensional elastic analyses showed that PCRV's with large horizontal turbomachinery cavities were structurally feasible. Related studies revealed that the cost of the PCRV to accommodate horizontal machinery was not as high as had been anticipated, and that the increased PCRV cost was more than offset by the elimination of the cost of the vertical generators. A secondary containment design concept of modest size and cost that can house the horizontal generators was identified and investigated.

Layout studies of a 3-loop plant with a turbomachine rating of 370 MW(e) was initiated. It was determined that the 370 MW(e) size turbomachinery could be designed to fit within essentially the same envelope as 275 MW(e) size machines and would then be rail shipable. The 370 MW(e) gas turbine still embodied the same features as the 275 MW(e) machine with only a small increase in stress levels. The advantage of the higher power conversion loop rating were seen to be; (1) reduced cost, (2) increased plant availability, (3) decreased plant complexity, and (4) enhanced plant growth potential. Compared to previous designs, the horizontal machinery configuration offered improved safety, potentially lower plant cost, more economical extrapolation to future increased plant output (higher reactor thermal rating), more conventional generator and turbomachinery design, and the potential for in-situ man access to the



GA-A14311

Fig. 4.21 Conceptual Overall View of GT-HTGR Plant

turbomachinery, these aspects are summarized on Table 4.4. The salient features of the primary system for the plant embodying three power conversion loops are given on Table 4.5.

4.2.2.1 Initial Plant Configuration with Horizontal Turbo-machinery

The initial configuration described in detail in Ref: 4.3 was only an interim solution and since it proved to represent only a stepping-stone towards a better arrangement it will be discussed only briefly. The overall primary system configuration is shown on Fig. 4.22. The configuration is characterized by the three gas turbine units installed radially in the bottom head of the PCRV. To minimize the size of the secondary containment building, a close-fitting cylindrical arrangement was selected with local cells to house the generators of conventional design, as shown on Fig. 4.23.

The power conversion loop embodies replaceable hot ducts, and two man access cavities for in-situ inspection and maintenance of the turbo-machine bearings. As can be seen from Fig. 4.24, a concentric heat exchanger arrangement was selected, and details of the recuperator and precooler assembly is shown on Fig. 4.25. The design rationale for this heat exchanger approach was simply to minimize unit size since this arrangement (as can be seen from Fig. 4.26) had essentially six recuperator and precooler assemblies. The recuperator assembly was well within transportation limits and it was planned to transport the modular, annular precooler in large self-headering sub-assemblies. A view of the 370 MW(e) helium turbomachine is given on Fig. 4.27, and it can be seen that the overall size of the machine is similar to that of a 70 MW(e) open-cycle industrial gas turbine.

As design studies progressed on this configuration some areas of concern were expressed regarding the heat exchangers, namely, (1) as more detailed mechanical design work was done there were indications that the diameters of both units would increase, thus tending to negate the advantages of this scheme, (2) mechanical interaction making installation, removal, and maintenance complex, (3) limited growth potential for the precooler for binary plant application, and (4) increasing exchanger costs for the concentric arrangement as the design definition increased. The above heat exchanger considerations led to further primary system configuration studies, involving location of the recuperators and coolers in their own vertical cavities.

4.2.2.2 Selected Plant Configuration with Horizontal Turbo-machinery

Continuing preliminary design efforts during 1975 were aimed at establishing a simpler plant which satisfied all of the safety, perform-

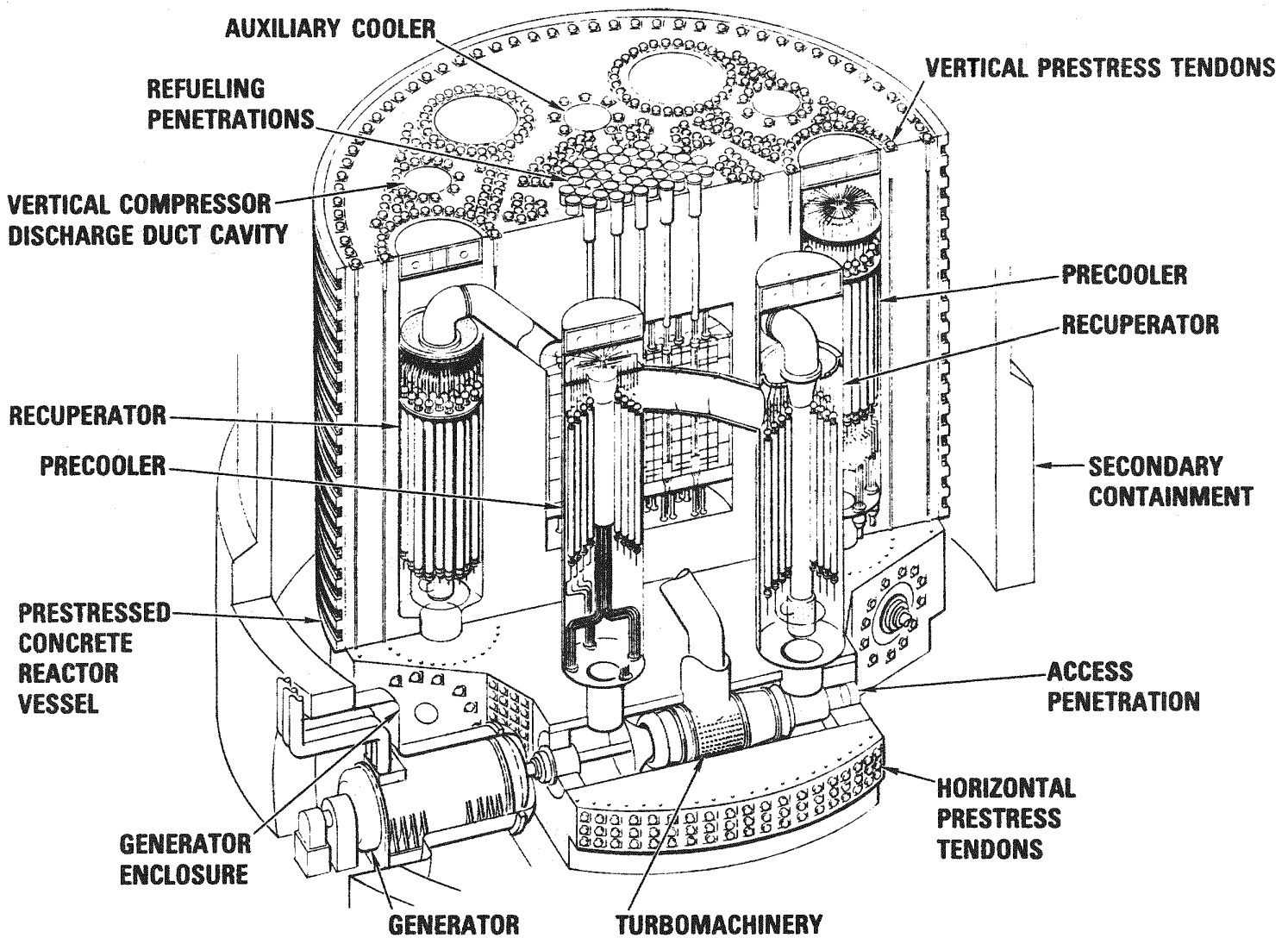
TABLE 4.4
ADVANTAGES OF HORIZONTAL TURBOMACHINERY

- In Situ Access Readily Achieved
- Conventional Orientation
- No Development for Horizontal Generator
- Reduced Thrust Bearing Requirements
- Avoids Interference with Refueling Operations
- Generators Removed from Proximity of Critical
Top Head Components

GA-A14311

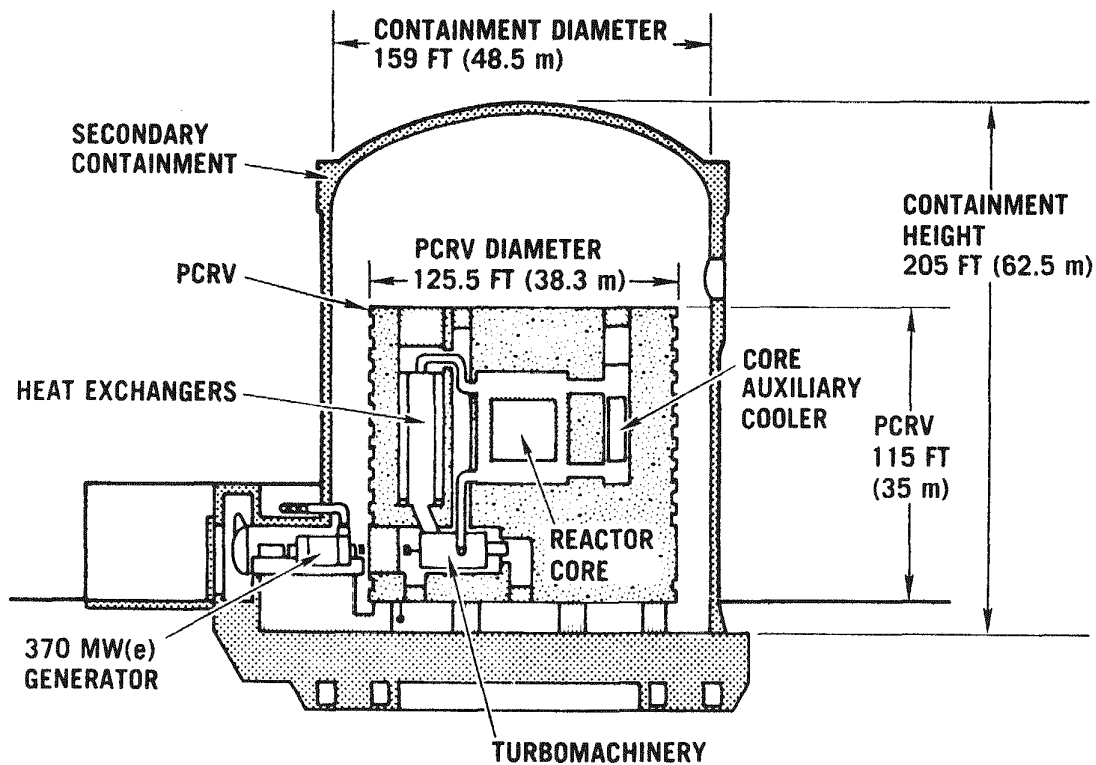
TABLE 4.5
SALIENT FEATURES OF PRIMARY SYSTEM FOR GT-HTGR POWER PLANT

- Integrated Design (Reactor, Turbomachinery, Heat Exchangers and Entire Helium Inventory)
- Enclosed Within PCRV)
- Multiple Gas Turbine Loops (3 for 3000 MW(t) Core)
- Horizontal Turbomachinery and Generator
 - Single-Shaft Turbomachine
- Man Access Provision for Turbomachinery Bearing Inspection and Maintenance
- Replaceable High-Temperature Ducts
- Recuperator and Precooler of Modular Construction with Tubular Matrix, and Axial Counter-flow Configuration
- Major Components Within Transportation Limits (Precooler Transported to Site in Quadrants)



GA-A14311

Fig. 4.22 Integrated 3-loop Plant with Horizontal Turbomachine



GA-A14311

Fig. 4.23 Simplified View of Integrated Plant

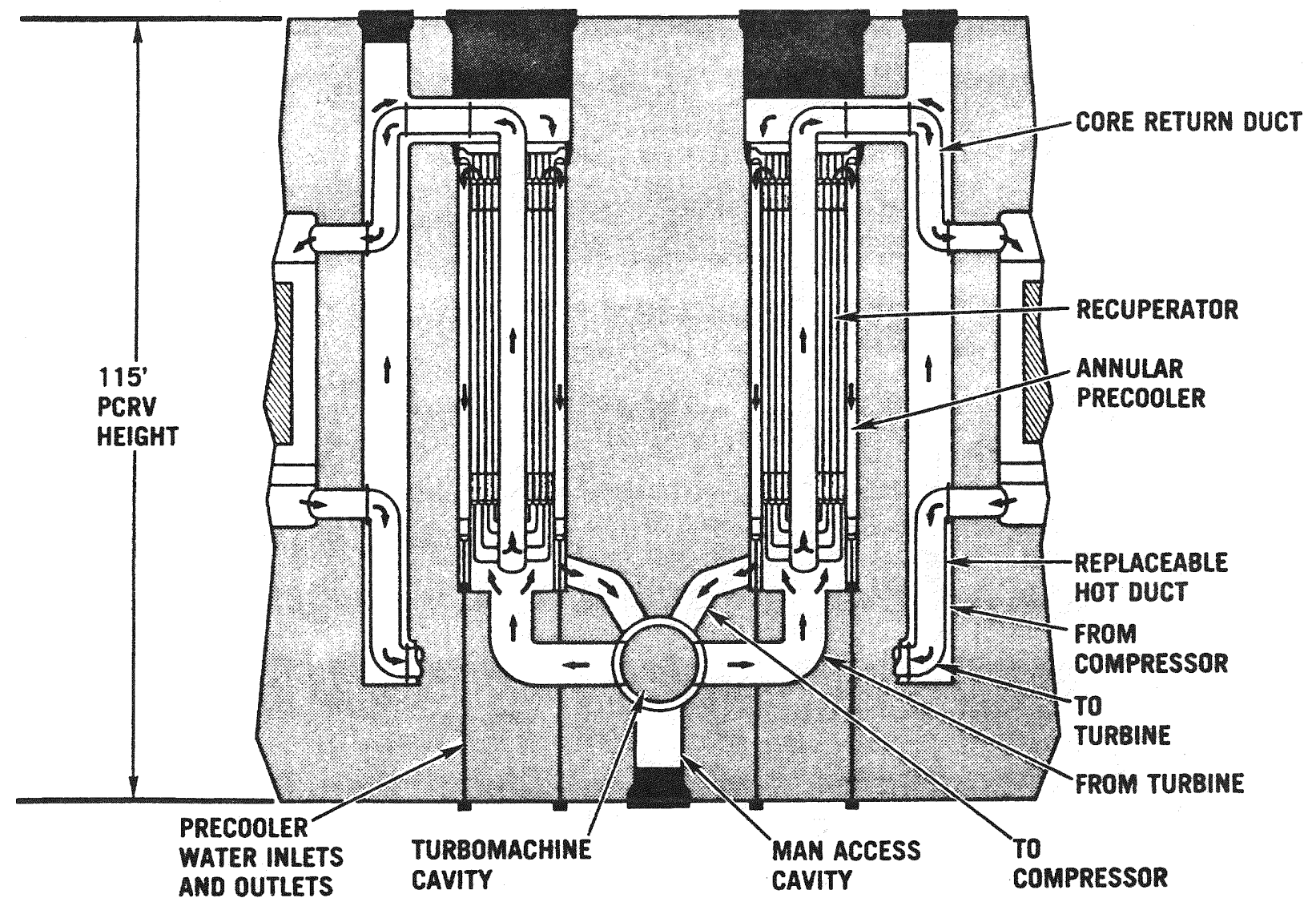
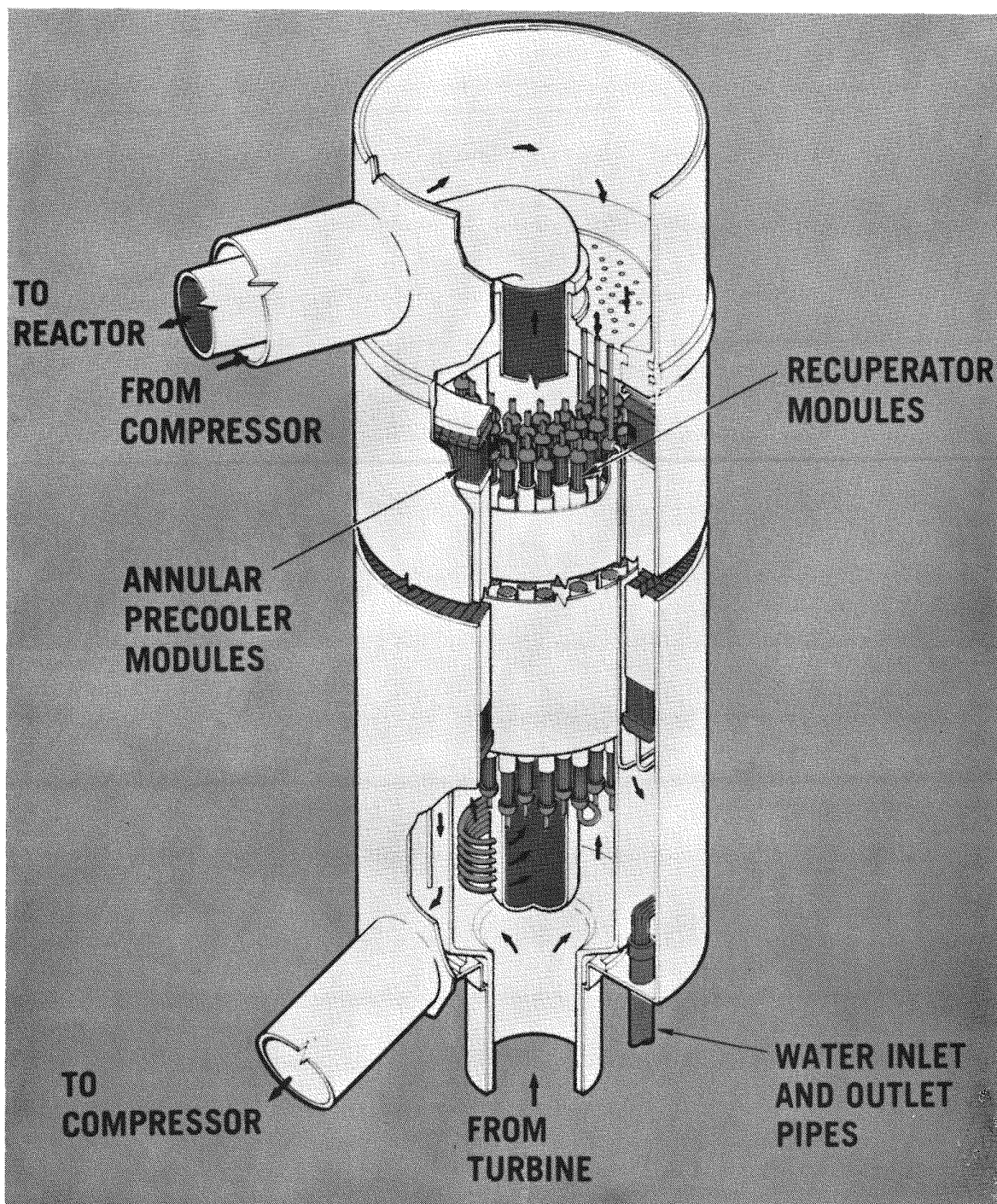


Fig. 4.24 Gas Flow Paths for Configuration with Concentric Heat Exchangers

GA-A14311



GA-A14311

Fig. 4.25 Concentric Heat Exchanger Arrangement

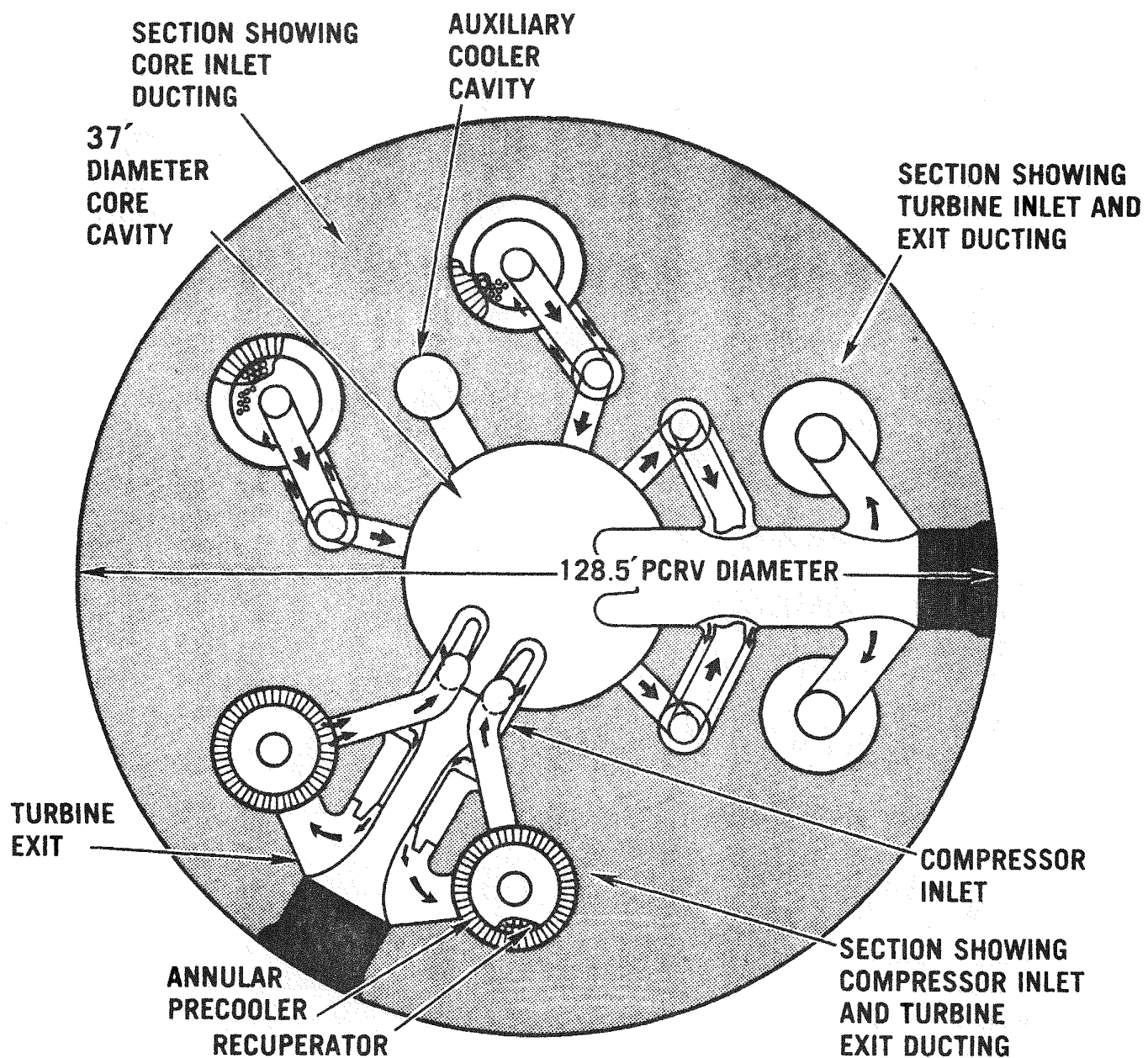
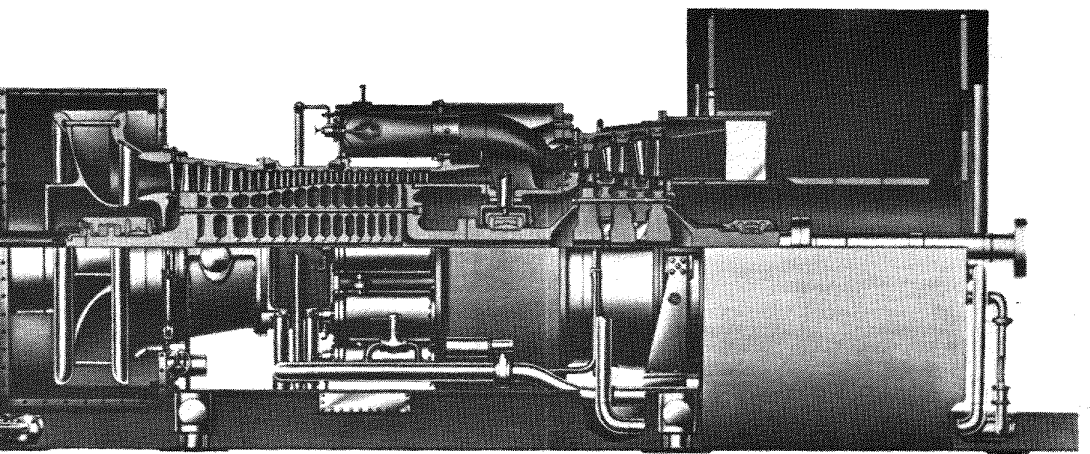


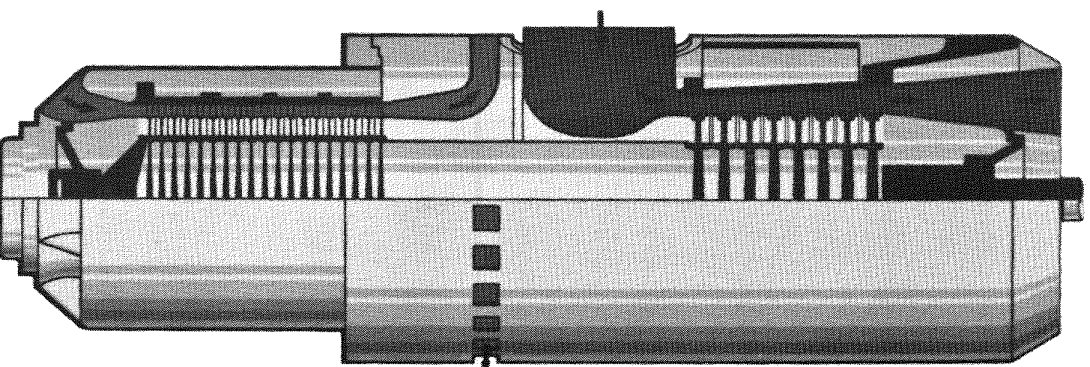
Fig. 4.26 Plan View of GT-HTGR PCRV

GA-A14311

**70 MWe
GENERAL ELECTRIC
MODEL 7000
OPEN CYCLE
GAS TURBINE**



**370 MWe
HTGR HELIUM
TURBOMACHINERY**



GA-A14311

Fig. 4.27 Comparative Sizes of Turbomachinery

ance, and economic goals and would become the reference configuration for the detailed Phase 3 Preliminary Phase. The main primary system design activity was centered on the heat exchanger location. Compared with the initial concentric configuration, design studies showed that the plant internal gas flow paths could be significantly simplified by eliminating the heat exchanger flow-split and having a single recuperator and precooler assembly per loop, in separate vertical cavities as shown on Fig. 4.28. This resulted in a less complex PCRV of lower cost. More detailed heat exchanger studies showed that, while assemblies were larger, there was economic gain because of design simplifications and their reduced number. This combined with less complex installation (no direct mechanical interaction between recuperator and precooler), improved maintenance capability and increased flexibility for binary cycle applied to the adoption of separate cavity recuperator and precooler arrangements for the plant primary system preliminary design.

Details of this plant have been given in Ref. 4.4 and are briefly given as follows: As shown in the simplified elevation views (Figs. 4.29 and 4.30) the GT-HTGR plant includes a secondary containment building that completely encloses the PCRV, the structure being of prestressed concrete construction with an oblate spheroidal dome. Power is generated in the classical regenerative Brayton cycle, and appears as 22,000 Kv electrical output on each of the three generators which are located outside the primary system. The heat exchangers are installed in vertical cavities arranged within the PCRV wall, two for each loop. A simplified (and schematically developed) vertical section through a power conversion loop is shown in Fig. 4.31. The simplified plan view (three sections shown) of the PCRV (Fig. 4.32) shows the orientation of the vertical cavities and the turbomachinery.

For the plant preliminary design emphasis has been placed on simplicity, and both heat exchangers are of tubular construction and embody plain tube geometries. A simple modular assembly approach was chosen to facilitate fabrication, handling, installation, and maintenance. Isometric views of the recuperator and precooler are shown on Figs. 4.33 and 4.34, respectively, and details are given in Table 4.6.

A simplified view of the 370 MW(e) turbomachine showing the salient dimensions is given on Fig. 4.35, and details of the aerodynamic and mechanical design are given on Table 4.7. For the design pressure ratio of 2.35 the numbers of compressor and turbine stages are 20 and 8, respectively. The machine has two journal bearings and the generator drive is from the compressor end of the machine. The thrust bearing is positioned outside of the PCRV for ease of inspection and access for maintenance

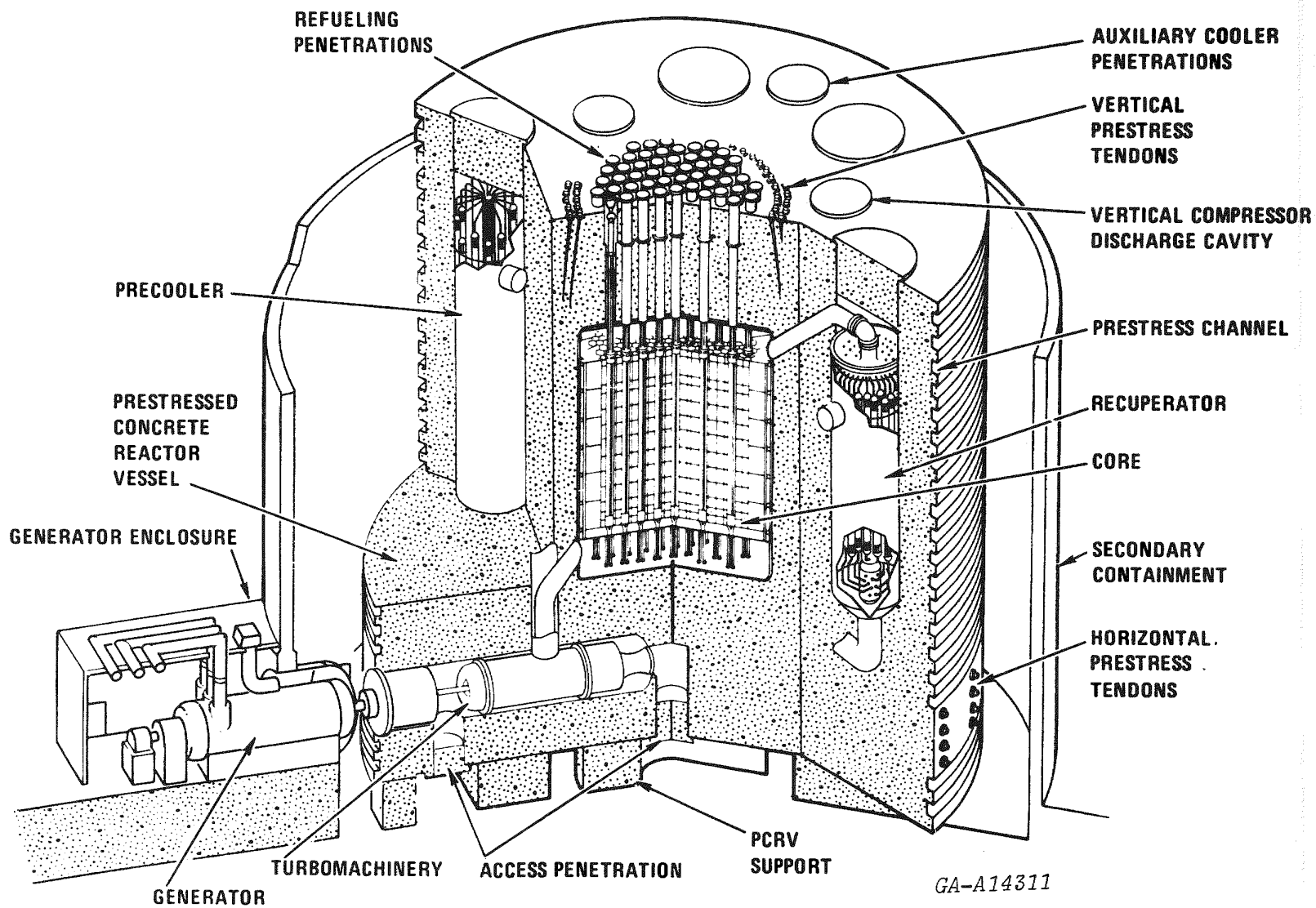


Fig. 4.28 Simplified 3-Loop GT-HTGR Configuration

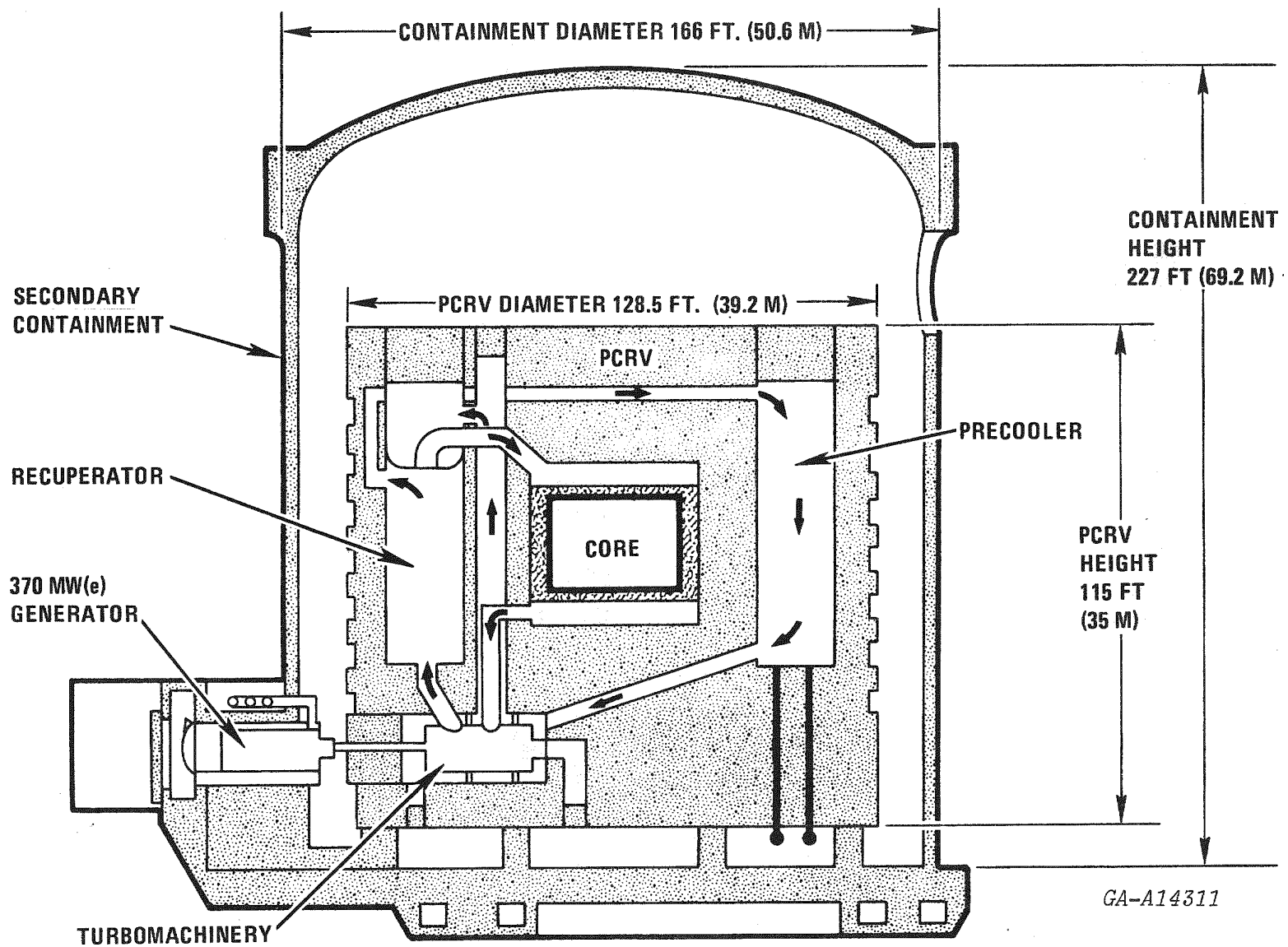


Fig. 4.29 Integrated Plant Configuration

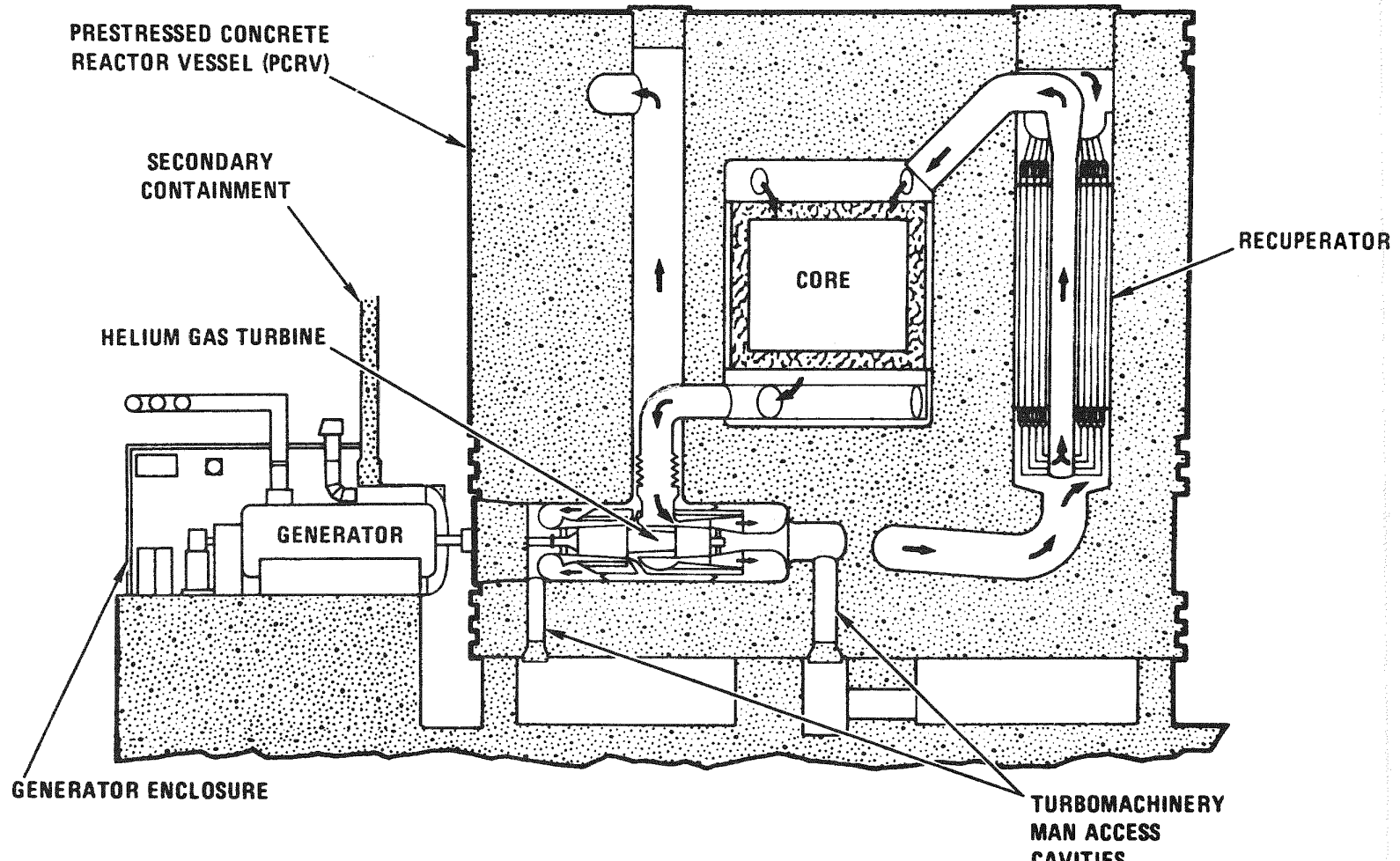
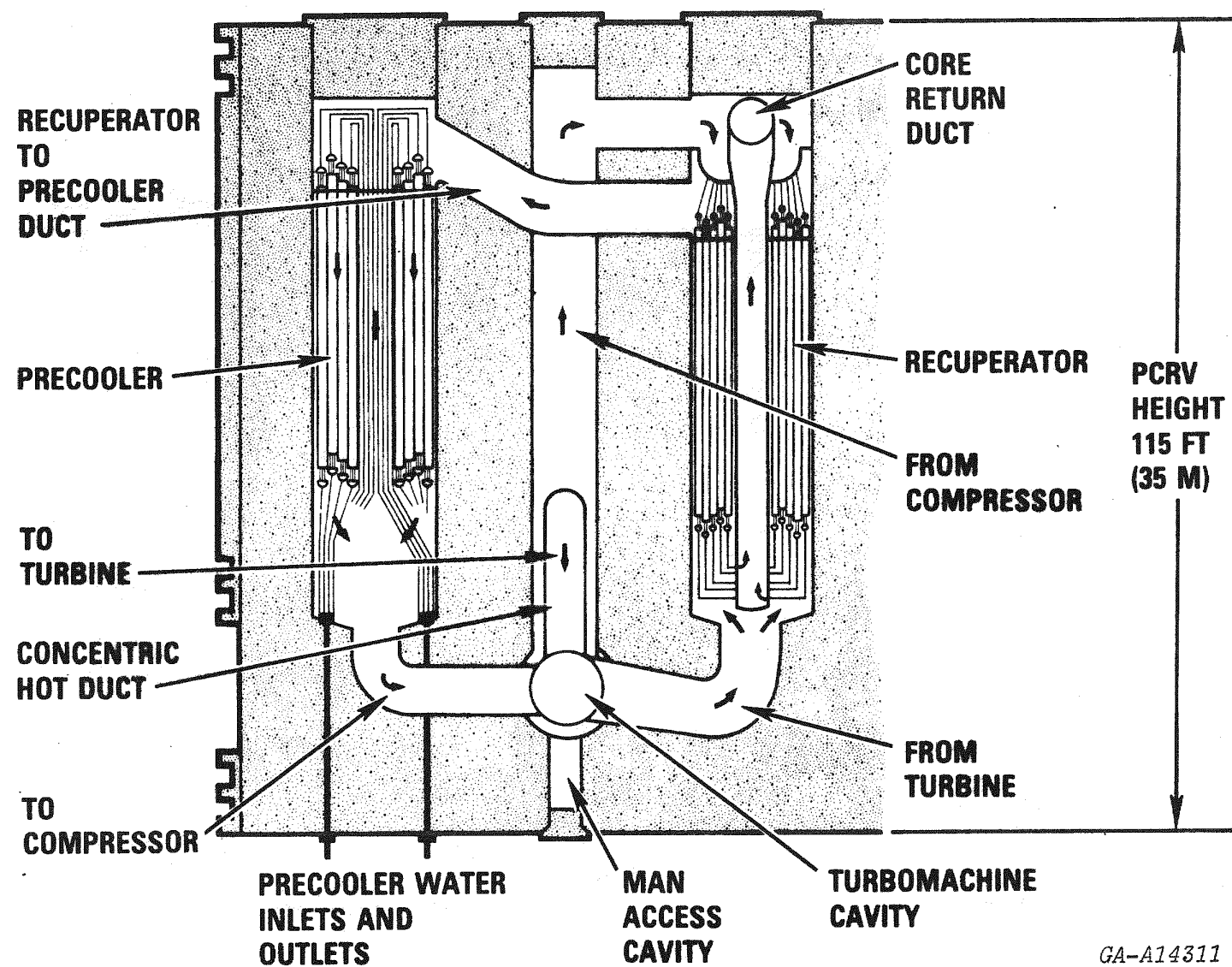


Fig. 4.30 View Through Power Conversion Loop



GA-A14311

Fig. 4.31 Elevation Through PCL

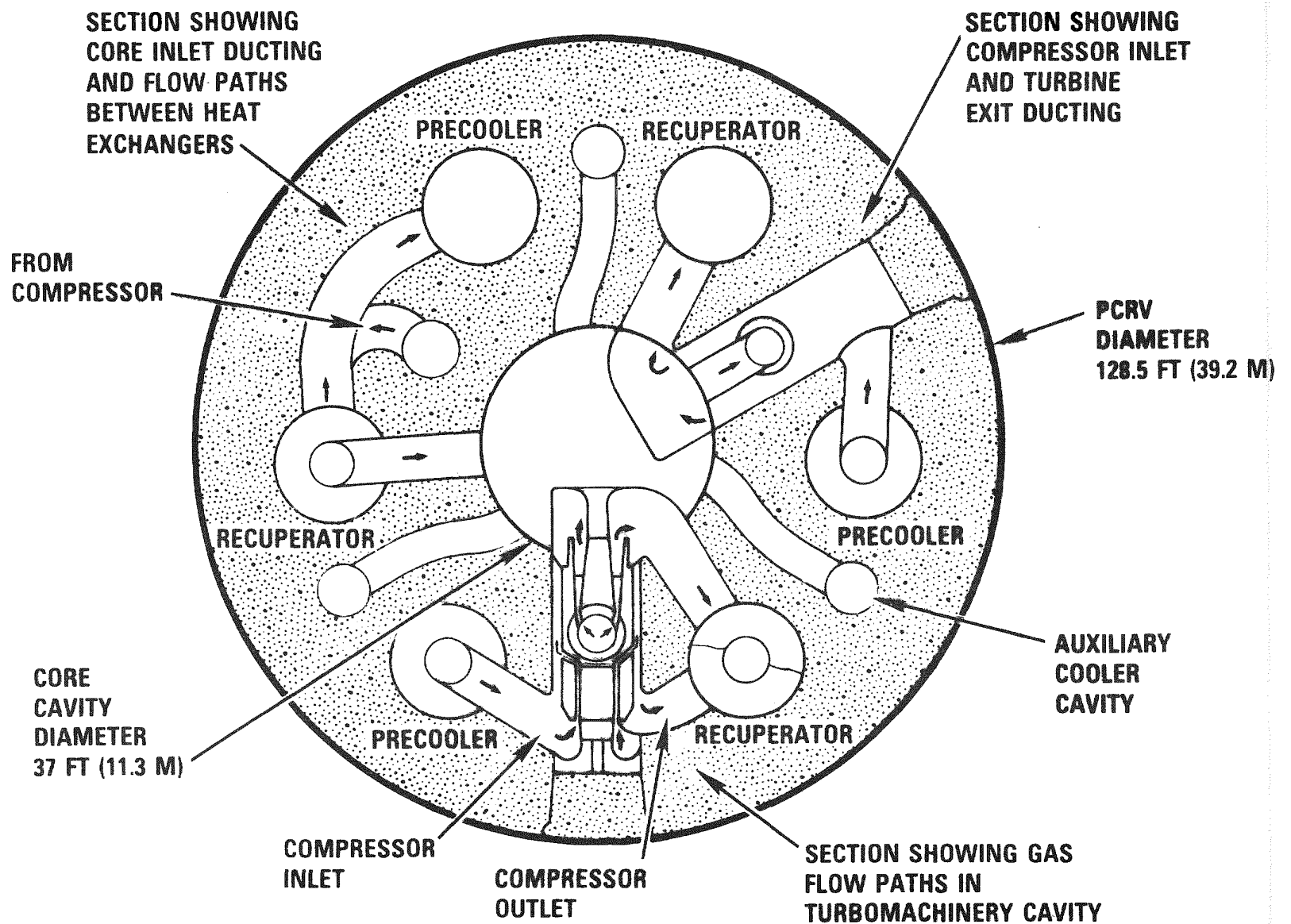
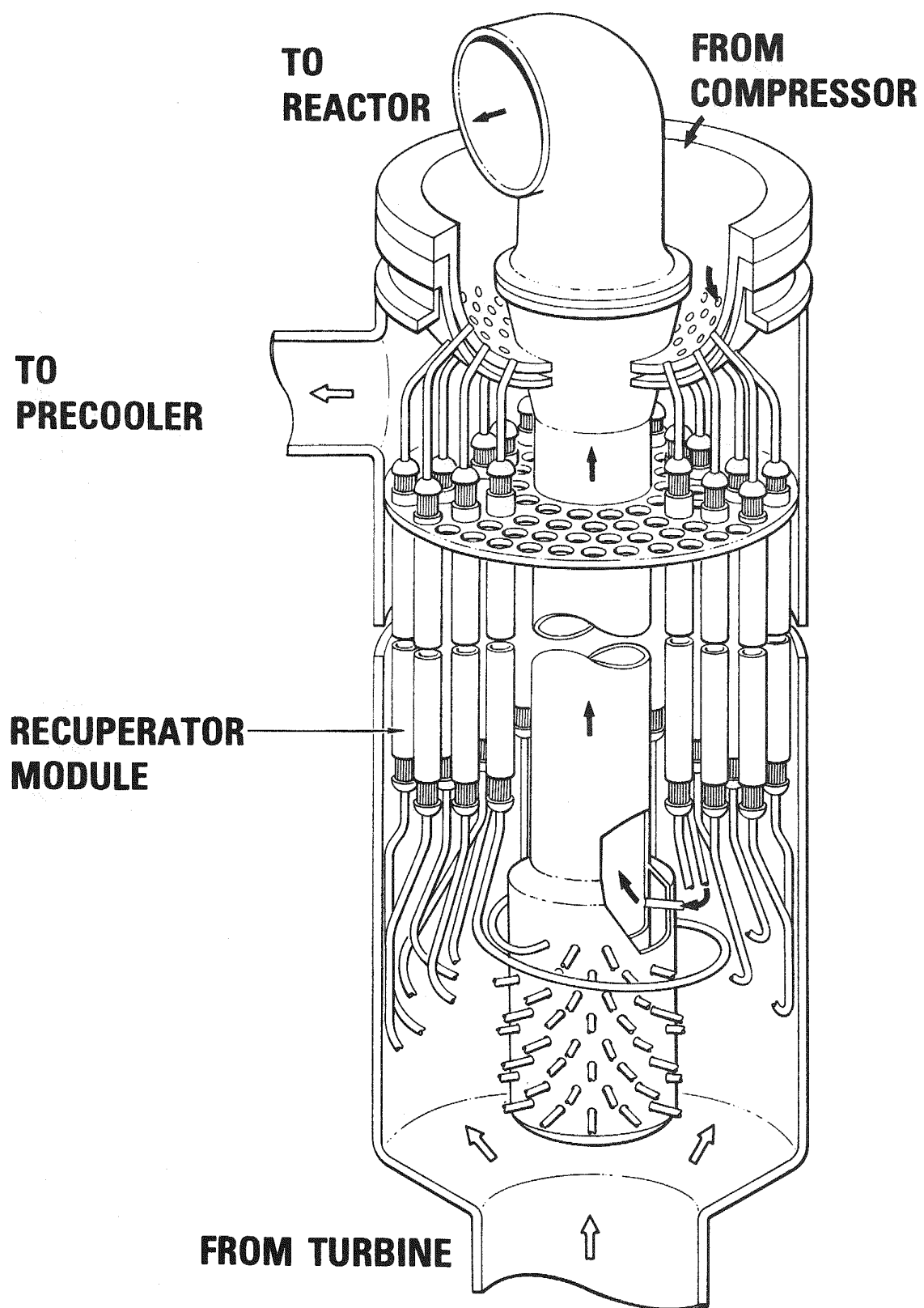


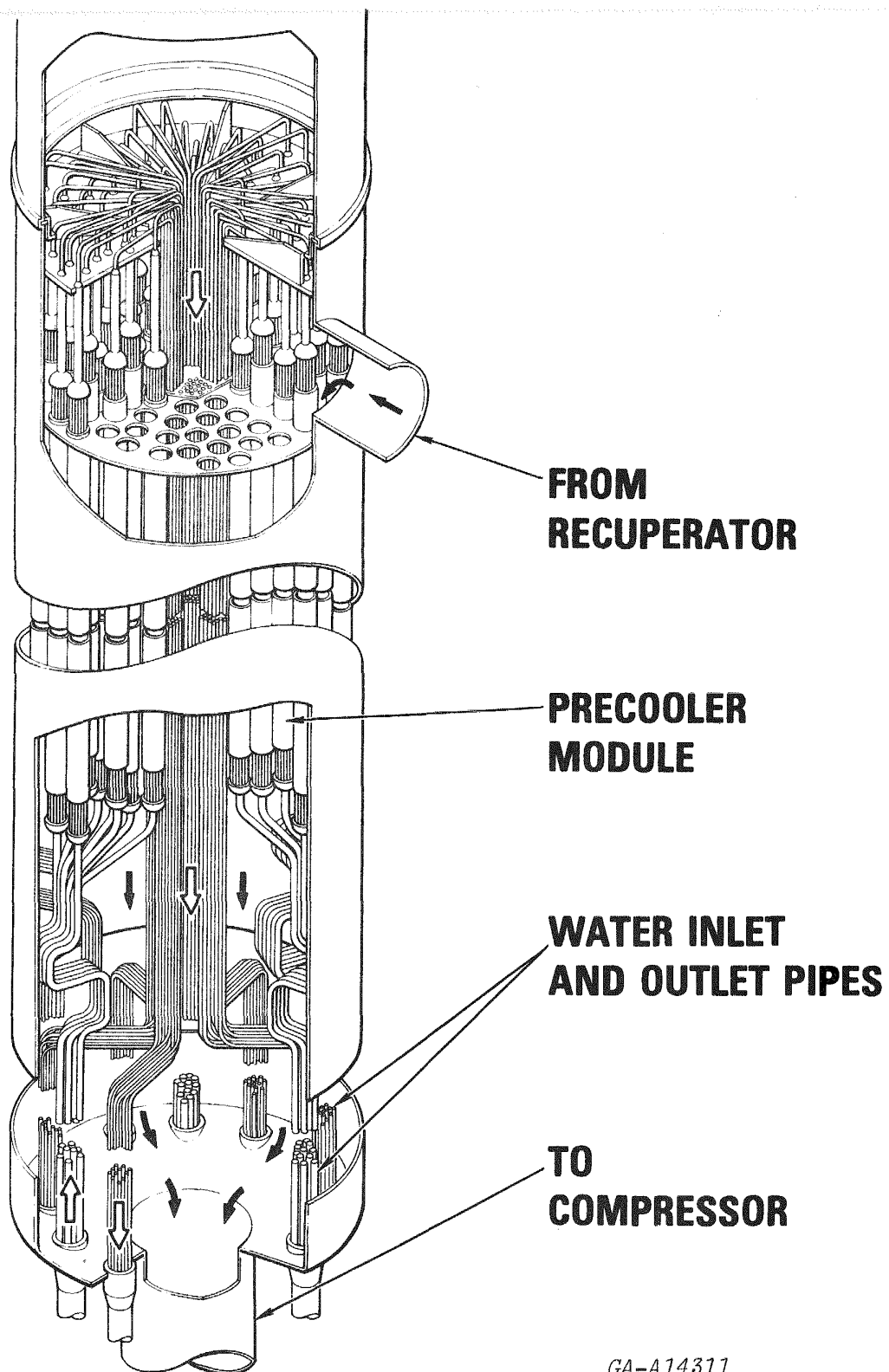
Fig. 4.32 Plan View of PCRV

GA-A14311



GA-A14311

Fig. 4.33 Recuperator Assembly



GA-A14311

Fig. 4.34 Precooler Assembly

Table 4.6

SUMMARY OF HEAT EXCHANGER PRELIMINARY DESIGNS FOR GAS TURBINE HTGR POWER PLANT

Exchanger	Recuperator	Precooler
Type		
Number per plant	3	3
Matrix type	Tubular	Tubular
Flow configuration	Counterflow	Counterflow
Construction	Modular	Modular
Thermal data		
Heat transfer rate, MW(t)	3094	1893
LMTD, °F (°C)	81.0 (45.5)	39.4 (21.9)
Effectiveness	0.890	0.972
Helium, ΔP/P	0.0266	0.0150
Surface geometry		
Tube outer diameter, in. (mm)	7/16 (11.1)	3/8 (9.5)
Tube wall thickness, in. (mm)	0.0375 (0.95)	0.049 (1.24)
Tube pitch arrangement	Triangular	Triangular
Pitch/diameter ratio	1.40	1.40
Maximum metal temp, °F (°C)	950 (510)	380 (193)
Material type	2-1/4 Cr - 1 Mo	Medium carbon steel
Tube bundle details		
Module diameter, in. (mm)	12.6 (320)	15.5 (394)
Modules/unit	180	96
Tubes/module	337	720
Effective tube length, ft (m)	42 (12.8)	41.5 (12.6)
Surface area/plant, ft ² (m ²)	883,000 (82,000)	842,000 (78,200)
Cavity diameter, ft (m)	18.0 (5.5)	17.5 (5.3)
Overall assembly		
Approximate overall length, ft (m)	65 (19.8)	73 (22.3)
Overall diameter, ft (m)	17.5 (5.3)	17.0 (5.2)
Module weight, lb (kg)	3630 (1647)	10,300 (4672)
Approximate assembly weight, tons	429	540

GA-A14311

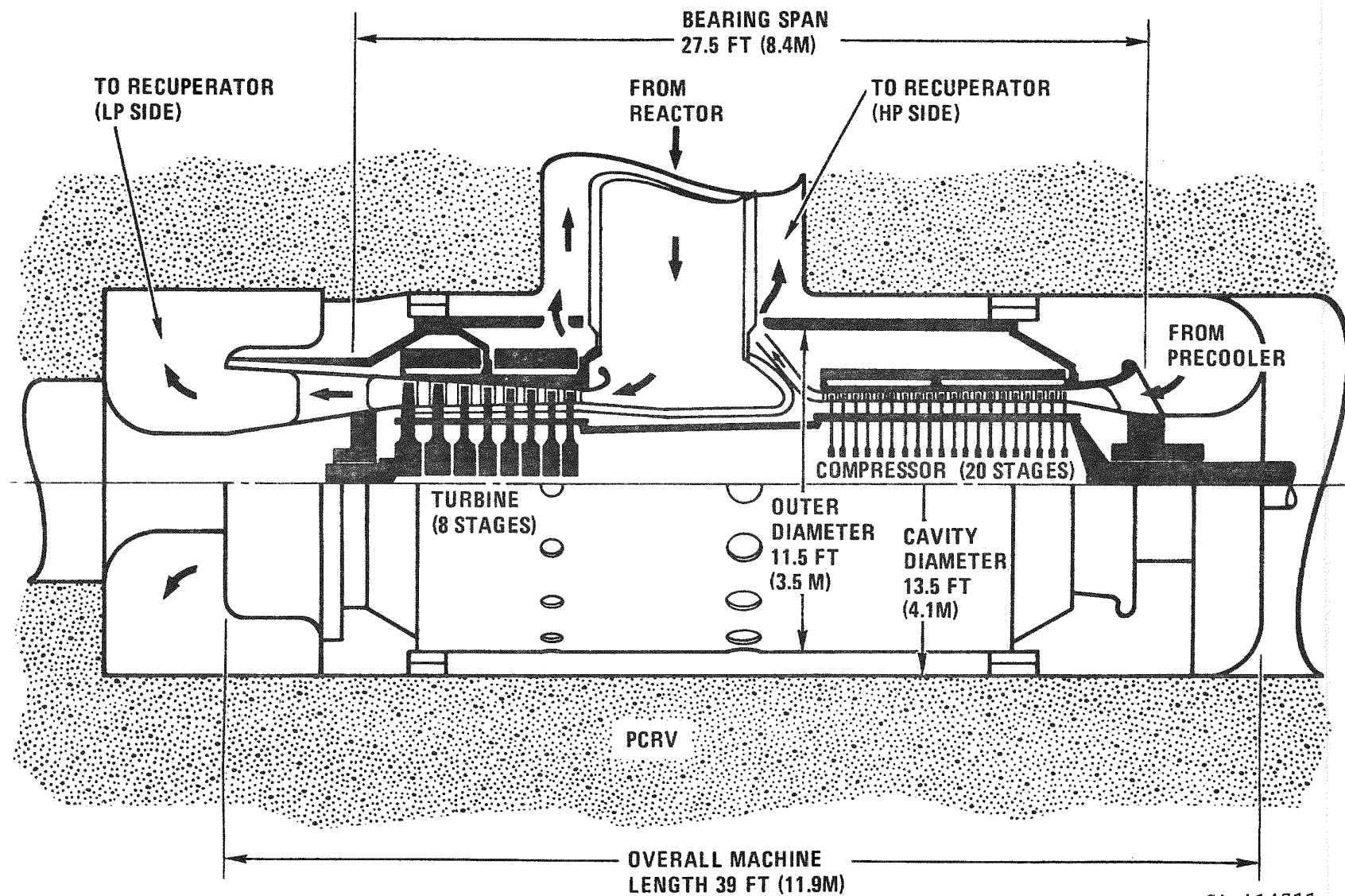


Fig. 4.35 Simplified Cross-Section of 370 MW(e) Helium Turbomachine

Table 4.7

TURBOMACHINE DESIGN DETAILS FOR 370 MW(e) HELIUM GAS TURBINE
(HORIZONTAL, SINGLE-SHAFT CONFIGURATION)

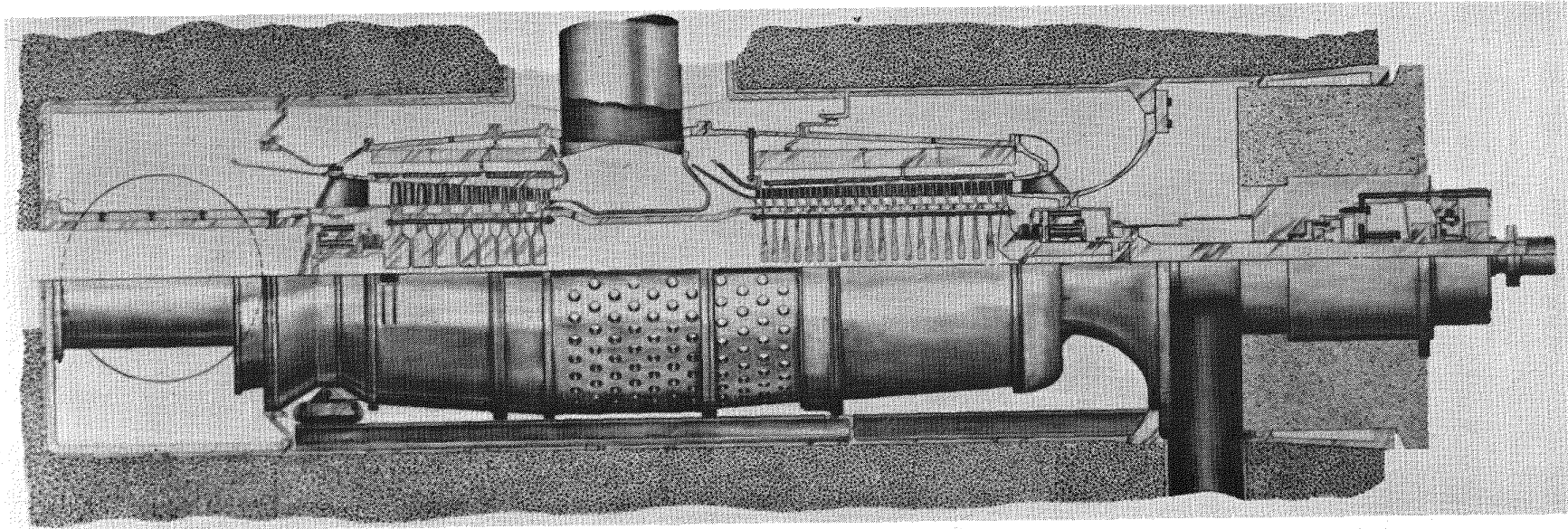
Machine	Compressor		Turbine	
Stage	First	Last	First	Last
Aerothermal data				
Rotational speed, rpm	3600		3600	
Inlet temperature, °F (°C)	95 (35)		1500 (815)	
Inlet pressure, psia (MPa)	426 (2.94)		950 (6.55)	
Pressure ratio	2.35		2.20	
Number of axial stages	20		8	
Axial velocity, ft/sec (m/sec)	650 (198)		850 (259)	
Maximum rotor mach number	0.39		0.29	
Stage loading factor	0.35		1.44	
Flow coefficient, V_a/U	0.60		0.75	
Reynolds number	6.4×10^6		2.3×10^6	
Degree of reaction	0.83		0.15 (root)	
Specific speed	250		120	
Specific diameter	0.90		0.95	
Cross power, MW	480		850	
Adiabatic efficiency	0.89		0.915	
Mechanical details and machine size				
Hub diameter, in. (m)	63.6 (1.62)	63.6 (1.62)	66.8 (1.7)	66.8 (1.7)
Tip diameter, in. (m)	73.7 (1.87)	70.2 (1.78)	78.0 (1.98)	83.5 (2.1)
Blade height, in. (mm)	5.05 (128)	3.30 (84)	5.6 (142)	8.35 (212)
Hub/tip ratio	0.863	0.905	0.855	0.80
Hub speed, ft/sec (m/sec)	1000 (305)	1000 (305)	1050 (320)	1050 (320)
Tip speed, ft/sec (m/sec)	1160 (354)	1104 (336)	1227 (374)	1310 (399)
Rotor blade chord, in. (mm)	3.90 (99)	3.20 (81)	4.0 (102)	4.8 (122)
Rotor aspect ratio	1.46	1.12	1.40	1.75
Rotor solidity	1.33	1.33	1.52	1.52
Number of rotors	65	83	80	67
Number of stators	81	106	57	51
Bending stress, lb/in. ² (MPa)	10,000 (69)	10,000 (69)	10,000 (69)	10,000 (69)
Centrifugal stress, lb/in. ² (MPa)	10,000 (69)	7100 (49)	12,000 (83)	16,100 (111)
Bladed length, in. (m)		124 (315)		80 (2.0)
Overall machine length, ft (m)			39.0 (11.9)	
Machine outer diameter, ft (m)			11.50 (3.50)	
Turbomachine weight, tons			295	

GA-A14317

or replacement. The turbine blading design is based on the utilization of existing nickel-base alloys and the stress levels are commensurate with a full plant operating life of 280,000 hours. From the more detailed view of the turbomachine shown on Fig. 4.36 it can be seen that the rotors of both the compressor and turbine are of bolted construction, the solid disks being held together with tie-bolts and located in accurate alignment. Incorporated in the structure of the turbomachine are disk catchers which will contain all the fragments associated with a disk failure up to 120% of the machine design speed. To be manufactured from laminated sheet, the formed cylindrical shields around the compressor and turbine can be clearly seen, and an appreciation of their magnitude is given by their combined weight which is on the order of 60 tons per turbomachine.

A summary of the salient features of the primary system for the plant configuration outlined above is given on Table 4.8, and from Table 4.1 it can be seen that this plant configuration has a power output of 1097 MW(e) and a station efficiency (dry-cooled) of 36.6%.

The following section gives a description of the current plant reference design which was established after in-depth cost optimization studies and extensive plant and component design work.



GA-A14311

Fig. 4.36 Overall View of 370 MW(e) Helium Turbomachine Installed In Horizontal Cavity

TABLE 4.8
GT-HTGR POWER PLANT SALIENT FEATURES OF PRIMARY SYSTEM

PLANT	NUMBER OF LOOPS LOOP RATING, MW(t) LOOP RATING, MW(e) TURBOMACHINERY ORIENTATION HEAT EXCHANGERS ORIENTATION	3 1000 370 HORIZONTAL VERTICAL
PCRV	DIAMETER, FT HEIGHT, FT HOT DUCT REPLACEABILITY MAN ACCESS FOR TURBOMACHINERY BEARING INSPECTION	128.5 115 YES YES
TURBOMACHINE	TYPE DIAMETER, FT LENGTH, FT APPROX. WEIGHT, TON	SINGLE - SHAFT 11.5 39 295
RECUPERATOR	NO. PER PLANT TYPE DIAMETER, FT LENGTH, FT APPROX. WEIGHT, TONS	3 MODULAR, AXIAL FLOW 17.5 65 475
PRECOOLER	NO. PER PLANT TYPE DIAMETER, FT LENGTH, FT APPROX. WEIGHT, TONS	3 MODULAR, AXIAL FLOW 17.5 73 540
PERFORMANCE (ISO RATING)	PLANT POWER MW(e) PLANT EFFICIENCY, %	1097 36.6

GA-A14311

REFERENCES

- 4.1 Adams, R. G., F. R. Bell, C. F. McDonald, and D. C. Morse, "HTGR Gas Turbine Power Plant Configuration Studies", ASME Paper No. 73-WA/Pwr-7.
- 4.2 Koutz, S. L., J. M. Krase, and L. Meyer, "HTGR Gas Turbine Power Plant Preliminary Design", ASME Paper No. 74-GT-104.
- 4.3 McDonald, C. F., R. G. Adams, F. R. Bell, and P. Fortescue, "Component Design Considerations for Gas Turbine HTGR Power Plant", ASME Paper No. 75-GT-67.
- 4.4 McDonald, C. F., P. Fortescue, and J. M. Krase, "Primary System Preliminary Design for Gas Turbine HTGR Power Plant", ASME Paper No. 76-GT-92.
- 4.5 McDonald, C. F., J. C. Bass, and H. Amtmann, "Primary System Design Studies for Advanced Direct Cycle Nuclear Gas Turbine Plant", Paper presented at ASME Gas Turbine Conference, Philadelphia, March 1977. (No. 77-GT-25).
- 4.6 Covert, R. E., J. M. Krase, and D. C. Morse, "Effect of Various Control Modes on the Steady-State Full and Part Load Performance of a Direct-Cycle Nuclear Gas Turbine Power Plant", ASME Paper No. 74-WA/GT-7.
- 4.7 Fortescue, P., "Advanced HTGR Systems", Paper presented at the Wingspread Workshop Conference, Racine, Wisconsin, May 14, 1975.
- 4.8 Fortescue, P., and R. N. Quade, "Direct-Cycle and Process Heat HTGR Development", Paper presented at ANS Topical Meeting on Gas-Cooled Reactors, Gatlinburg, Tennessee, May 8, 1974.
- 4.9 "Nuclear Gas Turbines", Proceedings of the International Conference organized by The British Nuclear Energy Society, London, April 8, 1970.
- 4.10 Waage, J. M., J. P. Gibbons, and K. W. Sieving, "Design of 2300 MW(e) Twin High Temperature Gas-Cooled Reactors for Philadelphia Electric", Proceedings of the American Power Conference, Vol. 34, pp.195-206, 1972.

5.0 GT-HTGR REFERENCE PLANT DESIGN

In 1975-76 studies of the GT-HTGR power plant were directed towards identification of a plant configuration with improved economic incentives over competing electric power plants. This section outlines the studies which led to the selection of the primary system for a plant with optimized parameters from the standpoint of minimum power generating cost. The studies outlined below led to changes in the PCRV geometry which had a significant impact by reduction in the size of the PCRV and attendant cost savings. Full details of this plant configuration are given in Ref. 5.1.

5.1 Optimization Studies

In the economic-performance and sensitivity studies analytical models of the major components and plant structures were generated, and an overall plant configuration and major cycle parameters selected to give minimum total cost of power. A summary of the parameters included in the optimization study is given in Table 5.1. With a turbine inlet temperature of 1562°F (850°C), a maximum system pressure of 1150 psia (7.93 MPa), and a compressor pressure ratio of 2.5, a plant efficiency of 40% is projected for the dry-cooled plant.

5.2 Thermodynamic Cycle and Performance

The plant design and performance data are based on a 3000 MW(t) reactor arrangement with a turbine inlet temperature of 1562°F (850°C), this representing a modest increase in the core outlet temperature that can be delivered now by HTGRs intended for steam application. This temperature is below the level where turbine blade cooling is necessary, and existing nickel-base alloys that are utilized in industrial open-cycle industrial gas turbines can be used. The salient cycle parameters are shown on Table 5.2 and the cycle diagram is shown on Fig. 5.1. For the given reactor outlet temperature the optimization studies identified the major cycle independent variables to give minimum power generating cost, and these are briefly discussed below.

Compared with previous studies the system maximum pressure was increased slightly to 1150 psia (7.93 MPa). This pressure level gives high gas density and compact turbomachinery, heat exchangers, and ducts, and is only a modest extension of PCRV structural design practice. The design point compressor pressure ratio was increased slightly to 2.50. With a recuperator effectiveness of 0.898, this pressure ratio is still slightly less than optimum for maximum efficiency, but it was chosen

TABLE 5.1
GT-HTGR PLANT OPTIMIZATION STUDIES

- COMPUTER PROGRAM CODER (COST OPTIMIZATION DESIGN EVALUATION ROUTINE)
 - A BASE-CASE/ALTERNATE-CASE APPROACH IS USED
 - BASE-CASE DESIGN IS DEFINED BY 350 DESIGN AND COST INPUT DATA
 - OPTIMIZATION FOR MINIMUM TOTAL TEST OF POWER
- THERMODYNAMIC, FLUID DYNAMIC, PERFORMANCE, COST, AND MECHANICAL DESIGN CRITERIA ARE EMBODIED IN SUBROUTINES FOR THE FOLLOWING AREAS:
 - PCRV
 - REACTOR CORE
 - TURBOMACHINERY
 - HEAT EXCHANGERS
 - SECONDARY CONTAINMENT BUILDING
- MAJOR DESIGN VARIABLES
 - REACTOR OUTLET TEMPERATURE
 - MAXIMUM HELIUM PRESSURE
 - COMPRESSOR PRESSURE RATIO
 - RECUPERATOR EFFECTIVENESS
 - PRECOOLER FLUID OUTLET TEMPERATURE

GA-A14311

Table 5.2 GT-HTGR Plant Cycle Parameters

Turbine Inlet Temperature, °F (°C)	1562 (850)
Compressor Pressure Ratio	2.50
Compressor Inlet Temperature, °F (°C)	79 (26)
Maximum System Pressure, psia (MPa)	1150 (7.93)
System Pressure Loss Ratio	0.0703
Recuperator Effectiveness	0.898
Cooling Water Outlet Temperature, °F (°C)	334 (168)
Turbine Isentropic Efficiency (across blading), %	91.8
Compressor Isentropic Efficiency (across blading), %	89.8
Turbine Disk Cooling Flow ^(a) , %	3.6
Turbomachine Bypass Leakage ^(a) , %	0.30
Recuperator Plus Precooler Bypass Leakage ^(a) , %	0.75
Generator Efficiency, %	98.8
Primary System Heat Loss, MW(t)	2 x 13.2
Station Auxiliary Power, MW(e)	2 x 10.5
Station Efficiency, %	40.0
Net Electrical Power, MW(e)	2 x 1200
Reactor Thermal Power, MW(t)	2 x 3000
Compressor Helium Flow Rate/Loop, 1b/sec (kg/sec)	1265 (574)

^(a) All bypass flows based on compressor flow rate.

GA-A14311

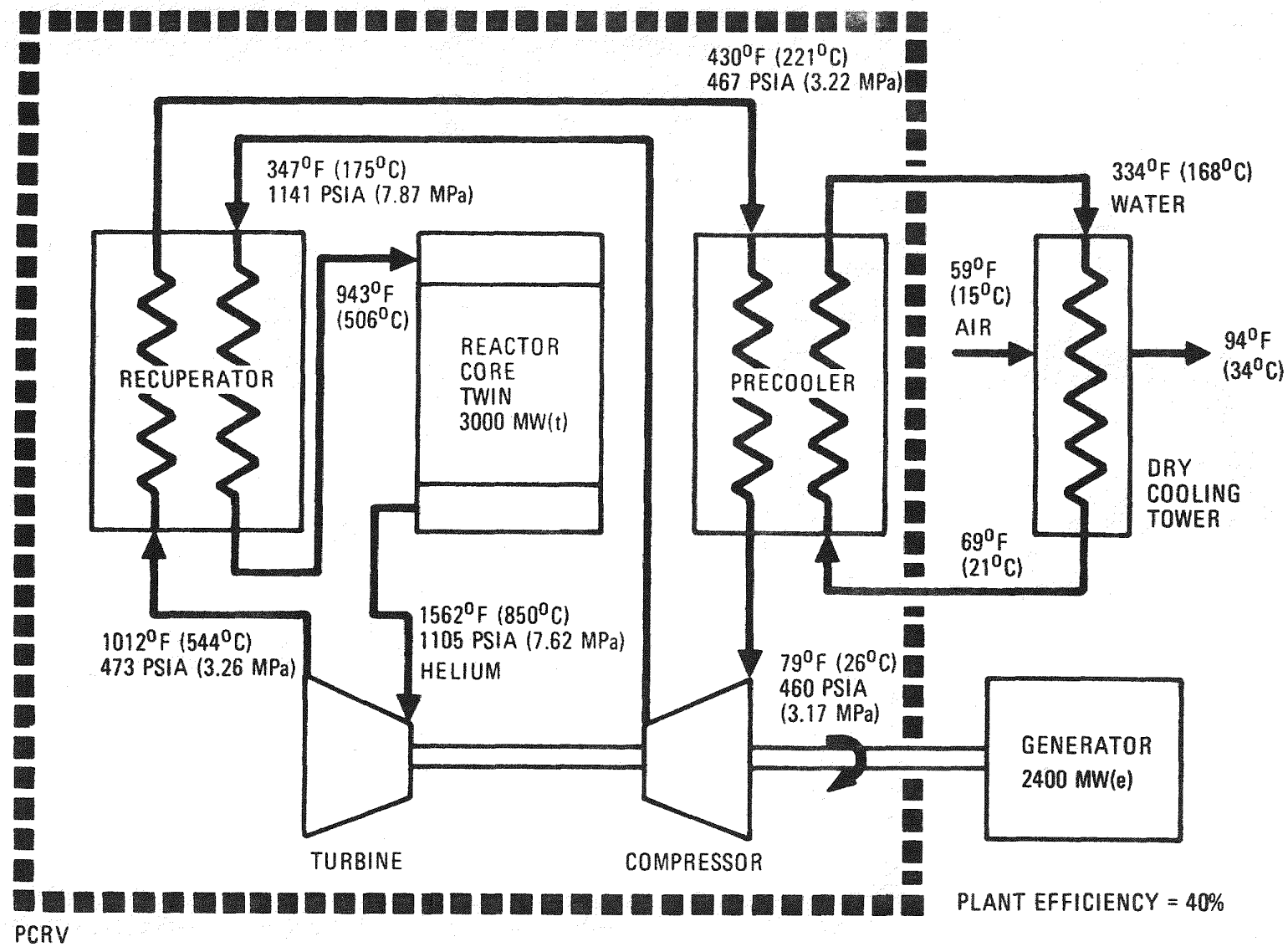


Fig. 5.1 Cycle Diagram for Dry-Cooled Twin Reactor Arrangement

to reduce the number of compressor and turbine stages which is strongly influenced by the low molecular weight, high specific heat, helium working fluid. In the plant and component layout studies emphasis was placed on selecting internal flow path geometries to minimize system pressure loss, since this has a significant effect on the performance of a closed-cycle gas turbine. The influences of the major parameters (from the optimization study) on GT-HTGR plant design and performance are summarized on Table 5.3.

5.3 Primary System Design

As for the previously described plant configuration an integrated primary system was adopted on the basis of both safety and economic considerations. The main features of the plant primary system are given on Table 5.4. A simplified isometric diagram of the GT-HTGR power plant primary system is shown in Fig. 5.2. All primary components, with the exception of the electric generators, are housed within the PCRV which is 118 ft. (36 m) in diameter and 111 ft. (34 m) high.

For the 3000 MW(t) core rating a preliminary primary system design embodying three gas turbine loops was selected. The resulting 400 MW(e), 60 Hz, turbomachine can be designed within current rail transportation limits, and can be accommodated in the PCRV horizontal cavities. For a machine of this rating a conservative design for the full life of the plant is possible with uncooled turbine blades made from existing nickel-base alloys. The reactor core in the GT-HTGR plant utilizes the same prismatic fuel and core configuration developed for the steam cycle HTGR. The core is contained in a central cavity 37 ft. (11.3 m) in diameter and 47 ft. (14.4 m) high. The power conversion loops are located symmetrically around the central core cavity as shown in the simplified plan view of the PCRV (Fig. 5.3). Each loop embodies a helium gas turbine, a recuperator, and precooler. The three turbomachines are oriented in a horizontal delta arrangement, and the heat exchangers are installed in vertical cavities arranged within the PCRV wall, two for each loop. The components are connected by large internal ducts within the PCRV. The internal surfaces of all PCRV cavities and ducts are lined with an impermeable steel membrane and covered with a thermal barrier designed to limit system heat losses and control concrete temperatures.

The horizontal turbomachine cavities are located directly below their associated loop heat exchangers, with the axis of the cavity oriented in a chordal direction rather than radial as reported for the previous plant reference design. This was a significant change permitting a reduction in vessel size since the length

TABLE 5.3

INFLUENCE OF MAJOR PARAMETERS (FROM OPTIMIZATION STUDY) ON PRIMARY SYSTEM DESIGN

REACTOR OUTLET TEMPERATURE INCREASE FROM 815°C (1500°F) TO
850°C (1562°F)

INCREASED PLANT EFFICIENCY
SAME MAXIMUM FUEL PARTICLE TEMPERATURE
UNCOOLED TURBINE BLADES RETAINED UTILIZING EXISTING
NICKEL-BASE ALLOYS
FERRITIC RECUPERATOR MATERIAL RETAINED
CONVENTIONAL HTGR TYPE THERMAL BARRIER RETAINED
850°C COMMON WITH EUROPEAN HHT PROGRAM

SYSTEM MAXIMUM PRESSURE INCREASE FROM 1000 PSIA (6.89 MPa) TO
1150 PSIA (7.93 MPa)

STRUCTURAL FEASIBILITY OF PCRV VERIFIED
REDUCED PRESSURE LOSS ($\Delta P/P$) IN DUCTS, HEAT EXCHANGERS
AND CORE
MORE COMPACT COMPONENTS

COMPRESSOR PRESSURE RATIO INCREASE FROM 2.35 TO 2.50

REDUCES HELIUM MASS FLOW RATE
UTILIZING ADVANCED TURBOMACHINERY TECHNOLOGY, THE
COMPRESSOR AND TURBINE EFFICIENCY GOALS CAN BE
REALIZED WITHOUT INCREASING THE NUMBER OF STAGES.

RECUPERATOR EFFECTIVENESS INCREASE FROM 0.89 TO 0.898

MODEST INCREASE CONTRIBUTES TO HIGHER PLANT EFFICIENCY
EXCHANGER ENVELOPE REDUCED WITH IMPROVED DESIGN

POWER CONVERSION LOOP RATING REMAINS THE SAME AT 1000 MW(t)

COMPONENT FABRICATION AND TRANSPORTATION LIMIT
CONSIDERATIONS
PERMITS USE OF EXISTING MATERIALS FOR TURBINE BLADING
IMPACT ON COMPONENT TESTING REQUIREMENTS
CONSTRUCTION SCHEDULE AND BOP COST
DELTA ARRANGEMENT OF PCRV FOR 3-LOOP (3000 MW(t) CORE)
RESULTS IN SIGNIFICANT COST SAVINGS

GA-A14311

TABLE 5.4
FEATURES OF GT-HTGR PLANT PRIMARY SYSTEM

- 40 PERCENT EFFICIENT PLANT WITH DRY COOLING
- NEW REFERENCE DESIGN BASED ON:
 - INTEGRATED CONFIGURATION
 - MULTIPLE GAS TURBINE LOOPS
 - NON-INTERCOOLED CYCLE
 - HIGH DEGREE OF HEAT RECUPERATION
 - DRY-COOLING
 - OPTIONAL WET-DRY COOLING
- DELTA ARRANGEMENT OFFERS THE FOLLOWING ADVANTAGES:
 - MINIMUM PCRV DIMENSIONS
 - MINIMUM SYSTEM PRESSURE LOSS
 - FEWER AND LESS COMPLICATED PRESTRESSING TENDONS
 - EASIER MAINTENANCE OF TURBOMACHINE AND HEAT EXCHANGERS
 - LOW POWER GENERATION COST

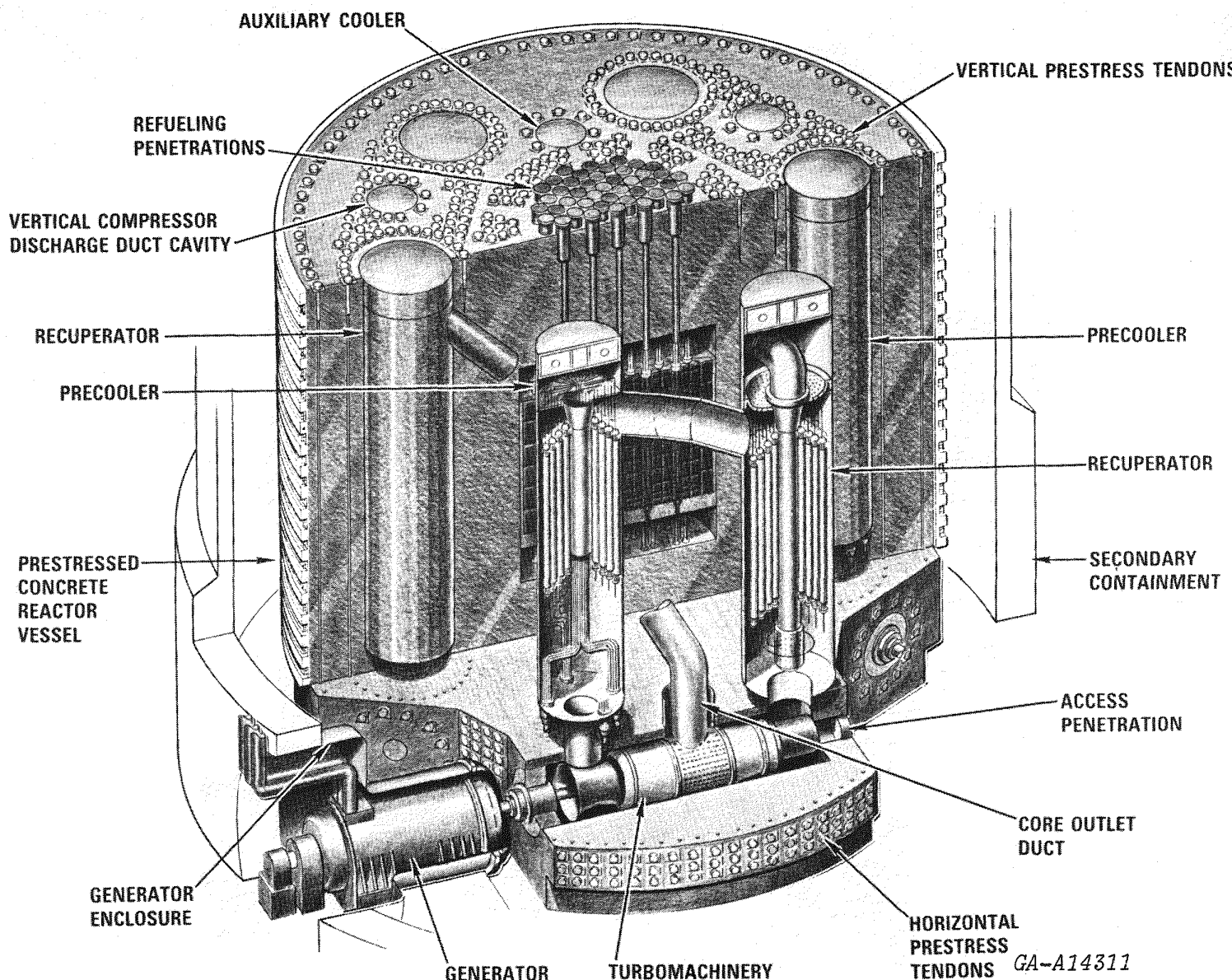


Fig. 5.2 3-Loop Integrated Plant Reference Design

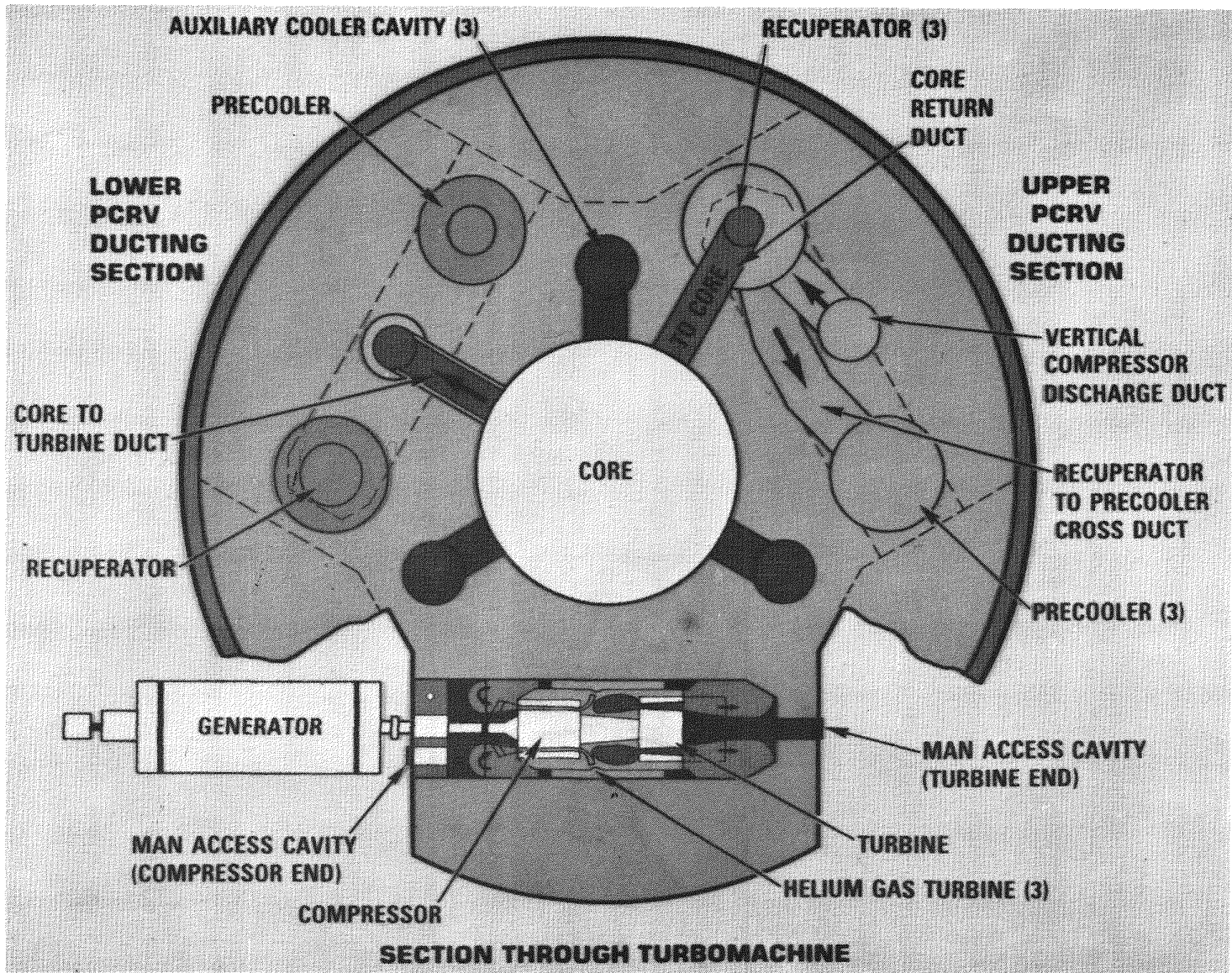


Fig. 5.3 Plan View of PCRV

GA-A14311

of the turbomachine no longer controls the diameter of the PCRV. This arrangement places the recuperator directly above the turbine exhaust, and the precooler above the compressor inlet and provides easy access to both ends of the turbomachine.

A simplified (and schematically developed) vertical section through a power conversion loop is shown on Fig. 5.4. Elevation views through the PCRV are given on Figs. 5.5 and 5.6 to show the core exit and inlet ducts, respectively. Referring to Figs. 5.3 through 5.6, the flow paths for each power conversion loop are as follows. The helium coolant flows downward through the reactor core, into the core outlet plenum. The hot gas from the core outlet plenum flows radially outward through the three large ducts to the turbine inlet which is located in the center of the machine. The vertical portion of the core outlet duct is concentric with the compressor outlet duct. The gas flows through the turbine and exits into a plenum located directly under the recuperator. It then flows upward through a short duct and enters the recuperator on the shell side, exiting below the upper recuperator tube sheet into the recuperator-precooler cross duct. The warm gas from the recuperator flows through the horizontal cross duct into the shell side of the water cooled precooler where its temperature is reduced further. The cool gas from the precooler flows downward through another short vertical duct into the compressor inlet plenum and passes through the compressor to exit near the center of the machine. High pressure compressor outlet gas then flows upward through a vertical duct to enter the inlet of the recuperator on the tube side. It flows downward through the tubes picking up heat from the shell side gas and exits into a central return duct at the bottom of the recuperator. The gas then returns upward through the central duct and enters the core inlet plenum through the inclined radial ducts at the top of the core cavity.

Although the reference design outlined in this paper is a three loop configuration, other reactor layouts with from one to four loops have been made using this basic arrangement. These have been investigated for use at core power levels of from 1000 MW(t) to 4000 MW(t). The plan view of a four loop plant for a 4000 MW(t) reactor is shown on Fig. 5.7.

There are several reasons that the non-radial or delta arrangement was selected for the reference plant design. Among them are:

Minimum loop pressure drop

Minimum thermal barrier cost

Easier maintenance of turbomachine and heat exchangers

Fewer and less complicated prestressing tendons

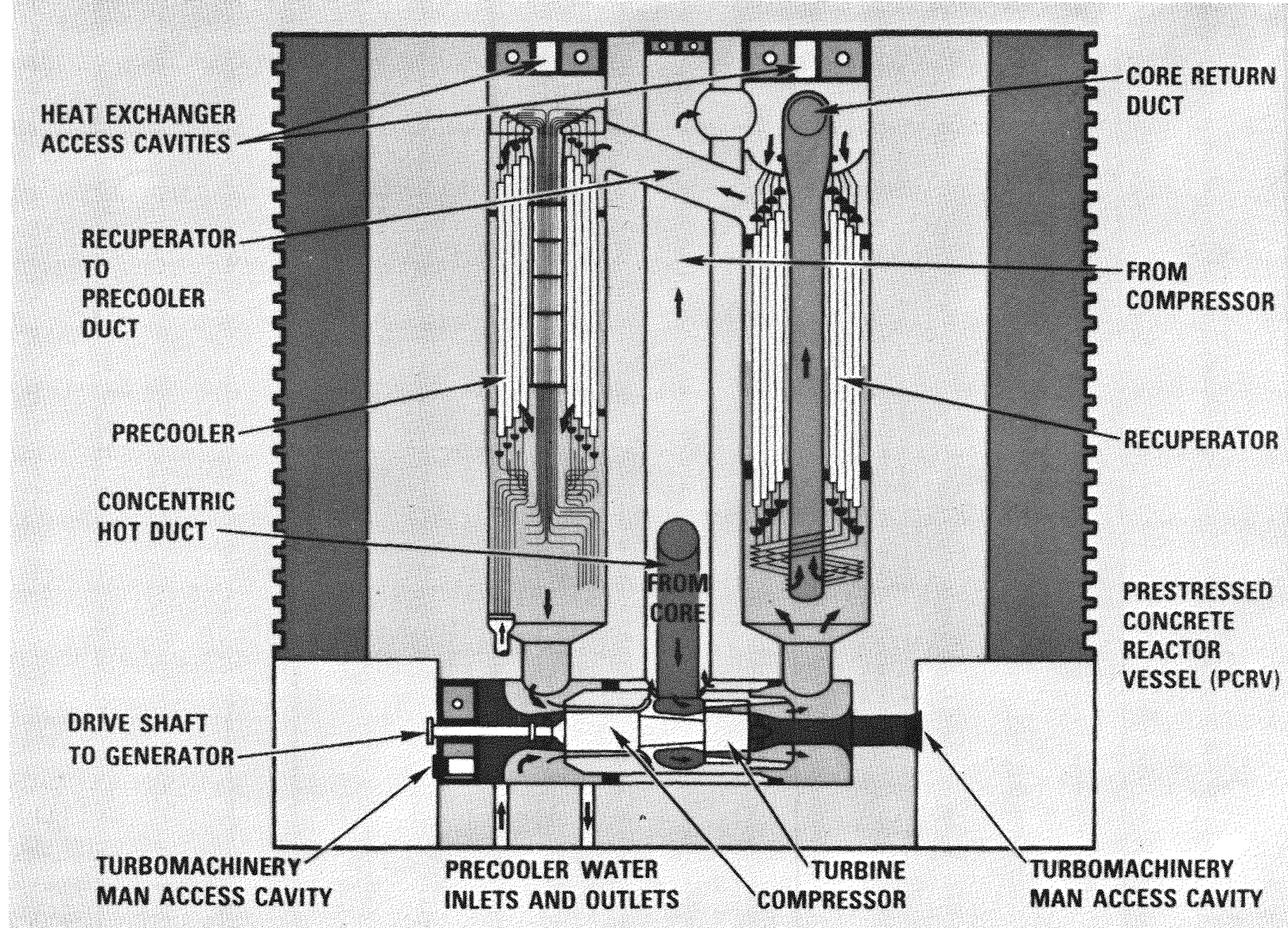
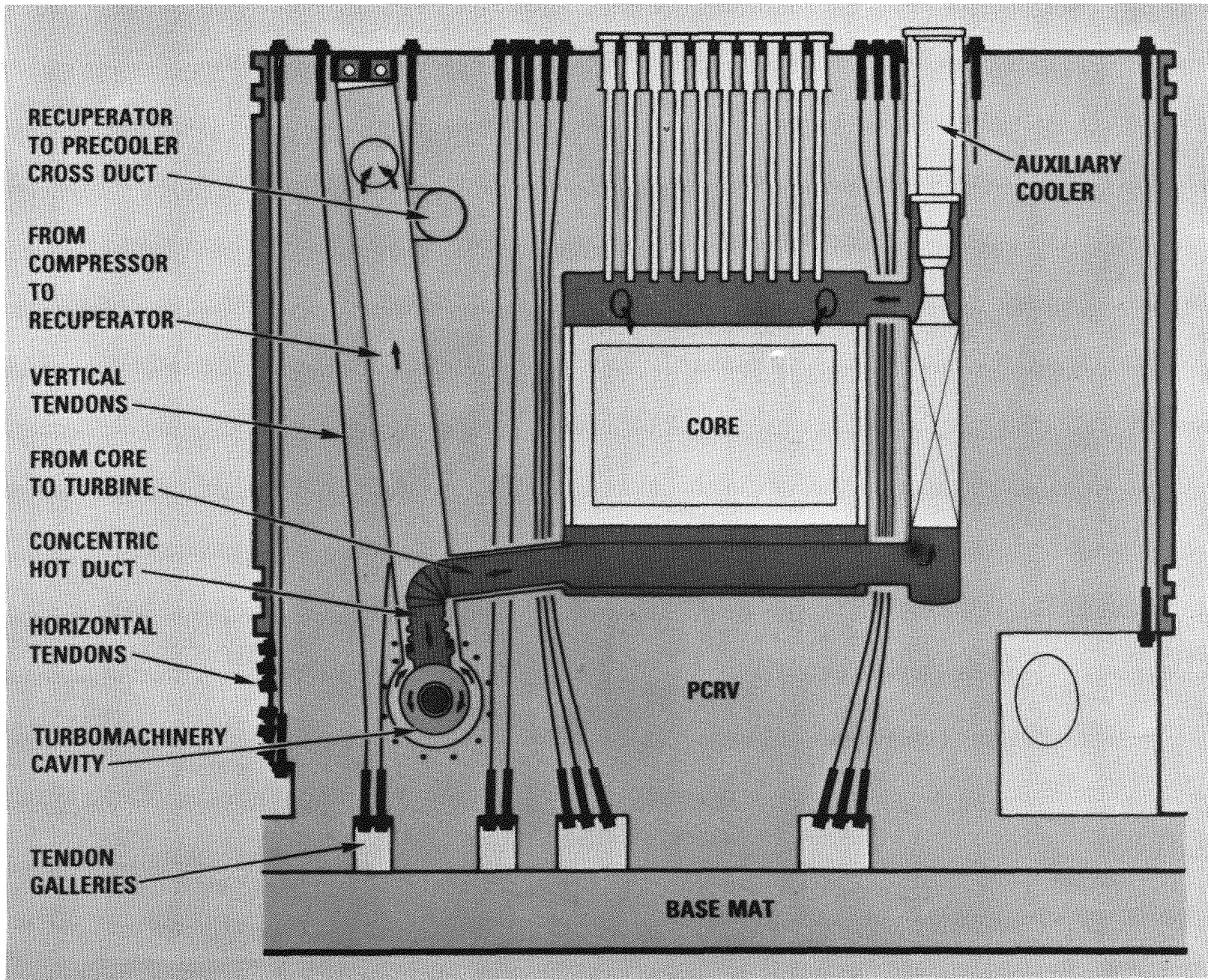


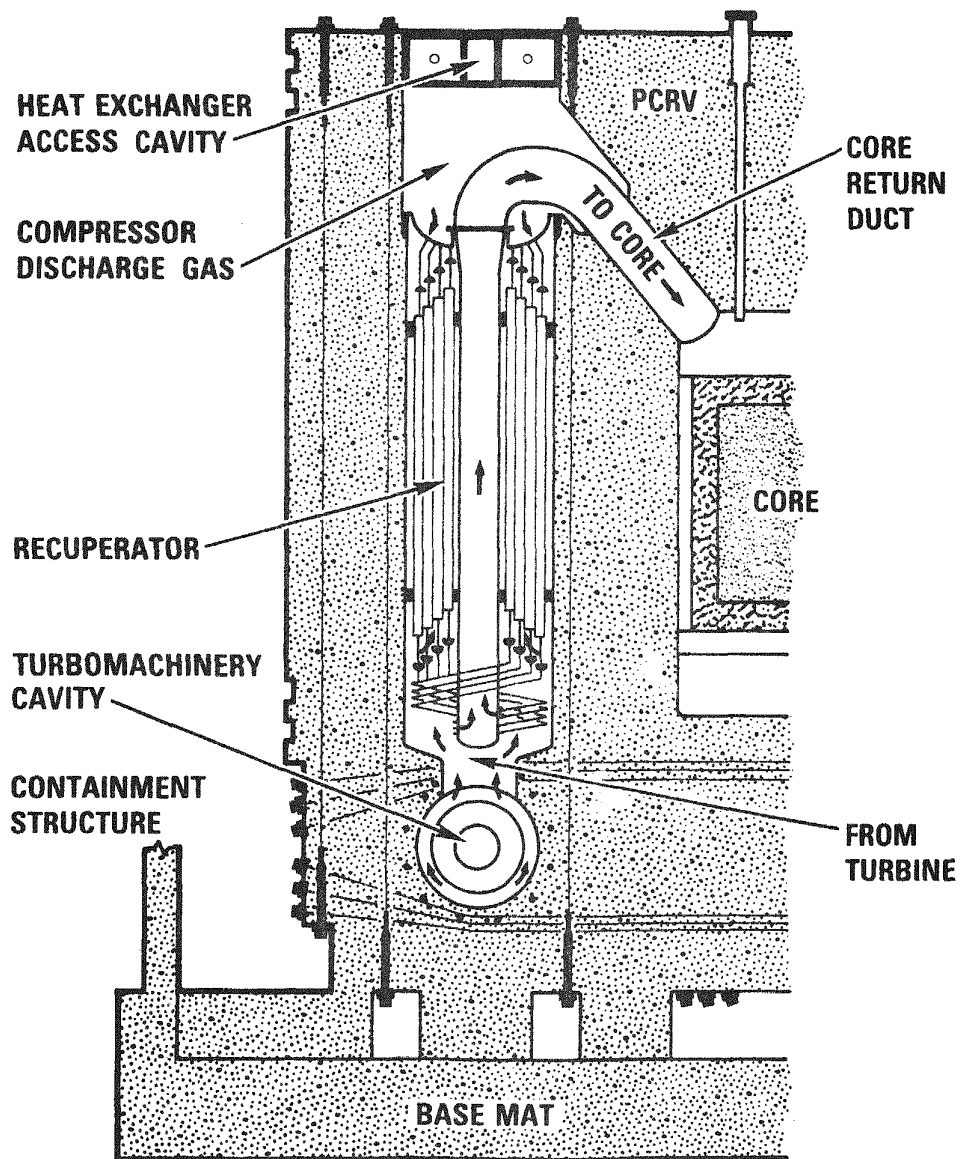
Fig. 5.4 Elevation View through PCL

GA-A14311



GA-A14311

Fig. 5.5 Elevation View Through PCRV



GA-A14311

Fig. 5.6 Section Through PCRV

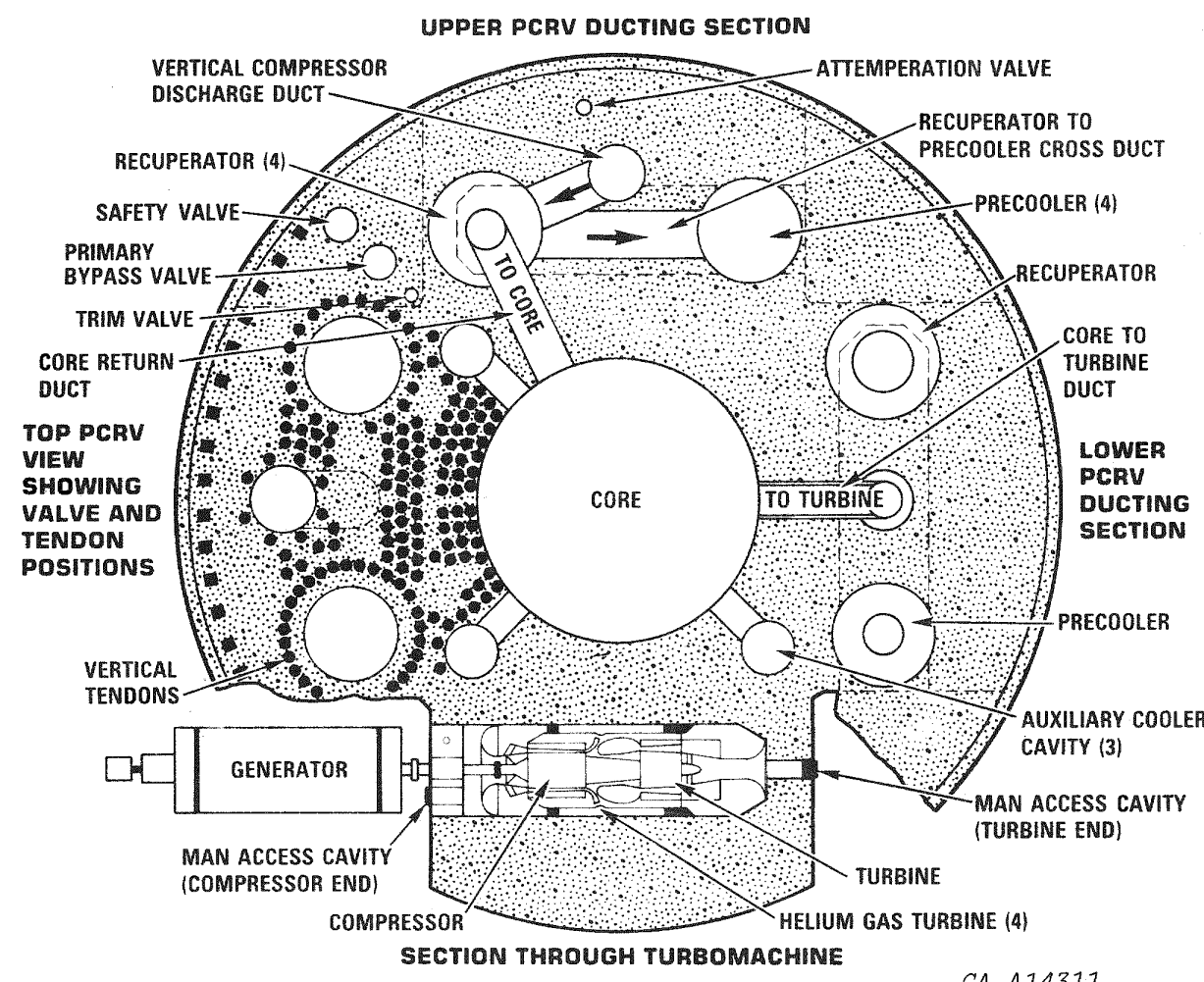


Fig. 5.7 Plan View of 4-Loop Configuration

Minimum PCRV dimensions

Provision for turbomachine growth

These advantages result in lower cost and increased cycle efficiency.

A summary of the main features of the primary system and power conversion loop is given in Table 5.5. Establishing the foregoing primary system preliminary design involved analyses and designs of the structures and major components to establish the internal gas flow path geometries for the selected integrated plant configuration. Significant aspects of the PCRV and major component designs are briefly outlined in the following sections.

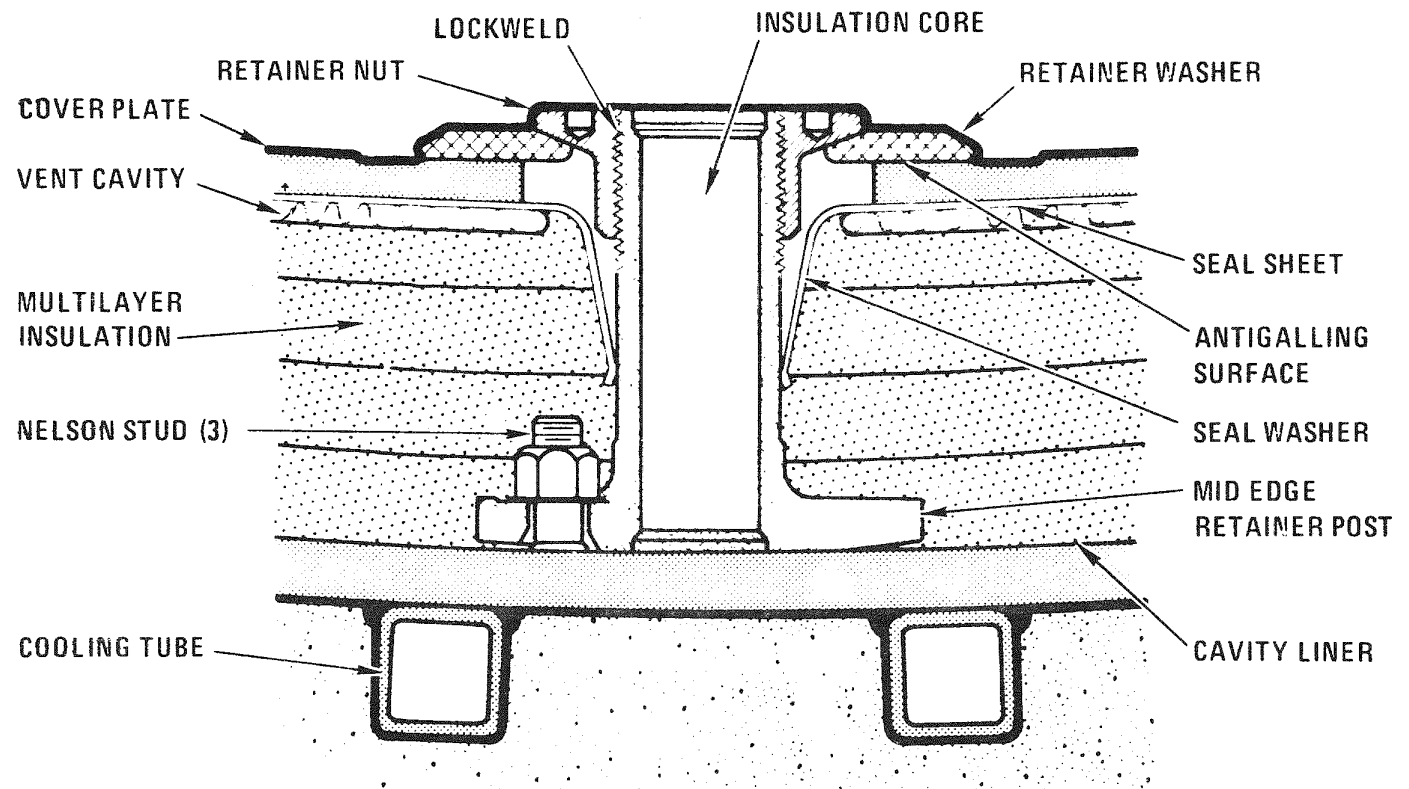
5.4 Prestressed Concrete Reactor Vessel (PCRV)

Criteria, design methods, and structural principles for the PCRV used in the GT-HTGR are essentially the same as those used for the steam cycle HTGR. Moreover, a specific PCRV design has been established due to the higher maximum system operating pressure, and the inclusion of the delta array of horizontal turbomachine cavities.

The PCRV is constructed of high strength concrete reinforced with steel bars. The PCRV is prestressed by three independent prestressing systems, (1) longitudinal prestressing system (LPS) which consists of tendons arranged around the cavities and ducts to counteract the cavity and duct pressures in the longitudinal direction, (2) circumferential prestressing system (CPS) which consists of multi-layered bands of wire strands wound under tension into channels precast in the surface of the vessel walls, and (3) a system of diagonal tendons which replace the wire winding of the CPS in the area of the horizontal T.M. cavities. The concrete walls and head sections are constructed around carbon steel liners for cavities and ducting. These liners serve as leak tight membranes to contain the reactor coolant within the PCRV cavities. The liners are anchored to the concrete by studs welded to the liners and embedded in the concrete. Operation of the PCRV requires control of its temperature environment at all times. This is achieved through temperature control of cooling water flowing through cooling tubes welded to the concrete side of the liner. In turn, the liner is protected from the high-temperature helium by a thermal barrier, which consists of special insulation. The thermal barrier consists in general of several layers of fibrous insulation placed adjacent to the cavity or duct liners, a layer of metallic screen material, a metallic seal sheet, and a metallic cover plate as shown on Fig. 5.8. The cover plate, which contains a number of small vent holes to allow the thermal barrier to vent during a rapid depressurization,

Table 5.5 PRIMARY SYSTEM SUMMARY FOR 3000 MW(t) TWIN ARRANGEMENT DRY-COOLED GT-HTGR PLANT

PLANT ARRANGEMENT	Reactor Thermal Rating, MW(t) Number of Reactors per Plant Heat Rejection Reactor Outlet Temperature, °F (°C) Power Conversion Loop Rating, MW(t) Number of Primary System Loops per Reactor	3000 Twin Arrangement Dry-Cooled Plant 1562 (850) 1000 3
PCRV	Arrangement Diameter, ft (m) Height, ft (m) Hot Duct Replaceability Man Access for Turbomachine Bearing Inspection Maximum System Pressure, psia (MPa)	Delta 118 (36) 111 (34.1) Yes Yes 1150 (7.93)
TURBOMACHINE	Turbomachine Type Compressor/Turbine Stages Compressor Pressure Ratio Generator Drive End Overall Diameter, ft (m) Overall Length, ft (m) Approx. Assembly Weight, Tons (Kg) Number of Journal Bearings Thrust Bearing Location	Single Shaft 18/8 2.50 Compressor 11.5 (3.5) 37 (11.3) 305 (276,800) 2 (tilting pad) External to PCRV
RECUPERATOR	Type (Modular Construction) Number per Reactor Overall Diameter, ft (m) Overall Length, ft (m) Assembly Weight, Tons (Kg) Tube Material Type ASME Code Class Fabrication Location	Tubular, Axial-Flow 3 16.75 (5.1) 62.0 (18.9) 474 (430,000) Ferritic, 2½ Cr-1 Mo Section VIII Factory
PRECOOLER	Type (Modular Construction) Number per Reactor Coolant Fluid Overall Diameter, ft (m) Overall Length, ft (m) Assembly Weight, Tons (Kg) Tube Material Type ASME Code Class Fabrication Location	Tubular, Axial-Flow 3 Water (Single Phase) 15.5 (4.72) 73 (22.3) 445 (404,000) Medium Carbon Steel Section VIII Factory
PERFORMANCE (ISO CONDITIONS)	Total Plant Power, MW(e) Plant Efficiency, %	2400 40.0



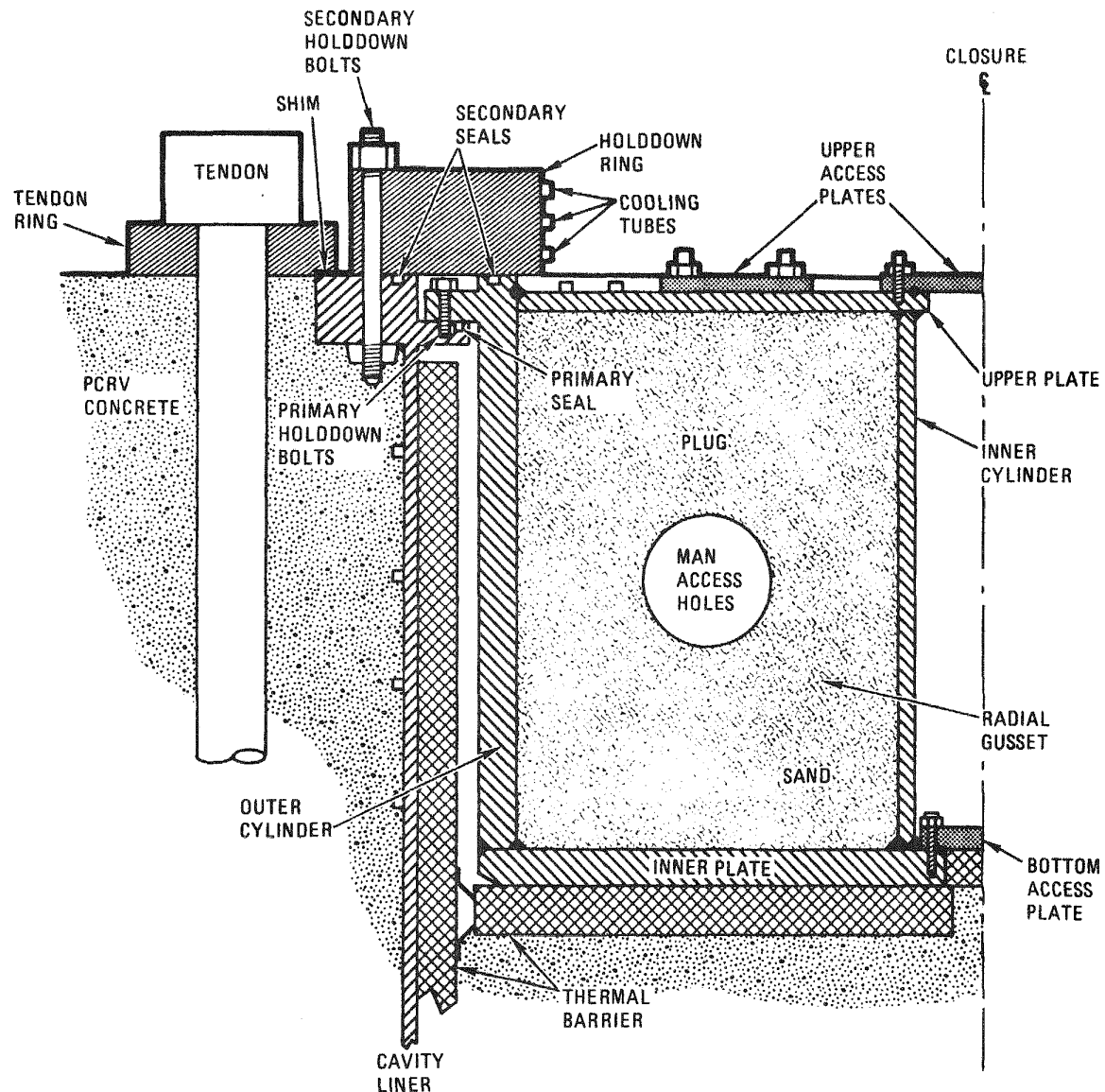
GA-A14311

Fig. 5.8 View of Typical Thermal Barrier for Main Cavities of GT-HTGR Plant

is held in place by one central fastener and eight edge fasteners which span the extension gap between adjacent cover plates.

The minimum height of the PCRV is determined by the core cavity height and the thickness of top and bottom heads. Important factors for the overall height of the PCRV of each configuration are the arrangement and dimensional requirements of the power conversion loop components, and in particular the placement of the horizontal turbomachine cavities directly under the heat exchanger cavities. An advantage of the delta arrangement is that the vertical tendons serve both the heat exchanger and turbomachine cavities, and this results in a cost savings because of the reduction in number of tendons. The delta arrangement, in which the turbomachinery cavities are placed into the wall section, and not under the core cavity as in previous designs, allows a minimum bottom head thickness and therefore a minimum PCRV height. The structural adequacy of the delta PCRV design approach has been demonstrated using three dimensional finite element elastic stress analysis. Each of the major cavities has a closure plug to facilitate installation and removal of the major components. The design concept of a typical steel closure assembly is shown in Fig. 5.9. The steel structure is substantially hollow, being formed of radial gussets covered by inner and outer circular plates and cylinders. During plant operation, the closure would be filled with boronated sand to improve its shielding characteristics; during periods of closure removal or in-service inspection of internal welds, the sand would be removed by a vacuum process. The plug and liner holddown includes the use of the vertical tendons surrounding the cavity to directly restrain the liner flange through an overlapping tendon ring. The steel closure is directly bolted to the liner flange, with secondary retention through an external holddown ring. Primary sealing is ensured because either double-weld failures or double-seal failures must occur simultaneously to allow helium leakage to the containment space. Notwithstanding this advantage, the secondary seals can be inspected or replaced without closure removal.

Compared with the previous reference plant design embodying radial turbomachinery cavities in the PCRV bottom head, the new delta arrangement permits a generator enclosure scheme which is more efficient from the space utilization standpoint. Layout of the generator enclosure is shown on Fig. 5.10. The generator is surrounded by a steel pressure vessel which permits an arrangement with the generator being accessible from outside the containment building. Locating the generator outside the secondary containment building results in simplification in the construction of the generator cell. This results in improved ability to control any hydrogen leakage from the generator.



GA-A14311

Fig. 5.9 PCRV Cavity Closure

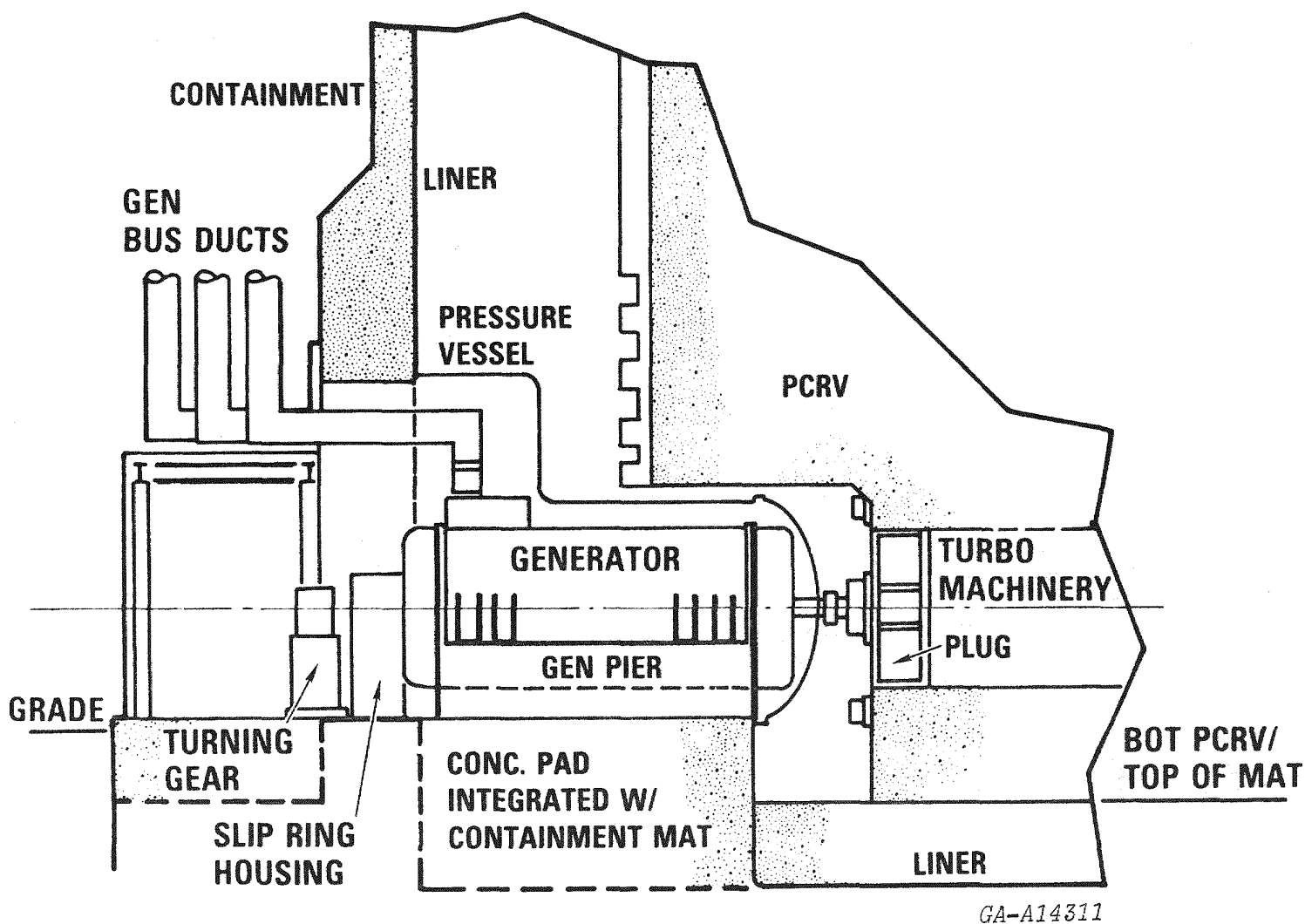


Fig. 5.10 Generator Enclosure for Integrated Plant

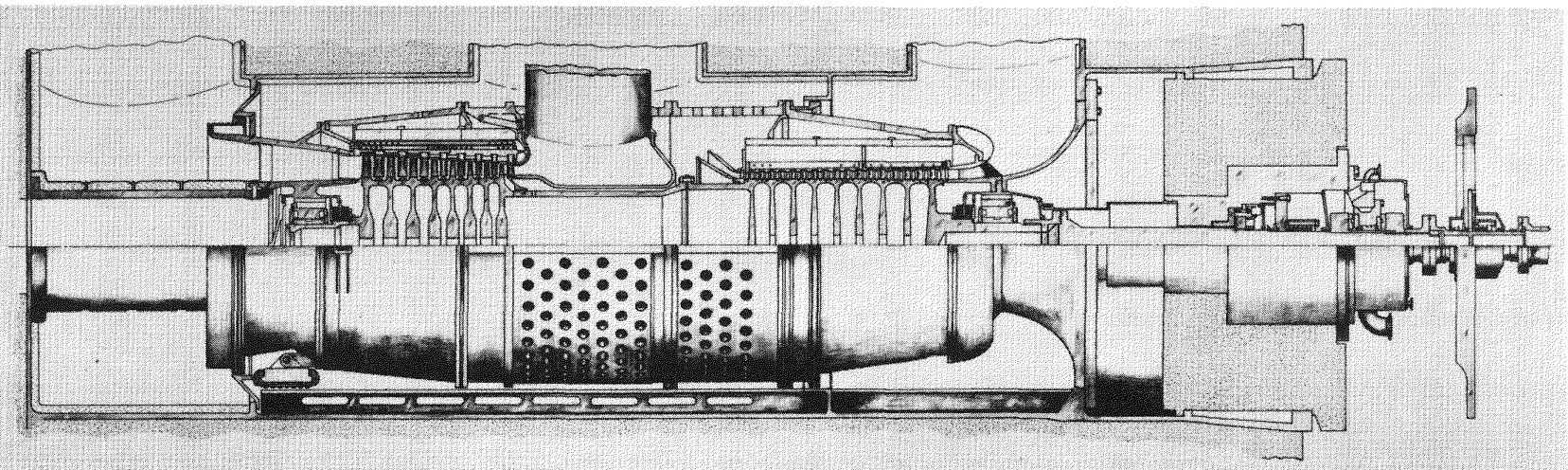
5.5 Component Design

It is not the purpose of this section to describe in detail the design considerations for the major components since these will be covered in Section 6. However, for an integrated plant the power conversion loop components cannot be treated as isolated units, and indeed, their design and the resolution of the interconnecting gas flow path geometries must be considered during the establishment of the plant primary system configuration. During the primary system design studies extensive layout work was done to identify the most attractive installation and orientation of the major components. The main PCL components which have a strong influence on the primary system design are the turbomachinery, heat exchangers, and to a much lesser extent, the control valves and a brief description of these are given below.

5.5.1 Turbomachinery

The turbomachinery design work for the GT-HTGR plant was done by the Power Systems Division and Pratt & Whitney Aircraft Division of United Technologies Corporation. The arrangement of the 400 MW(e) helium turbomachine is shown on Fig. 5.11, and details of the design are given in Ref. 5.2. An extremely simple arrangement consisting of a single-shaft direct-drive turbomachine was chosen for the GT-HTGR plant. The use of a two-bearing rotor, feasibility of which has been confirmed by critical speed analyses, maintained the smallest number of individual parts for the turbomachine, and tended to minimize the overall cost of the machine, and ease inspection and maintenance requirements. Aero-thermodynamic analyses showed that for a 400 MW(e) size machine, a single turbine inlet duct (from the reactor) could be utilized, the pressure losses and flow inlet geometry to the turbine bladed section being satisfactory. The turbomachine utilizes portions of the PCRV cavity as its gas inlet and exit plenums and volutes to the maximum extent. To achieve this, the cavity is divided into three main chambers by large diameter sliding seals located around the outer casing. This arrangement is felt to be better than the alternate approach of having flanged joints at all of the turbomachine-to-PCRV interfaces because, (1) the integrally formed scrolls and volutes are of larger cross-section (within the imposed constraint on machine diameter) resulting in reduced pressure losses, and (2) the number of mechanical joints which must be remotely actuated is minimized. In the proposed design only one duct (core-to-turbine) must be retracted remotely for machine installation and removal, and a conceptual arrangement of this is shown on Fig. 5.12.

The well-established fact that the optimization (for maximum cycle efficiency) of a highly recuperated, closed-cycle system gives a relatively low compressor pressure ratio is fortunate for a high specific heat gas as helium. The



GA-A14311

Fig. 5.11 400 MW(e) Helium Turbomachine

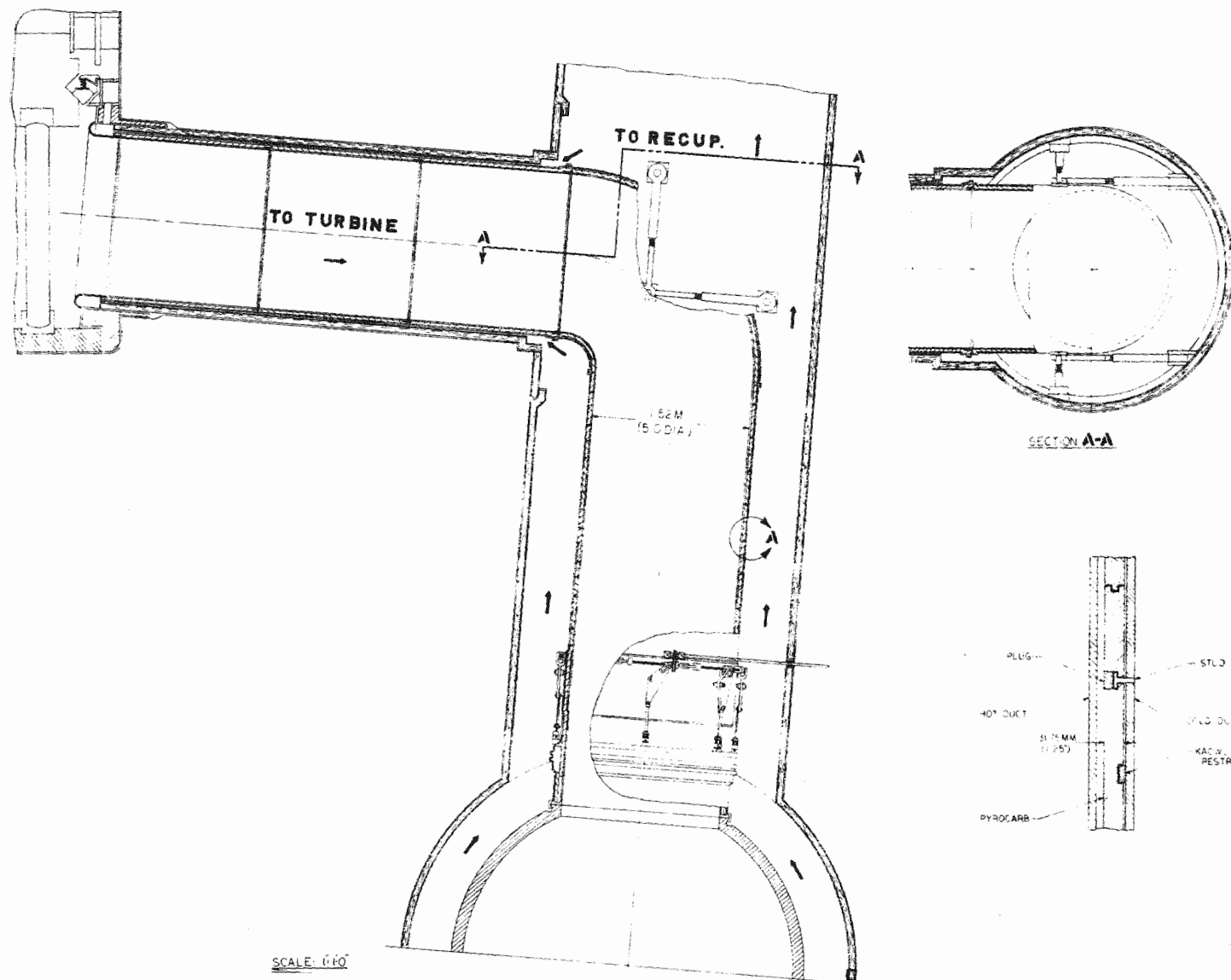


Fig. 5.12 View of Reactor-to-Turbine Duct

GA-A14311

selected value of 2.50 is slightly less than optimum, but was chosen to reduce the number of compressor and turbine stages. The selected number of stages (18 compressor and 8 turbine) are comparable with much higher pressure ratio air-breathing, open-cycle industrial gas turbines. Details of the turbomachinery are given on Table 5.6.

The overall machine dimensions are within the limitations imposed for rail shipment capability. In fact, the design basis casing diameter of 11.5 ft. (3.5 m) allows for addition of a shielded shipping container for rail transport of a radioactively contaminated unit. The overall length and approximate weight of the turbomachinery are 37 ft. (11.3 m) and 305 tons (277,000 Kg), respectively. The high density of the working fluid works to the advantage of the overall design, since the external dimensions of the 400 MW(e) helium gas turbine are approximately equal to those of 100 MW(e) air-breathing, open-cycle industrial gas turbine.

5.5.2 Heat Exchanger Design

While details of the heat exchangers have been discussed previously (Ref. 5.3), it is meaningful to discuss them briefly in the context of this paper since they are large components and have a significant influence on the integrated primary system. The combined effects of the size constraint (integration in the PCRV side-wall cavities), in-service inspection, in-situ repair, and maintenance and fabrication considerations have a significant effect on the choice of surface geometry, flow configuration, and mechanical design.

For the plant preliminary design emphasis has been placed on simplicity, and both heat exchangers are of tubular construction. A simple modular array was chosen to facilitate manufacture, installation and maintenance. Both the recuperator and precooler have a high effectiveness and thermal conductance requirements and a straight tube axial counterflow configuration was chosen to minimize the surface area and pressure loss.

In an integrated plant, the heat exchangers exert a direct influence on the overall size of the PCRV, thus creating a strong incentive for a surface compactness not generally imposed on ordinary industrial heat exchangers. While the counterflow tubular configuration approach used in the design of the recuperator and the precooler yields dimensions particularly suited for PCRV cavity installations, the actual packaging of the heat transfer matrix to minimize heat exchanger frontal area requirements (thus minimizing PCRV cavity diameter requirements) is of vital importance. With the possibility of packaging both heat exchangers as full, homogeneous tube arrays within their respective cavities ruled out by practical considerations, the approach taken toward modularization of the heat transfer matrix must be

Table 5.6

DESIGN DETAILS FOR 400-MW(e) HELIUM GAS TURBINE

Machine	Compressor	Turbine	
Inlet Temperature, °F (°C)	79.0 (26)	1562 (850)	
Inlet Pressure, psia (MPa)	460 (3.17)	1105 (7.62)	
Pressure Ratio	2.50	2.32	
Mass Flow Rate, lb/sec (kg/sec)	1265 (574)	1214 (551)	
Rotational Speed, rpm	3600	3600	
Number of Stages	18	8	
Blading Adiabatic Efficiency, %	89.8	91.8	
Stage Number	1	18	18
Tip Diameter, in. (mm)	71.9 (1826)	68.3 (1735)	76.5 (1943)
Hub Diameter, in. (mm)	62 (1575)	62 (1575)	66.6 (1691)
Hub/Tip Ratio	0.86	0.91	0.87
Blade Height, in. (mm)	4.95 (126)	3.15 (80)	4.95 (126)
Number of Vanes, stator	78	121	90
Number of Blades, rotor	77	120	124

Turbomachine Overall Data

Overall Length, ft (m)	37 (11.3) (excluding exhaust plenum)
Overall Diameter, ft (m)	11.5 (3.5)
Rotor Weight, tons (kg)	67 (60,800)
Stator and Case Weight, tons (kg)	238 (216,000)
Total Machine Weight, tons (kg)	305 (276,800)
Bearings:	
Number of Journal Bearings	2
Type of Journal Bearings	5 pad tilting pad jet lubricated
Thrust Bearing Type	8 pad tilting pad, double acting
Bearing Span, ft (m)	29.0 (8.8)

GA-A14311

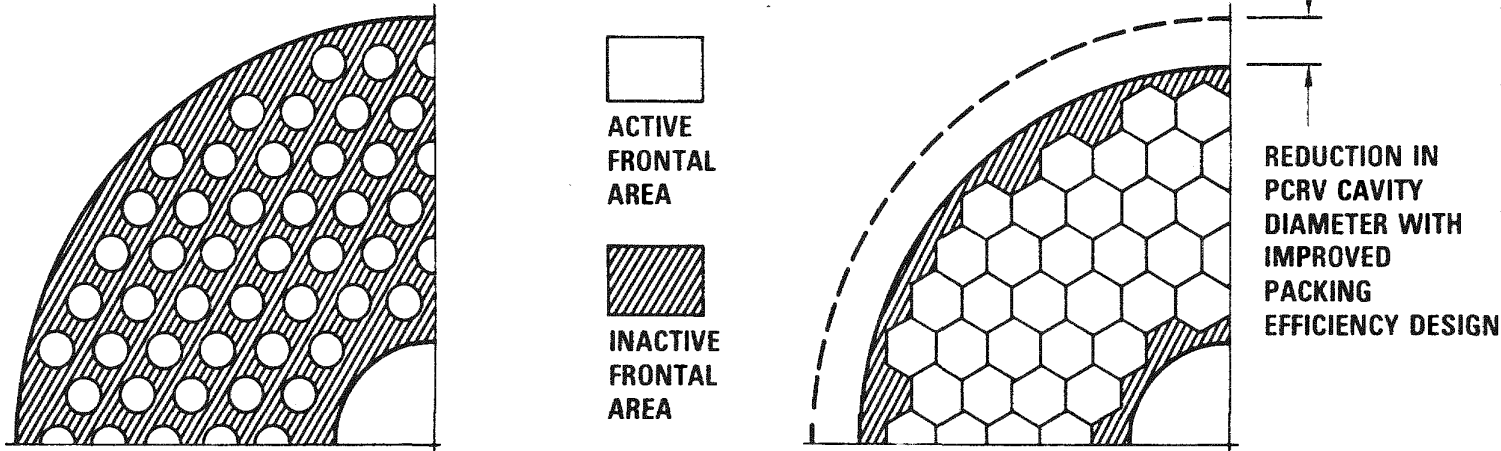
selected carefully. Since homogeneous tube arrays produce the minimum possible PCRV cavity diameters, the module shape and size for a given heat exchanger design should be the combination which most nearly produces the ideality of a homogeneous tube field while satisfying the mechanical design requirements for handling and thermal growth flexibility.

Compared with the circular modules reported previously (Refs. 5.3 and 5.4), recent innovations in module subheadering and shrouding techniques have resulted in a configuration of much improved packaging efficiency which has made possible a reduction in heat exchanger diameter for the same unit performance. A comparison of the two designs is shown schematically on Fig. 5.13. With a novel subheadering arrangement, in which the tube plate itself lies within the tube field, a contiguous hexagonal array of modules results in a more efficient utilization of frontal area. Mutually shared partitions between modules, rather than individual cans or shrouds, are possible, thus eliminating the need for intermodule bypass seals, increasing the rigidity of the modular array and facilitating provision for shell-side mixing (via perforated or discontinuous partitions).

A simplified schematic of the recuperator assembly is shown on Fig. 5.14. The recuperator consists of 144 hexagonal vertically oriented modules connected in parallel to a tubesheet at the top end, and to a high pressure bottom drum header that is connected to a cylindrical return duct passing up through the center of the modular array. The unit is supported from its upper tubeplate, and with no mechanical connections at the bottom of the assembly (hot end) unrestrained growth capability downward is provided. The recuperator arrangement provides for removability, in-service inspection, and lead tube plugging. A summary of the salient features of the recuperator is given in Table 5.7.

A simplified schematic of the precooler assembly is shown on Fig. 5.15. With 144 hexagonal modules the overall assembly is similar to the recuperator. The support system is similar to the recuperator, except that the modular array is anchored to a top support plate instead of a primary pressure carrying tubeplate. Both the precooler water inlet and outlet lead tubes penetrate the bottom head of the PCRV, and between the modules and bottom tubesheets, the lead tubes are coiled to produce the flexibility required to accommodate differential thermal expansion. In addition to failure isolation and external lead tube plugging capability, the precooler provides for removability and in-service inspection. A summary of the salient features of the precooler is given in Table 5.7.

Even though relatively high heat transfer coefficients can be realized with the single-phase working fluids, large surface areas are necessary due



REFERENCE DESIGN WITH CIRCULAR MODULES

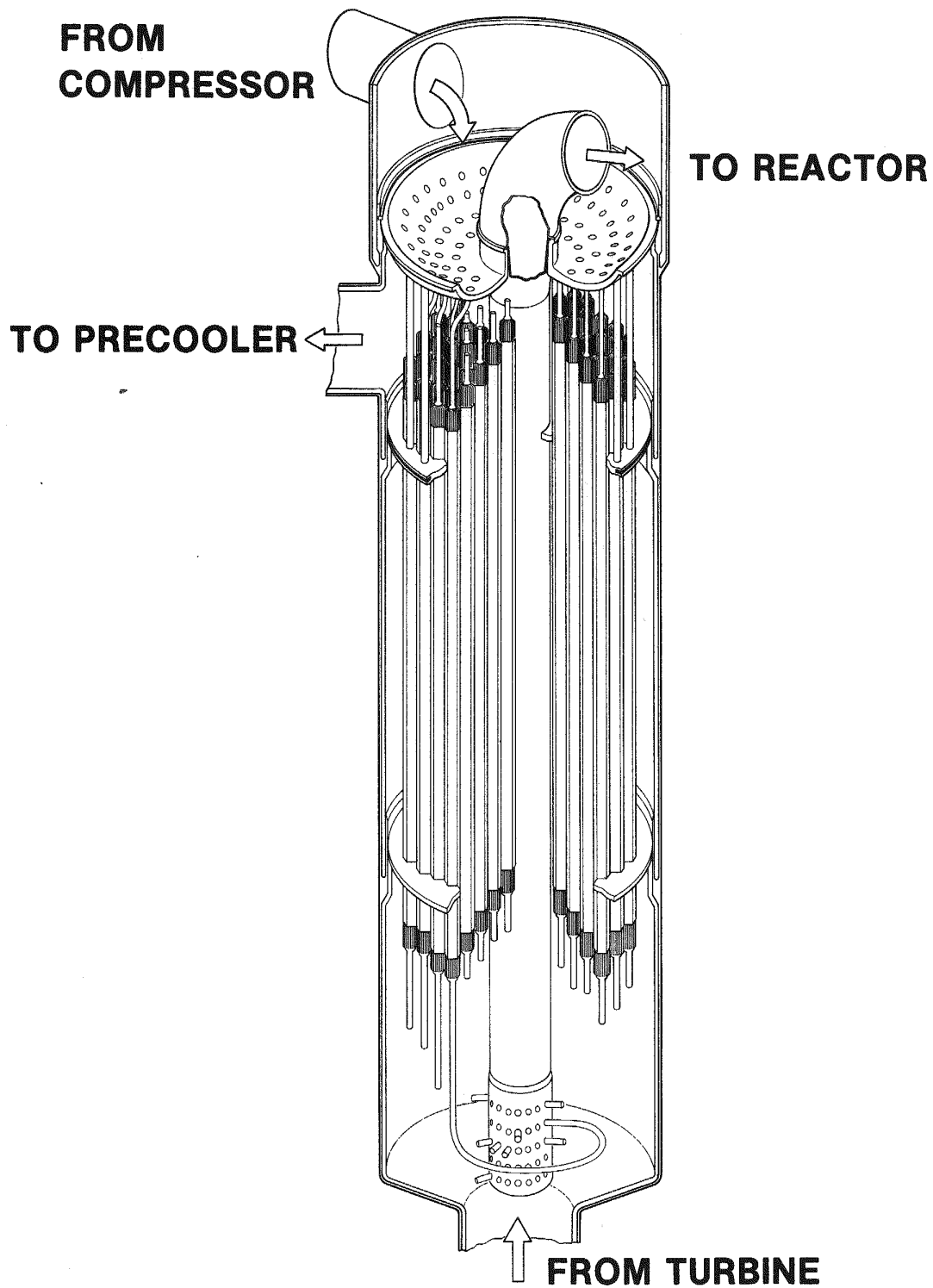
- MODULE STAGGERING MANDATORY
- LARGE INACTIVE FRONTAL AREA
- COMPLEX INTERSTITIAL SEALS

IMPROVED HEXAGONAL MODULE ARRANGEMENT

- REDUCTION IN EXCHANGER DIAMETER
- INTERSTITIAL SEALS ELIMINATED
- SHELL-SIDE GAS MIXING POSSIBLE

GA-A14311

Fig. 5.13 Heat Exchanger Module Comparison



GA-A14311

Fig. 5.14 Recuperator Assembly

TABLE 5.7
SUMMARY OF HEAT EXCHANGER PRELIMINARY DESIGNS

TYPE	EXCHANGER	RECUPERATOR	PRECOOLER
	NUMBER PER REACTOR	3	3
SURFACE GEOMETRY	MATRIX TYPE FLOW CONFIGURATION CONSTRUCTION	TUBULAR AXIAL COUNTERFLOW MODULAR	
	TUBE OUTER DIAMETER, INS (MM) TUBE WALL THICKNESS, INS (MM) MAXIMUM METAL TEMP., °F (°C) INTERNAL PRESSURE DIFFERENTIAL, PSI (MPa)	7/16 (11.1) 0.045 (1.14) 968 (520) 670 (4.61)	3/8 (9.5) 0.049 (1.24) 357 (81) 150 (1.03) He>H ₂ O
	TUBE MATERIAL TYPE	FERRITIC, 2 1/4Cr-1Mo	MEDIUM CARBON STEEL
MODULE DETAILS	MODULE DIMN. (ACROSS FLATS), INS (MM) SUB-HEADERING TYPE MODULES PER UNIT TUBES PER MODULE EFFECTIVE TUBE LENGTH, FT (M) SURFACE AREA/REACTOR, FT ² (M ²)	14.2 (361) CONICAL 144 547 39.8 (12.13) 1,080,000 (100,000)	13.2 (335) CONICAL 144 631 37.0 (11.3) 990,000 (91,900)
OVERALL ASSEMBLY	APPROX. OVERALL LENGTH, FT (M) OVERALL DIAMETER, FT (M) MODULE WEIGHT, LB (KG) APPROX. ASSEMBLY WEIGHT, TONS (KG) FABRICATION LOCATION	62 (18.9) 16.75 (5.1) 5230 (2375) 474 (430,000) FACTORY	73 (22.3) 15.5 (4.72) 5980 (2715) 445 (404,000) FACTORY

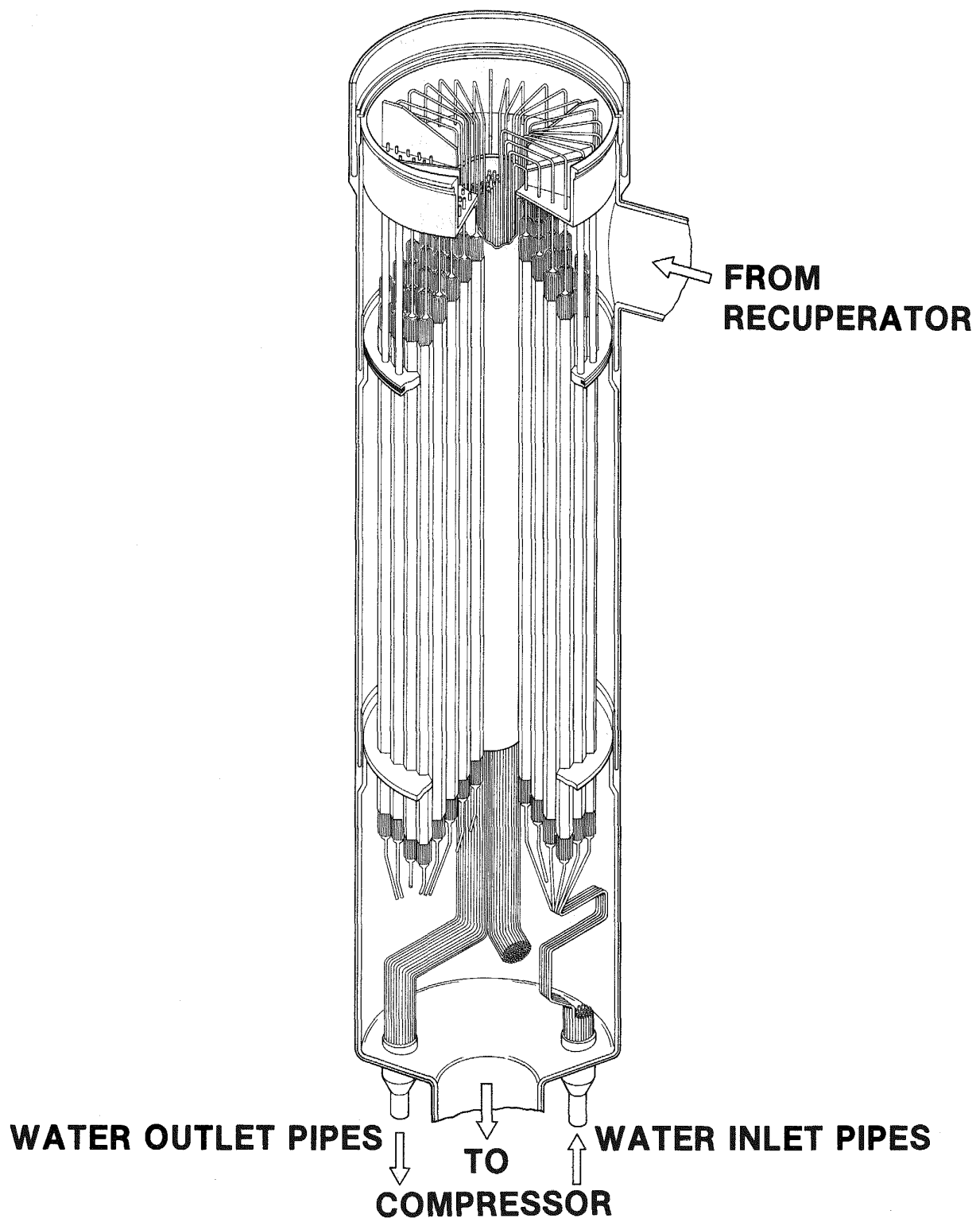


Fig. 5.15 Precooler Assembly

GA-A14311

to the large quantity of heat transfer. Because of the modest metal temperatures, the use of code approved lower grade alloys of reduced cost is possible. The ferritic materials selected for both exchangers have been used extensively in industrial and nuclear plant heat exchangers. While the exchanger assemblies described above are large, state-of-the-art manufacturing methods apply and the modular approach eases fabrication, handling, and assembly. The overall size and weight of both the recuperator and precooler are similar to contemporary steam generators; and transport methods, handling and installation techniques developed for these units are equally applicable to the heat exchangers for the nuclear gas turbine plant.

5.6 Maintenance Considerations

With all of the power conversion machinery installed inside the reactor vessel maintenance aspects must be considered during the plant conceptual design phase. Some of the component maintenance considerations observed in the plant layout studies are given on Table 5.8.

The primary criterion of the GT-HTGR plant maintenance and inspection plan is to provide, at a reasonable cost, maintenance and inspection facilities, equipment and component design that will permit the realization of maximum plant availability. It is therefore a matter of policy to design all of the related maintenance facilities for economy and convenience, both for planned and unplanned maintenance. All primary system equipment will be designed for full plant lifetime, with no limited-life parts. Moreover, all components except some in the reactor cavity are designed for removal and replacement. The removal and replacement of primary system components from the PCRV after depressurization will, in general, be performed by remote handling techniques with equipment that provides for retention of the helium atmosphere within the PCRV, and also provides any needed radiation shielding. Typically, the primary system components are moved to a service facility for decontamination for either remote or contact maintenance work, or for shipment off-site to other facilities. The maintenance requirements must thus provide for the replacement of some items which have been designed to last the plant lifetime, but fail due to unforeseen circumstances. The items in this category are the heat exchangers, valves, and some portions of the ducting. Turbomachinery changeout is regarded as a planned maintenance activity.

An important part of the formulation of the maintenance plan has been to provide for in-situ maintenance whenever practical. The degrees to which in-situ and service facility maintenance operations can be carried out depend upon the

TABLE 5.8
COMPONENT MAINTENANCE CONSIDERATIONS IN GT-HTGR PLANT LAYOUT STUDIES

TURBOMACHINERY

- IN SITU MAINTENANCE ACCESS
- ACCESS SPACES SHIELDED, PURGED AND FREE OF CONTAMINANTS
- OPTICAL INSPECTION OF TURBINE BLADING FROM OUTSIDE PCRV
- INSTALLATION AND REMOVAL POSSIBLE WITHOUT MAN ACCESS

HEAT EXCHANGERS

- MAINTENANCE ACCESS AT BOTH ENDS OF RECUPERATOR AND PRECOOLER
- OPTICAL INSPECTION OF TUBE PLATES AND SUPPORT STRUCTURE
- IN SITU LEAD TUBE PLUGGING OF EXCHANGER MODULES
FROM OUTSIDE PCRV

GA-A14311

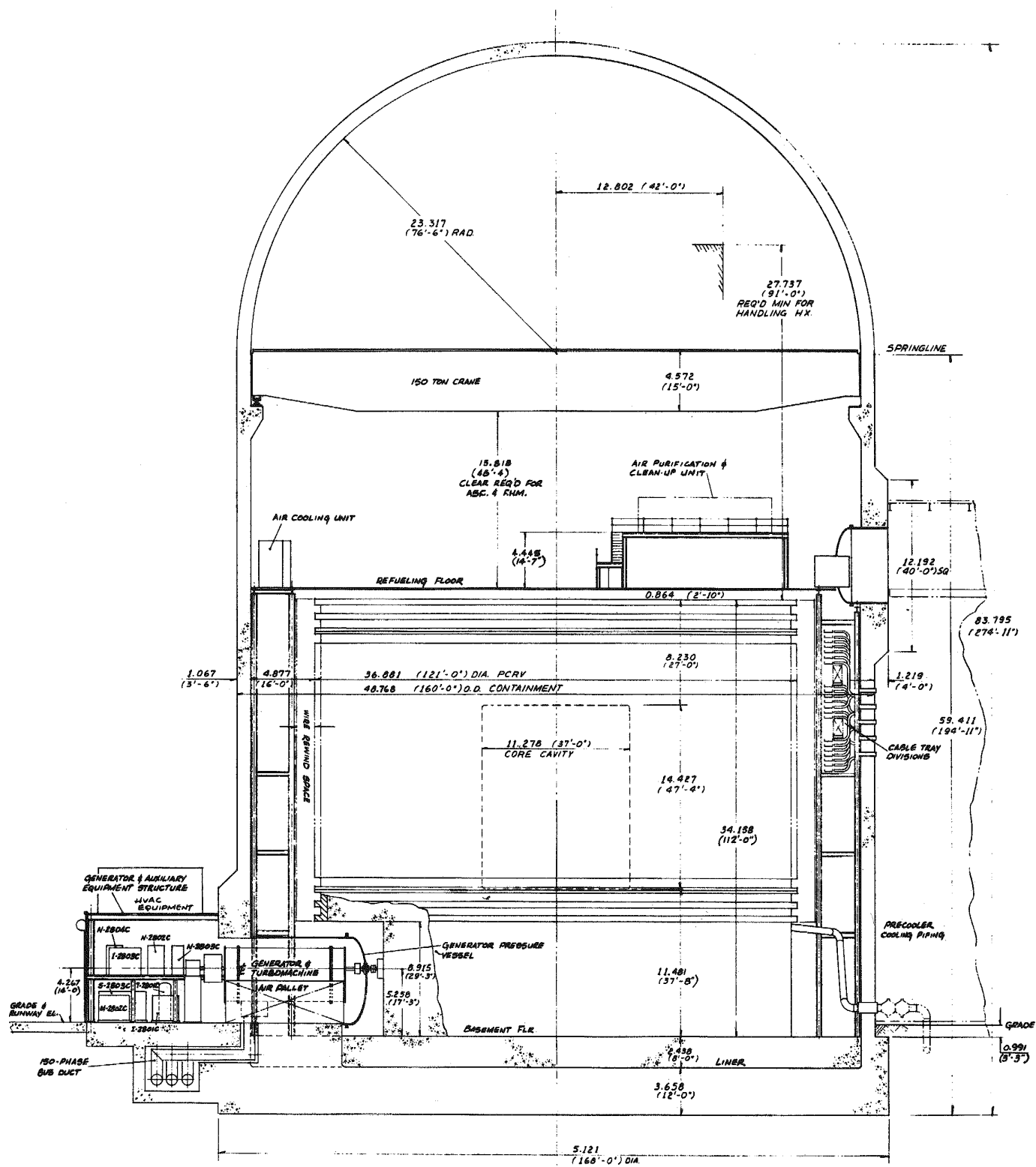
radiological environment in and around the equipment in question. The maintenance equipment will be designed so that it is convenient for the more economical direct contact approach if the activity levels are acceptable. The maintenance plan, however, will be formulated for conservatively high activity levels. The objective will be to provide equipment to deal economically with anticipated activity levels; at the same time, the plan will permit advantages to be taken of low activity levels when they occur. For the GT-HTGR plant, heavy emphasis will be placed on diagnostics and, where possible, a large portion of the periodic inspection and repair should be performed in-situ. Turbomachine blading, bearings, instrumentation and service systems should be accessible.

In general, equipment will be removed for maintenance and overhaul only if the records raise a question concerning the ability of the component to perform satisfactorily. Reliance on performance monitoring and measurements of deflections, eccentricity, vibration, acoustics, critical clearances and lubrication parameters, in addition to temperature and pressure, are key items in the successful implementation of this approach.

5.7 Overall Plant Configurations

From Fig. 5.16 it can be seen that a close-fitting cylindrical secondary containment building encloses the PCRV. The secondary containment together with the PCRV incorporate safety features which limit loss of primary coolant, and missile damage in the event of failures in the turbomachinery, shaft seals, generator, heat exchangers, or PCRV primary closures. A major feature of the integrated nuclear gas turbine plant is the location of the power conversion system components within the PCRV, this eliminating the need for buildings such as the traditional turbine hall, and gives a compact overall arrangement as shown on the artist's rendition of the GT-HTGR on Fig. 5.17.

A concept for the plot plan in Fig. 5.18 illustrates the general layout of buildings and dry-cooling towers in a twin 3000 MW(t) GT-HTGR plant. The reactor service building and fuel storage facilities are shared by the two reactor units. Separate control buildings and safety-related auxiliaries are provided for each unit. A runway system and rail access are provided for turbomachinery and generator handling. It can be seen that space is allocated on the plot plan for an ammonia turbine building should the binary cycle option be selected. In the reference GT-HTGR dry-cooled plant, the generator evaporative cooling system is the only significant water consuming system. Other cooling requirements are met with dry-cooling systems.



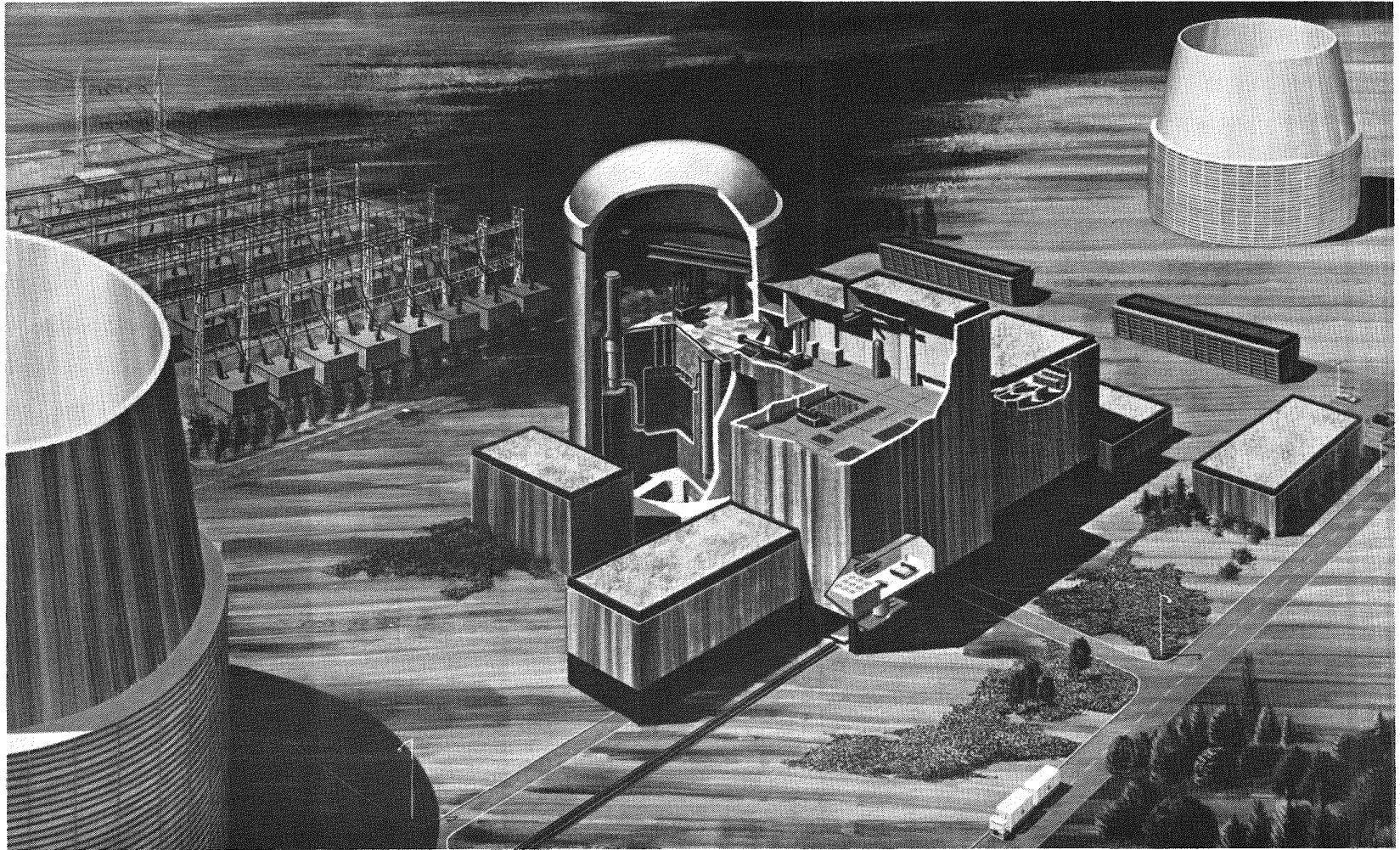
NOTE:
ALL DIMENSIONS ARE
IN METERS UNLESS
OTHERWISE SPECIFIED.

5000 MW(t)
GT - HTGR
CONTAINMENT
SECTION A-A

SECTION A-A

GA-A14311

Fig. 5.16 View of GT-HTGR Plant Containment Building



GA-A14311

Fig. 5.17 Overall Conceptual View of GT-HTGR Plant

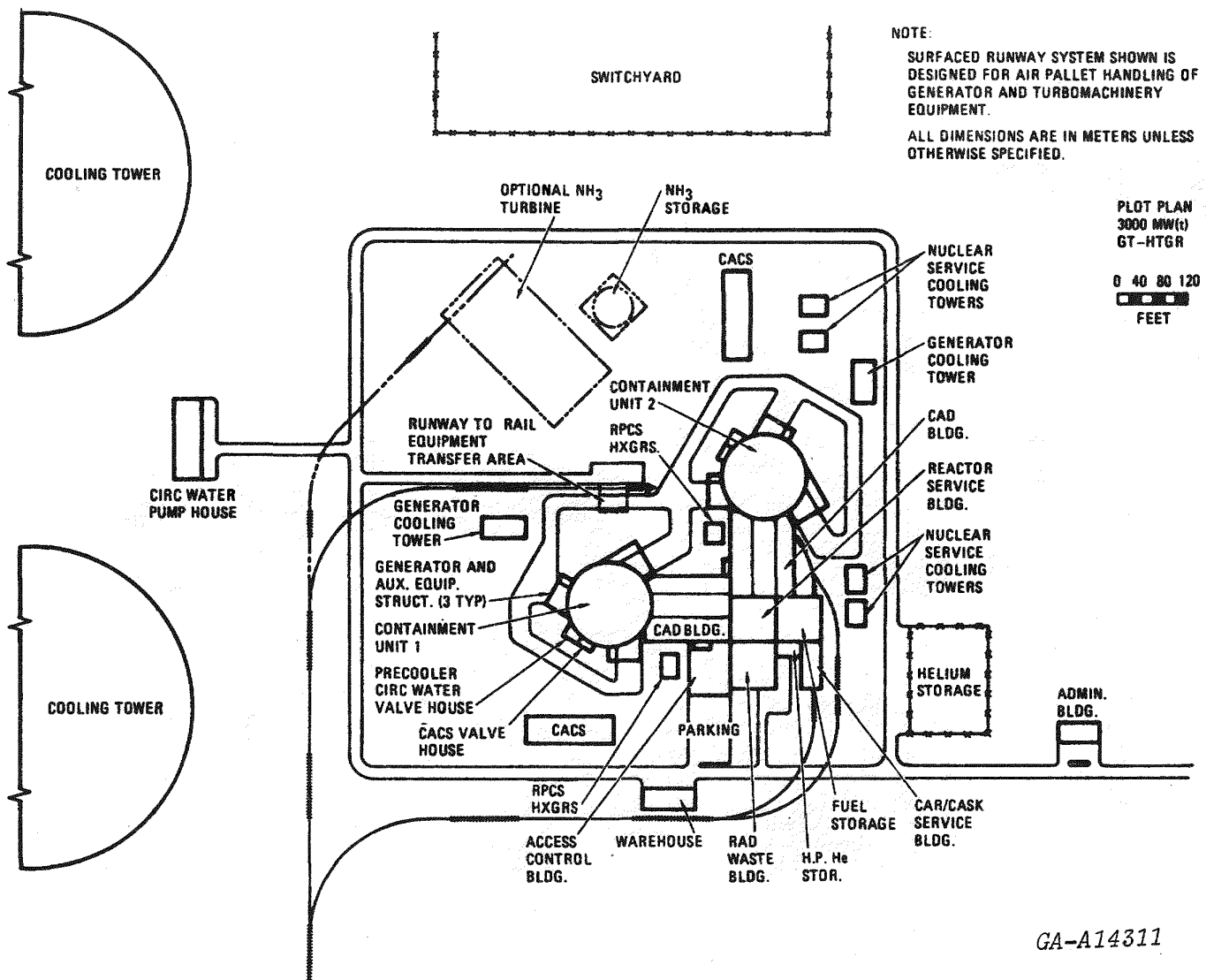


Fig. 5.18 Plot Plan for GT-HTGR Plant with Twin Reactors

5.8 Summary

The primary design studies were done for a 3000 MW(t) reactor plant with dry-cooling. The reference plant design still utilizes a multiloop gas turbine approach and a modest turbine inlet temperature (compared with open cycle industrial gas turbines) of 1562°F (850°C), thus permitting the use of uncooled turbine blades made from existing nickel-base alloys. The combination of comprehensive optimization and primary system layout studies lead to a simpler plant arrangement of improved performance and reduced capital cost.

From the analytical sensitivity studies changes in the following areas were made compared with the previous reference design: (1) slightly increased reactor outlet temperature, (2) higher system maximum pressure (3) compressor pressure ratio increased from 2.35 to 2.5, and (4) slightly higher heat exchanger thermal conductance requirements.

The plant layout studies resulted in a substantially improved configuration with much simplified gas flow paths, which results in a decrease in system pressure loss. The adoption of an improved heat exchanger subheadering configuration with better utilization of flow frontal area resulted in recuperator and precooler cavity diameter reduction for the same performance. This design improvement extended beyond just the heat exchangers themselves, since it allowed a reduction in diameter of the PCRV and secondary containment building, this resulting in a substantial cost savings. The reduction in diameter of the PCRV was also made possible by changing the horizontal orientation of the turbomachinery cavities from radial to a delta configuration for the three loop plant. With this arrangement the length of the turbomachine no longer controls the diameter of the vessel. A significant advantage of the delta arrangement is the improved access to the turbomachine for inspection and maintenance.

REFERENCES

- 5.1 McDonald, C. F., J. C. Bass, and H. Amtmann, "Primary System Design Studies for Advanced Direct Cycle Nuclear Gas Turbine Plant", ASME Paper No. 77-GT-25.
- 5.2 Adams, R. G., and F. H. Boenig, "The Design of Turbomachinery for the Gas Turbine (Direct Cycle) HTGR Power Plant", ASME Paper No. 77-GT-38.
- 5.3 McDonald, C. F., T. H. Van Hagan, and K. Vepa, "Heat Exchanger Design Considerations for the Gas Turbine HTGR Power Plant", ASME Paper No. 76-GT-53.
- 5.4 McDonald, C. F., J. M. Kruse, and P. Fortescue, "Primary System Preliminary Design for Gas Turbine HTGR Power Plant", ASME Paper No. 76-GT-92.

6.0 COMPONENT DESIGN CONSIDERATIONS

The integrated plant configuration, with all the major power loop components inside the PCRV, has formidable envelope limitations and demanding maintenance requirements for the high performance, high reliability machinery, and these requirements have a strong influence on the component design considerations. The major components which have a direct bearing on the overall layout and cost of the power conversion loop; namely, the turbomachinery, heat exchangers, and to a lesser extent the valves, are briefly discussed below. The various aerodynamic, heat transfer, structural and design criteria discussed are generalized (i.e. not specifically related to the latest reference design plant) and are included to emphasize that for an integrated plant the design of the major components cannot be done in an isolated manner, but must be coordinated with the overall design of the plant primary system.

6.1 Turbomachine Design

Since high turbomachinery efficiencies are required, it is important that minimum loss ducts to and from the compressor and turbine be incorporated, thus necessitating close attention to the interfacing of the gas turbine with the other components in the power conversion loop. Minimum loss ducts with carefully contoured geometries to give good flow distribution into the compressor and turbine tend to require large volutes and scrolls; however, with a limited machine diameter and the requirement of minimizing the bearing span to give satisfactory rotor dynamic characteristics (critical speed margin), large flow areas are not available and trade-offs are necessary to satisfy both aerodynamic and structural requirements for the selected primary system.

6.1.1 Compressor Aerodynamic Design Considerations

Since axial compressor aerothermodynamic design techniques have been well documented, it is not the intent to describe detailed analyses in this paper, but rather to outline how the fluid properties of helium influence the flow path geometries, and to emphasize that the aerodynamic procedures used are essentially identical to conventional air-breathing gas turbine practice.

The choice of working fluid affects the turbomachinery primarily in two ways: (1) the number of compressor stages for the attainment of the required pressure ratio and high efficiency, and (2) the machine size for a high-pressure closed system. The specific heat of helium is five times that of air, and since the stage temperature rise varies inversely as the specific heat (for a given limiting blade speed), it follows that the temperature rise available per stage when running with helium will be only one-fifth that of air. The pressure ratio is given by

$$R = 1 + \left(\frac{\eta \Delta T}{T_1} \right)^{\gamma/\gamma-1}.$$

It can be seen that the combination of the temperature rise and the reduced value of $\gamma/\gamma-1$ results in more stages being required for a helium compressor. As discussed previously, it is fortunate that the optimization (for maximum cycle efficiency) of a highly recuperated closed-cycle system gives a relatively low pressure ratio; hence, the number of compressor stages is comparable with existing open-cycle industrial gas turbines.

Substitution of helium for air greatly modifies aerodynamic requirements by removing Mach number limitations; the problem then becomes that of trying to induce the highest possible gas velocities that stress-limited blades will allow. For the selected single-shaft turbomachinery the compressor rotational speed is, of course, fixed at the generator synchronous speed of 3600 rpm for a 60 Hz machine. The size of the machine is thus dictated by the choice of blade speed, there being an incentive to use the highest values possible commensurate with stress limits to reduce the number of stages since the stage loading factor is inversely proportional to the blade speed squared.

For the specified design conditions the required number of stages was determined and a complete blading design performed, including annulus dimensions, number of blades, blade chords, and stagger angles (which enable the compressor bladed length to be determined). Aerodynamic design techniques developed extensively over the years for open-cycle gas turbines are directly applicable to the helium compressor. It is known from experience that certain aerothermodynamic parameters have a strong influence on compressor design, namely flow coefficient (V_a/U), stage loading factor ($\Delta H/U^2$), and diffusion factor (D). Initially a 20-stage compressor design was selected with both aerodynamic and dynamic loading parameters consistent

with conservatively designed, long-life industrial gas turbines. While a small gain in efficiency could be realized by increasing the number of stages, a penalty would have to be paid in compressor length. With 20 axial stages the maximum diffusion factor (aerodynamic loading factor) is on the order of 0.39, which is acceptable for conservatively designed industrial gas turbines and should give a satisfactory surge margin.

Helium compressors for closed cycle gas turbines are characterized by small blade heights, high hub-to-tip ratios, and low aspect ratios. Based on work done by General Atomic, for a 20-stage compressor design, the effects of varying the blade and gas velocities are typically shown in Fig. 6.1. Increasing the hub speed and gas axial velocity above the selected values of 1000 ft/sec (305 m/sec) and 650 ft/sec (198 m/sec), respectively, would reduce the machine length, but the rear stage blade height would be significantly reduced and the hub-to-tip ratio would be higher than the accepted upper limit of about 0.90 for high efficiency compressors. With high pressure helium, the blade heights are small and end wall losses become significant and thus careful mechanical design is necessary to minimize tip clearance effects. While the end wall effects have an adverse influence on efficiency, two factors that will partially offset the tendency for lower efficiencies are the very high Reynolds number (6×10^6) and the very low Mach number (0.39). The specific speed and diameter values for the initially selected 20-stage machine are typical for high efficiency axial compressors.

Examples of additional axial compressor parameter studies done by General Atomic during the early part of the turbomachinery design phase are shown in Figs. 6.2 through 6.6. It can be seen that aerodynamic design work was done for both single and split-shaft arrangements with differing numbers of compressor stages. A representative compressor map for use in plant performance and control studies is shown in Fig. 6.7.

The in-depth studies of the turbomachine for the GT-HTGR plant were done by United Technologies and details of the machine for the reference plant design are given in Ref. 6.1. Table 6.1, taken from this source, gives the details of the compressor design. For the reference design, with a pressure ratio of 2.5, it was possible to reduce the number of compressor stages from 20 to 18 and still maintain a high level of efficiency, by utilizing advanced technology from open-cycle industrial gas turbines (Ref. 6.2). The compressor adiabatic efficiency (across the blading) of 89.8 percent is based on a design system of existing data.

NOTES:

20 AXIAL STAGES

ROTATIONAL SPEED = 3600 RPM

ZERO INLET AND EXIT SWIRL

HELIUM FLOW = 1393 LB/SEC (632 KG/SEC)

FREE VORTEX DESIGN

INLET PRESSURE = 425 PSIA (2.93 MPa)

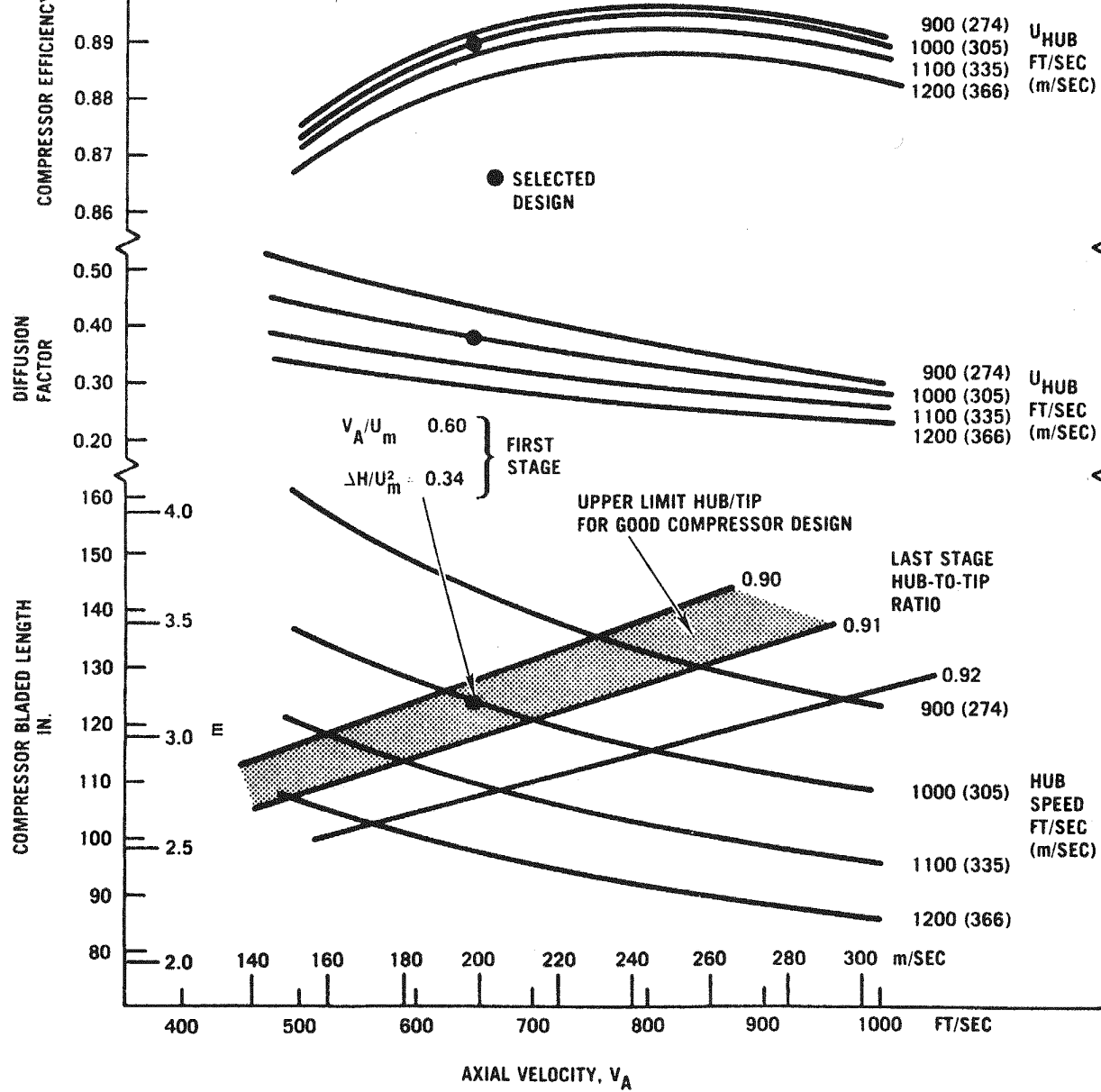
MAXIMUM STRESS LEVEL 10,000 PSI (68.9 MPa)

INLET TEMPERATURE = 95 F (35 C)

PRESSURE RATIO = 2.35

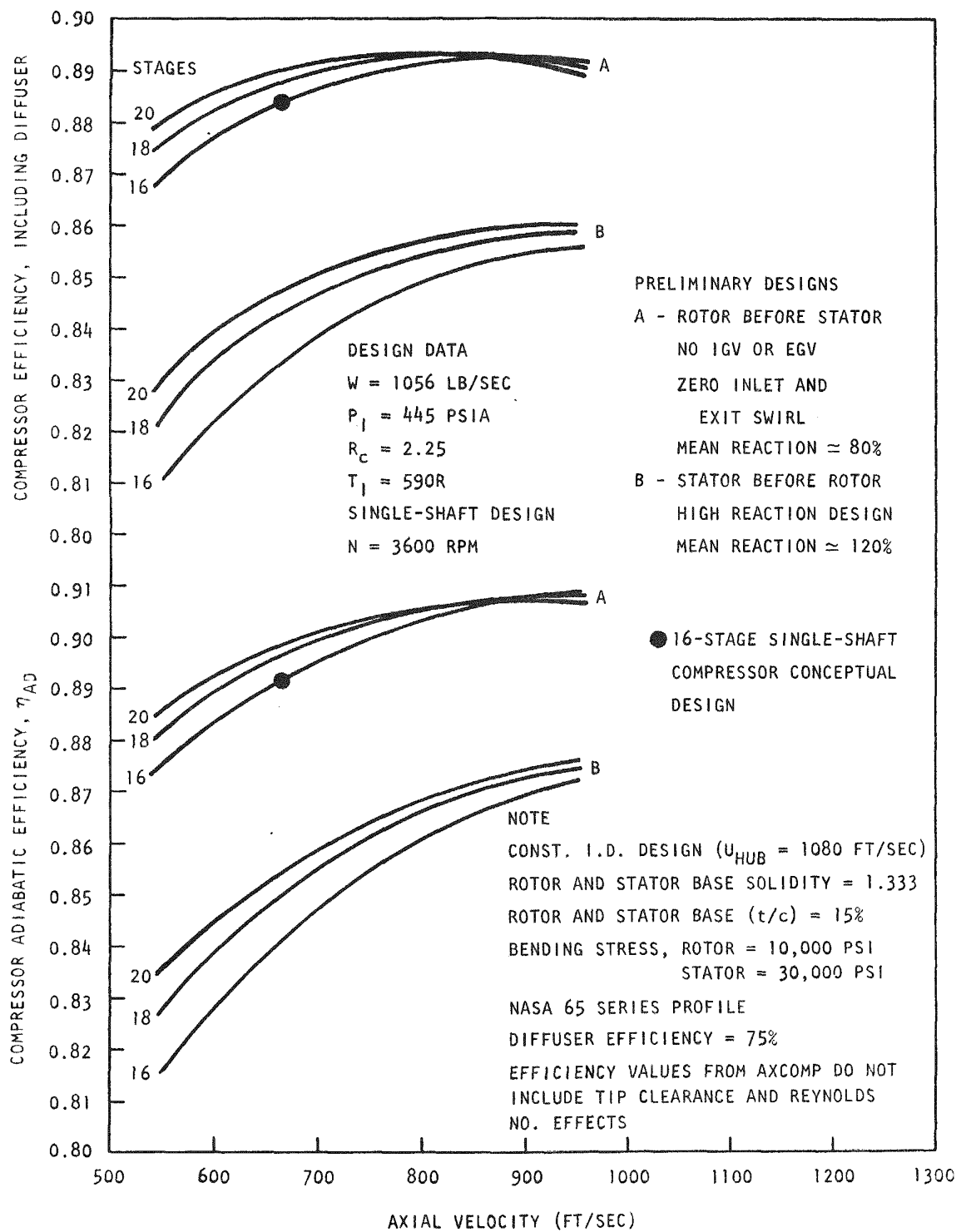
COMPRESSOR AERODYNAMIC LOADING PARAMETER, DEFINED

$$D \quad (1 - \frac{\cos \beta_1}{\cos \beta}) - \frac{S}{C} \frac{\cos \beta_1}{2} (\tan \beta_1 - \tan \beta_2)$$



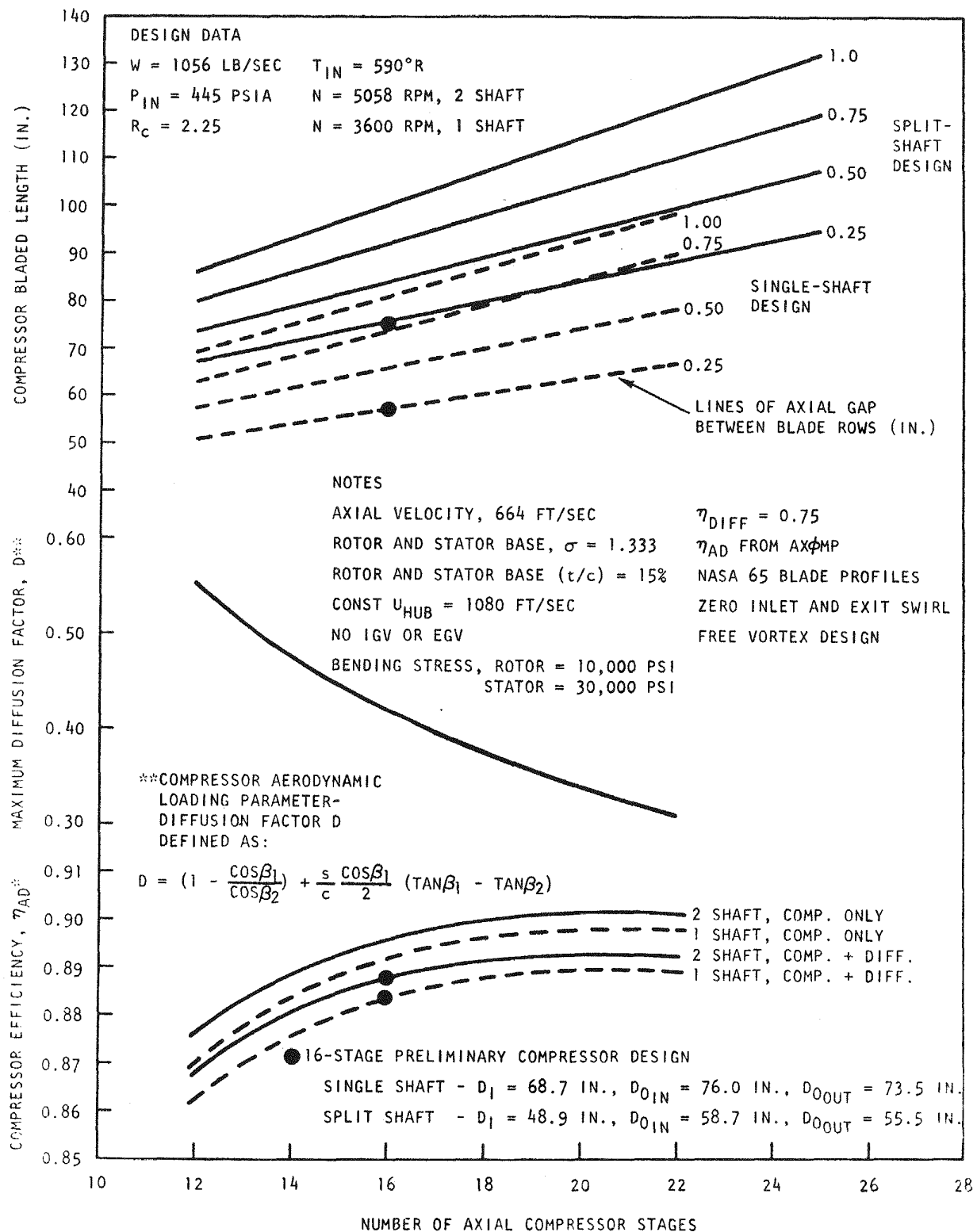
GA-A14311

Fig. 6.1 Conceptual Axial Compressor Design Parameters for 370 MW(e) Helium Gas Turbine



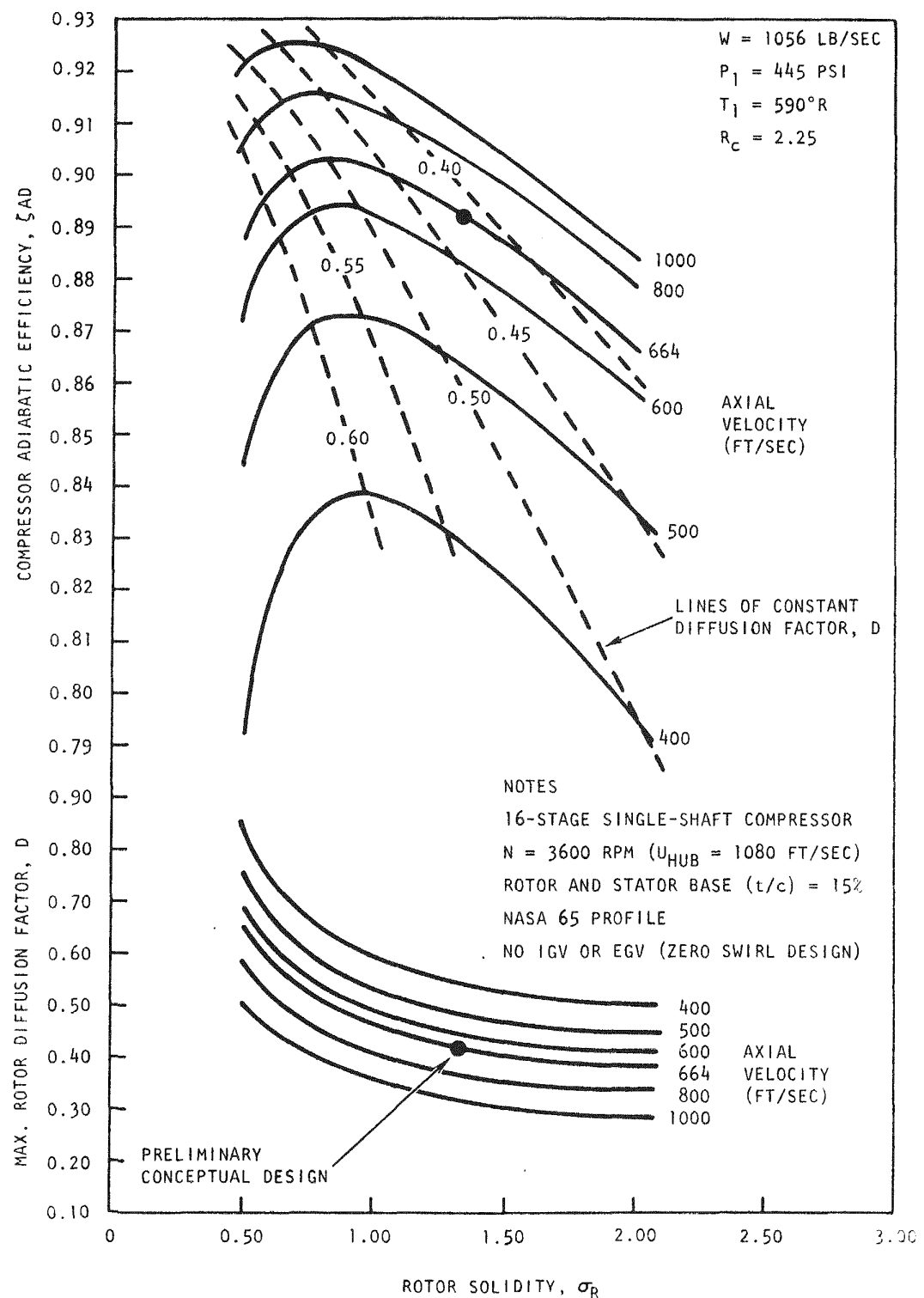
GA-A14311

Fig. 6.2 Influence of Axial Velocity and Number of Stages of Efficiency for Medium and High Reaction Compressor Designs



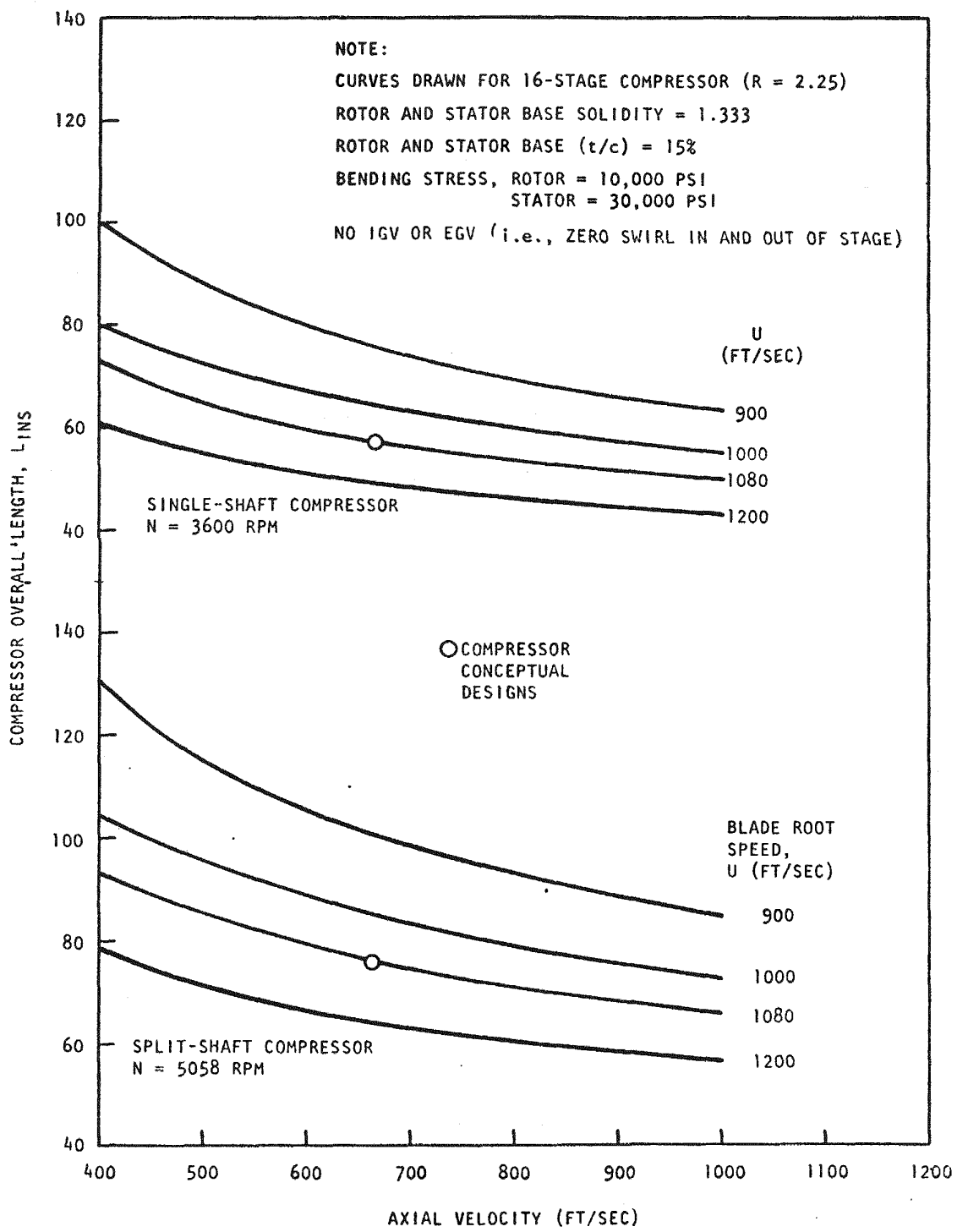
GA-A14311

Fig. 6.3 Influence of Number of Stages on Helium Axial Compressor Parameters



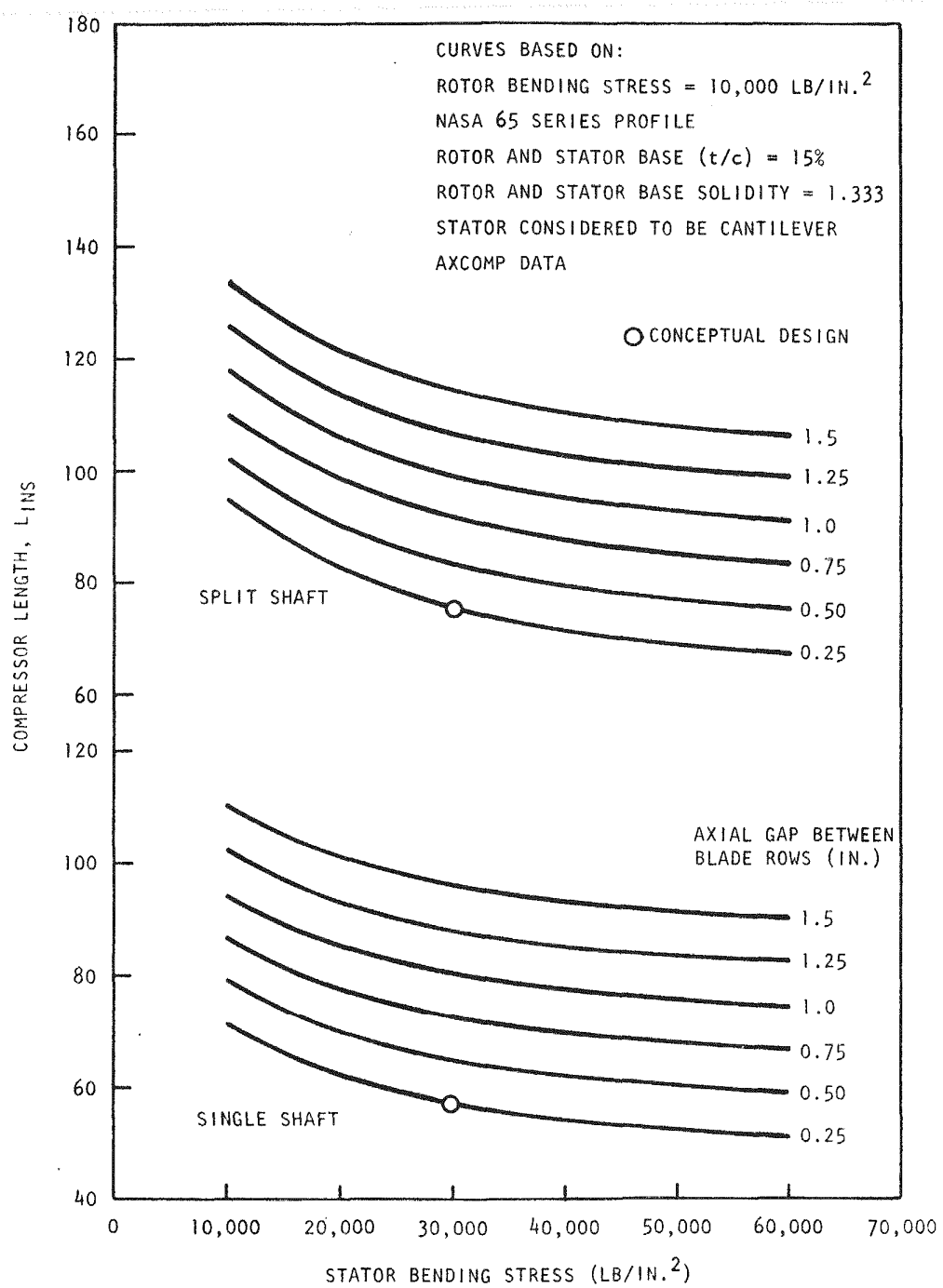
GA-A14311

Fig. 6.4 Influence of Blade Solidity on Compressor Efficiency and Aerodynamic Loading



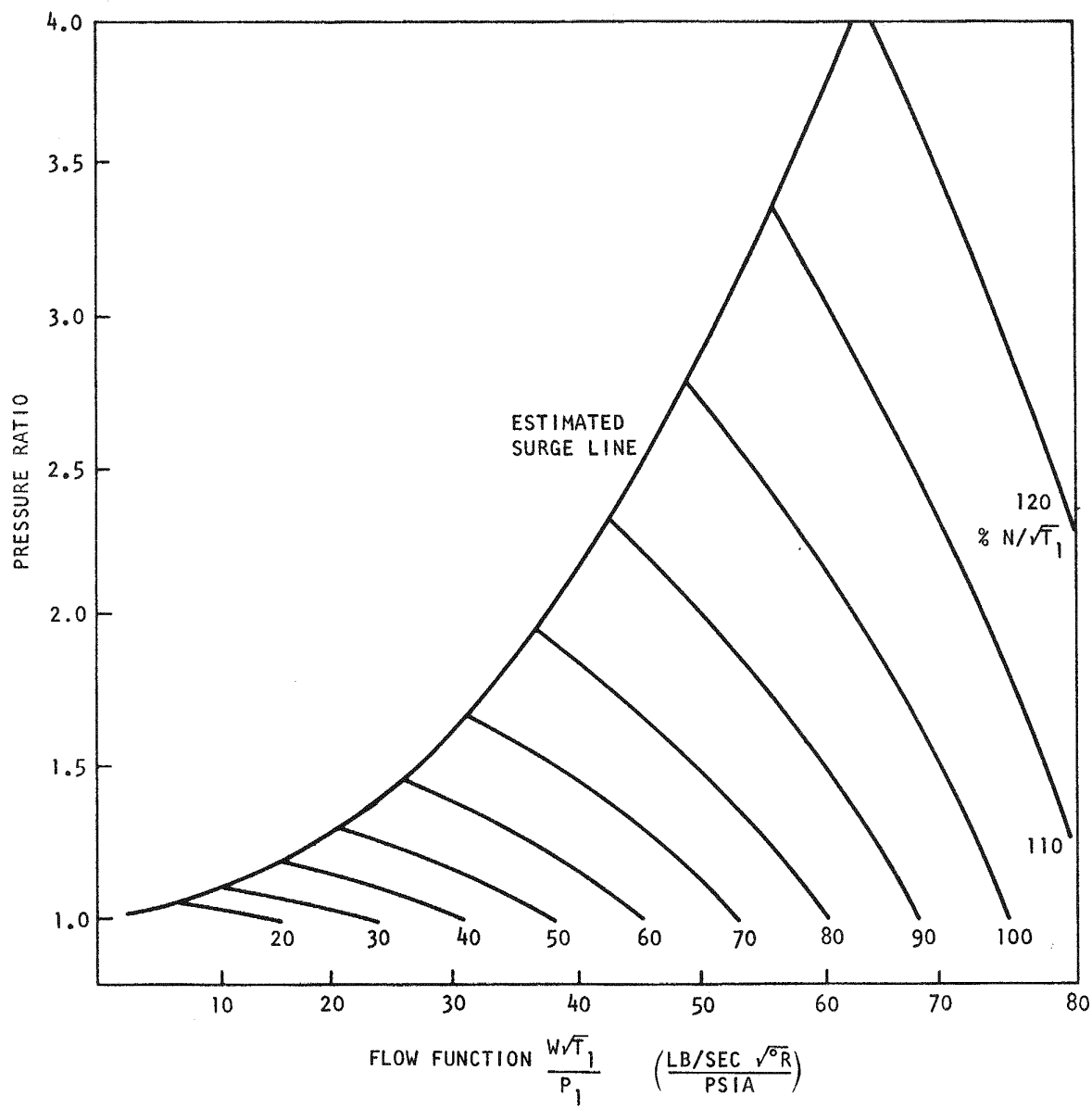
GA-A14311

Fig. 6.5 Influence of Axial Velocity and Blade Speed on Compressor Length



GA-A14311

Fig. 6.6 Effect of Stator Bending Stress or Compressor Overall Length



GA-A14311

Fig. 6.7 Simplified Helium Compressor Map

TABLE 6.1
SUMMARY OF GT-HTGR TURBOMACHINERY DESIGN

	<u>Compressor</u>		<u>Turbine</u>	
Inlet temperature, °F (°C)	79 (26)		1562 (850)	
Inlet pressure, psi (MPa)	460 (3.17)		1109 (7.6)	
Exit temperature, °F (°C)	350 (177)		991 (533)	
Exit pressure, psi (MPa)	1050 (7.93)		476 (3.3)	
Mass flow rate, lb/s (kg/s)	1268 (575)		1195 (542)	
Rotational speed, rpm	3600		3600	
Number of stages	18		8	
Stage number	1	18	1	8
Tip diameter, in. (mm)	71.9 (1826)	68.3 (1735)	76.5 (1943)	86 (2184)
Hub diameter, in. (mm)	62 (1575)	62.0 (1575)	66.6 (1691)	62.6 (1590)
Number of vanes, stator	78	121	90	50
Number of blades, rotor	77	120	124	68
Blade height, in. (mm)	4.95 (126)	3.15 (80)	4.95 (125.7)	11.7 (297.2)
Blade chord, in. (mm)	3.1 (79)	2.0 (51)	2.46 (62.5)	5.0 (127)
Vane height, in. (mm)	4.9 (124)	3.1 (79)	4.95 (125.7)	11.2 (284.5)
Vane chord, in. (mm)	3.0 (76)	1.9 (48)	4.34 (110)	8.3 (211)
Blade effective stress, psi (MPa)	--	--	15500 (107)	31000 (214)
Disk avg. tang. stress, psi (MPa)	59000 (407)	52000 (358)	42640 (294)	36000 (248)
Disk max. radial stress, psi (MPa)	69000 (476)	75000 (517)	48600 (335)	45000 (331)

TURBOMACHINE OVERALL DATA

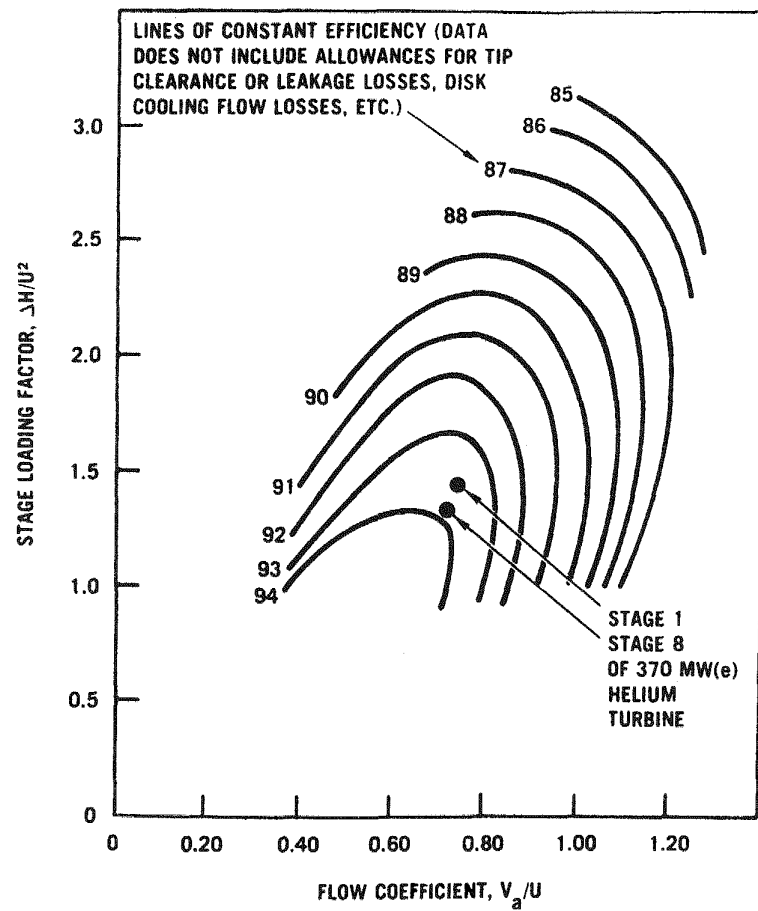
Length overall, ft (m)	36.84 (11.2) (not including exhaust plenum)
Diameter overall, ft (m)	11.5 (3.51)
Rotor weight, lbs (kg)	133,500 (60,505) (includes output shaft)
Stator and case weight, lbs (kg)	476,500 (216,140) (incl. plug seal assembly)
Total machine weight, lbs (kg)	610,000 (276,696)
Bearings: No. of journal bearings	2
Type of journal bearings	5 pad tilting pad oil lubricated
Journal diameter, in. (mm)	20 (508)
Thrust bearing type	8 pad tilting pad, double acting oil lubricated
Thrust bearing OD, in. (mm)	30 (762)
Length of shaft over bearing centers, ft (m)	29 (8.8)

6.1.2. Turbine Aerodynamic Design

The properties of helium affect the turbine in very much the same way as they affect the compressor. That is, for a given overall expansion ratio the total number of stages for a helium machine will be much greater than for an air-breathing gas turbine. Because it is desirable to have as high a blade speed as possible in order to reduce the number of stages to a minimum, the most critical stress conditions are those of the first stage since the rotor blade metal temperature is close to the reactor outlet temperature.

Performance analysis of a large number of turbine rig tests produces an empirical relationship between stage loading factor ($\Delta H/U^2$), axial velocity/mean blade speed, and efficiency. Figure 6.8, constructed from test data (Ref. 6.3.) from many different rig turbines, shows this in simplified form. The aim in any new design of turbine is to place the design point within the high efficiency areas. This figure shows that if high efficiency is the sole criterion, the optimum values of stage loading factor and flow coefficient are between 1.0 and 1.2 and between 0.5 and 0.6, respectively. Factoring stress considerations into the turbine design, blade speed and blade height can be reduced to below their aerodynamic optimum values by raising both the stage loading factor and flow coefficient slightly without any serious penalty in efficiency. An early eight-stage turbine design done by General Atomic has stage loading factors between 1.44 and 1.34, which, in conjunction with flow coefficients of around 0.74, give an overall design in the "maximum efficiency" island as shown in Fig. 6.8. Although the efficiency values shown in Fig. 6.8 do not include allowances for tip clearance, leakage losses, and disk cooling losses, the position of the efficiency contours is not changed by these factors and the figure is useful as a preliminary design tool to establish a practical design.

For this initial eight-stage axial flow turbine, preliminary considerations of disk strength indicated that a rim speed of around 1050 ft/sec (320 m/sec) would be consistent with a conservative, highly reliable design. The turbine blade centrifugal stress (for a given geometry) is proportional to the $rpm^2 \times$ annulus area, the latter being determined by the selection of axial velocity at 850 ft/sec (259 m/sec). This value of axial velocity, while higher than customary in air-breathing, open-cycle gas turbines, permits small enough blade heights to give reasonable centrifugal stresses without at the same time producing unacceptably high exit losses. The high specific heat of



GA-A14311

Fig. 6.8 Generalized Axial Turbine Blading Efficiency Contours

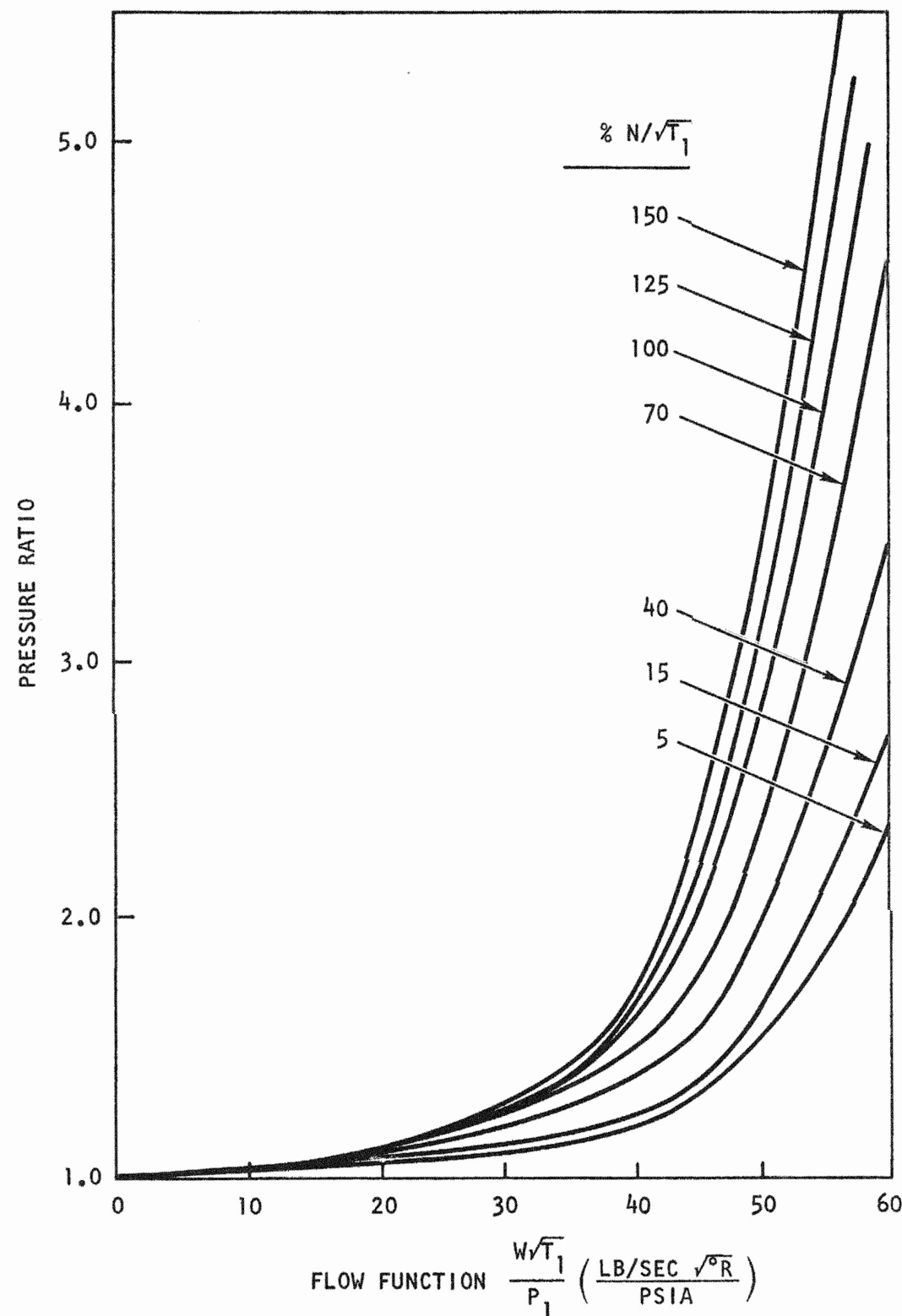
helium again produces a significant difference between air-breathing and helium turbines in that a given level of leaving loss characterizes a higher axial velocity in helium. The preliminary turbine design outlined in this paper has been based on the use of existing nickel-base alloys that have been used extensively in open-cycle turbines. A representative turbine map used in plant performance and control studies is shown on Fig. 6.9.

As mentioned above the in-depth turbomachinery design studies were done by United Technologies and details of the 8 stage turbine are given in Table 6.1. The high turbine efficiency of 91.8 percent (across the blading) again reflects the influence of technology from demonstrated advanced technology industrial and aircraft gas turbines.

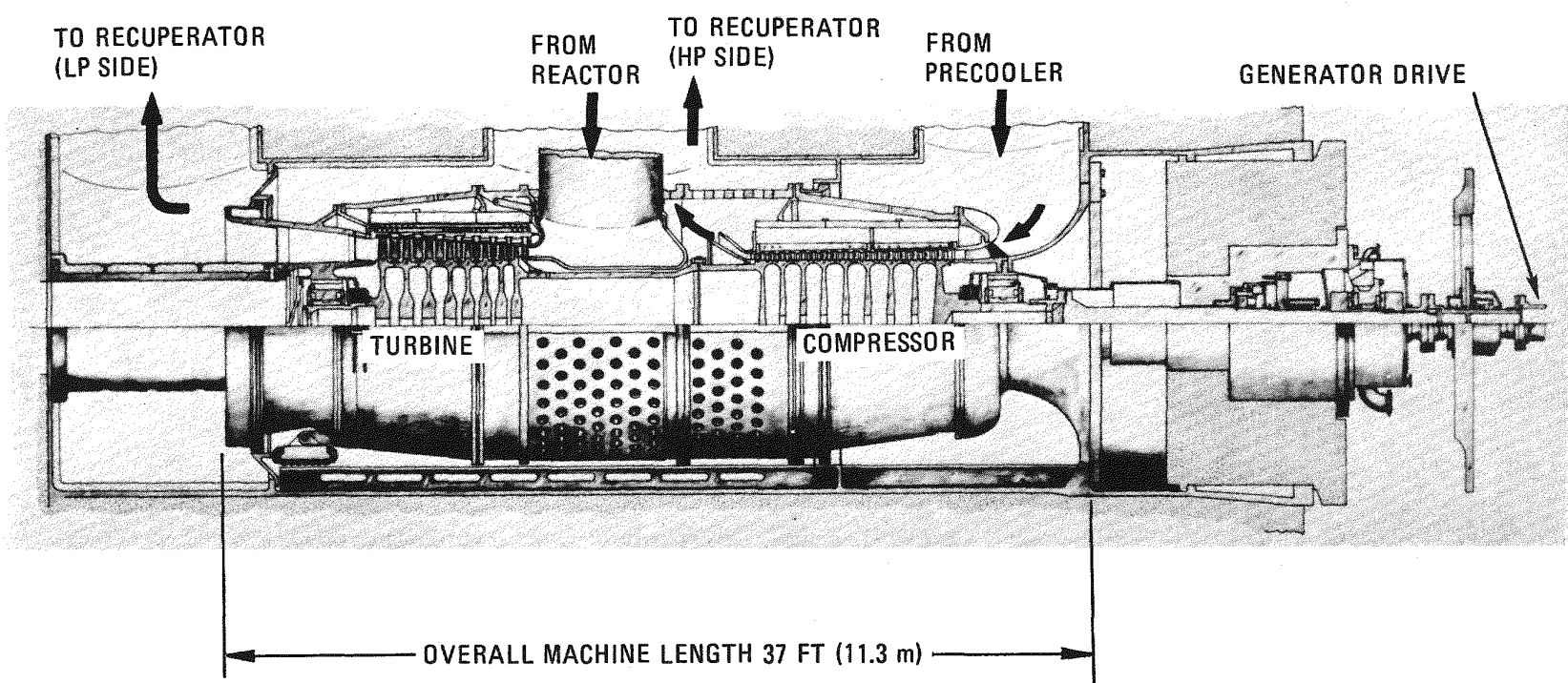
While the helium turbomachinery differs from air-breathing gas turbines in that large disks and small blade heights are essentially dictated by the nature of the working fluid and the high degree of pressurization, many of the aerodynamic procedures used are identical to conventional open-cycle industrial and aircraft gas turbine practice. A helium turbine is substantially smaller than an equivalent air-breathing turbine because the enthalpy drop in the helium turbine is many times greater. The specific power of the helium turbine (at 850°C inlet temperature) is on the order of 450 hp/lb/sec (0.73 MW/Kg/sec), which is considerably higher than can be achieved in advanced air-breathing turbines.

6.1.3 Turbomachine Mechanical Design

The turbomachine for the reference plant design has a power rating of 400 MWe at 60 Hz. As shown on Fig. 6.10, the machine is single-shaft and non-intercooled. The compressor and turbine have 18 and 8 stages, respectively. The rotor is of welded construction as opposed to earlier use of bolted rotor assemblies. Welded rotors have a long, successful history in European gas and steam turbines. The view of the compressor rotor in Fig. 6.11 shows the welded disk construction, the tangential blade attachments and dual blade rows mounted on each disk. This design reduces weight, machining time and number of parts. The turbine design shown on Fig. 6.12 also employs the welded rotor concept. It has an insulated case to reduce materials cost and control tip clearance. Tangential blade attachments are used to minimize turbine secondary cooling requirements and improve performance.

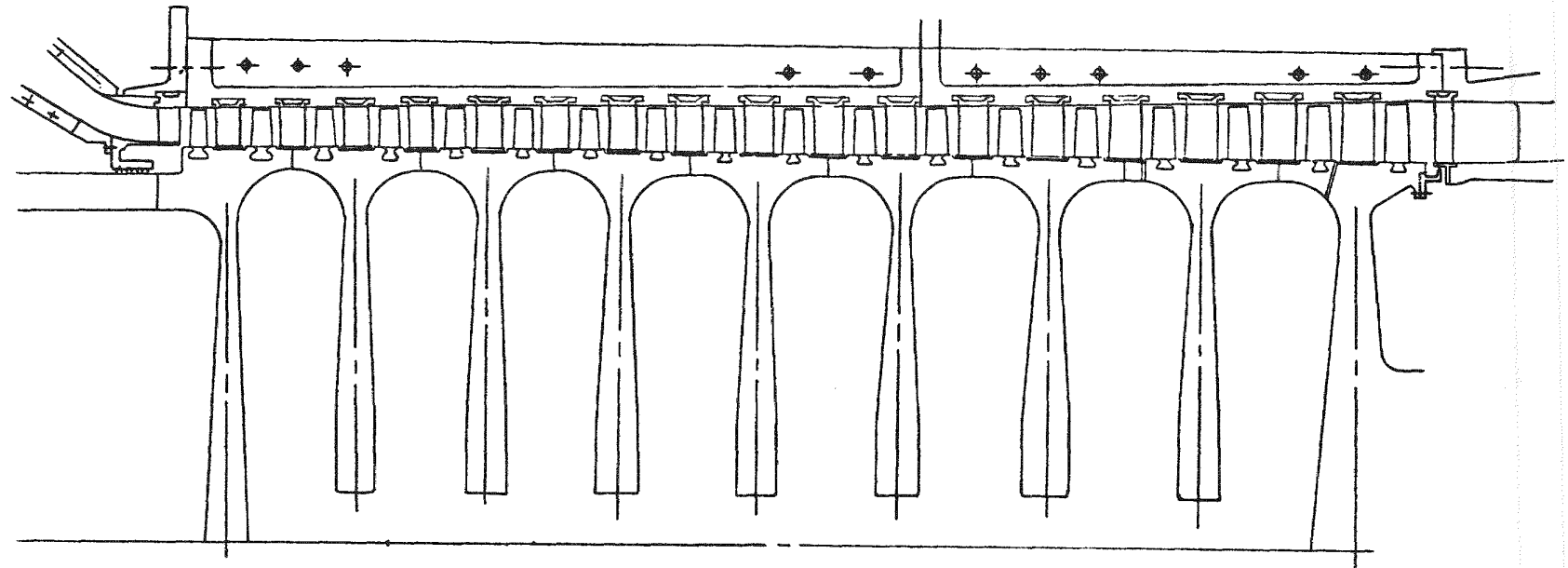


GA-A14311
Fig. 6.9 Simplified Helium Turbine Map



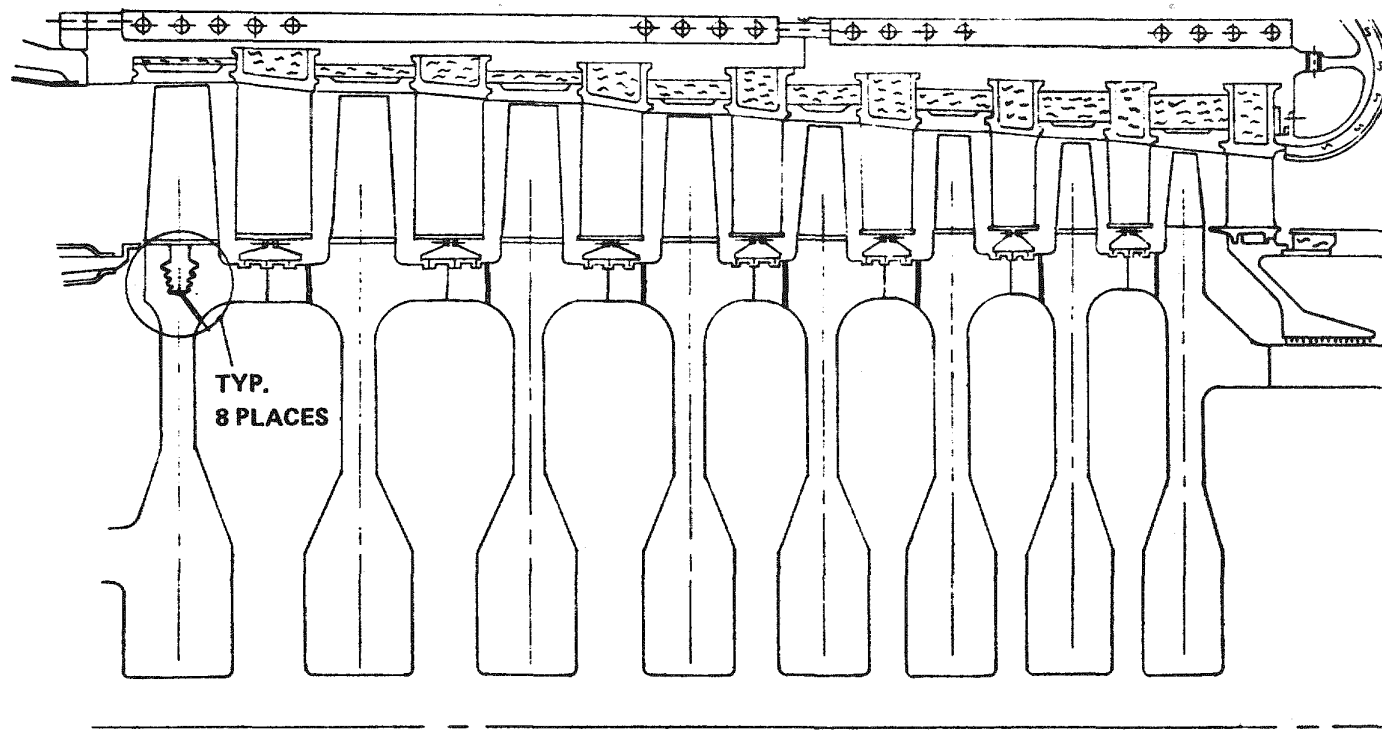
GA-A14311

Fig. 6.10 400 MW(e) Helium Gas Turbine



GA-A14311

Fig. 6.11 View of Compressor Rotor



GA-A14311

Fig. 6.12 View of Turbine Rotor

Table 6.1. includes the stress levels calculated for the various rotating elements of the turbomachine. Comparison with the capabilities of proposed materials for the turbomachine showed that the stressing of the first turbine stage was the most critical for the required operational life of the machine. The stress level shown for this component is well within the limits for projected 1% creep of the alloy IN-100 at 280,000 hours, which is the design life of the blading. The steady-state bending stresses produced in the blading by the gas turning forces are balanced by a component of the centrifugal force produced by a non-radial alignment of the centroids of the airfoil sections.

The mechanical analysis of the turbomachine included a complete determination of transverse and torsional critical speeds and axial vibration response. The results of the critical speed analysis, following several iterations with design modifications to remove potential problems are given below.

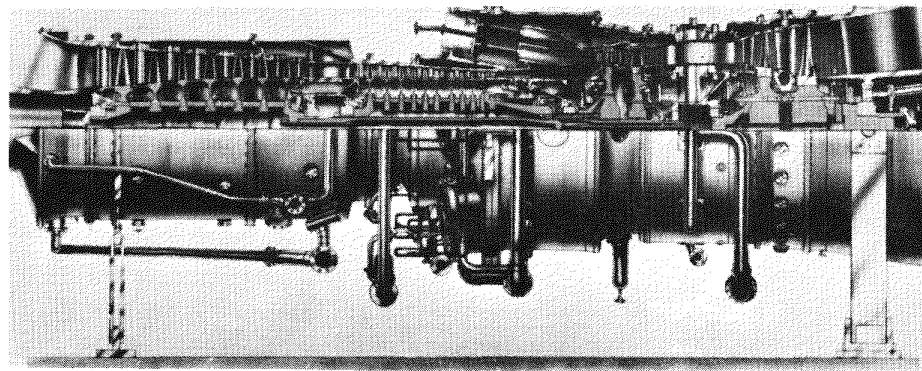
<u>Mode Type</u>	<u>N_c, rpm</u>
Gas Turbine Bounce	400
Gas Turbine Pitch	1450
Gas Turbine Bounce (Case out of Phase)	1440
First Shaft Bending	2900
Gas Turbine Ditch (Case out of Phase)	2400
Gas Turbine Free-Free	5000

From the above figures it can be seen that the turbomachine generator set has to "run through" several critical speeds in accelerating to its running speed. However, most of these are the so-called "bounce and pitch" modes which do not pose a threat to the integrity of the machine. The lowest critical speed which poses a threat to the integrity of the rotor is the "gas turbine free-free mode" which the analysis shows to be 5000 rpm. This is 39 percent higher than the design running speed of 3600 rpm and 15 percent higher than the maximum design overspeed of the machine which is 4320 rpm. Torsional natural frequencies were calculated to ensure that no resonance would occur with generator electrical frequencies. The first

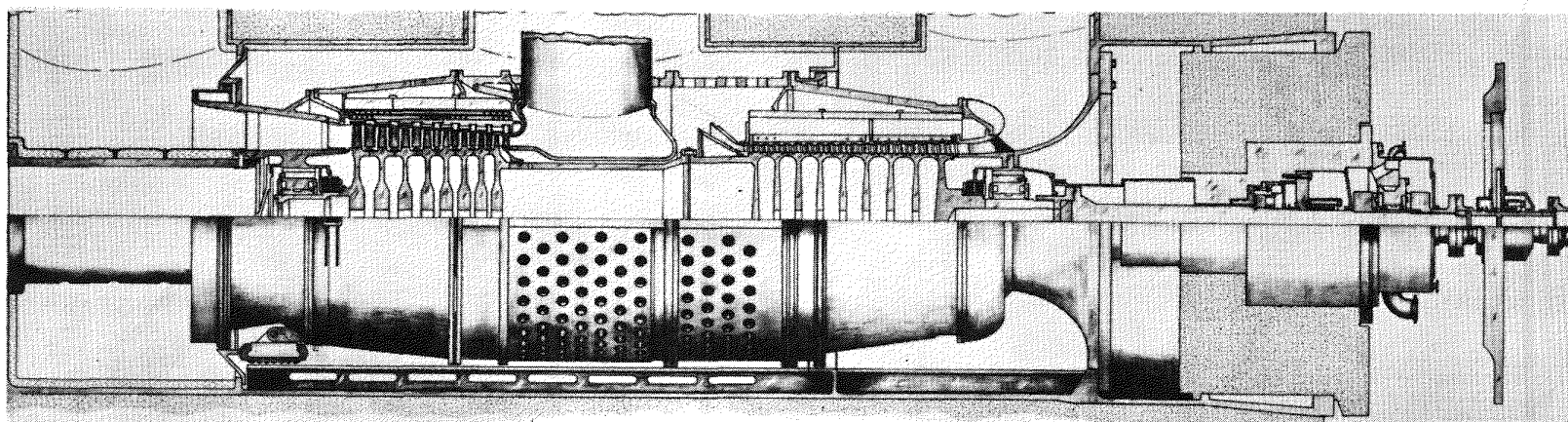
two natural frequencies are at 12 Hz and 138 Hz, the lower frequency giving a 90 percent margin below the fundamental 60 Hz frequency of the electrical generator, and the higher frequency giving a 16 percent margin above the 120 Hz first harmonic of the generator electro-mechanical excitation.

Oil lubricated bearings were chosen for the GT-HTGR turbomachine since in general minimum film thicknesses for oil bearings were found to be 1.3 to 2.0 times as great as those for water bearings with the same L/D ratio, and maximum allowable misalignments were found to be approximately twice as great for oil bearings as for water bearings. The journal bearings are subjected to high radial loading during normal operation and must be capable of withstanding temporary overload due to a seismic event. Tilting pad bearings were selected wherever possible because of their self-aligning capability, which is essential, and their inherent stability. A tilting pad type of double-acting arrangement was selected for the oil-lubricated thrust bearing. With an outer diameter of 30 inches (762 mm) and a running speed of 3600 rpm, the thrust bearing is slightly beyond current thrust bearing experience. However, it is the opinion of bearing manufacturers who have been consulted that the design is attainable with little more in the way of development than a demonstration test.

The overall length of the turbomachine is 37 ft (11.3 m). The overall diameter of 11.5 ft (3.5 m) was a design constraint to facilitate rail transportation including the turbomachine when contaminated and installed in a shielded cask. The overall weight of the machine is 305 Ton (277,000 Kg). Rotor burst protection is incorporated in the machine design in the form of burst shields around the compressor and turbine rotor bladed sections. Design criteria and details of these burst shields are given in Ref. 6.4. From Fig. 6.13 it can be seen that the overall size of the 400 MWe helium gas turbine is similar to that of a 100 MWe open-cycle industrial gas turbine. Fig. 6.14 is of interest since it vividly compares the projected size of a helium turbine blade with that of a 136 MWe steam turbine; the full impact of such a comparison would be more dramatic if a rear stage blade from a modern low-pressure steam turbine had been portrayed.



100 MWe UNITED TECHNOLOGIES FT50 ADVANCED OPEN-CYCLE INDUSTRIAL GAS TURBINE

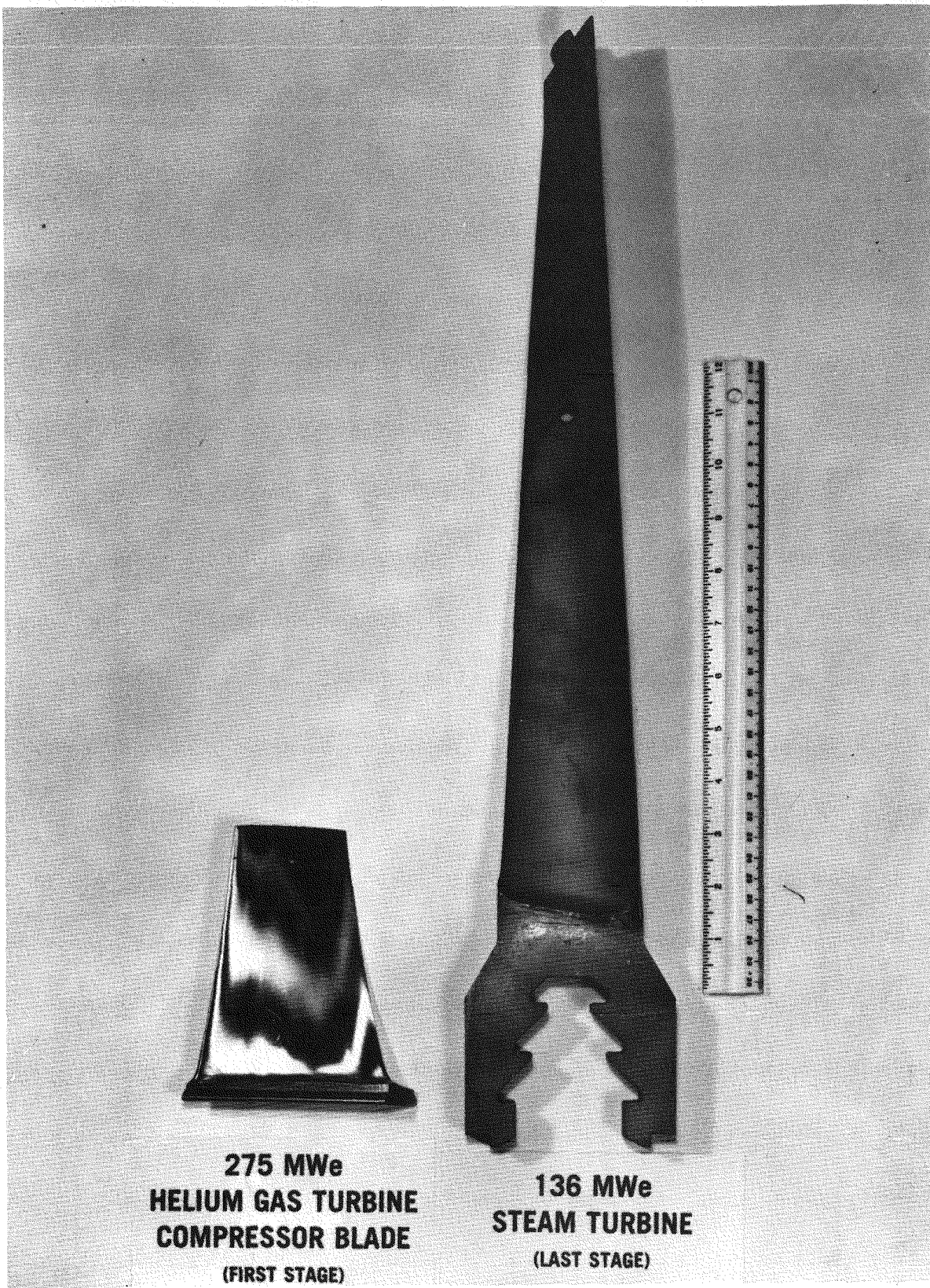


400 MWe HTGR HELIUM TURBOMACHINE (UNITED TECHNOLOGIES DESIGN)



GA-A14311

Fig. 6.13 Comparative Sizes of Open- and Closed-Cycle Turbomachines



GA-A14311

Fig. 6.14 Blade Size Comparison

6.1.4. Turbomachine Installation and Removal

When repairs to the machine or a thorough inspection are necessary, it will be removed from the PCRV cavity, since the confined space and possibility of radiation from plated-out fission products render impractical all but the simplest inspection and maintenance (that of the bearings). Removal of a turbomachine will be the most extensive maintenance task accomplished at the power station site. Special air pallet units, casks, portable winches, miscellaneous handling tools, fixtures, and alignment tools are some of the equipment needed. An analysis of the procedures and time necessary to remove and replace the turbomachinery has indicated that an estimated 21 working days (utilizing 2 shifts per day) to remove and replace the turbomachine is realistic. Under normal maintenance schedules this operation would be done during plant refueling.

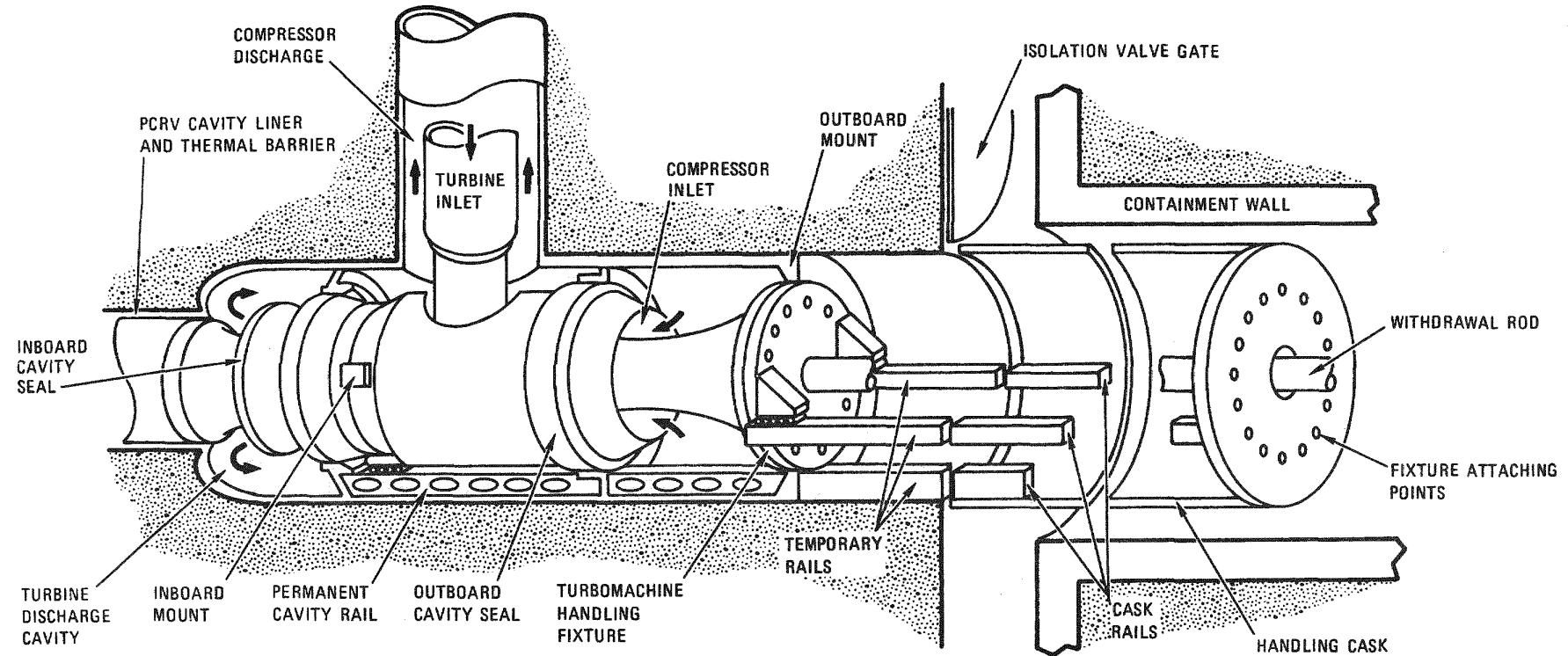
Transfer of the turbomachine between the PCRV cavity and the handling cask during removal or installation is effected by rolling the machine into the cavity. Fig. 6.15 shows the turbomachine being moved on its roller system. The cask and plug cavity are purged of air and filled with helium. The inflatable seals on the turbomachine are then de-energized. Next the turbomachine is pulled into the cask using a power winch. With the turbomachine in the cask, the rail sections in the temporary rails shown in Fig. 6.15 are retracted by their pneumatic cylinder actuators and the valve closed. The cask pallet is withdrawn and then moved along the surfaced runway to the siding (shown earlier in the plant plot plan) where two rented crawler cranes are used to lift it off the pallet and onto the railcar. The installation of a spare machine is accomplished by a reversal of the above sequence.

6.1.5. Rating Potential for 60 Hz Non-Intercooled Turbomachine

A very simplistic approach is given below for the portrayal of the basic data leading to identification of machine size. The main point of interest for a given turbine inlet temperature (850°C) is the influence of machine power on the life expectancy for a given blade material. The simplistic curves presented are based on the assumption that the stress level in the turbine blading is the life controlling function.

6.1.5.1. Blade Stresses

It was assumed that bending stresses are off-set by blade tilt; that is, if the blade section centroids are arranged along non-radial lines so



GA-A14311

Fig. 6.15 Turbomachine Installation and Removal

that the centrifugal force tends to counteract the bending effect of the deflection of gas on the rotor blading. A further simplification was made: while realizing that the blade effective stress is a combination of centrifugal and untwist stresses, only the centrifugal stress was considered in this brief study.

The centrifugal stress was computed from the simple relationship:

$$f_c = 2\pi\rho \frac{N^2}{g} A.T.$$

where ρ = blade material density, lb/ft^3

N = rotational speed, rpm

A = annulus area, ft^2

T = blade taper factor (0.70 assumed)

The above equation for blade centrifugal stress then reduces to:

$$f_c = 1.274 A(N/100)^2 \text{ for IN-100 blade material}$$

$$f_c = 1.68 A(N/100)^2 \text{ for TZM blade material}$$

The difference in constants merely reflects the 32% higher density of the refractory material.

6.1.5.2. Material Properties

For the 850°C turbine inlet temperature case, the candidate blade material was assumed to be IN-100, which is a nickel-base precipitation hardenable, vacuum cast alloy. For comparison purposes, an arc-cast molybdenum-base TZM was also evaluated.

The important properties (from the standpoint of blade life at elevated temperature) are shown on Fig. 6.16. The creep-rupture allowance is taken to be 0.80 of the average data, and the data shown are for a temperature of 850°C . At the exit from the turbine (where the gas temperature is around 550°C) the creep criteria is no longer the life governing factor and it is assumed that the Ultimate Tensile Strength (2/3 of the minimum value taken) of the material limits the rear stages, if indeed this is the lesser of the allowables. UTS data for IN-100 and TZM are given on Fig. 6.16 for a temperature of 550°C .

CREEP DATA AT 850°C (1562°F)	MATERIAL	IN-100	TZM
CREEP RUPTURE ALLOWABLE SHOWN	NICKEL-BASE	NICKEL-BASE	REFRACTORY
PLOTTED EQUALS 80% AVERAGE VALUE	MINIMUM UTS AT 850°C, PSI	108,000	82,000
	MINIMUM UTS AT 550°C, PSI	128,000	100,000
	DENSITY, LB/FT ³	0.28	0.369
	α , IN/IN°F AT 800°C	7.5×10^{-6}	3.0×10^6

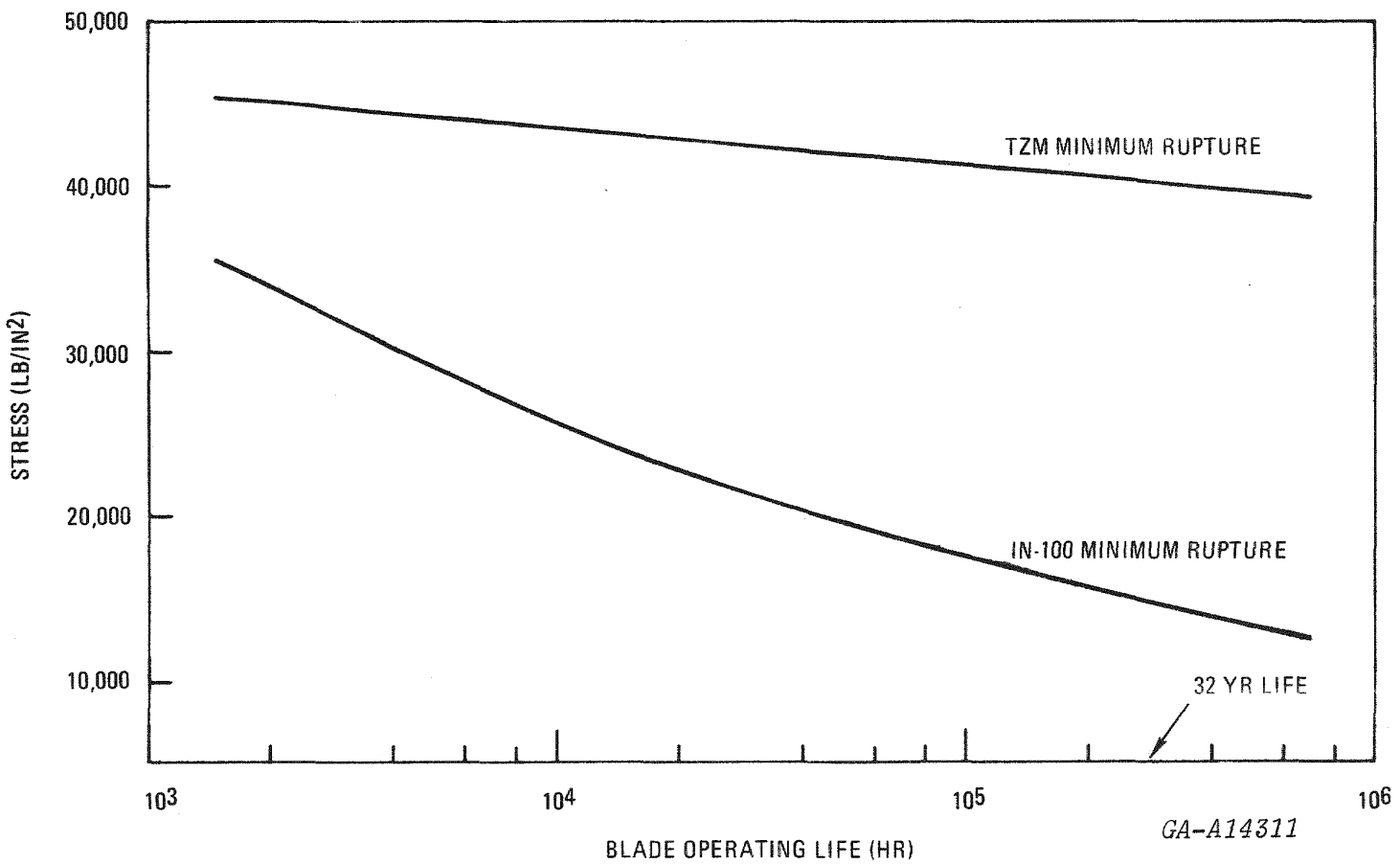


Fig. 6.16 Structural Properties of Turbine Blade Materials

6.1.5.3. Turbomachine Size Limits

6.1.5.3.1. Nickel-Base IN-100 Blade Material

The inter-relationship between first stage blade centrifugal stress and creep rupture-life is shown on Fig. 6.17. A quick check on the rear stage showed that 2/3 of the UTS was very much higher than the blade centrifugal stress, hence the rear stages are not limiting. The curves clearly show that a single non-intercooled turbomachine of 1200 MWe at 60 Hz (for a 3000 Mwt core) is not feasible with un-cooled blades. The 400 MWe machine for the 3 loop reference plant has conservative stresses. For the simplified assumptions made it can be seen that for the full operating life of 280,000 hours (i.e. 40 years at 80% utilization) the machine upper limit is around 530 MWe. With more detailed analysis, and slight adjustment to the annulus area it is postulated that a 600 MWe machine (2 loop plant) could be designed to meet the life goal.

6.1.5.3.2. TZM Blade Material

It can be seen from Fig. 6.17. that with the very high creep rupture strength of TZM, the life of the machine is not dictated by the first stage blade centrifugal stresses. At the turbine exit, however, the UTS of TZM is less than IN-100. If all 8 stages of the turbine had TZM blading, then the power of the machine would be limited to about 720 MWe by the rear stages. If the rear stages had IN-100 blades then the power limit would be increased to about 920 MWe. Because of the over two to one (IN-100/TZM) difference in coefficient of expansion, a turbine with dual blading might be difficult from the standpoint of tip clearance control. This limited study has shown that, even with the use of an advanced material such as TZM for the turbine blading, a single 60 Hz machine (non-intercooled) of 1200 MWe for a 3000 Mwt reactor is not feasible.

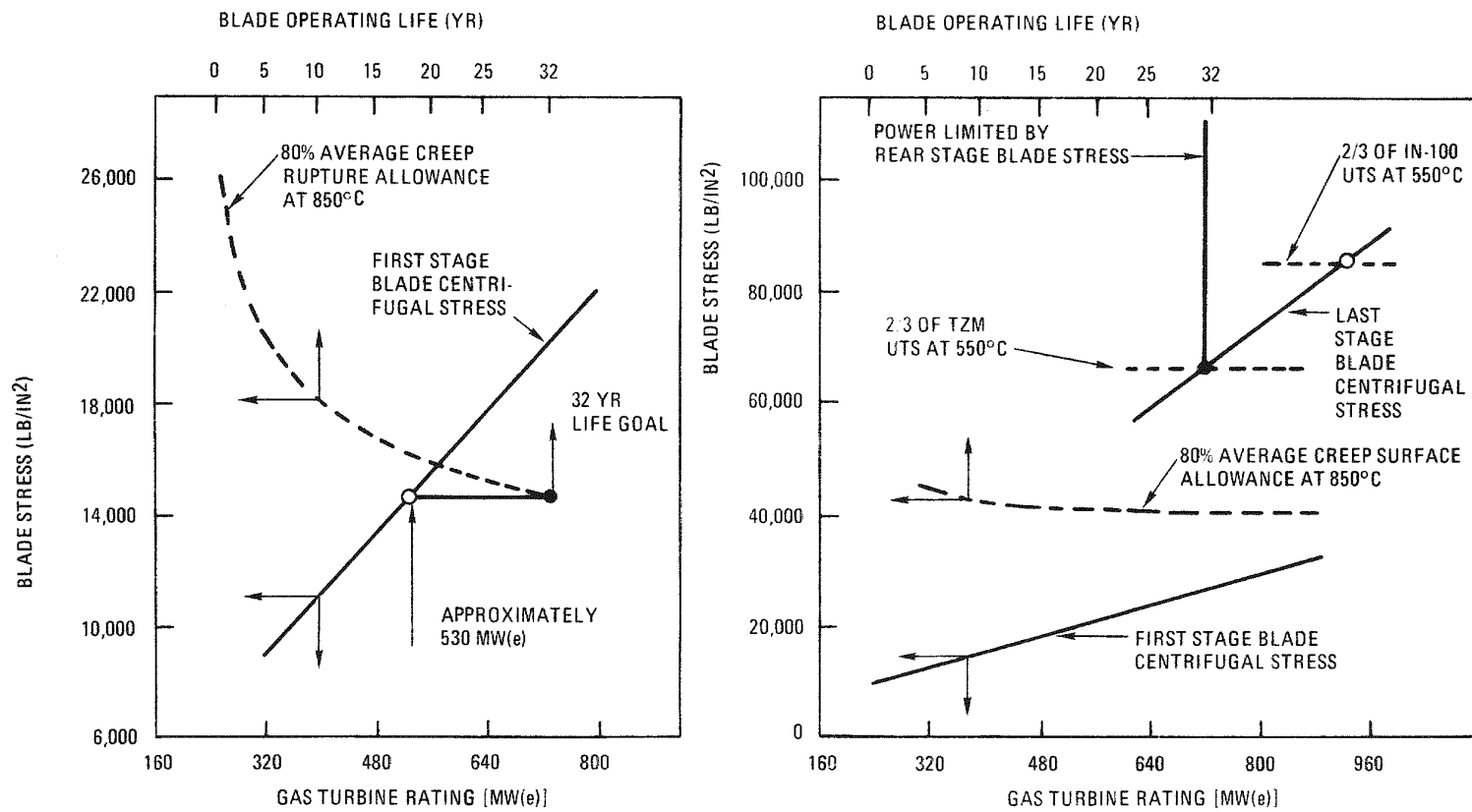
6.2. Heat Exchanger Design Considerations

Since the design aspects of the GT-HTGR heat exchangers have been covered comprehensively in a recent paper (Ref. 6.5) they will be only briefly covered in this report. The heat exchangers are large components and they have a significant influence on the integrated primary system. The combined effects of size constraint (integration in the PCRV side-wall cavities), in-service inspection, in-situ repair, and maintenance and fabrication considerations

• DATA FOR UNCOOLED BLADES, TURBINE INLET 850°C, TURBINE OUTLET 550°C

A) NICKEL-BASED
IN-100
BLADE MATERIAL

B) REFRACTORY
TZM
BLADE MATERIAL



GA-A14311

Fig. 6.17 Rating Potential for Nonintercooled 60 Hz Turbomachine

have a significant effect on the choice of surface geometry, flow configuration, and mechanical design.

A ground rule for the recuperator and precooler is that they must be designed for the full 40 year life of the plant which, with a 80% load factor, corresponds to a service life of 280,000 hours. Design objectives for the heat exchangers are given on Table 6.2. From the heat exchanger design data (Table 6.3.) it can be seen that the heat transfer rates are very high. The magnitude of the interval energy transfer within the cycle for the 3 recuperators (3094 Mwt) is on the same order as the reactor thermal input of 3000 Mwt. In the case of the precooler, the system reject heat of 1893 Mwt is transferred via a closed water loop to the dry cooling towers, where it is dissipated to the atmosphere in air-cooled exchangers.

Because of the nature of the gas turbine cycle, the combined surface area requirements of the recuperator (gas-to-gas exchanger) and precooler [gas-to-water (pressurized to suppress phase change)] are much higher than for the steam generator for the HTGR plant. Since it is desirable to limit the heat exchanger diameter for (1) minimum cavity size in PCRV, (2) reasonable fabrication limit, and (3) ease of transportation to the site, the much higher surface area requirements of the GT-HTGR plant have necessitated the use of smaller hydraulic diameter passages than in contemporary steam generators. From the standpoints of tubesheet thickness, fabrication, maintenance, repair, and flow distribution, it is not practical to consider a full array of small tubes in a bundle of approximately 16.5 ft (5 m) diameter; thus modularization is necessary.

With the integrated plant concept there is limited freedom in the selection of the heat exchanger fluid flow paths within the primary system. Detailed design studies have shown that satisfactory gas flow paths (with acceptable pressure loss) within the primary system could be achieved with an axial flow arrangement (counterflow) in both exchangers.

Tubular types of construction were selected for both the recuperator and precooler. The main reason for this selection was that it represents the only type of construction that has been proven to have the structural integrity for long life electrical utility power service. The much more compact type of plate-fin surface geometries used for open-cycle gas turbine recuperators (Ref. 6.6.) have only been demonstrated at low pressure levels. The basic design decisions mentioned above are summarized on Table 6.4.

TABLE 6.2
DESIGN OBJECTIVES FOR GT-HTGR HEAT EXCHANGERS

- Select Geometries and Arrangements of Proven Construction
- Simplicity of Design
- Use of Code-APPROVED Materials
- Use Existing HTGR Technology to the Maximum
- Use Conservative Design Parameters

Heat Exchanger Configurations Presented have been
Design for the Full 40-Year Plant Life (280,000
Operating Hours)

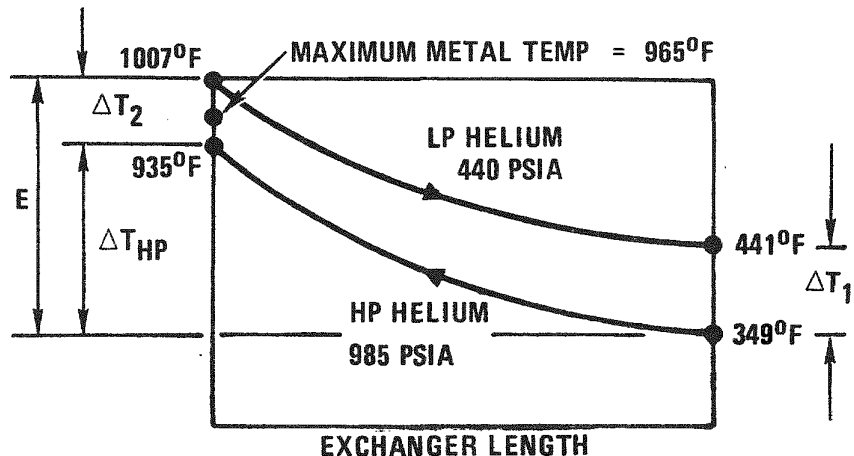
- Major Attention Given to Safety, Reliability, Maintenance,
and Repair Considerations in Conceptual Design Phase

GA-A14317

TABLE 6.3

HEAT EXCHANGER DESIGN DATA

RECUPERATOR



$$\text{EFFECTIVENESS} = \Delta T_{HP}/E = 0.89$$

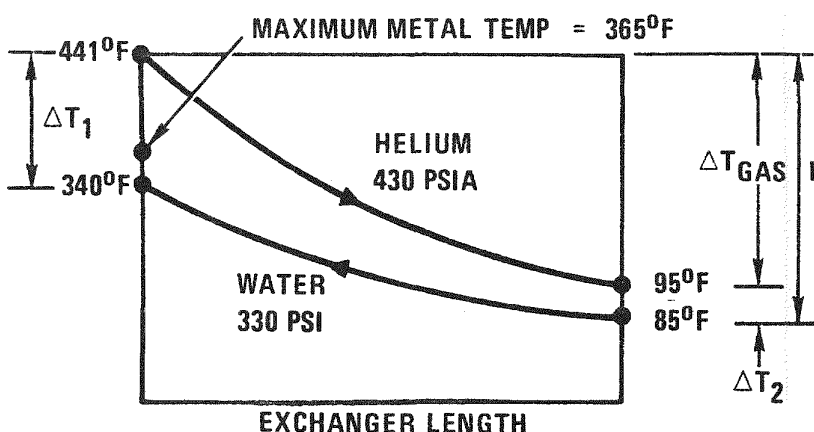
$$\text{HEAT TRANSFER Q/PLANT} = 3094 \text{ MW(t)}$$

$$\text{LOG MEAN TEMPERATURE DIFFERENCE (LMTD)} = \frac{\Delta T_1 - \Delta T_2}{\log \Delta T_1 / \Delta T_2} = 81^\circ\text{F}$$

$$\text{THE CONDUCTANCE} = Q/\text{LMTD} = 130 \times 10^6 \text{ BTU/HR}^\circ\text{F (UA)}$$

$$\text{PRESSURE LOSS} \quad \sum(\Delta P/P) = \frac{\Delta P_{HP}}{P_{HP}} + \frac{\Delta P}{P_{LP}} < 3\%$$

PRECOOLER



$$\text{HELIUM EFFECTIVENESS} = \Delta T_{GAS}/E = 0.972$$

$$\text{HEAT TRANSFER Q/PLANT} = 1893 \text{ MW(t)}$$

$$\text{LMTD} = \frac{\Delta T_1 - \Delta T_2}{\log \Delta T_1 / \Delta T_2} = 39.4^\circ\text{F}$$

$$\text{CONDUCTANCE (UA)} = Q/\text{LMTD} = 165 \times 10^6 \text{ BTU/HR}^\circ\text{F}$$

$$\text{HELIUM PRESSURE LOSS} \quad \frac{\Delta P_{LP}}{P_{LP}} < 1.5\%$$

$$\text{WATER PRESSURE LOSS} = \text{APPROX. 30 PSI}$$

TABLE 6.4
PRELIMINARY HEAT EXCHANGER DESIGN DECISIONS

- Recuperator and Precooler in Separate Cavities
 - Simple Installation
 - Maintenance Simplified Because no Direct Interaction Between Exchangers
 - Added Flexibility for Waste Heat Power Plant Application
- Modular Assembly
 - Simplified Construction
 - Installation and Handling
 - Ease of Maintenance
 - Reduced Tubesheet Stress
- Tubular Surface Geometry
 - Pressure Containment and Structural Integrity
 - Simple Tubesheet Joints
 - Minimum Cost
- Axial Counterflow Configuration
 - Minimum Surface Area (For High Effectiveness)
 - Low Pressure Loss
 - Tube Vibration Effects Minimized
 - Thermal Stress Effects Minimized
 - Simple Headering
 - Size Compatible with Installation in PCRV Sidewall Cavities

GA-A14311

While the counterflow tubular configuration approach used in the design of the recuperator and the precooler yields dimensions particularly suited for PCRV cavity installations, the actual packaging of the heat transfer matrix to minimize heat exchanger frontal area requirements (thus minimizing PCRV cavity diameter requirements) is of vital importance. With the possibility of packaging both heat exchangers as full, homogeneous tube arrays within their respective cavities ruled out by practical considerations, the approach taken toward modularization of the heat transfer matrix must be selected carefully. Since homogeneous tube arrays produce the minimum possible PCRV cavity diameters, the module shape and size for a given heat exchanger design should be the combination which most nearly produces the ideality of a homogeneous tube field while satisfying the mechanical design requirements for handling and thermal growth flexibility.

Compared with the circular modules reported previously (Ref. 6.5.) recent innovations in module subheadering and shrouding techniques have resulted in a configuration of much improved packaging efficiency which has made possible a reduction in heat exchanger diameter for the same unit performance. With a novel subheadering arrangement, in which the tubeplate itself lies within the tube field (as shown in Fig. 6.18), a contiguous hexagonal array of modules results in a more efficient utilization of frontal area. Mutually shared partitions between modules, rather than individual cans or shrouds, are possible, thus eliminating the need for intermodule bypass seals, increasing the rigidity of the modular array and facilitating provision for shell-side mixing (via perforated or discontinuous partitions). Both the recuperator and precooler embody this type of construction, and details of these units are given below.

6.2.1. Recuperator Design

For a representative surface geometry, the influence of recuperator effectiveness on exchanger length, pressure loss, and surface area can be seen on Fig. 6.19. For the reference plant design an effectiveness value of 0.898 was selected. The results of a typical recuperator thermal sizing study are shown on Fig. 6.20. The passage of each pressure loss curve through a unique minimum illustrates an additional constraint typical of counterflow exchangers. The 7/16 in (11.1 mm) O/D tube on a 1.4 p/d surface geometry selected for the reference design has a pressure loss near the minimum. Details of the selected recuperator are given in Table 6.5.

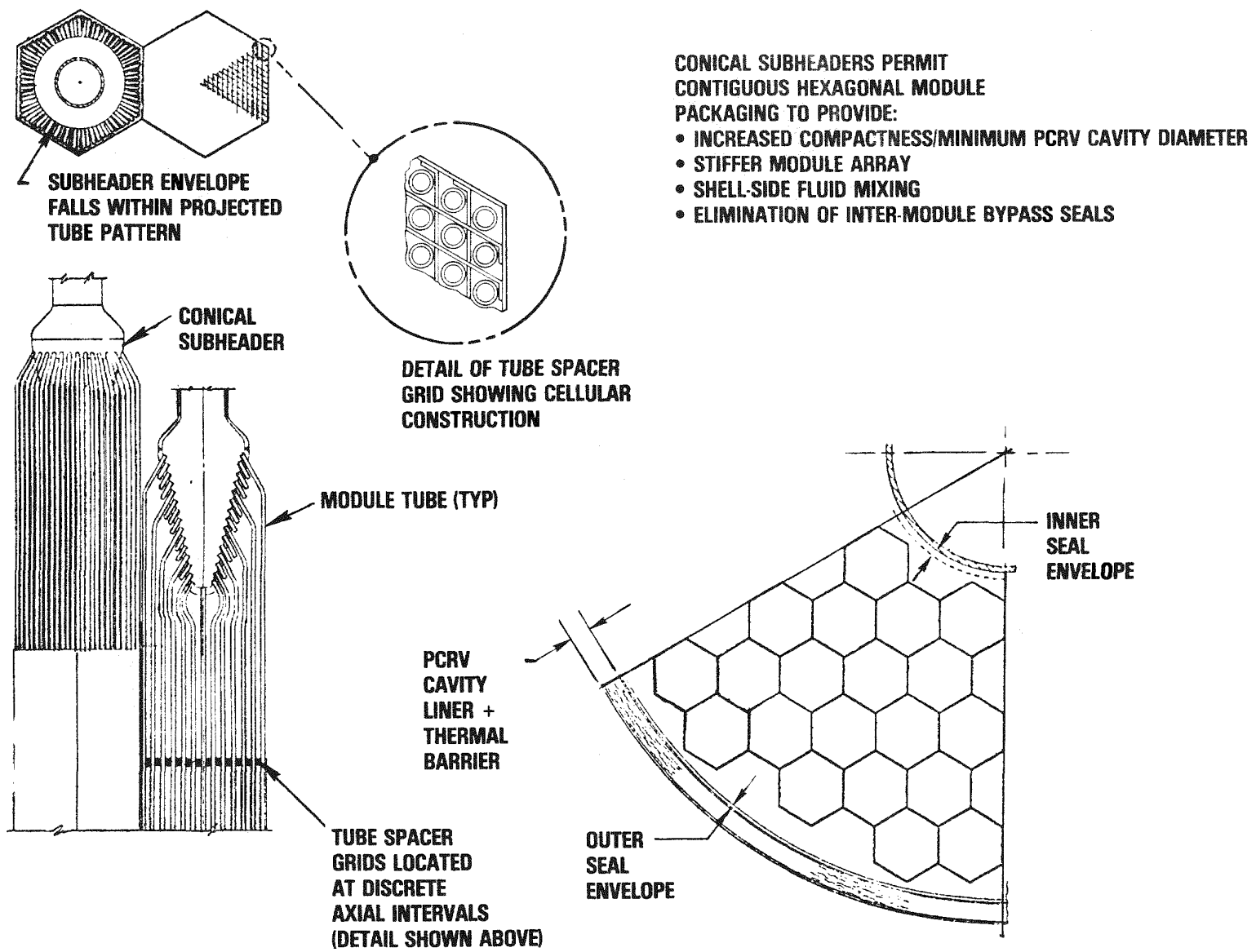
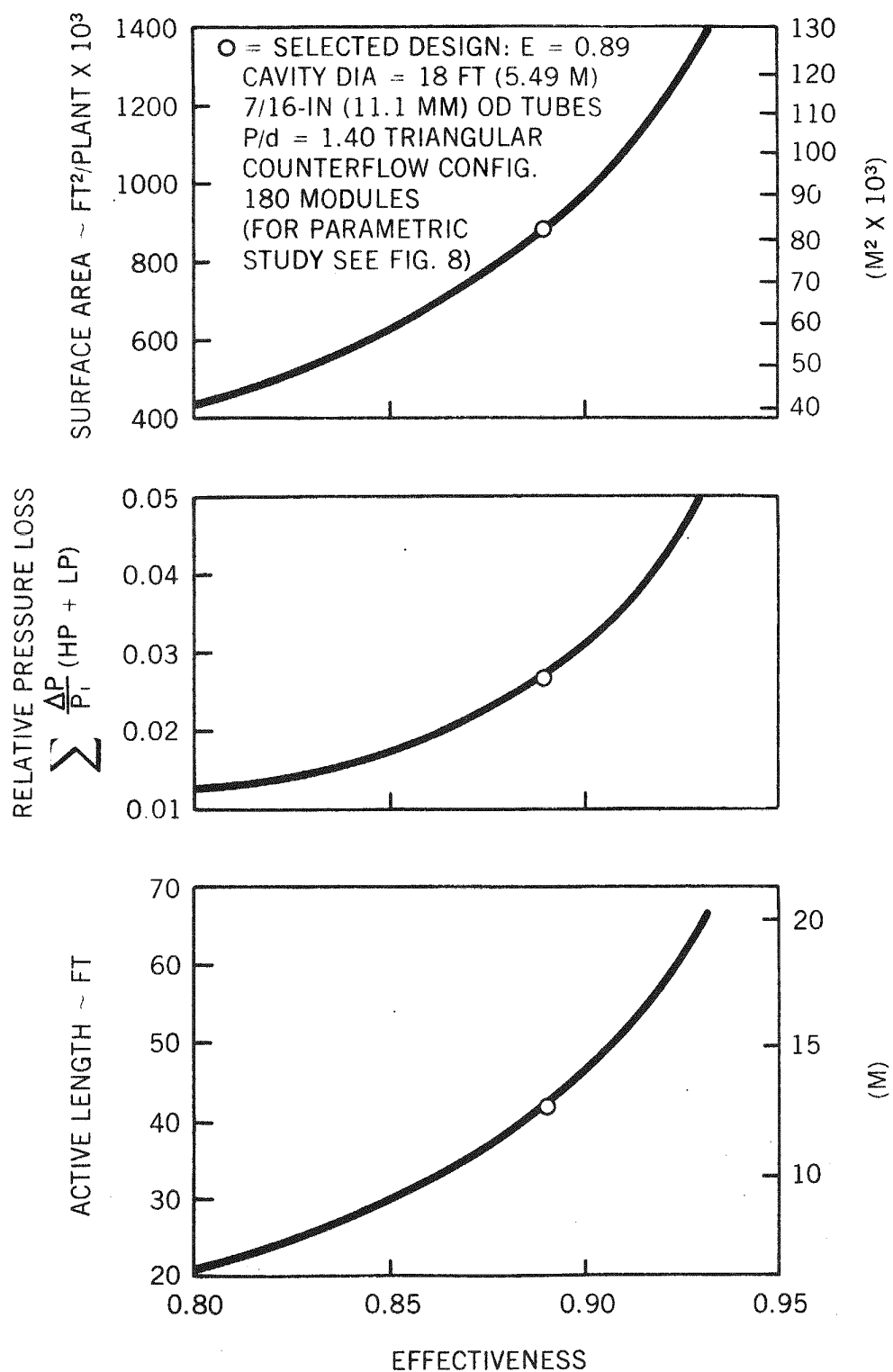


Fig. 6.18 Heat Exchanger Module Details

GA-A14311



GA-A14311

Fig. 6.19 Influence of Effectiveness on Recuperator Size

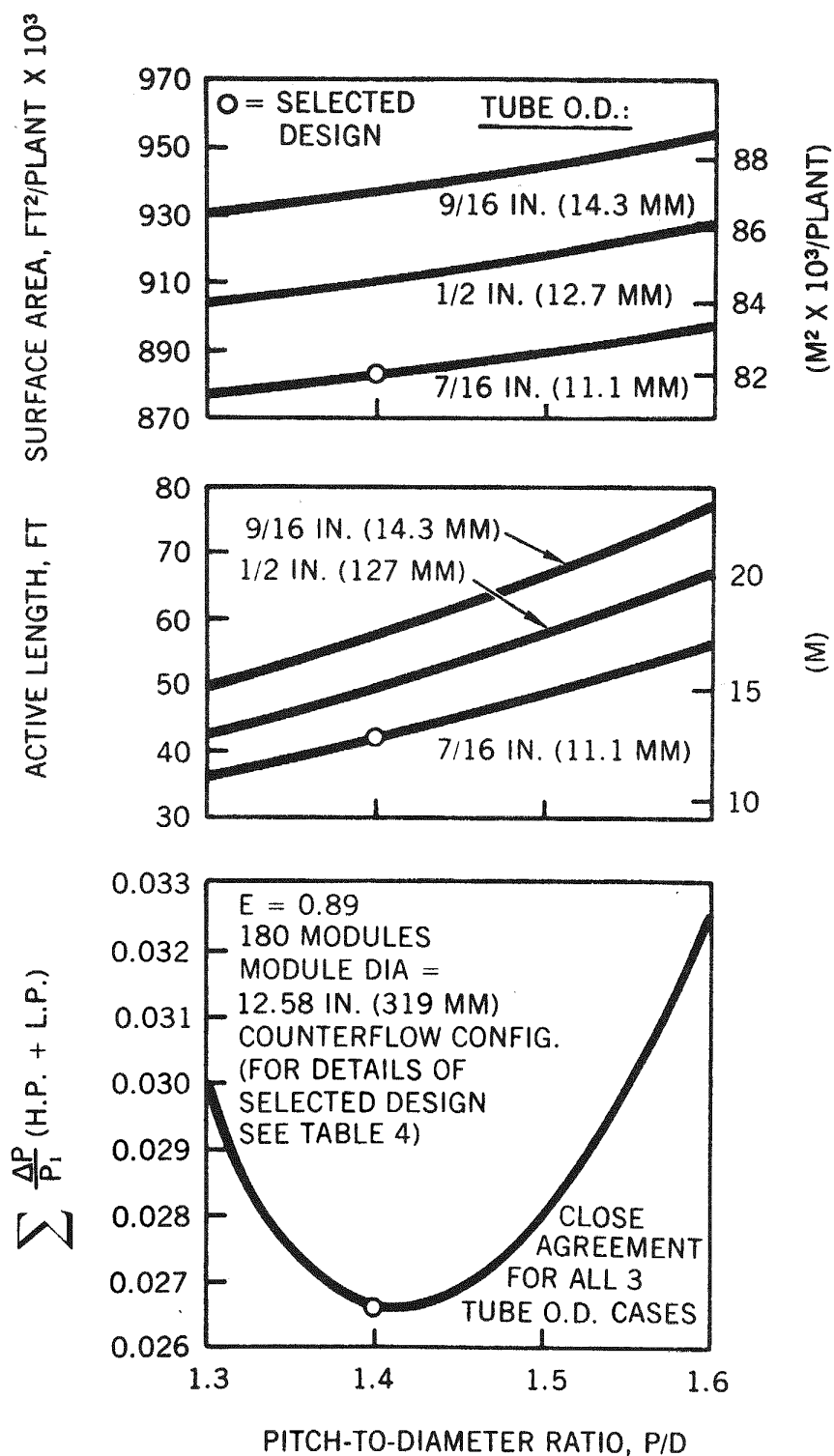


Fig. 6.20 Influence of Surface Geometry on Recuperator Size and Performance

GA-A14311

Table 6.5 Summary of GT-HTGR Heat Exchanger Design

	Exchanger	Recuperator	Precooler
Type	Number per Reactor	3	3
	Matrix Type	Tubular	Tubular
	Flow Configuration	Counterflow	Counterflow
	Construction	Modular	Modular
Thermal	Heat Transfer Rate, MW(t) per Reactor	2860	1740
	LMTD, °F (°C)	75.3 (41.8)	38.0 (21.1)
	Effectiveness	0.898	0.972
	Helium ($\Delta P/P$)	0.0184	0.010
Surface Geometry	Tube Outer Diameter, in. (mm)	0.4375 (11.1)	0.375 (9.5)
	Tube Wall Thickness, in. (mm)	0.045 (1.14)	0.049 (1.24)
	Tube Pitch Arrangement	Triangular	Triangular
	Pitch/Diameter Ratio	1.374	1.38
	Maximum Metal Temperature, °F (°C)	968 (520)	357 (81)
Tube Bundle Details	Material Type	2-1/4 Cr - 1 Mo	Med. Carbon Steel
	Hexagonal Module Dimension, in. (mm)	14.2 (361) A/F	13.2 (335)
	Modules/Exchanger	144	144
	Tubes/Module	547	631
	Effective Tube Length, ft (m)	39.8 (12.13)	37.0 (11.28)
Overall Assembly	Surface Area/Reactor, ft ² (m ²)	1.08×10^6 (100,000)	990,000 (91,900)
	Cavity Diameter (ITB), ft (m)	17.25 (5.26)	16.0 (4.9)
	Approximate Overall Length, ft (m)	62 (18.9)	73 (22.3)
	Overall Diameter, ft (m)	16.75 (5.1)	15.5 (4.72)
	Module Weight, lb (kg)	5230 (2375)	5980 (2715)
	Approximate Assembly Weight, tons (kg)	474 (430,000)	445 (404,000)
	Fabrication Location	Factory	Factory

GA-A14311

Details of the recuperator are shown on Fig. 6.21, and in a simplified schematic form on Fig. 6.22. The recuperator consists of 144 hexagonal vertically oriented modules connected in parallel to a tube sheet at the top end, and to a high pressure bottom drum header that is connected to a cylindrical return duct passing up through the center of the modular array. The unit is supported from its upper tubeplate, and with no mechanical connections at the bottom of the assembly (hot end) unrestrained growth capability is provided. In addition to performing their headering function, the lower set of lead tubes is coiled to provide the necessary flexibility for the accommodation of differential expansion.

Studies on the applicability of enhanced surface geometries (i.e., roughened and finned-tubes) for the recuperator showed that, while the length of the exchanger could be reduced, this did not manifest itself in a cost reduction; accordingly, plain tubes were selected. Support of the small diameter tubes within the module shrouds is provided by means of cellular spacer grids located at axial intervals along the tube bundles.

The temperature and pressure levels in the recuperator are low enough to permit the selection of a ferritic alloy (2-1/4 Cr - 1 Mo) as the material for the tubes and most of the structural members. At the high temperature end of the unit the lower lead tubes are fabricated from an austenitic material (316 St St), this being necessary to give the 280,000 hour life requirements, since in this region of the exchanger creep considerations are dominant. The design stress intensity curves for the heat exchanger materials in the temperature range of interest are shown on Fig. 6.23.

6.2.2. Precooler Design

With a water inlet temperature of 85°F (29.4°C), the approach temperature (between helium and water) and the level of the water outlet temperature (to the cooling tower) have a significant effect on the surface area of the precooler as can be seen on Fig. 6.24. A water outlet temperature of 340°F (171°C) was selected from precooler/dry-cooling tower performance and trade-off studies, and this gives a plant water flow in the closed coolant loop for the three precoolers on the order of 50,000 gpm. The results of a typical precooler thermal sizing study are shown in Fig. 6.25, which indicates that the solutions for the given PCRV cavity envelope become more optimal as tube diameter and pitching are decreased. The design selection was thus governed

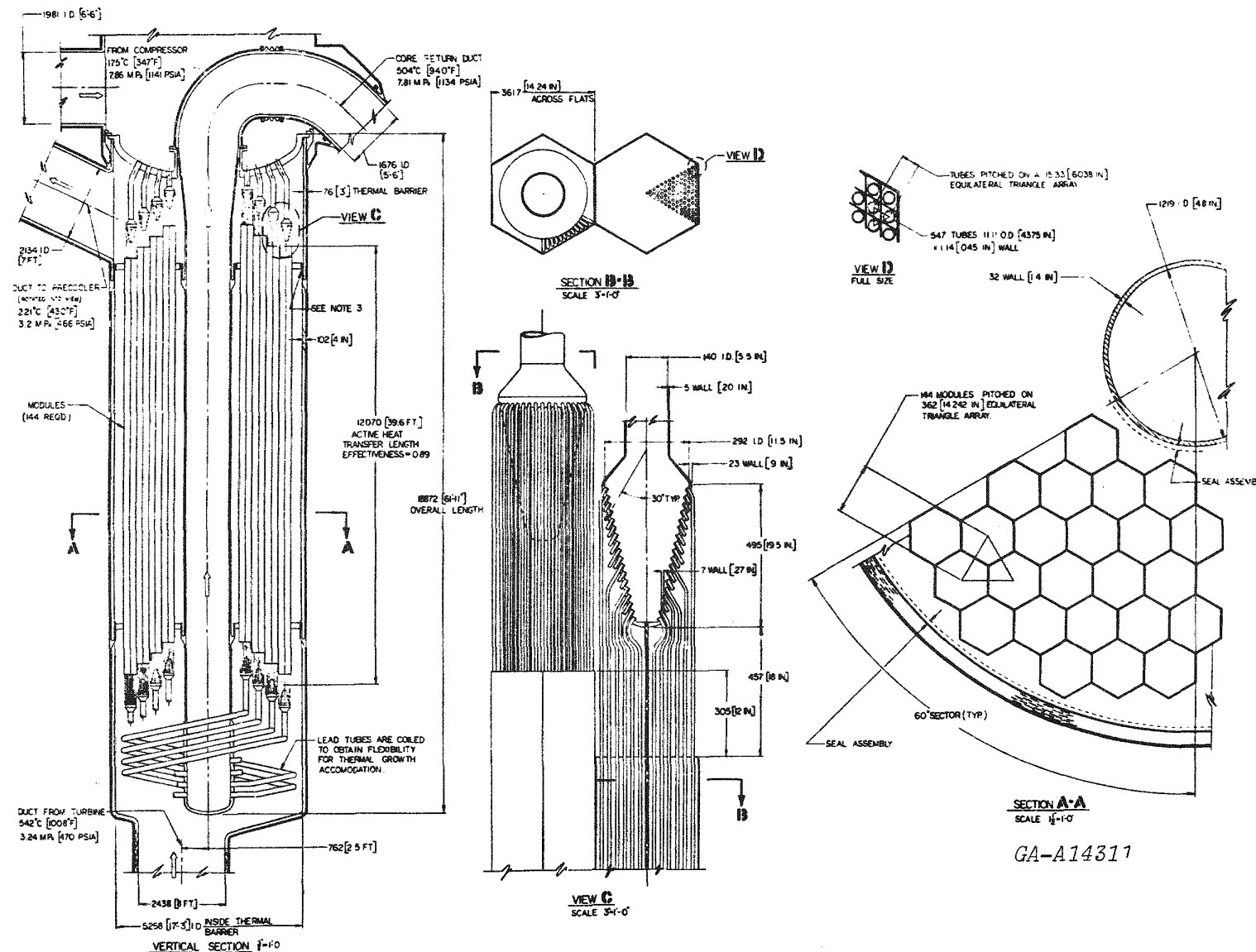
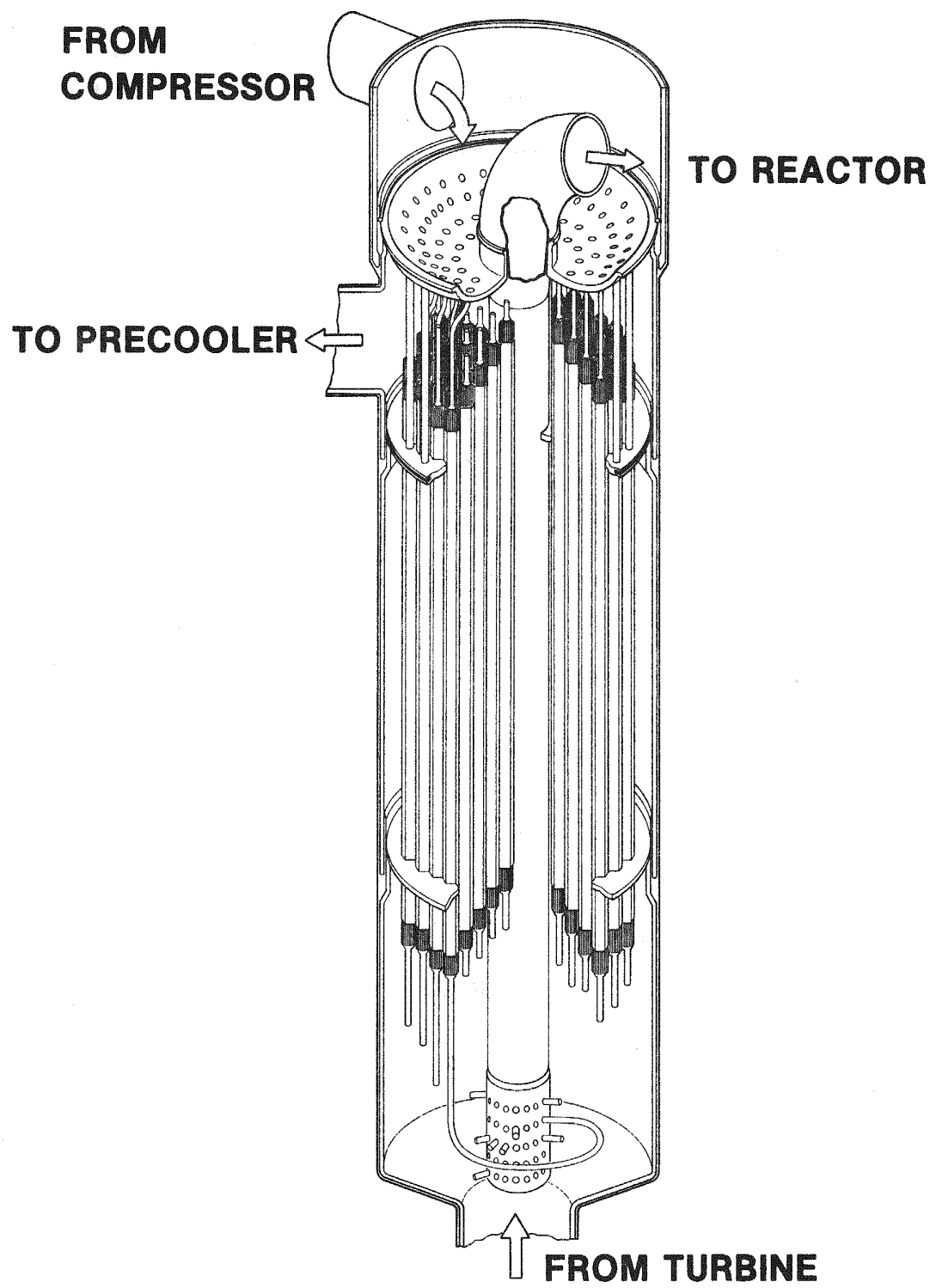


Fig. 6.21 Recuperator Details



GA-A14311

Fig. 6.22 View of Recuperator Assembly

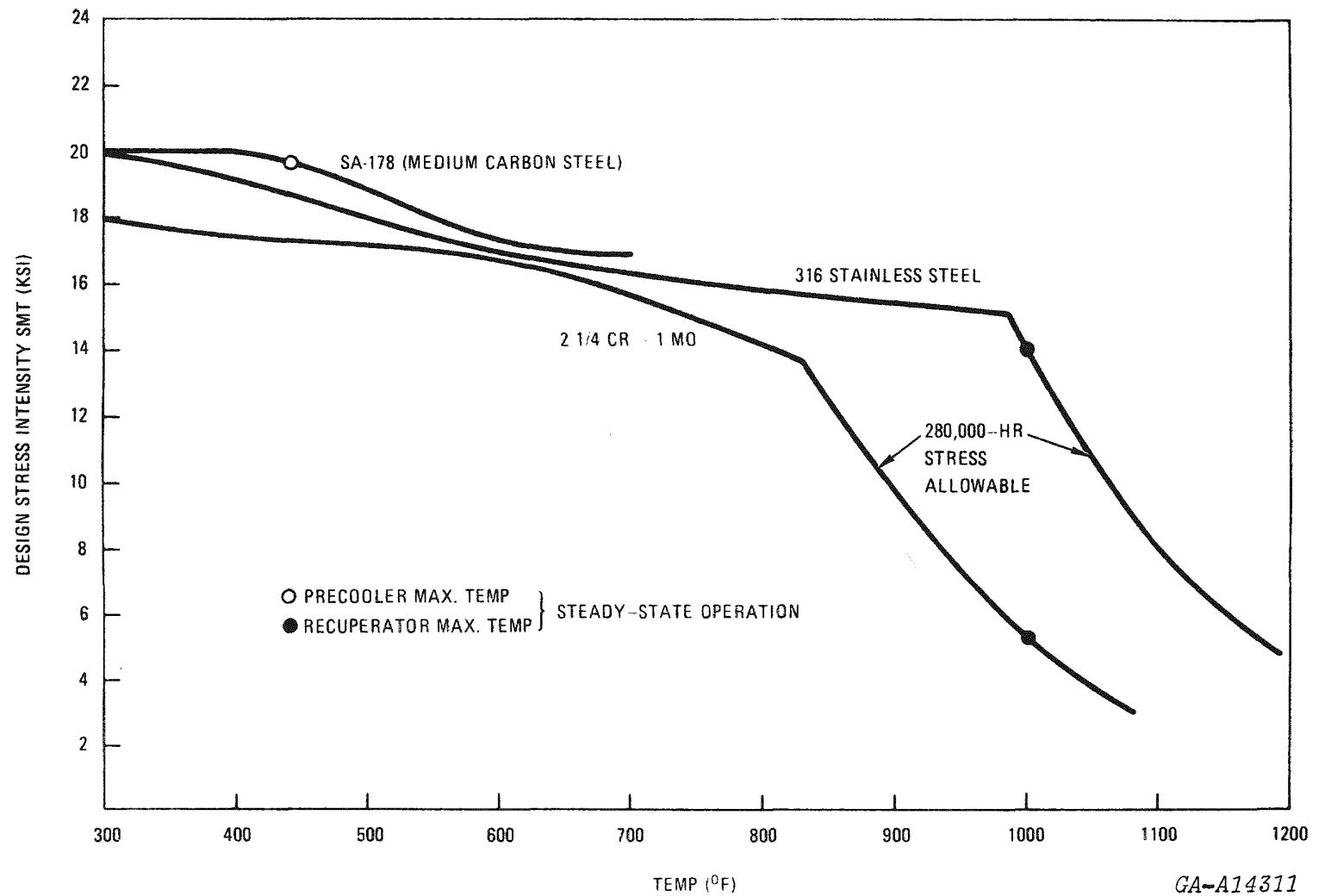
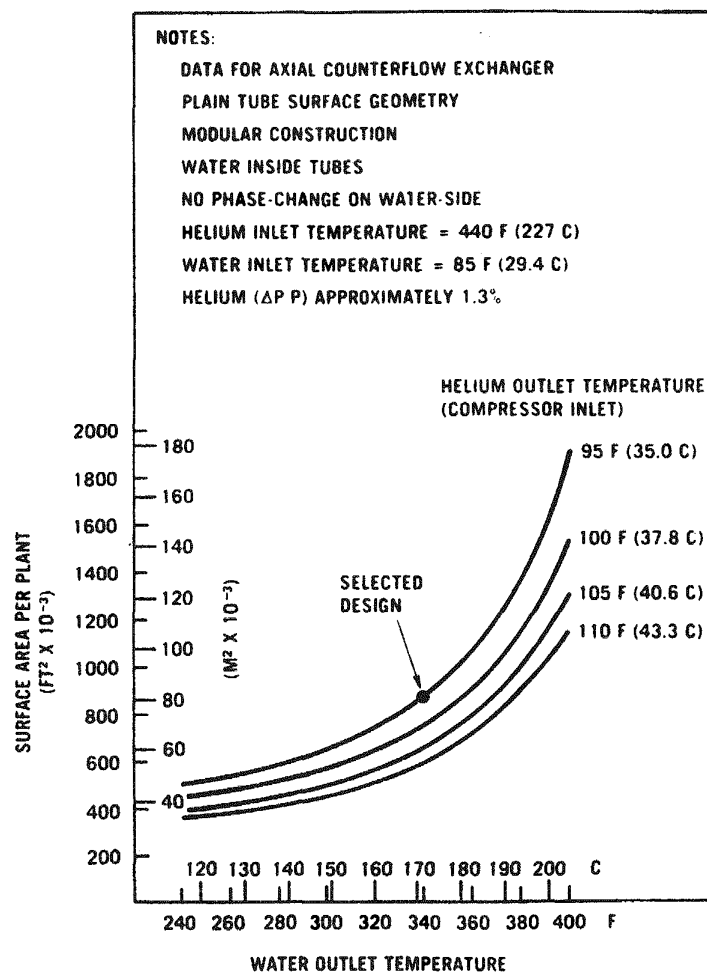


Fig. 6.23 Heat Exchanger Materials Structural Properties



GA-A14311

Fig. 6.24 Effect of Gas and Water Temperatures on Precooler Surface Area Requirements

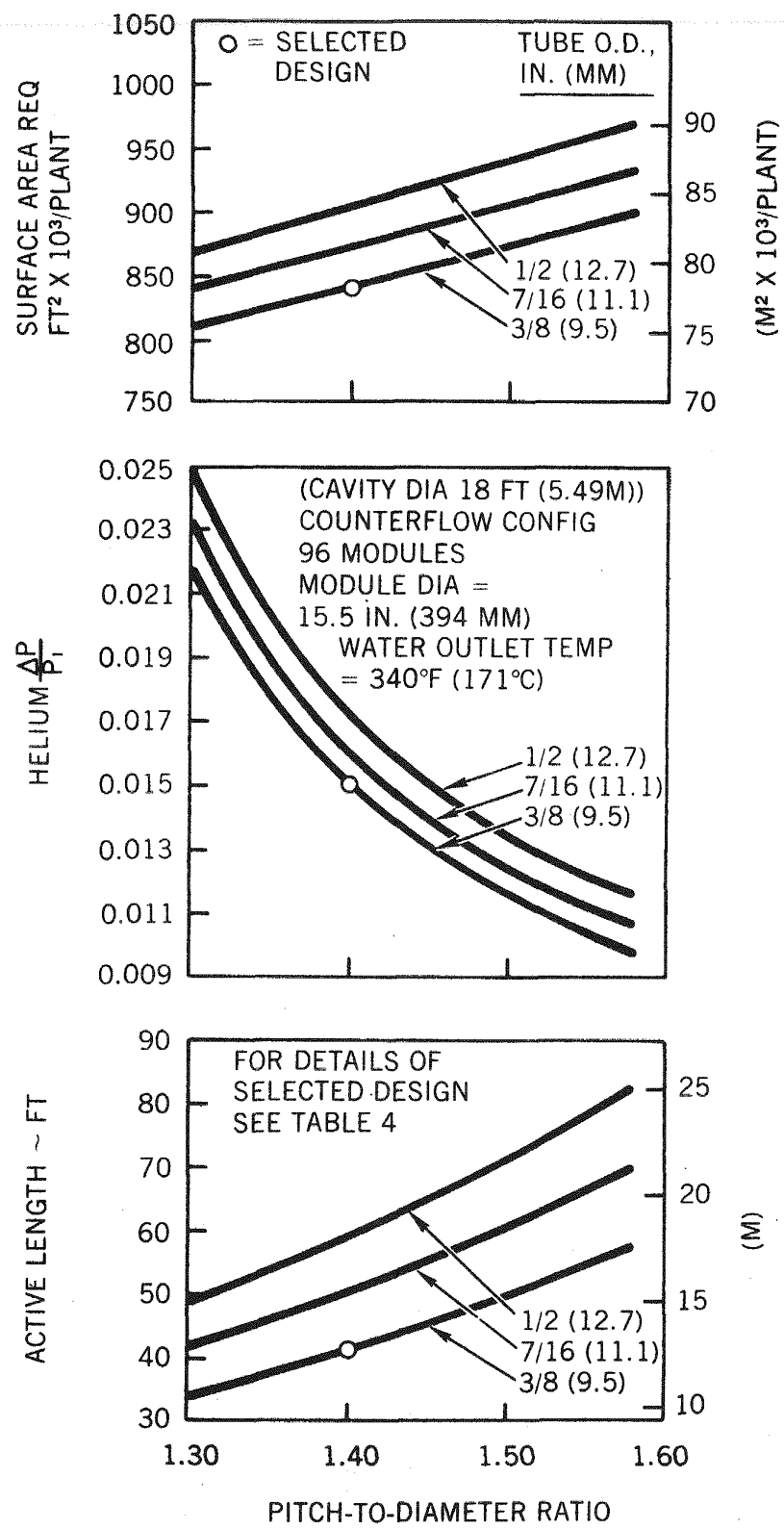


Fig. 6.25 Influence of Surface Geometry on Precooler Size

GA-A14311

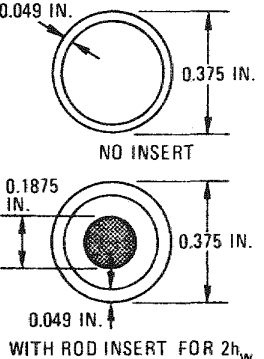
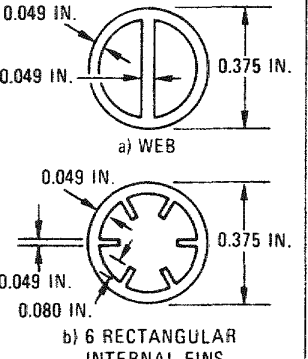
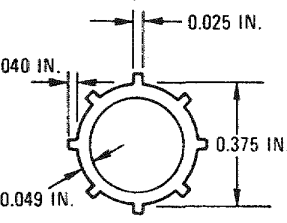
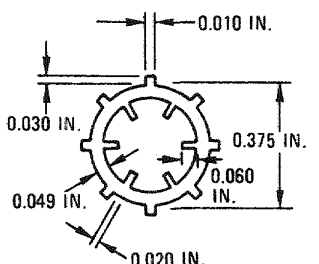
by the assumed minimum fabrication limits of 1.4 on the tube pitch-to-diameter ratio, and 3/8 in (9.5 mm) on the tube diameter. Details of this design solution are presented in Table 6.5.

During the thermal sizing it was observed that the large frontal area required to minimize helium pressure loss led to a large number of tubes, and the resultant water velocities inside the tubes produced heat transfer coefficients lower than in conventional liquid heat exchangers. This has an adverse impact on precooler size, and while the helium side is controlling (i.e., h_A water > h_A gas) surface enhancement and/or secondary surfaces to improve the water side conductance became necessary to reduce the precooler length to the point where it was no longer controlling the height of the PCRV. After considerable analytical investigation of surfaces of the type shown on Table 6, it was determined that internal longitudinal finning offered the best chance to achieve the desired envelope goals without unduly penalizing system performance or incurring unacceptable costs.

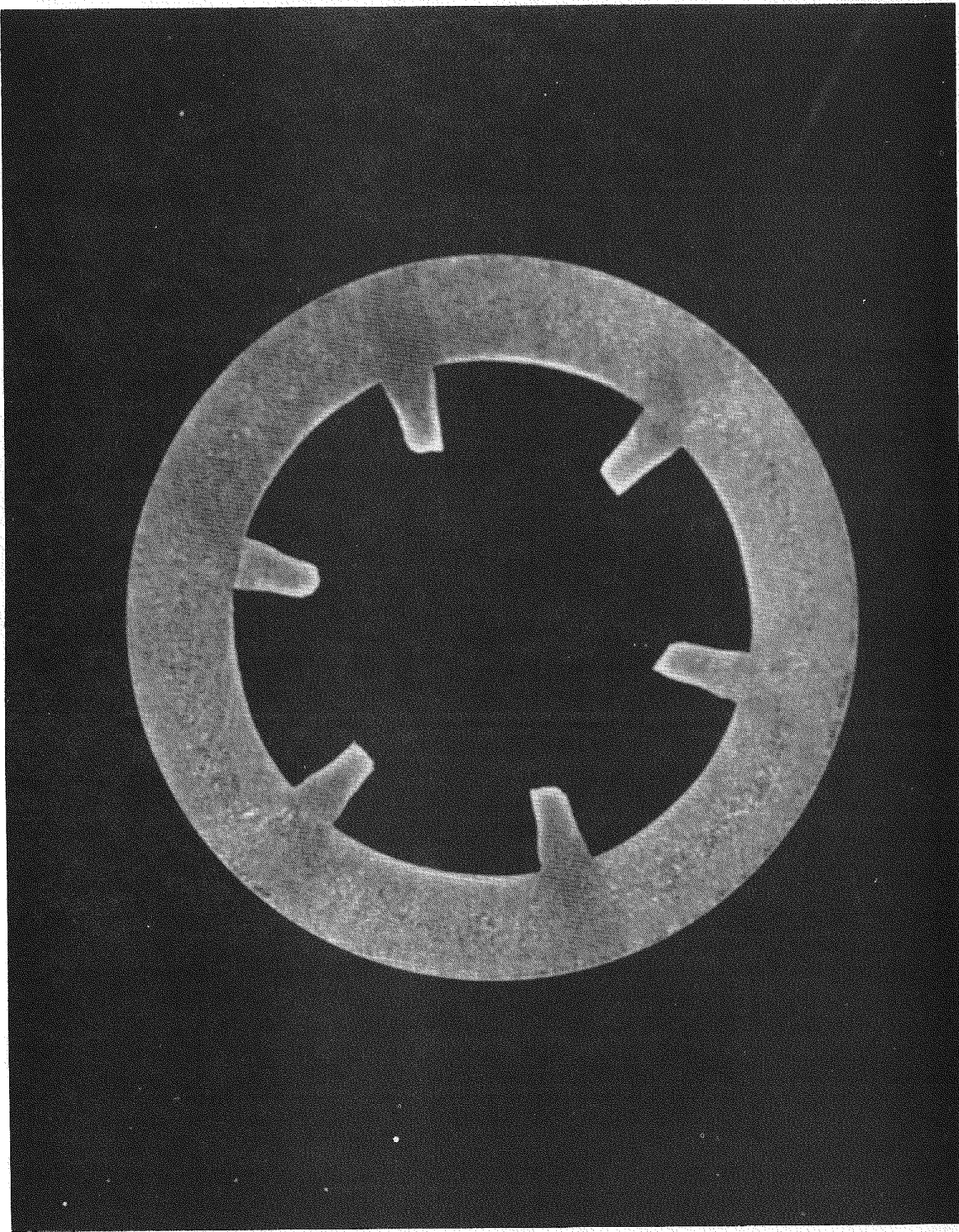
The analytical portion of this effort culminated in the selection of a candidate finned-tube geometry for manufacturing feasibility and economic evaluation. The candidate has six internal longitudinal rectangular fins, 0.080 in (2 mm) high by 0.049 in (1.24 mm) thick, formed symmetrically as an integral part of the inside surface of a 3/8-in (9.5 mm) outside diameter x 0.049-in (1.24 mm) wall tube.

The results thus far obtained from a comprehensive survey of U.S. and foreign tube vendors indicate that the technology exists for producing this type of surface in medium carbon steel. One vendor in particular, the Forge-Fin Division of Noranda Metal Industries, has voluntarily supported this investigation by forwarding medium carbon steel pilot samples of finned tubing both geometrically and dimensionally similar to the candidate's surface (see Fig. 6.26) along with budgetary production cost data. The samples were produced by a proven manufacturing process in which a heavier-walled tube of larger diameter is fed continuously into a swaging machine. Inside the tube is a mandrel that contains grooves of the same dimensions as the fins to be formed in the tube. As the dies in the swaging machine impact on the outside of the tube, the metal is forced to flow into the grooves in the mandrel, producing the inner fins. The resulting finned tube is pulled out of the swaging machine in continuous lengths as the fins are being formed, and the tube is then sunk to the desired diameter by drawing it through a die.

TABLE 6.6
HEAT EXCHANGER FINNED-TUBE GEOMETRIES EVALUATED FOR PRECOOLER

SOLUTION	PLAIN TUBE REFERENCE DESIGN	INTERNAL AXIAL FINS	EXTERNAL AXIAL FINS	INTERNAL & EXTERNAL AXIAL FINS	
EXCESSIVE HX LENGTH FOR INSTALLATION IN PCRV					
	NO INSERT WITH INSERT	p/d = 1.40		p/d = 1.40	
TUBE L EFFECTIVE, FT	53.0	41.5	a) 38.2 b) 37.0	40.0	31.0
HX L OVERALL, FT	84.5	73.0	69.7 68.5	71.5	62.5
HELIM (ΔP/P)	0.0185	0.015	0.0139	0.0129	0.027
TUBE WT/UNIT, TON	350	410	293	328	280
HX WT/UNIT, TON	480	540	423	458	410
					353

GA-A14311



GA-A14311

Fig. 6.26 Enlarged View of Precooler Tube Showing Internal Fin Geometry (Actual OD = 9.5 mm (3/8 in.))

In addition to demonstrating the fabricability of the desired geometry, the Forge-Fin specimens also show that it is possible to manufacture this particular geometry with spiral fins rather than straight ones. This is of particular interest in the precooler design, which is characterized by low water velocities, because the resulting centrifugal flow field promotion may offer the possibility of additional heat transfer augmentation combined with suppression of the turbulent-to-laminar flow transition regime and its associated lower heat transfer characteristics.

Details of the precooler are shown on Fig. 6.27, and in a simplified schematic form on Fig. 6.28. With 144 hexagonal modules the overall assembly is similar to the recuperator. The support system is similar to the recuperator, except that the modular array is anchored to a top support plate instead of a primary pressure-carrying tubeplate. Both the precooler water inlet and outlet lead tubes penetrate the bottom head of the PCRV, and between the modules and bottom tubesheets, the lead tubes are coiled to produce the flexibility required to accommodate differential thermal expansion. In addition to failure isolation and external lead tube plugging capability, the precooler provides for removability and in-service inspection.

Compared with the recuperator the lower operating temperatures and pressures in the precooler, in conjunction with the close water chemistry control standards required for the cooling water system, enable the entire precooler assembly to be made from medium carbon steel. With a precooler maximum metal temperature on the order of only 380°F (193°C), creep considerations are not the dominant design criteria as was the case for the recuperator.

6.2.3. Heat Exchanger Fabrication Considerations

In general, the heat exchanger types chosen for the gas turbine plant represent a very simple design approach: tubular, modular, axial counter-flow with straight plain tubes. While long lengths of small diameter tubing are required, the modular approach helps from the fabrication standpoint. In the preliminary designs presented, there has been a tendency to favor small modules (less than 10,000 lb (4500 kg)) to ease fabrication and handling.

To ensure that the basic goals of plant simplicity and minimum cost were being met, manufacturing aspects of the recuperator and precooler designs were reviewed concurrently with the analytical study, leading to the adoption of the assumed minimum practical limits previously discussed.

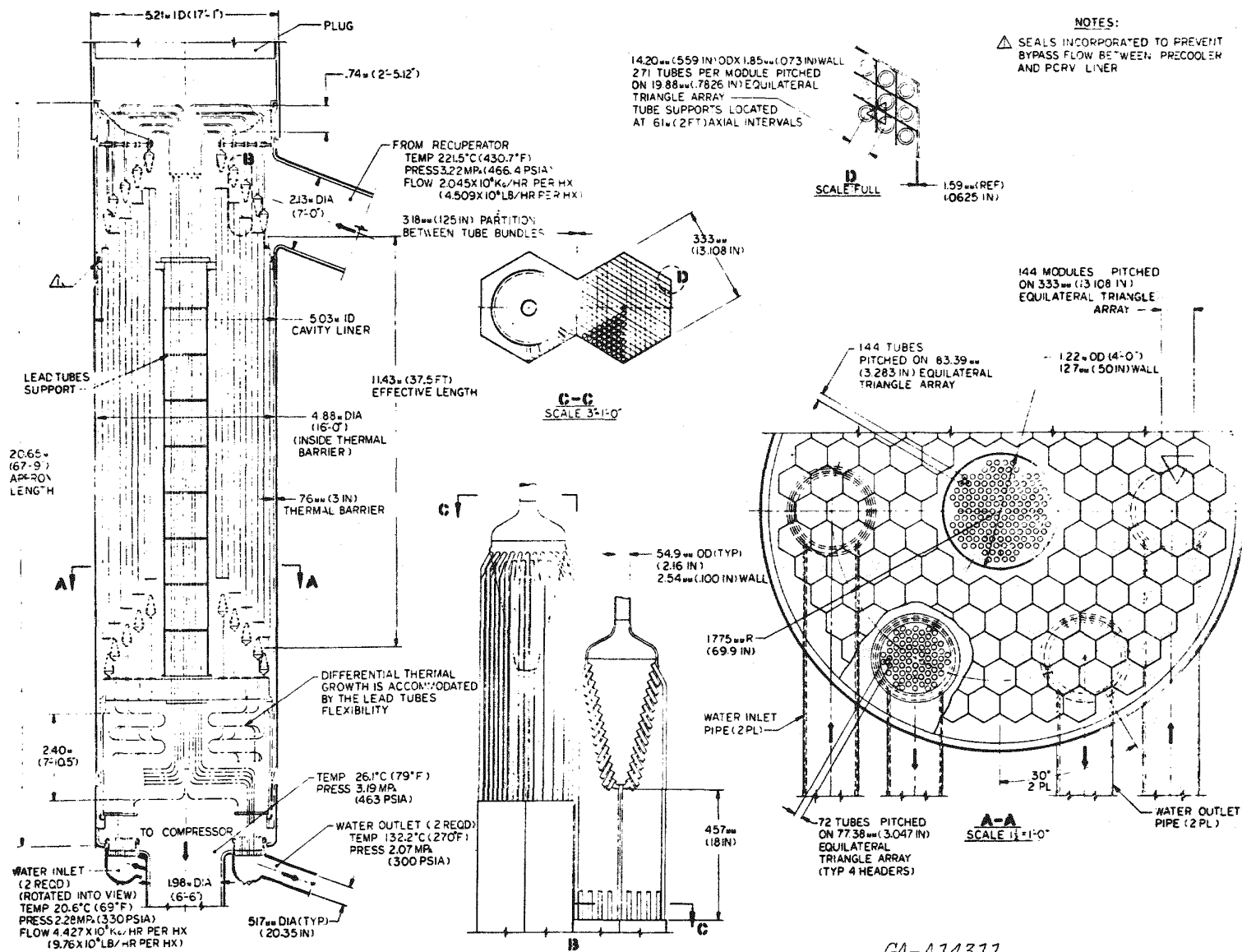
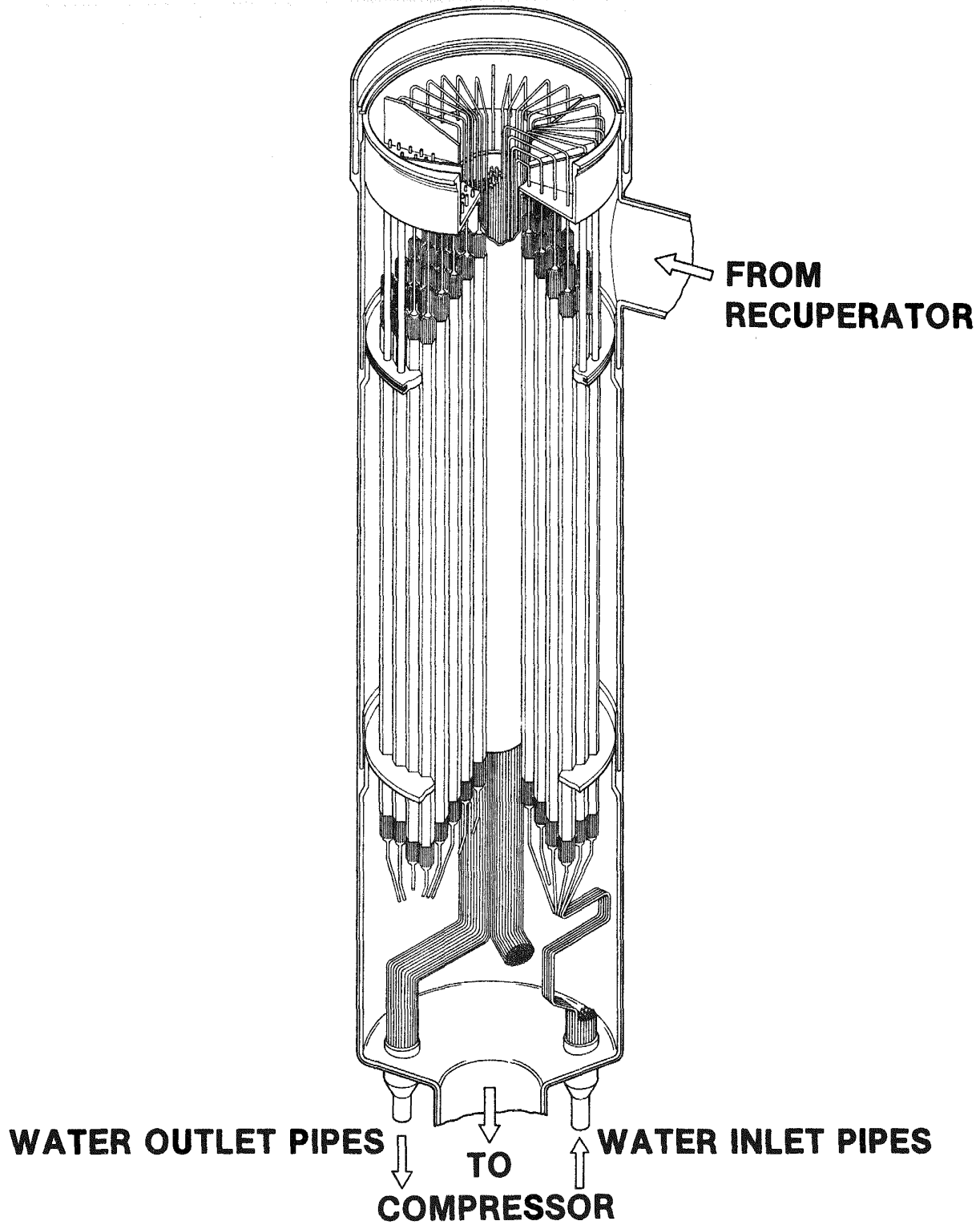


Fig. 6.27 Precooler Details



GA-A14311

Fig. 6.28 View of Precooler Assembly

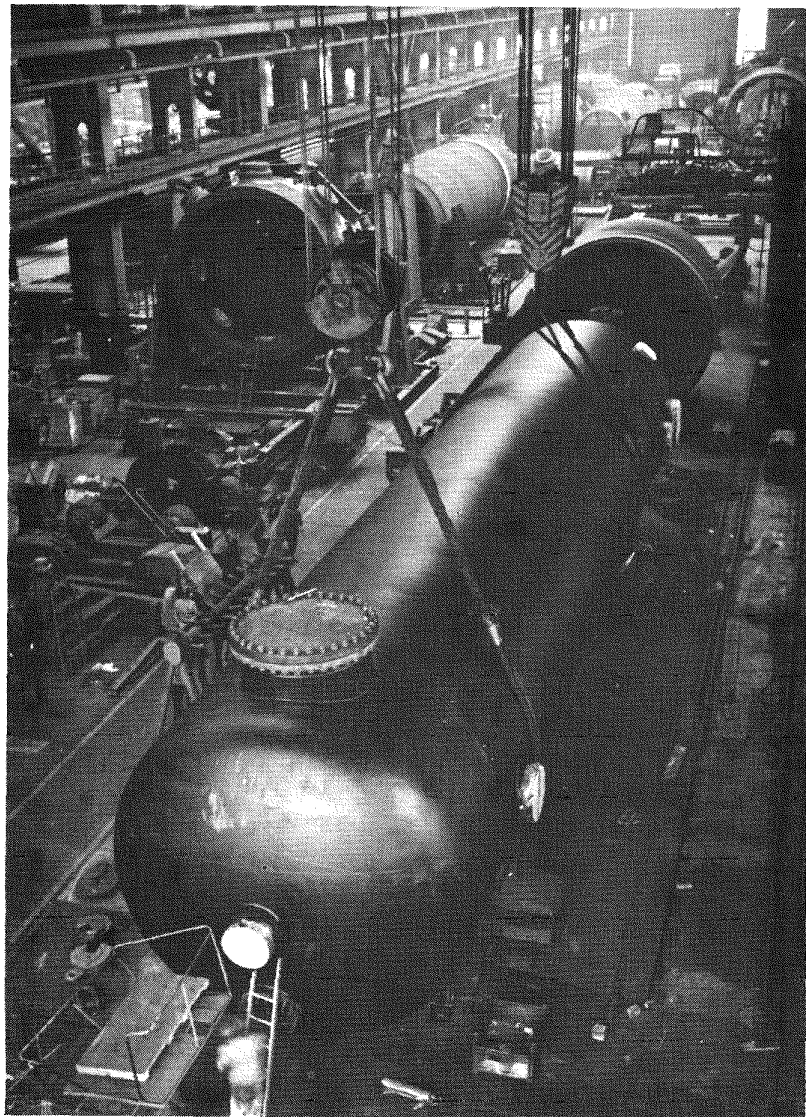
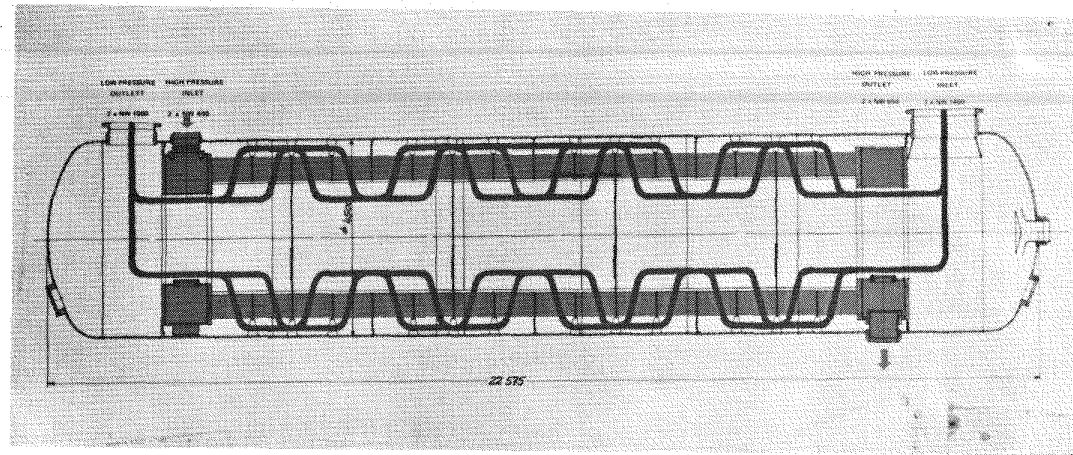
A large recuperator embodying similar tube diameters and pitching arrangement has been fabricated for a helium gas turbine (Ref. 6.7), and is currently under test. Details of this unit are shown on Fig. 6.29.

While substantially different from contemporary steam generators, the heat exchangers presented herein are considered to be within the bounds of conventional fabrication technology. Some manufacturing development in support of critical areas in the detailed mechanical design (e.g., tube-to-tubesheet joints) is anticipated in the program development plan. The large recuperator support plate is within current manufacturing dimensions for a ferritic alloy such as 2-1/4 Cr - 1 Mo. The size and weight of the gas turbine heat exchangers is such that they can be transported from the factory to the site on special rail cars. With the modular configuration, an alternative approach would be to transport the various subassemblies to the site and complete the fabrication in the field.

6.2.4. Heat Exchanger Installation, Handling, and Maintenance

The size and weight of both the recuperator and precooler are similar to those of steam generators for contemporary nuclear power plants. The installation approach taken for both units is based on a top support arrangement with top access to the PCRV cavity. Both the recuperator and the precooler will be lowered into the PCRV cavities (either by overhead crane or, more likely, by a system of hydraulic jacks) during construction, and they are expected to remain in place during the life of the plant. A heat exchanger would be replaced only if it were deemed economically desirable in order to increase plant output and efficiency.

The recuperator assembly is supported from its main top tubesheet, which rests on a circumferential ring anchored in the cavity sidewall. In addition to providing unrestrained thermal growth capability, the absence of mechanical connections to the PCRV below this upper support plane makes removal and reinstallation of the recuperator relatively straightforward, if conditions so warrant. The recuperator does not form a primary pressure boundary, and failure of the small individual tubes causes relatively small plant performance loss. If a lead tube (5 in. diameter (127 mm)) fails, the level of leakage rate would necessitate repair. Plugging of the failed module is done from the top of the PCRV, and requires a special-purpose machine which would plug both ends of the lead tube, thus isolating the faulty module.



GA-A14311

Fig. 6.29 Overall View of Recuperator for Oberhausen II Helium Turbine Plant (by Courtesy GHH)

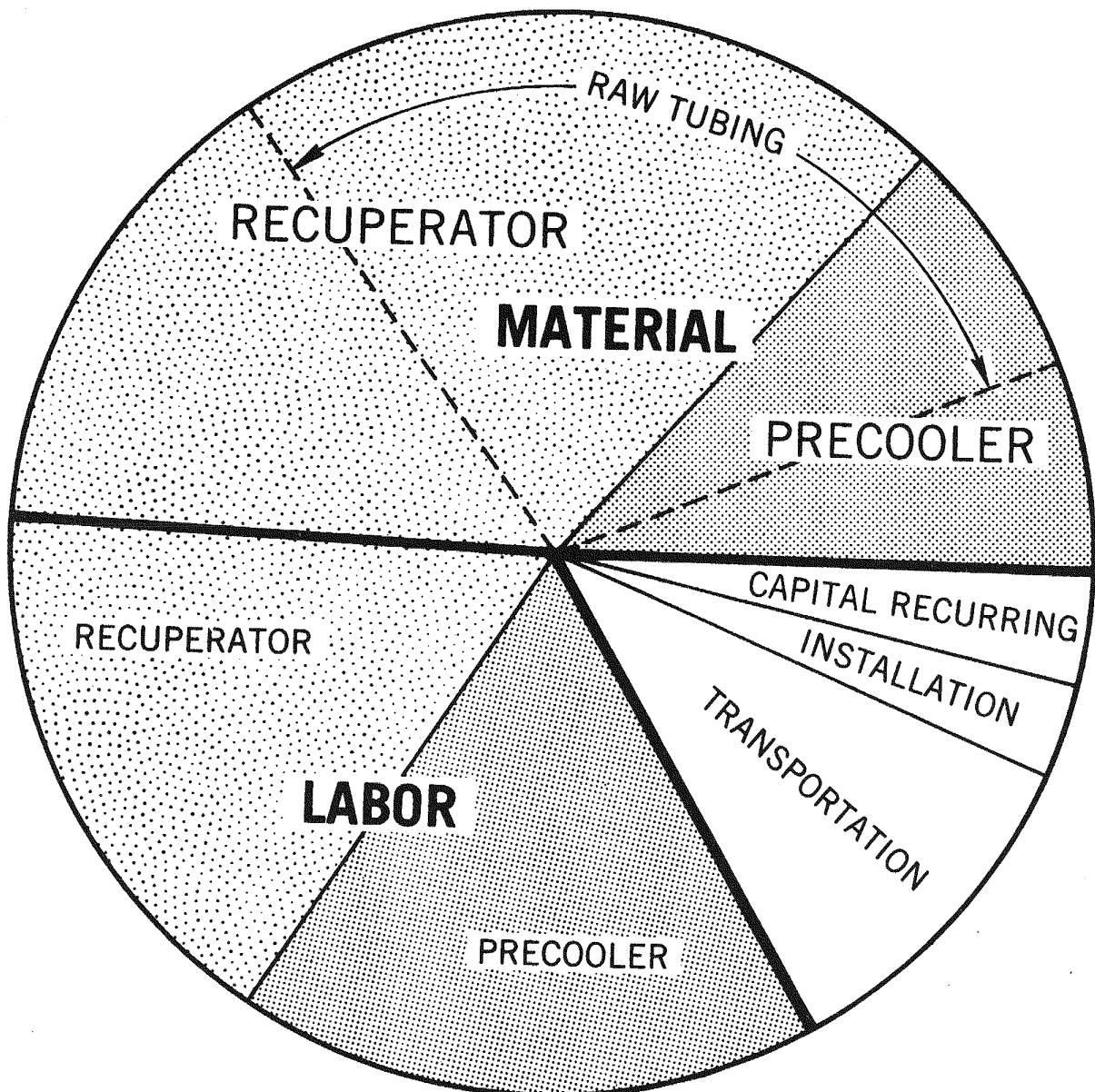
The installation and removal of the precooler is similar to that of the recuperator but, since the water connections are at the bottom of the PCRV, an additional operation is necessary. The water pipes penetrating the bottom head of the vessel must be cut and rewelded in a plane below the main tubesheets for the unlikely case of precooler removal and reinstallation. Tube plugging of the precooler, in the event of a failure, is executed below the PCRV by plugging individual inlet and outlet lead tubes (2-1/2 in. diameter (64 mm)) thus isolating the faulty module.

6.2.5. Heat Exchanger Economic Considerations

Because of the nature of the closed-cycle gas turbine and the selection of single-phase working fluids (helium and water), the surface area requirements are larger than in steam generators for the HTGR; however, their lower operating temperatures and pressure differentials permit the use of less expensive alloys in thinner gauges. The heat exchangers are obviously important capital equipment items in the gas turbine plant, and economic studies to identify areas of potential savings are a necessary part of the preliminary design. While detailed discussions of heat exchanger costs are beyond the scope of this paper, the relative importance of the major cost elements in the recuperator and precooler designs presented are shown in Fig. 6.30. This simple cost breakdown diagram suggests that cost reduction efforts should be concentrated in lowering both material and labor costs. Alternate design approaches, aimed at reducing the size and cost of the heat exchangers for the gas turbine HTGR plant, are being studied.

6.2.6. Heat Exchanger Design Summary

Even though relatively high heat transfer coefficients can be realized with the single-phase working fluids (helium and water), large surface areas are necessary because of demanding thermal conductance requirements associated with the large heat transfer rates. Because of the modest metal temperatures and internal pressure differentials compared with modern steam generators, the use of code-approved lower-grade alloys of reduced cost is possible. The ferritic materials selected for both exchangers have been used extensively in industrial and nuclear plant heat exchangers. While the exchanger assemblies are large, state-of-the-art manufacturing methods apply, and the modular approach actually eases fabrication, handling, and assembly. The overall



GA-A14311

Fig. 6.30 Relative Importance of Major Cost Elements for GT-HTGR Heat Exchanger

size and weight of both the recuperator and precooler are similar to contemporary steam generators, and transport methods, handling, and installation techniques developed for these units will be equally applicable to the heat exchangers for the nuclear gas turbine plant.

The design decisions involving selection of surface geometry, flow configuration, modular approach, and overall mechanical design, are in close agreement with those established independently in Europe for heat exchanger design studies in support of the HHT program (Refs. 6.8 and 6.9).

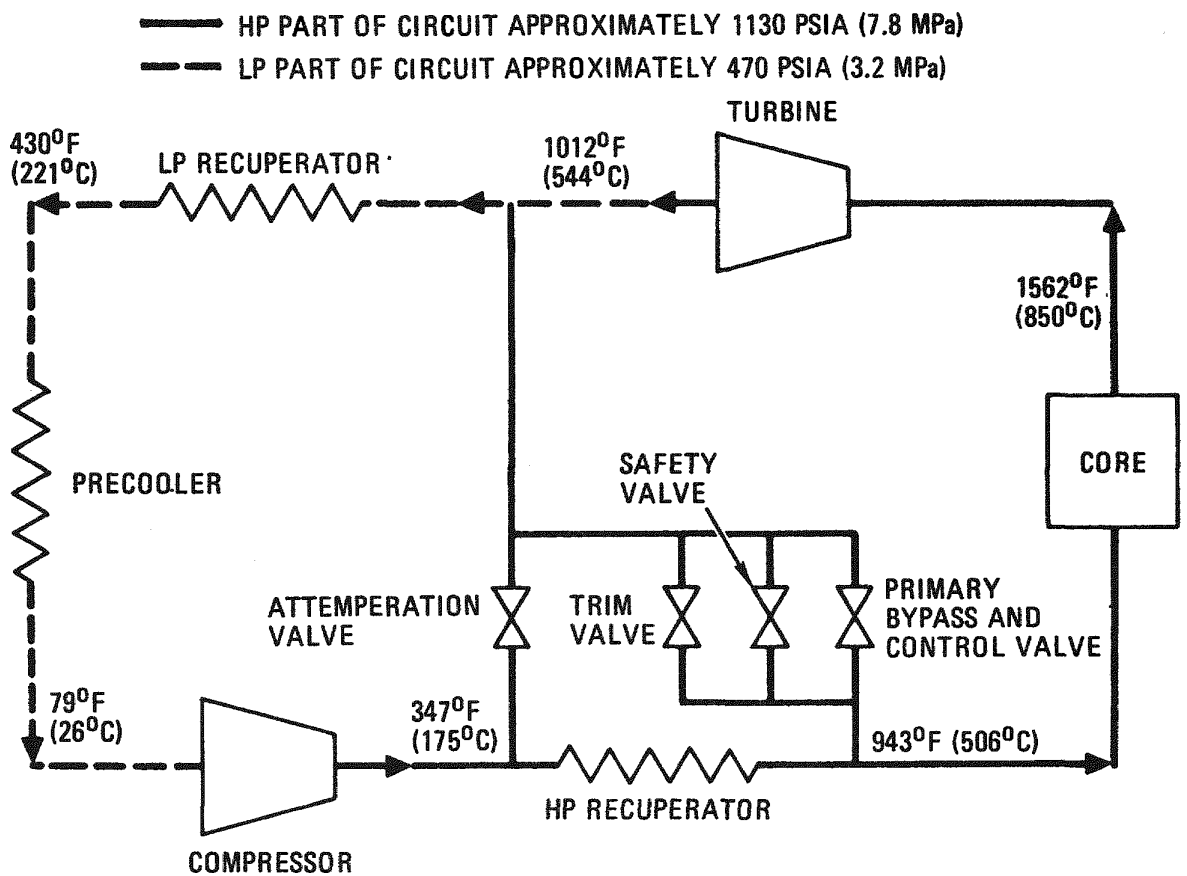
6.3. Control Valve Design

In the GT-HTGR plant the helium control valves are integrated in the primary system, and since there are four valves per power conversion loop their overall size and configuration must be considered during plant layout studies. Full details of the plant control scheme have been described previously (Ref. 6.10), so only aspects of the valve configuration and sizing will be mentioned in this paper.

Figure 6.31 is a simplified control valve diagram showing the position of the valves in the flow circuit. Helium inventory control and reactor outlet temperature control are useful in maximizing plant efficiency during extended part-load operation, but their response times are too great for short-term speed and load control. The prime control system must, therefore, be based on fast-acting primary loop valves.

The main requirement of the valve bypass system is that it be capable of limiting turbine overspeed to less than 20% for all accidents or events up through the worst case of a coupling failure with trip on backup overspeed detection. Control studies have shown that connection and gas routing from high- to low-pressure zones of the primary system is the only bypass that will satisfy the worst-case overspeed protection. Single-point bypass (from compressor discharge to turbine discharge) methods are undesirable because of extreme temperature excursions to the heat exchangers and reactor.

As shown in Fig. 6.31, there are four valves in the split-flow bypass configuration of each power conversion loop. The trim, safety, and primary bypass valves connect the core inlet to the turbine exit of each loop; the attemperation valve connects the compressor exit to the turbine exit. The primary bypass can be used in two modes: 1) it can be modulated by the



GA-A14311

Fig. 6.31 Simplified Control Valve Diagram for GT-HTGR Plant

control system for plant load control; or 2) it can be operated in a binary (open/shut) mode, if the safety valve fails to open, by a separate actuator as part of the plant protection system. The safety valve (non-modulated) is actuated by the plant protection system and is a binary (open/shut) valve used primarily for turbine overspeed/overpressure protection. This valve cannot be used for load control purposes. The small trim valve makes fine adjustments of turbine speed and load and is of particular use when synchronizing with the electric power network. The attemperation valve is used to mix gases (compressor discharge and core inlet), thereby minimizing thermal shock to the heat exchangers and core during transients.

The four valves, operating in a helium environment at elevated temperature are by no means "off-the-shelf" components, and conceptual designs have been established to satisfy all of the plant requirements. A summary of the control valve conceptual design considerations is given in Table 6.7. The initial mechanical designs followed conventional valve design practice as closely as possible. This led to the selection of isolated units with large, thick, cast valve bodies to withstand the high pressures and temperatures, and the use of many features of conventional valves. Installation of these "isolated" valve assemblies into cavities in the PCRV proved to be difficult because of the space consuming thermal expansion devices, necessary because of the rigid valve-to-PCRV duct interfaces, and the resulting large growth from ambient to operating temperature. With this isolated valve approach, the valve assembly envelopes were excessive for installation in individual PCRV cavities.

At this stage it was clear that the design of the valves must be integrated with the PCRV. The conceptual design approach for all four valves involved eliminating the large cast valve bodies (pressure bearing), and installing the valve assemblies directly in individual cavities in the vessel. The complete valve assembly (including the seat) can be readily installed and removed from the cavity. Elimination of the pressurized body eases thermal expansion problems, and thermal shock effects during transient operation will be minimized. A simplified view of the integrated approach for the safety valve is shown on Fig. 6.32. The four valves are installed in separate cavities in the top heat of the PCRV, and are accessible for inspection and maintenance. The position of the valve cavities in the vessel were established from layout studies to determine the simplest routing of the interconnecting ducts for the four valves in each PCL.

TABLE 6.7
SUMMARY OF CONTROL VALVE CONCEPTUAL DESIGN

- LINEARLY-ACTIVATED PLUG TYPE VALVES SELECTED
- INTEGRATED VALVE APPROACH SELECTED
- COMPLETE VALVE ASSEMBLY CAN BE READILY INSTALLED
OR REMOVED FROM PCRV CAVITY
- ACCESSIBLE FOR INSPECTION AND MAINTENANCE
- PRESSURIZED VALVE BODY EASES HIGH TEMPERATURE STRUCTURAL
PROBLEMS, THERMAL EXPANSION CONSIDERATIONS AND THERMAL
SHOCK EFFECTS DURING TRANSIENTS
- EACH OF 4 VALVES IN SEPARATE CAVITIES IN THE PCRV TOP HEAD

GA-A14311

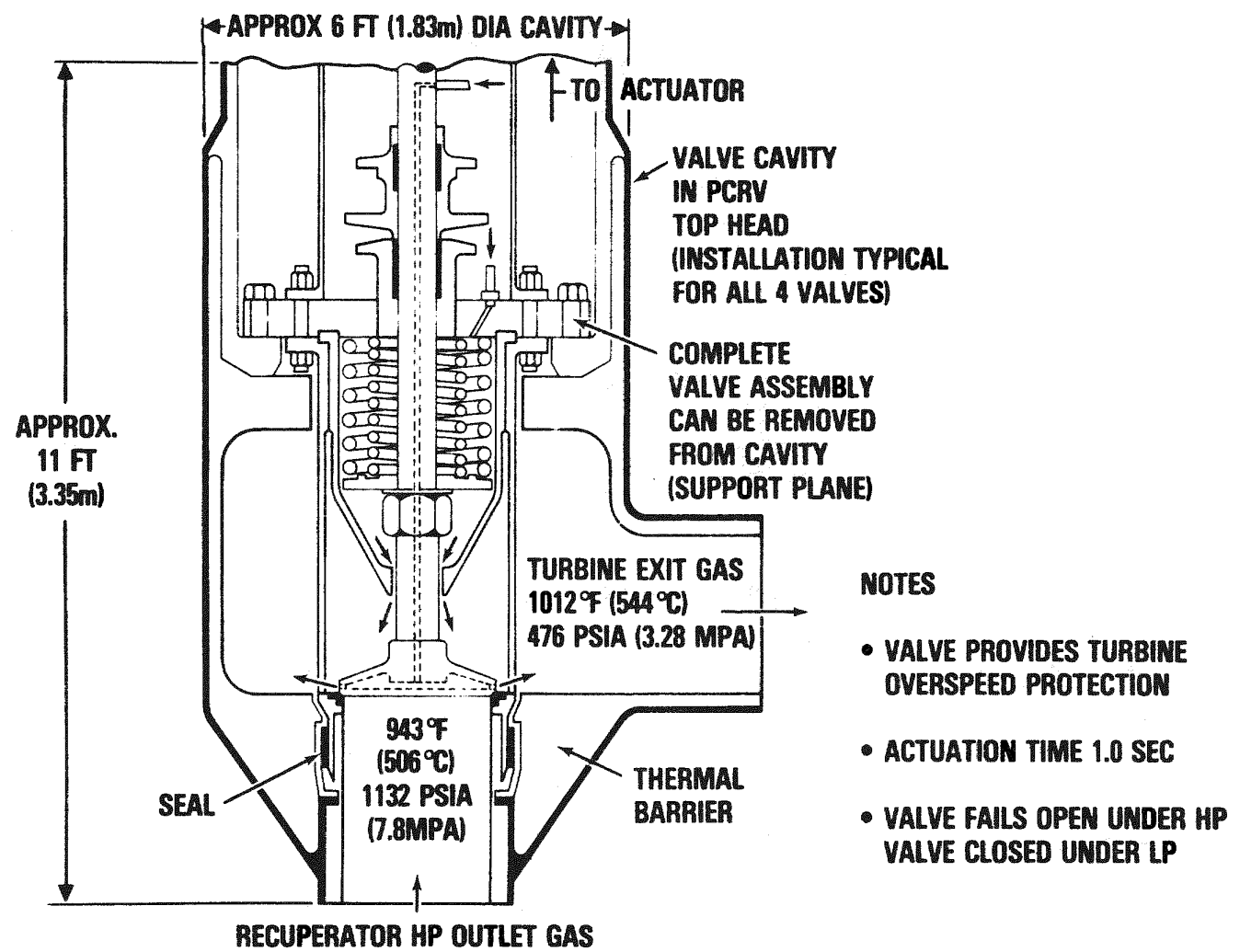


Fig. 6.32 Simplified View of Safety Valve Showing Valve Assembly Integrated in the PCRV

With the selected control valve scheme, the effect on temperatures in the primary system can be seen from Fig. 6.33 for the case of loss of electrical load. It is significant to note that temperature excursions are minimal, obviating thermal shock in the two heat exchangers, eliminating the possibility of boiling in the precooler, and perhaps most important, the reactor core inlet temperature remains almost constant.

6.4. Materials Testing Program

The GT-HTGR plant will be required to operate for approximately 280,000 hours. Power conversion loop components will be designed for extended lifetimes in order to insure reliability and to minimize inspection, maintenance and repair requirements. The proper selection and application of structural alloy materials in the high temperature, high pressure, helium environment of the GT-HTGR will be primary factors in attaining these goals. Although it is anticipated that conventional structural and high temperature alloys will be employed in the gas turbine plant, the long-term behavior of these materials in possible reactor helium environment must be characterized and environmental effects on properties must be quantified. Active degradation mechanisms such as oxidation and/or carburization from coolant impurity interactions must be identified and the occurrence of these effects must be correlated with helium impurity levels and alloy composition.

The candidate alloys for the major components described above include low alloy steels, high alloy steels, austenitic stainless steels, high nickel or nickel-base superalloys, and possibly more advanced materials such as molybdenum or dispersion strengthened alloys, depending on service temperatures which could range from below 400°F (205°C) to about 1800°F (982°C). For the alloys of interest, creep or stress rupture properties will be important for design of components operating above about 900°F (482°C). Candidate alloys in the test program, in support of the component design activities, are shown on Table 6.8. Other important properties may include short-term tensile or compression behavior, high and low cycle fatigue resistance, cycle and static flow growth rates, fracture toughness, thermal aging resistance and helium impurity corrosion rates depending on the component design environment.

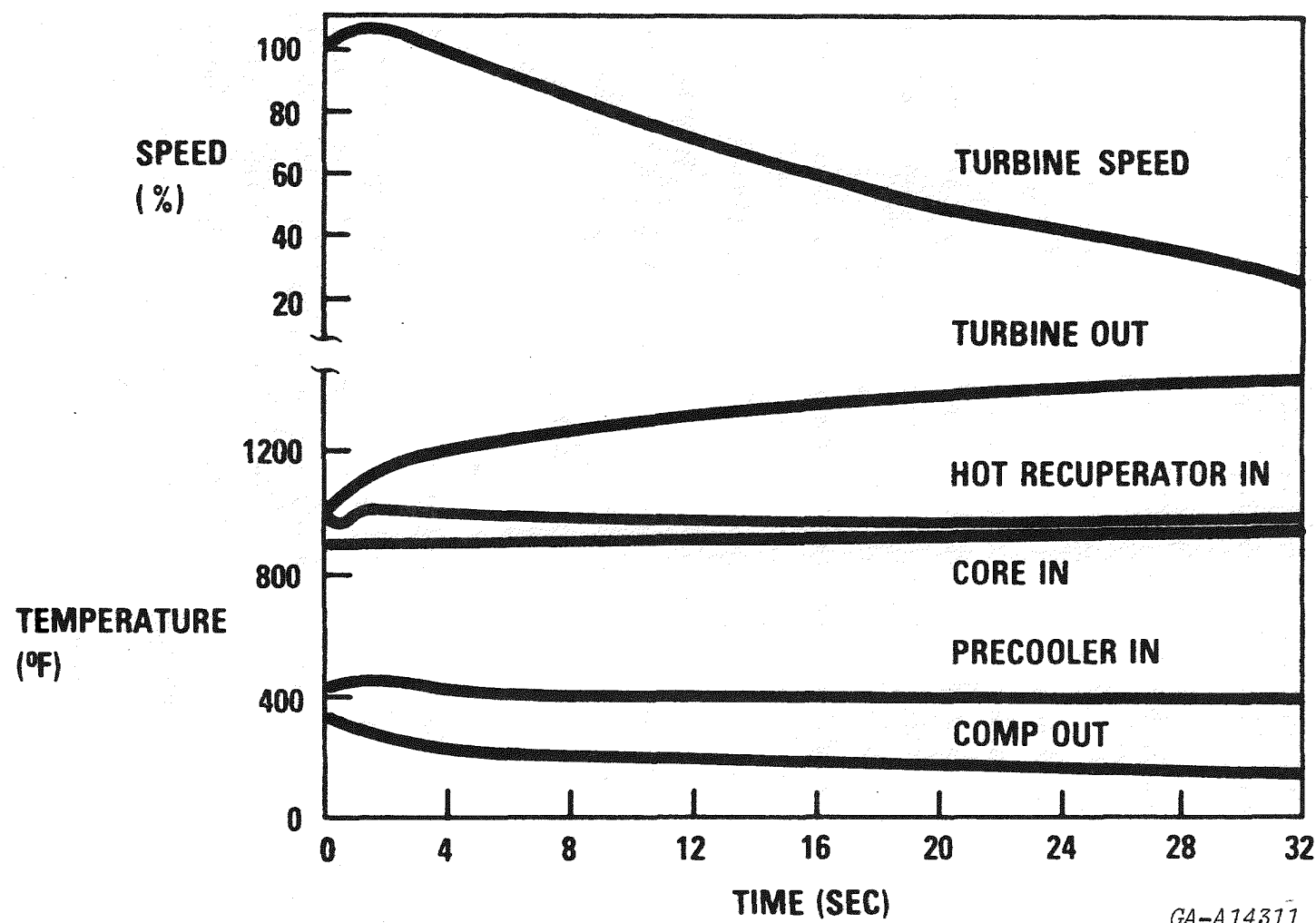


Fig. 6.33 GT-HTGR Plant Transients for Selected Bypass Control Valve System (Loss of Load Case)

TABLE 6.8
ALLOYS IN GT-HTGR TEST PROGRAM

ALLOY DESIG.	TYPE	APPLICATION
IN. 100 IN. 713C MM004 M21(LC) IN. 738 RENE 100	VAC. SHELL CAST	TURBINE BLADES & VANES
MoTzm	WROUGHT	T. BLADES, VANES, HOT DUCTS
HASTELLOY X INCONEL 617	WROUGHT	HOT DUCTS, CASINGS
MA753 MA754	MECH. ALLOYED	
IN. 519	CENT. CAST	
INCONEL 706 INCONEL 718 A286	WROUGHT	TURBINE DISKS
422 316L 800 2-1/4 Cr/Mo	WROUGHT	HEAT EXCHANGERS, DUCTS

In summary, the purpose of the materials screening test program (which has been underway for several years) is to identify and evaluate structural alloys for application in the power conversion loop components. The general approach has been to establish the applicability of candidate materials by determining possible environmental effects on pertinent structural properties through screening tests, diagnostic metallurgical evaluations, and analyses.

REFERENCES

- 6.1. Adams, R. G., and F. H. Boenig, "The Design of Turbomachinery for the Gas Turbine (Direct Cycle) HTGR Power Plant", ASME Paper 77-GT-38.
- 6.2. "FT 50 Design Shortcut to 1980 Technology", Gas Turbine World, November 1975.
- 6.3. Smith, S. F., "A Simple Correlation of Turbine Efficiency", Journal of the Royal Aeronautical Society, 69, 467 (1965).
- 6.4. Chmielewski, R., K. Vepa, L. Cheng, and J. Bowyer, "Fault Analysis of a Gas Turbine HTGR", ASME Paper No. 76-GT-99.
- 6.5. McDonald, C. F., T. Van Hagan, and K. Vepa, "Heat Exchanger Design Considerations for Gas Turbine HTGR Power Plant", ASME Paper No. 76-GT-53.
- 6.6. McDonald, C. F., "Gas Turbine Recuperator Technology Advancements", ASME Paper No. 72-GT-32.
- 6.7. Zenker, P., "The Oberhausen 50 MW Helium Turbine Plant", Combustion, April 1976.
- 6.8. Bieri, H., R. Naegelin, and M. Weber, "Designing the Heat Exchangers for Integrated Gas Turbine Cycles of High-Temperature Reactors," Sulzer Technical Review, NUCLEX 75, special issue.
- 6.9. Naegelin, R., and G. Varadi, "Thermohydraulic Design of Heat Exchangers for Direct Cycle Integrated Gas Turbine Plants", Paper IAEA-SM-200/6, International Symposium on Gas Cooled Reactors, Julich, Germany, October 1975.
- 6.10. Openshaw, F. L., E. Estrine, and M. Croft, "Control of a Gas Turbine HTGR", ASME Paper No. 76-GT-97.

7.0 SECONDARY POWER CYCLE (BINARY PLANT)

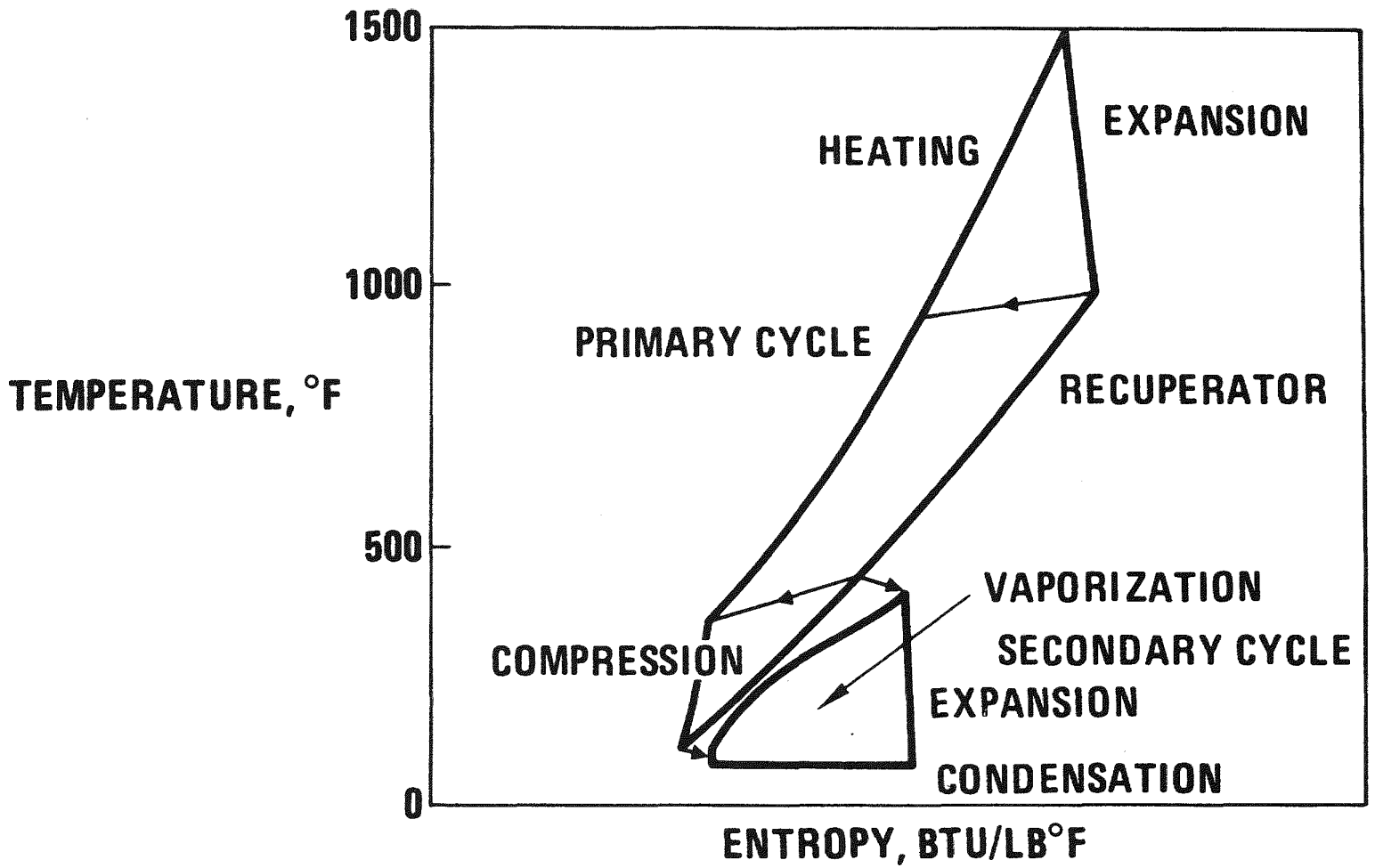
Although primary emphasis has been placed on the dry-cooled GT-HTGR, the merits of the high reject temperature have been recognized (Refs. 7.1 through 7.5). In the smaller European cities the reject from the fossil-fired closed-cycle gas turbines has been used to advantage for urban and industrial district heating. As outlined in Ref. 7.6 the utilization of the hot water from the gas turbine heat exchangers results in overall plant fuel utilization of over 60 percent. The use of the reject heat from the GT-HTGR plant for district heating has been considered (Ref. 7.7), but apart from small systems in some of the cities in the United States, the necessary infrastructure in the form of distribution grids does not yet exist, so that utilization of heat from a large nuclear gas turbine plant comes under the category of a long range goal.

With added emphasis in the U.S. on fuel conservation and minimum impact on the environment by future power generating systems, studies have been carried out for utilization of the waste heat from the GT-HTGR power plant in a secondary cycle that can raise the overall efficiency of the combined cycle into the range of 50 percent. The attraction of usefully employing the relatively high-grade waste heat from a nuclear closed-cycle gas turbine goes beyond that of achieving higher efficiency. Because the extra power is obtainable without major penalty to the output of the primary helium turbine system, not only is this extra power free of fuel cost, it is also free of the capital cost of most of the rest of the nuclear plant.

As outlined below system studies and equipment conceptual designs were done for an advanced version of the GT-HTGR in an effort to evaluate the economic and performance potential.

7.1 Working Fluid Selection

By far the most important initial decision concerning the secondary power cycle was the choice of working fluid. To minimize novelties one would naturally wish to use steam. Unfortunately, steam would be a poor choice for several reasons, which are perhaps best appreciated by observation of the temperature-entropy diagram shown in Fig. 7.1. It is necessary, in other words, to form the approximately triangular-shaped bottom cycle diagram to best fit the space shown available for the bottom cycle's operation in this figure, and this can only be done in the absence of the input temperature plateau which normal evaporation would have caused.



GA-A14311

Fig. 7.1 GT-HTGR Binary Cycle

Since the critical temperature of steam is too high for the available temperature levels, steam is at a considerable efficiency disadvantage. This is not the only one. The vapor pressure of water at a sink temperature is far too low, for the low enthalpy drop associated with bottom cycle duty entails high mass flows which could not be readily accommodated by steam without resort to the enormous last stages which were so happily eliminated by the closed cycle gas turbine.

An extensive study of many possible working fluids (Ref. 7.8 and 7.9) led to the conclusion that, provided supercritical operation was possible, there was little to choose on efficiency grounds between many candidate fluids; the principal criterion for selection was much more concerned with the practicality of the pressure involved and the size of the necessary heat exchangers and turbines and pumps and, of course, chemical stability and compatibility, not only with available circuit components, but also with the reactor core, in the advent of heat exchanger failure. Ammonia was selected, by a considerable margin as being the most effective working fluid for the GT-HTGR secondary power cycle. The principal factors favoring ammonia were, (1) its extremely good heat transfer ability, (2) high effective specific heat, and (3) high vapor pressure at the sink temperature. These factors led to a very considerable advantage in terms of machinery, duct, and heat exchanger bulk, and hence minimum cost. The magnitude of the advantage of ammonia is best illustrated by the following table, which lists just a few of the parameters that influence component sizes for several contending fluids.

Fluid	Ammonia	Isobutane	Propylene	Freon-12	Propane
Turbine Annulus relative area	1.0	5.8	3.9	7.4	4.2
Relative Condensing Coefficient	1.0	0.4	0.5	0.2	0.3
Relative Precooler Heat Transfer Coefficient	1.0	0.3	0.3	0.1	0.4

7.2 Secondary Power Cycle Conditions

The plant performance data are based on an advanced version of the primary cycle using a reactor outlet temperature of 1742°F (950°C). In addition, a relatively large plant size was investigated involving a twin 4000 MWe reactor. The secondary power cycle with an efficiency of just over 19 percent contributes 920 MW(e) to the overall plant output. Cycle conditions and component arrangement are illustrated schematically in Fig. 7.2.

The helium Brayton cycle with recuperation is combined with a supercritical ammonia Rankine cycle for evolution into the binary GT-HTGR plant. Some of the design parameters for the binary plant are set primarily by the design conditions that have been established for the dry-cooled plant in order to avoid extensive redesign of the primary system components.

Evaporative cooling was assumed as the method of heat rejection from the binary plant, and the wet bulb temperature taken is 9.7°C (49.5°F), which corresponds to an International Standards Organization (ISO) day dry-bulb temperature of 15°C (59°F) and 50% relative humidity. An ammonia condensation temperature of 32.2°C (90°F) was selected based on an optimization of the entire heat rejection system.

The secondary cycle is basically a supercritical Rankine power cycle as shown on Fig. 7.3; thus its components, operation, and controls are similar to Rankine cycle steam power plants. The ammonia turbine inlet pressure of 16.1 MPa (2334 psia) was selected from system studies, this involving certain criteria to be established (as outlined below) to ensure component thermodynamic compatibility for the fixed ammonia turbine inlet temperature of 250°C (482°F). From the temperature-entropy diagram on Fig. 7.3, it can be seen that for the supercritical cycle the ammonia precooler heating curve is well-matched to the helium heat rejection curve. There is, however, a pinch-point in the heat source exchanger which has a significant influence on the surface area requirement of this unit, and in the cycle studies, a minimum pinch point temperature difference of 5.6°C (10°F) was imposed to ease the thermal conductance requirements of the precooler. With the condensation temperature (hence pressure) established from plant heat rejection characteristics, another important criteria was that of establishing the turbine exhaust condition very close to the saturated vapor line. A few degrees

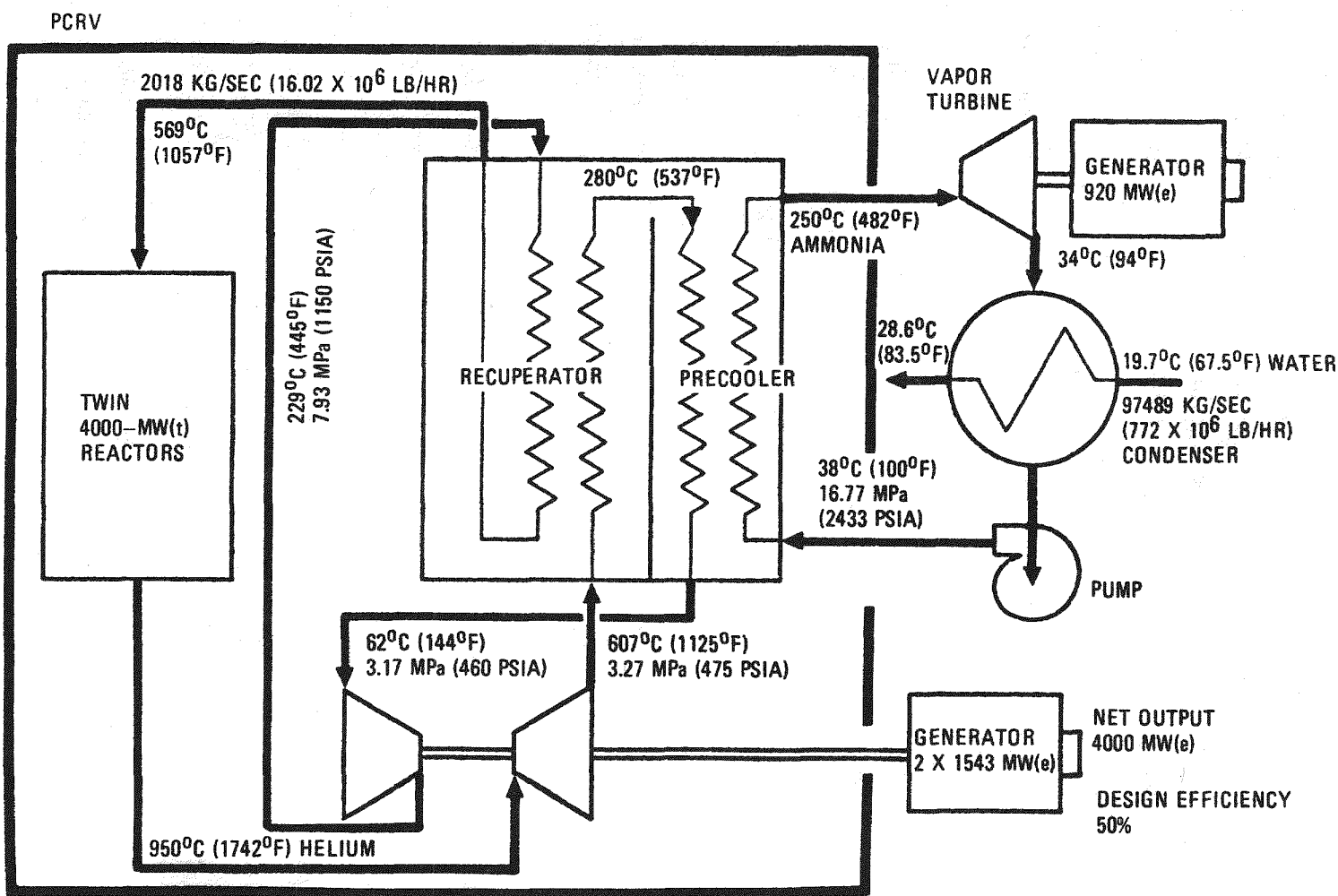


Fig. 7.2 Cycle Diagram for GT-HTGR Plant with Ammonia Bottoming Cycle

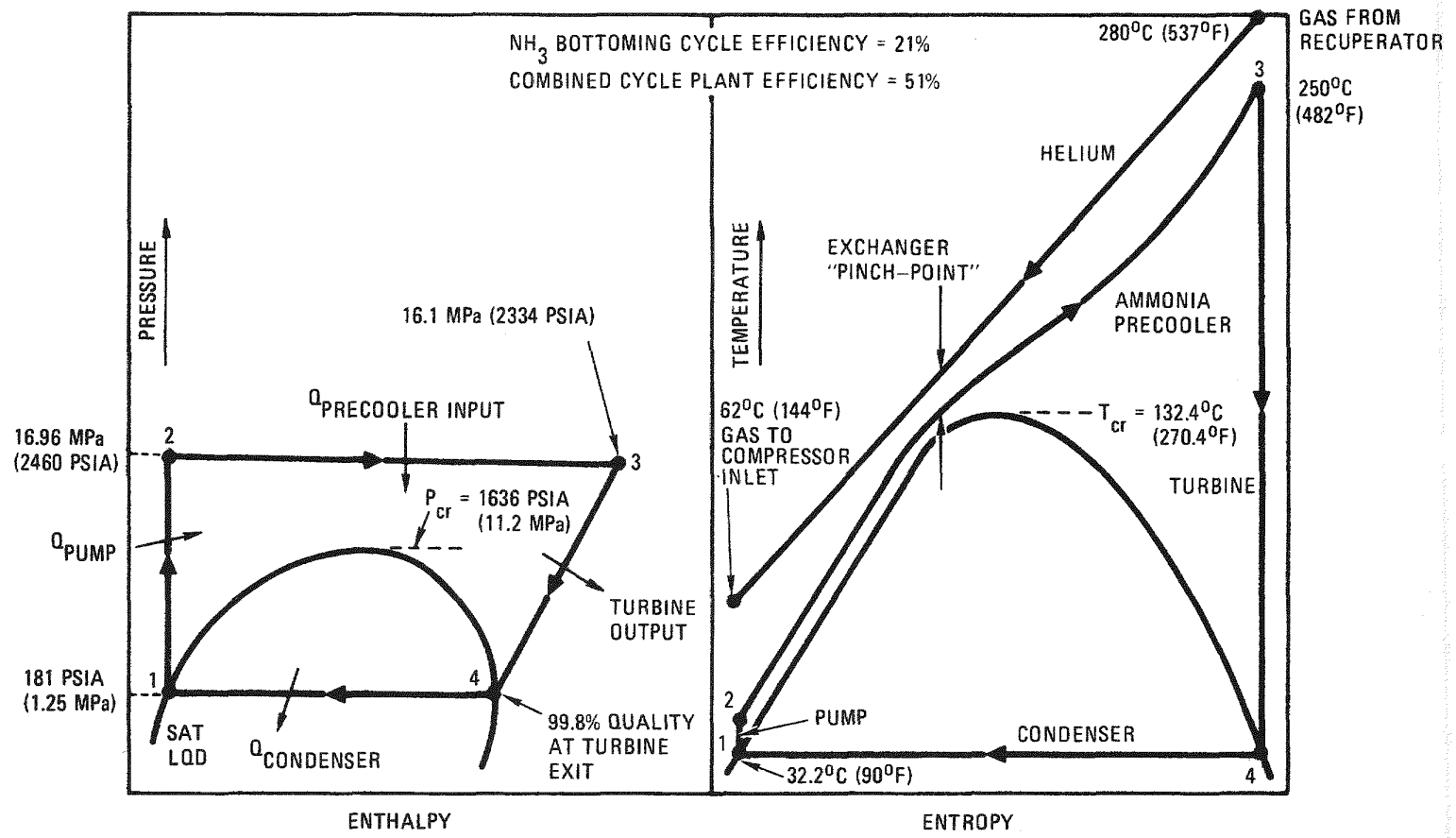


Fig. 7.3 Supercritical Ammonia Bottoming Cycle Diagram for GT-HTGR Plant

of superheat would have an adverse effect on the already large condenser and over-expansion in the turbine would result in efficiency loss and erosion problems because of the moisture content. From the pressure-enthalpy diagram on Fig. 7.3, it can be seen that with a turbine exit quality of 99.8%, and the criteria mentioned above, the turbine inlet pressure of 16.1 MPa (2334 psia) was established.

The supercritical ammonia fluid is heated in the primary system plant pre-coolers which are located inside the prestressed concrete reactor vessel. The heated fluid from the precoolers in both reactor units is transported to the single waste heat (secondary cycle) plant. Multiple shell-and-tube condensers reject the heat from the cycle. The secondary cycle ammonia flow is circulated by turbine-driven feedpumps. A surge tank upstream from the feedpumps isolates pressure transients in the system. A simplified flow diagram for the waste heat plant is shown on Fig. 7.4. Safety studies have shown that the system with direct helium-to-ammonia heating as shown on Fig. 7.4 is acceptable; however, the turbo-machinery design considerations outlined here would not be affected by possible future introduction of an intermediate heat transfer loop.

7.3 Component Design Considerations

Component design considerations (particularly the turbine and condenser, because of their cost impact) are briefly outlined below. Initial design considerations have been reported previously (Ref. 7.10). The conceptual designs of the secondary power cycle components are conceptual in nature and should not be interpreted as final design solutions. They were done in sufficient detail to:

(1) establish their feasibility, (2) satisfy performance and economic requirements, (3) seek industry participation for more detailed design and balance-of-plant cost studies, and (4) to assist in plant layout studies. The cycle conditions for the secondary power cycle components are given on Table 7.1.

7.3.1 Ammonia Turbine Design

One of the early design considerations for the binary plant involved the selection of the number of turbines. Realizing the economic merits of a single unit, a conceptual design of a 920 MW(e) turbine was completed. A review of this design concluded that it was indeed technically feasible, but from the overall plant availability standpoint, two turbines would be more attractive.

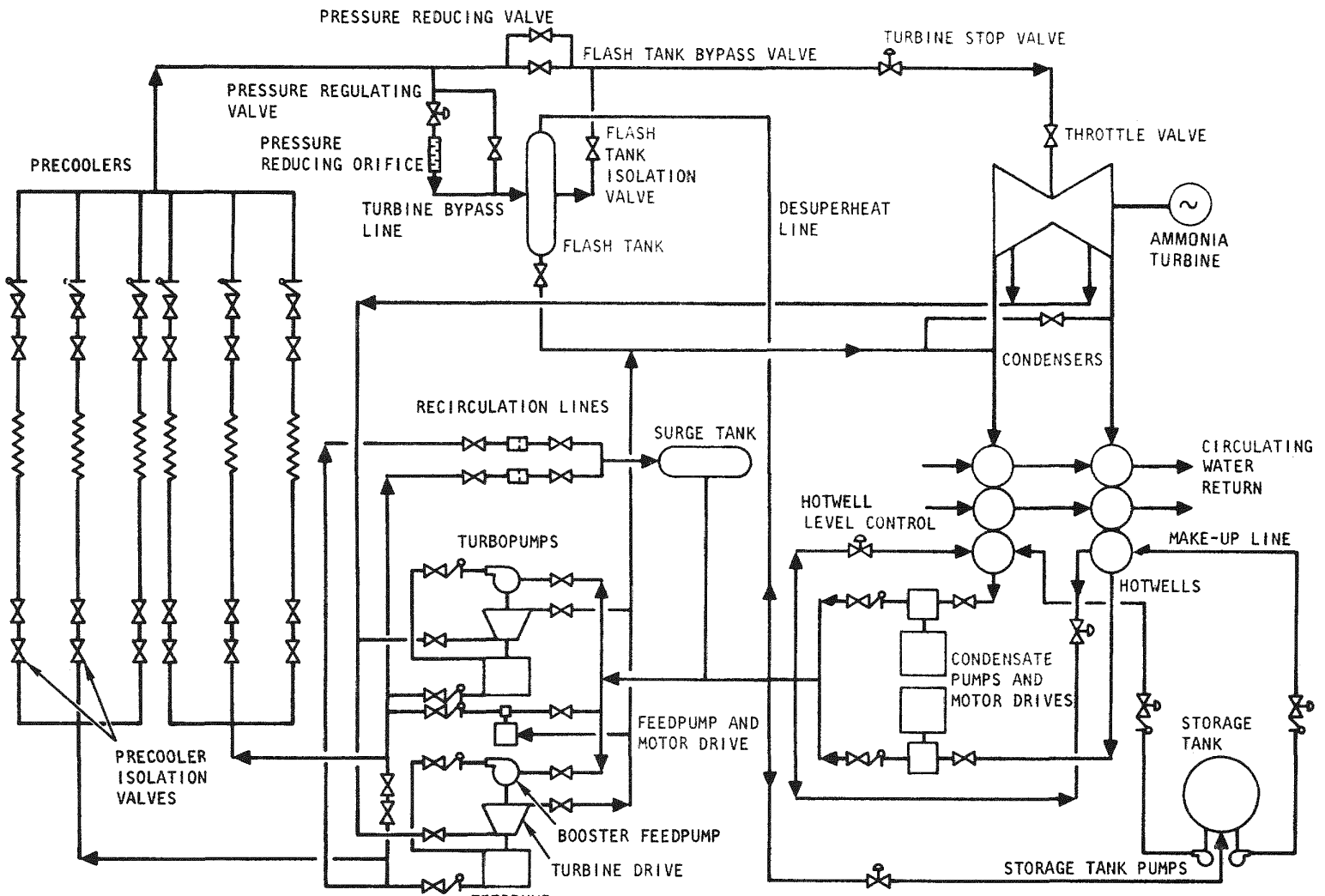


Fig. 7.4 Flow Diagram for Ammonia Bottoming Cycle

BINARY PLANT GT-HTGR DESIGN PARAMETERS AND PERFORMANCE

OVERALL PLANT	Reactor Thermal Rating, MW(t)	Twin 4000 MW(t) Units
	Reactor Type	HTGR
	Reactor Outlet Temperature, °C (°F)	950 (1742)
	Plant Type	Integrated Primary System
	Net Electrical Output, MW(e)	4000
	Power Plant Efficiency, %	50.0
	Mode of Heat Rejection	Natural Draft Evaporative Cooling Tower
PRIMARY SYSTEM	Electrical Output, MW(e)	3086
	Efficiency, %	38.6
	Power Conversion System	Helium Gas Turbines
	Number of Power Conversion Loops	4 Per Reactor
	Turbine Inlet Temperature, °C (°F)	950 (1742)
	Turbine Efficiency, %	91.5
	Compressor Inlet Temperature, °C (°F)	62 (144)
	Compressor Pressure Ratio	2.50
	Maximum Helium Pressure, MPa (psia)	7.93 (1150)
	Compressor Efficiency, %	89.0
	Recuperator Effectiveness, %	90.0
SECONDARY SYSTEM	Electrical Generator Efficiency, %	98.6
	Electrical Output, MW(e)	920
	Efficiency, %	19.3
	Power Conversion System	Supercritical Rankine Cycle
	Working Fluid	Ammonia
	Turbine Inlet Pressure, MPa (psia)	16.1 (2334)
	Turbine Inlet Temperature, °C (°F)	250 (482)
	Turbine Type	2 Double - Flow Axial Units
	Turbine Expansion Ratio	12.1
	Turbine Exit Gas Condition	99.8% Quality
	Turbine Efficiency, %	90.0 (Across Blading)
	Feed Pump Type	4 Turbine Driven Centrifugal Units
	Pump Efficiency, %	85.0
	Condenser Heat Load, MW(t)	3900
	Condensing Pressure, MPa (psia)	1.25 (181)
	Ambient Dry Bulb Temperature, °C (°F)	15 (59)
	Ambient Wet Bulb Temperature, °C (°F)	9.7 (49.5)

Accordingly, two turbines were adopted with a unit rating of 460 MW(e), and it is details of this ammonia turbine that are presented herein. The next major decision involved the choice of a single-flow or double-flow configuration. A double-flow arrangement was chosen for the following reasons: (1) it is essentially self-balancing, thus eliminating complex thrust balancing devices; (2) it results in low values of blade stresses; and (3) the double-flow exit system is well-suited to the piping configuration for transporting the vapor to the multiplicity of condenser shells. These considerations were viewed as more important than the main merit of the single-flow system which lies in the area of reduced number of discs, blades, and machine structure.

The high density working fluid in the ammonia secondary cycle results in a very compact power conversion system, compared with steam turbines and open-cycle industrial gas turbines. The ammonia turbine is characterized by short blades, and high hub-to-tip ratios that result from a combination of the properties of ammonia and the high degree of pressurization, particularly at the turbine exit. The waste-heat plant cycle conditions have been selected so that the ammonia is dry-saturated (99.8% quality) at the end of expansion, so that in the absence of wetness the aerodynamic design procedures used are identical to conventional gas and high pressure steam turbine practice. Design conditions for the ammonia turbine are given on Table 7.2.

The conceptual design of the turbine was done with the assistance of a comprehensive computer code which has been used extensively for steam turbine design. With the substitution of ammonia properties for steam, this code, which embodies thermodynamic, aerodynamic, and structural subroutines, was used for the turbine blading design. Studies were done to evaluate the blading design for differing number of stages and gas flow path geometries, with emphasis placed on high efficiency solutions. Details of the selected 8 stage design are shown on Table 7.2. The stress levels are consistent with the turbine design life goal of 40 years.

Correlation of efficiency can be based on the stage loading and flow coefficient. Such a simple correlation gives a measure of the vector diagram on stage efficiency, although it must be appreciated that the detailed choice of

Table 7.2

DATA FOR CONCEPTUAL AMMONIA POWER TURBINE DESIGN

Turbine Type	Double-Flow Axial Arrangement	
Number of Turbines per Plant	2	
Turbine Power, MW(e)	460	
Ammonia Outlet Flow, kg/sec (lb/sec)	1536 (3385)	
Rotational Speed, rpm	3600	
Number of Axial Stages	8	
Turbine Expansion Ratio	12.1	
Turbine Inlet Pressure, MPa (psia)	16.1 (2334)	
Turbine Inlet Temperature, °C (°F)	250 (482)	
Turbine Efficiency Goal, %	90.0 (Across Blading)	
Machine Overall Length, m (ft)	6.1 (20.0)	
Machine Overall Diameter, m (ft)	3.2 (10.5)	
Power Output/Exhaust Area, MW/m ² (MW/ft ²)	430 (40)	
Stage	First	Last
Tip Diameter, m (in.)	0.844 (33.2)	1.46 (57.5)
Hub Diameter, m (in.)	0.728 (28.7)	1.207 (47.5)
Blade Height, mm (in.)	58 (2.25)	126.5 (5.0)
Hub-to-tip Ratio	0.864	0.826
Hub Speed, m/sec (ft/sec)	137.3 (450)	227.6 (747)
Tip Speed, m/sec (ft/sec)	159.1 (522)	275.1 (903)
Gas Axial Velocity, m/sec (ft/sec)	66.7 (219)	113.1 (371)
Rotor Blade Chord, mm (in.)	37.5 (1.48)	49.6 (1.95)
Rotor Aspect Ratio	1.52	2.56
Hub Solidity	1.49	1.48
Number of Rotor Blades	94	110
Specific Speed, N_s	91	114
Specific Diameter, D_s	1.25	1.0
Degree of Reaction	0.55	0.55
Flow Coefficient	0.45	0.45
Stage Loading, $\Delta H/U^2$	0.90	0.90
Maximum Rotor Mach Number	0.32	0.65
Reynolds Number	11×10^6	9.4×10^6
Centrifugal Stress, MPa (psi)	29.23 (4,240)	88.5 (12,850)
Rotor Bending Stress, MPa (psi)	137.9 (20,000)	137.9 (20,000)

GA-A14311

design parameters such as blade loading, profile shape, aspect ratio, tip clearance, may all affect the overall efficiency. Performance analysis of many gas turbine rig tests produces an empirical relationship between stage loading factor, flow coefficient, and efficiency. Fig. 7.5 constructed from test data (Ref. 7.11) shows this in a simplified form. With an initial assumption of 8 stages it can be seen that the aerodynamic factors are consistent with a high efficiency design. Although the efficiency values shown on Fig. 7.5 do not include allowances for tip clearance and leakage losses, the position of the efficiency contours is not significantly changed by these factors, and the figure is useful as a preliminary design tool. Superimposing the same turbine aerodynamic loading factors on similar curve arrays for typical high-pressure steam turbines (Ref. 7.12) shows that the 90% efficiency goal should be realizable for a conservatively designed multistage axial ammonia turbine.

The map of specific speed vs. specific diameter for axial turbines (Ref. 7.13) shown on Fig. 7.6 is particularly useful at the conceptual design stage. Initial calculations are based on operating in the middle of the maximum efficiency island, then modifying the design as necessary to satisfy stress criteria, stage matching, and mechanical limitations. From this figure it can be seen that the 8 stage conceptual design is in the proper regime for high efficiency.

A simplified view of the double-flow, eight stage ammonia turbine is shown on Fig. 7.7. The overall length and width are 20 ft. (6.1m) and 10.5 ft (3.2m), respectively. The 460 MW(e) turbine has four exits as shown, each duct transporting ammonia vapor to a bank of three condenser shells. The turbine layout was prepared to get an appreciation for the overall plant size, and to assist in binary cycle balance-of-plant studies. In this conceptual phase of the program, the mechanical design aspects of the rotor, bearings, seals, and structures were not addressed, and indeed in these areas, inputs from a turbine company with experience in large power generating machinery are necessary.

The general response from the turbine industry was that while an ammonia turbine has not been built and operated, its design would be well within the state-of-the-art, and with a molecular weight very similar to steam, existing aerodynamic data would be applicable. On Fig. 7.8, a comparison is shown between a

LINES OF CONSTANT EFFICIENCY FROM A WIDE
RANGE OF AXIAL TURBINE TEST RESULTS
(DIFFERING REACTIONS AND EXIT SWIRL, ETC.)
DATA DO NOT INCLUDE ALLOWANCES FOR
TIP CLEARANCE OR LEAKAGE LOSSES

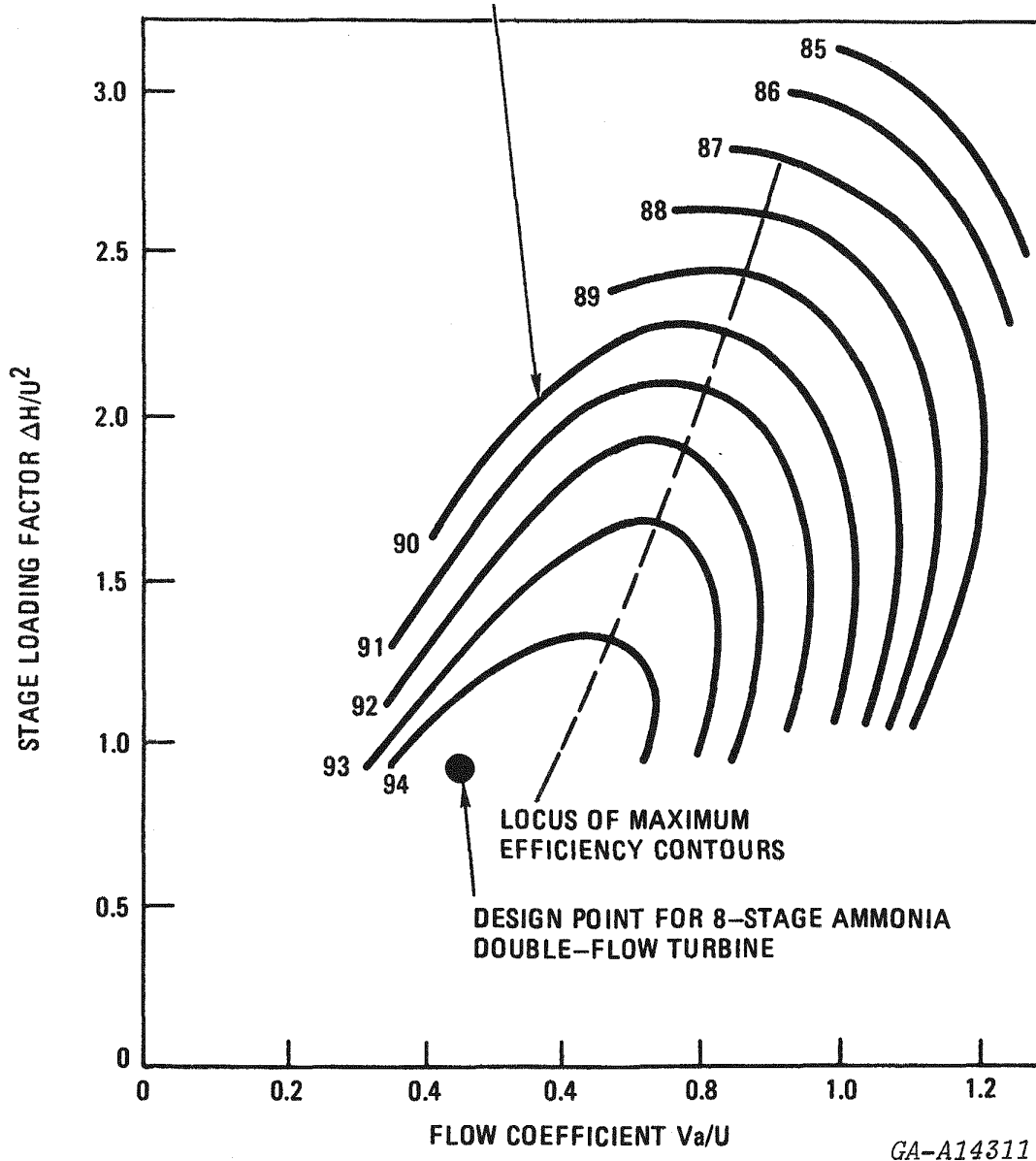


Fig. 7.5 Generalized Axial Turbine Blading Efficiency Contours

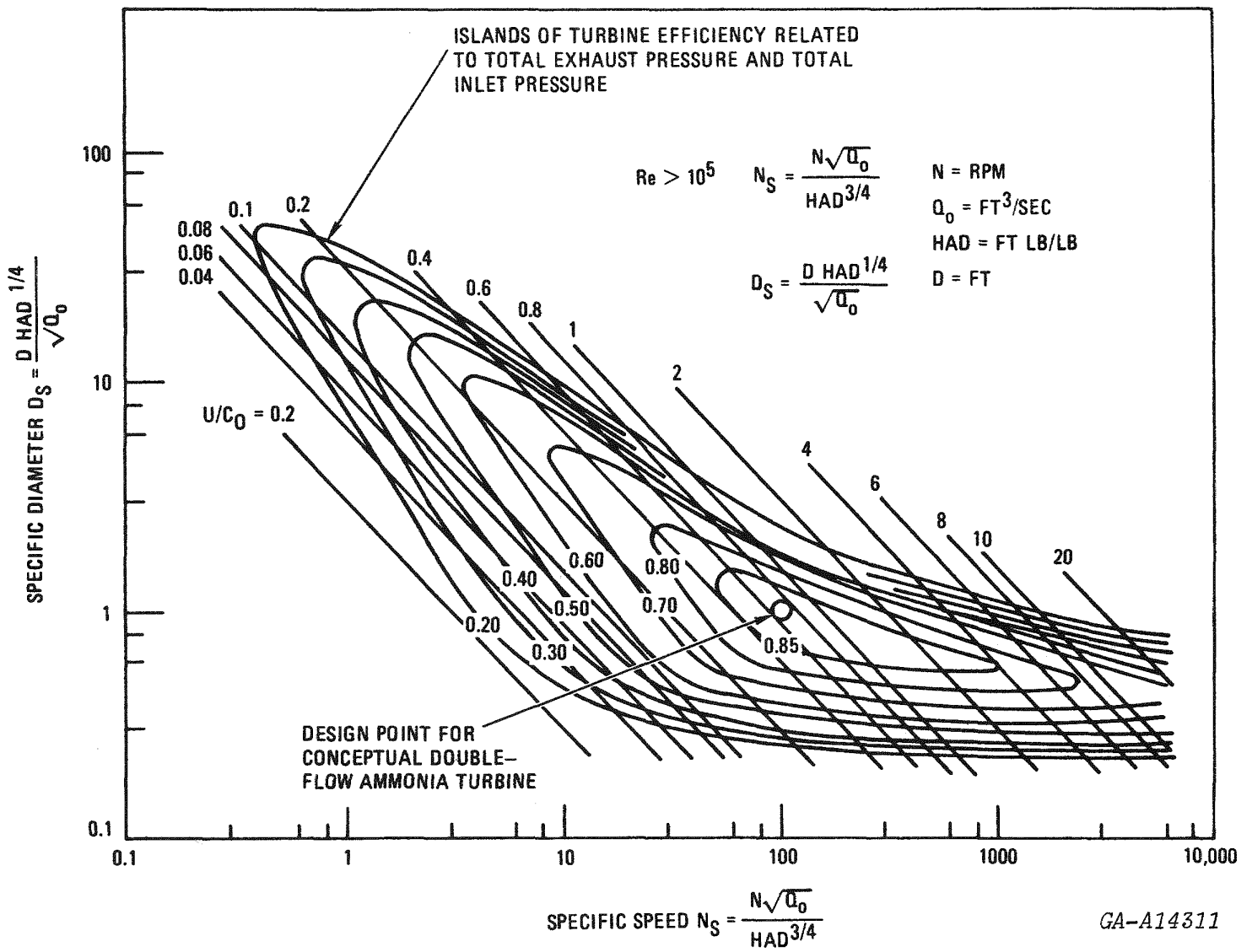


Fig. 7.6 Specific Speed-Diameter Relations for Axial Flow Turbine

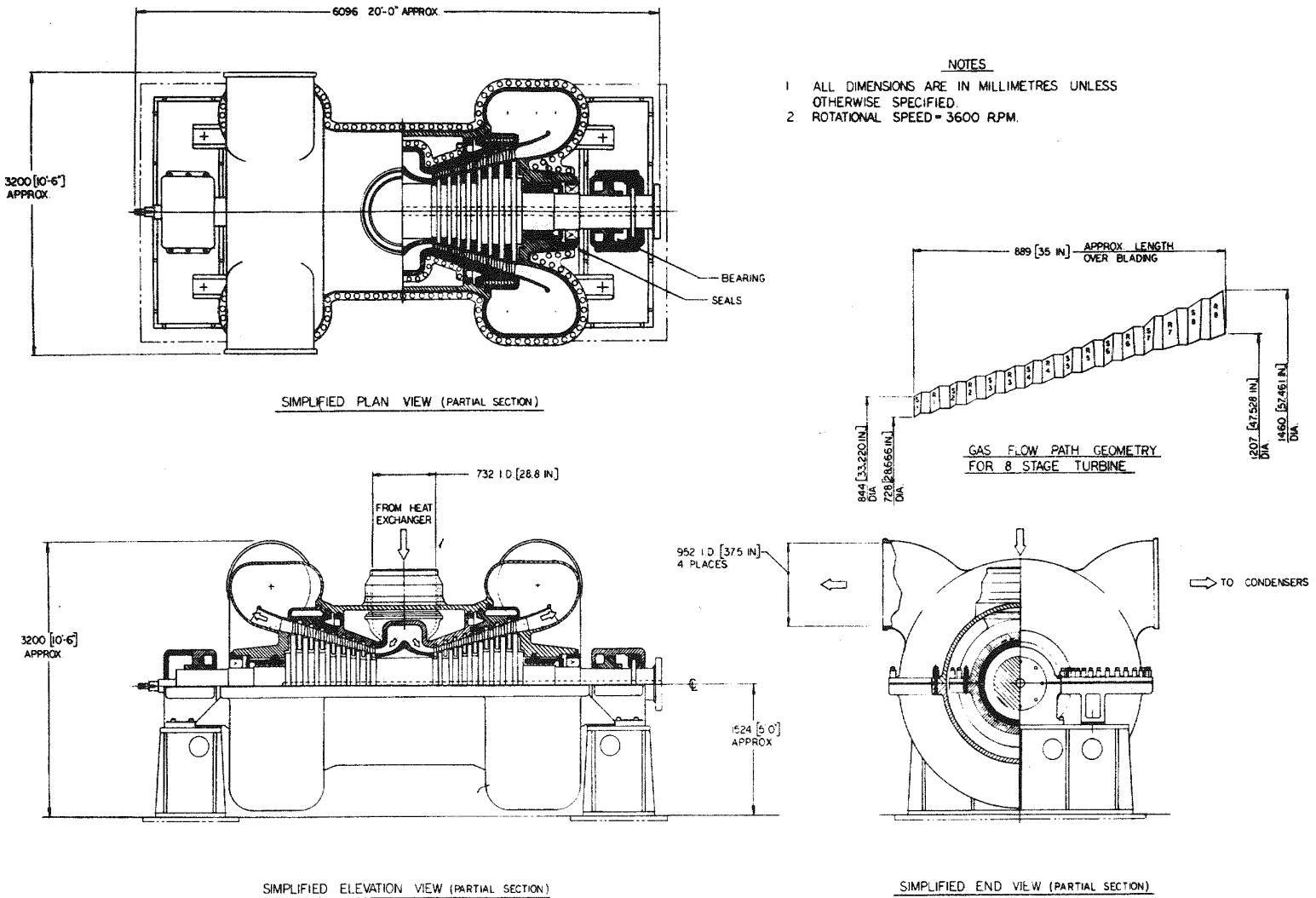


Fig. 7.7 Conceptual Design of 460 MW(e) Ammonia Turbine

GA-A14311

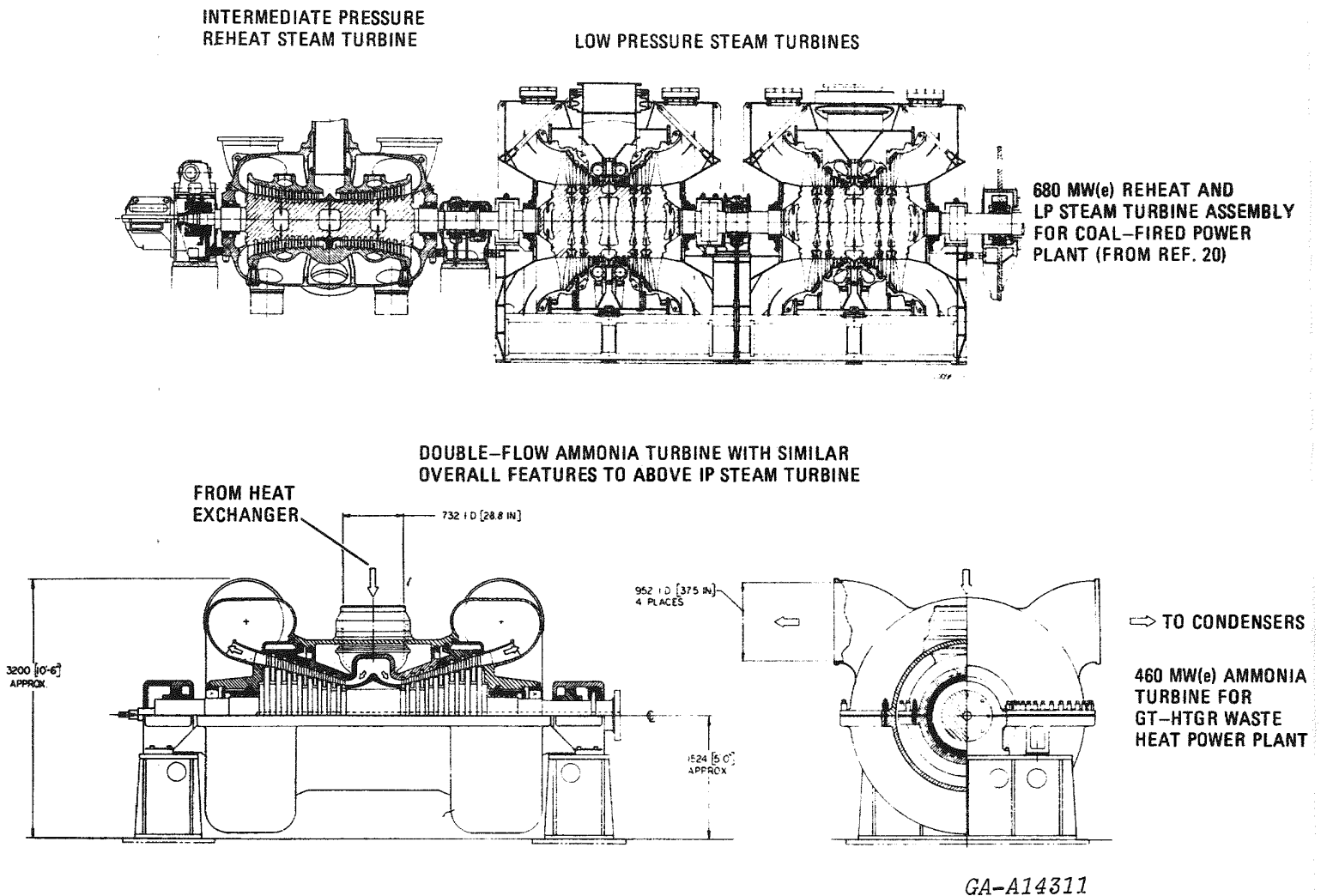


Fig. 7.8 Comparison of Features Between Ammonia Turbine and Modern Reheat Steam Turbine (Steam Turbine
Figure by Courtesy of BBC)

modern reheat steam turbine (Ref. 7.14) and the conceptual ammonia turbine outlined herein. From this figure and Table 7.3, it can be seen that, from the overall configuration and size standpoints, there is considerable similarity. This substantiates the fabricability of the ammonia turbine since exiting manufacturing techniques could be directly applied.

A comprehensive outline of the ammonia turbomachinery design is given in Ref. 7.15.

7.3.2 Turbine-Driven Ammonia Feedpump

Unlike boiler-feed water pumps in contemporary steam plants, the ammonia pump for the binary plant is not an "off-the-shelf" component, and to assist in balance-of-plant studies and cost estimates, a conceptual design was carried out. With secondary plant total pumping power requirements in excess of 100 MW(e), an ammonia turbine drive for the pump was selected, and the complete pump package is briefly outlined herein. For the conceptual design, four parallel pumps were selected, each with a flow in the order of 1.47m^3 (23,000 gpm), which is similar to existing boiler-feed water pumps used in large commercial steam power generating plants. In the cycle calculations, an ammonia pump efficiency of 85% was assumed, and one of the goals of the conceptual design study was to confirm the feasibility of realizing this efficiency level.

Ammonia bleed from the fifth stage of the main turbine has the right thermodynamic condition to make a single-axial-stage pump drive turbine feasible. Each of the four pumps has a power requirement on the order of 27 MWe. In order to achieve an adequate NPSH (Net Positive Suction Head) it was necessary to provide a booster pump, driven off the same shaft as the drive turbine through a reduction gear. Details of the two-stage centrifugal pump are given on Table 7.4, and a summary of the main features of the single stage drive turbine are given on Table 7.5.

With an overall length and height of 15 ft (4.6m) and 6 ft. (1.8m) respectively, it can be seen from Fig. 7.9 that the ammonia feed pump package is a compact unit. The design, fabrication, and operability of the feed-pump unit

Table 7.3

COMPARISON OF AMMONIA TURBINE AND MODERN INTERMEDIATE
PRESSURE (REHEAT) STEAM TURBINE

Turbine	Ammonia Turbine	Reheat (IP) Steam Turbine * (Ref. 20)
Status	Conceptual Design	Ordered for Amos 3 and Gavin 1 & 2 coal-fired plants.
Turbine Rating	460	410
Turbine Type	Double-Flow Axial	Double-Flow Axial
Number of Stages	8	9
Rotational Speed, rpm	3600	3600
Blade Height		
First Stage, mm (ins)	58 (2.25)	139 (5.47)
Last Stage, mm (ins)	126.5 (5.0)	241 (9.49)
Machine Overall length, m (ft)	6.1 (20.0)	7.8 (25.6)
Machine Overall Diameter, m (ft)	3.2 (10.5)	4.8 (15.7)
Power Output/Exhaust Area		
MW/m ² (MW/ft ²)	430 (40)	384 (35.7)
Specific Power		
MW/kg1Sec (hp/lb/Sec)	0.30 (182)	0.45 (271)
Turbine Efficiency, %	90.0	89.5

GA-A14311

* Steam Turbine data courtesy of BBC, Brown Boveri and Company, Limited

Table 7.4

DETAILS OF AMMONIA PUMP(S) CONCEPTUAL DESIGN

<u>Ammonia Feed Pump</u>	
Type	Two-stage centrifugal
Number per Plant	4
Mass Flow, kg/sec (lb/sec)	870 (1917)
Volumetric Flow, m^3 /sec (gpm)	1.47 (23,312)
Inlet Pressure, MPa (psia)	1.24 (180)
Suction Temperature, °C (°F)	34.3 (93.8)
Discharge Pressure, MPa (psia)	16.96 (2460)
Available NPSH	0
NPSH Required, m (ft)	275 (900) from booster pump
Rotational Speed, rpm	9000
Impeller Exit Diameter, mm (in.)	384 (15.1)
Width, mm (in.)	45.8 (1.8)
Peripheral Speed, m/sec (ft/sec)	181 (594)
Efficiency, %	85.0
Power, MW (hp)	27.2 (36,460)
<u>Ammonia Boost Pump</u>	
Type	Single-stage centrifugal
Suction Temperature, °C (°F)	32.2 (90)
NPSH (available), m (ft)	24.4 (80)
Rotational Speed, rpm	1500
Impeller Exit Diameter, mm (in.)	908 (36)
Impeller Exit Width, mm (in.)	81 (3.2)
Peripheral Speed, m/sec (ft/sec)	71.3 (234)

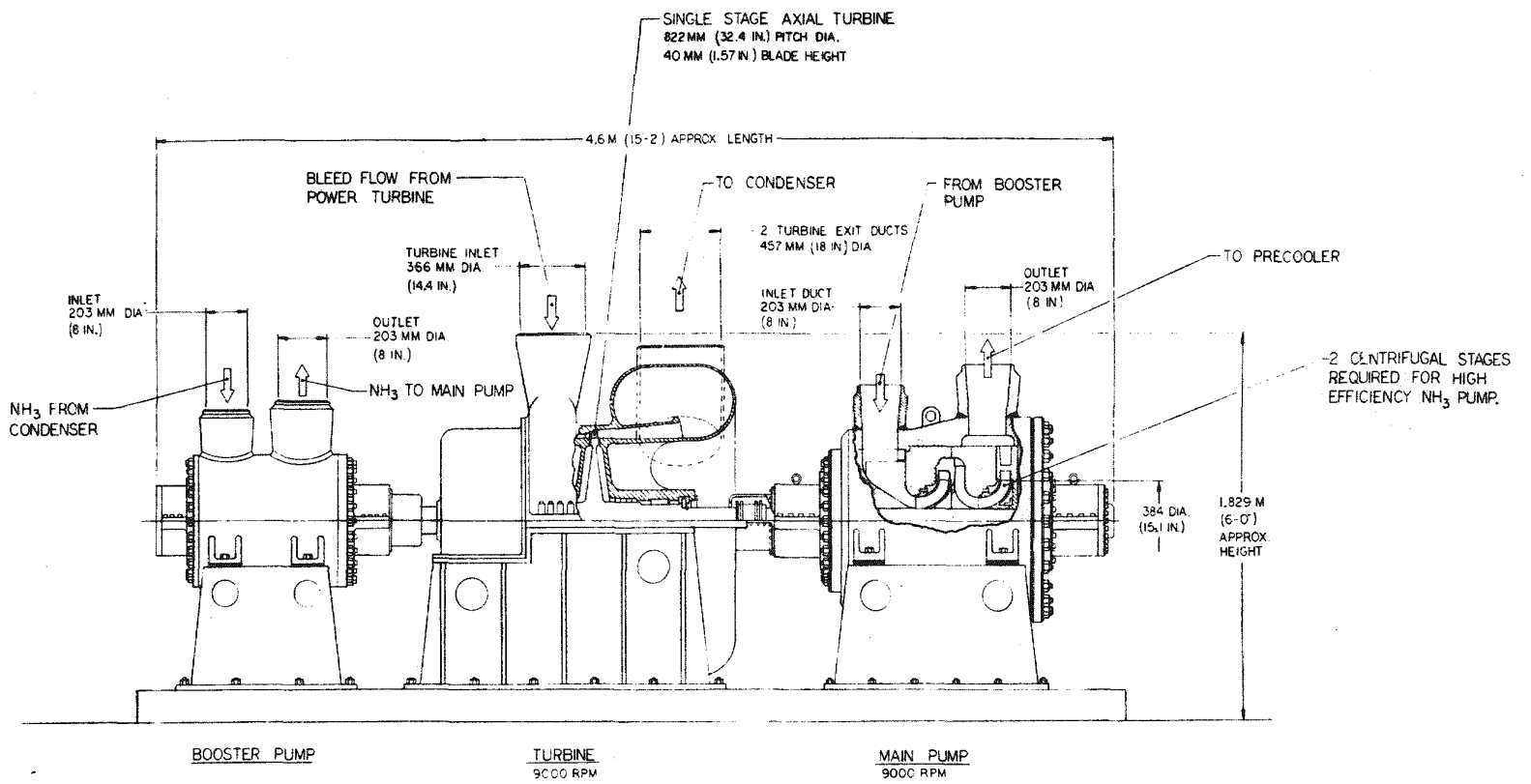
GA-A14311

Table 7.5

DETAILS OF AMMONIA PUMP DRIVE TURBINE

Type	Single-Stage Axial Flow
Ammonia Flow Rate, kg/sec (lb/sec)	205 (451.3)
Inlet Temperature, °C (°F)	155 (311)
Inlet Pressure, MPa (psia)	6.11 (886)
Efficiency, %	85.0 (Across Blading)
Rotational Speed, rpm	9000
Flow Coefficient, V_a/U	0.50
Stage Loading Coefficient, $\Delta H/U^2$	1.0
Hub Diameter, mm (in.)	782 (30.8)
Tip Diameter, mm (in.)	864 (34.0)
Blade Height at Exit, mm (in.)	41 (1.6)
Nozzle Height/Pitch Diameter	0.0156
Specific Diameter	1.52
Specific Speed	71.0
Blade Tip Speed, m/sec (ft/sec)	407 (1335)
Enthalpy Drop, kJ/kg (Btu/lb)	149.9 (64.4)
Blade Centrifugal Stress, MPa (psi)	114.6 (16,600)
Feed-Pump-Turbine Assembly	
Approximate Overall Length, m (ft)	4.6 (15)
Approximate Overall Height, m (ft)	1.8 (6)

GA-A14311



GA-A14311

Fig. 7.9 Conceptual Design of Turbine Driven Ammonia Feed Pump

represent existing technology, and while detailed design is necessary, the development effort to satisfy the high efficiency design goal should be minimal.

7.3.3 Condenser Conceptual Design

The ammonia condenser design differs from conventional steam design in two major respects: (1) the ammonia condensing pressure is much higher than the steam pressure; and (2) the condensing heat transfer, although good, is not as good as steam. The condensers are designed with the cooling water flow inside the tubes and condensing ammonia vapor flowing in cross-flow over the tube banks. Heat transfer is augmented in the condenser design to reduce the physical size and cost. A spirally-corregated tube was chosen for the condenser design based on improved performance and reduction in cost.

Design data for the condenser are given on Table 7.6. The high vapor pressure does restrict the maximum shell diameter, so multiple shells are used, with a constraint put on shell diameter of 15 ft. (4.57m) to facilitate shop fabrication and shipment of the site of a complete assembly. Design studies led to the selection of a U-tube configuration since this inherently provides for the differential expansion between the tubes and the shell. The ammonia condenser is shown on Fig. 7.10 and 7.11, and a possible support structure is shown on Fig. 7.12. Each condenser train consists of three units mounted one above the other as shown on Fig. 7.12. The ammonia vapor from the turbine comes in at the top of the top unit, and an equal amount is assumed to condense in each unit and be drawn off as a liquid through the four nozzles at the bottom of each shell.

Figure 7.10 shows horizontal and vertical sections and an end view of the top unit. Figure 7.11 is a cross-section taken through the vapor nozzles. The U-tubes are in the horizontal plane, with the cooling water entering at one side and leaving at the other. Two inlet and two outlet pipes were provided to keep the pipe size and entry openings small, but the sizes will make it easy to provide for two half-size water circuits if they are considered desirable. On the ammonia side, the vapor enters the top nozzle and is deflected by the circular impingement plate. It then divides, some of it flowing down the sides of the bundle in the spaces shown in Fig. 7.11 and some of it entering the center part of the bundle through the void formed by the inner U-tubes. The vapor thus enters the tube

Plant	Reactor thermal rating, MW(t) Number of condensers/plant Heat exchanger type Type of construction Flow configuration Orientation	Twin 4000-MW(t) arrangement 24 Tubular Shell and tube U-tube, cross flow (shell) Horizontal
Thermal Data	Heat transfer Q, MW(t)/plant LMTD, °C (°F) Conductance UA/plant, MW/°C (Btu/hr-°F) Ammonia pressure loss, kPa (psi) Water pressure loss, kPa (psi)	3873 7.16 (12.9) 540.4 (1025 x 10 ⁹) 8.96 (1.3) 103.4 (15)
Surface Geometry	Number of passes Tube type Tube o.d., mm (in.) Tube wall thickness, mm (in.) Number of tubes/unit Effective tube length, m (ft) Surface area/plant, m ² (ft ²) Maximum metal temperature, °C (°F) Operating internal pressure differential, MPa (psi) Tube material type ASME Code class Safety class	2 Spirally corrugated 28.5 (1.125) 1.24 (0.049) 11388 9.3 (30) 224,358 (2.4149 x 10 ⁶) 32.2 (90) 0.93 (135) 304 SS Section VIII Nonnuclear
Overall Assembly	Shell design pressure, MPa (psig) Normal operating pressure, MPa (psia) Maximum vapor temperature, °C (°F)	2.06 (300) 1.24 (180.6) 48.9 (120)

GA-A14311

Fig. 7.6 Conceptual Design Data for Ammonia Condenser

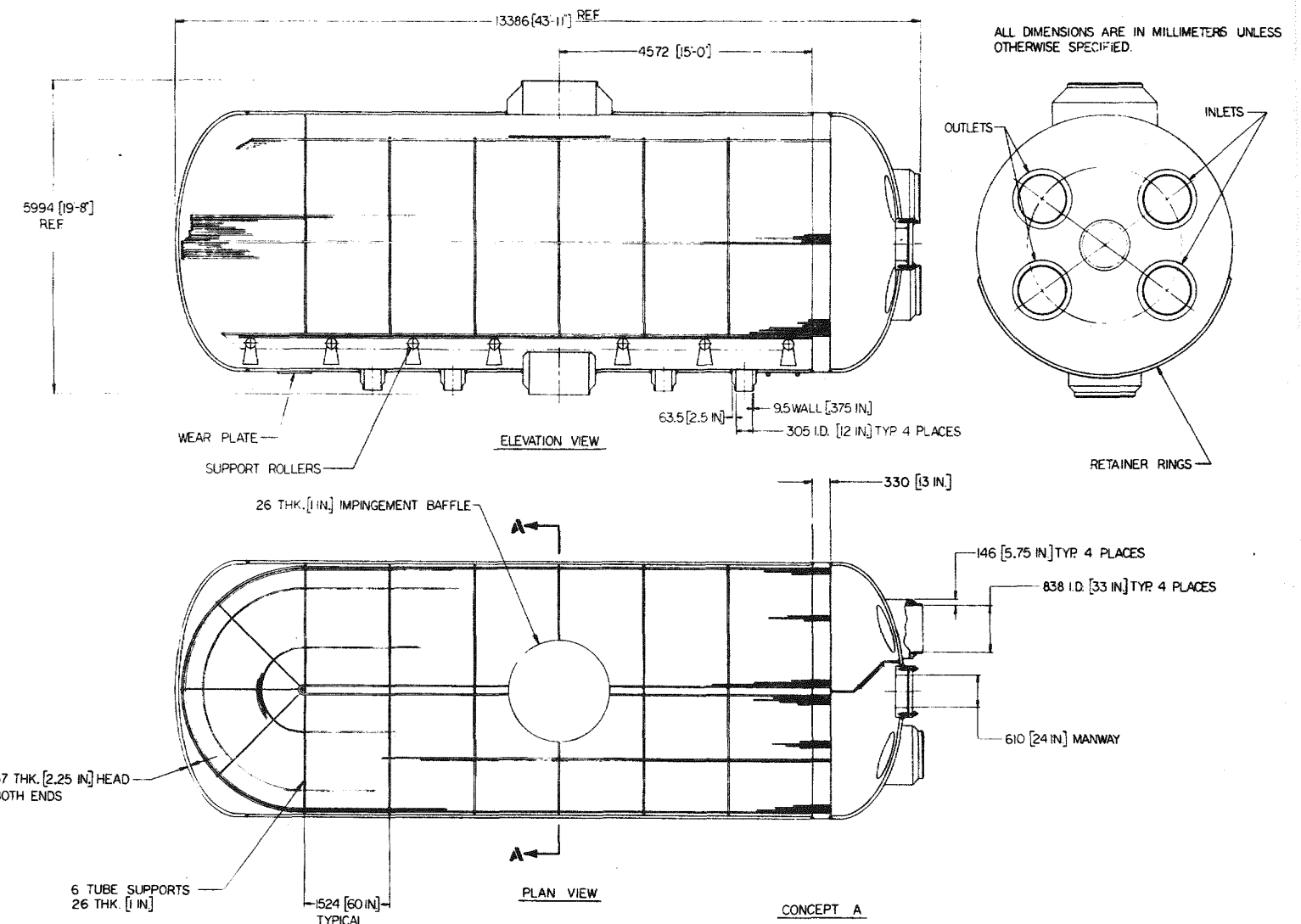


Fig. 7.10 Ammonia Condenser Arrangement

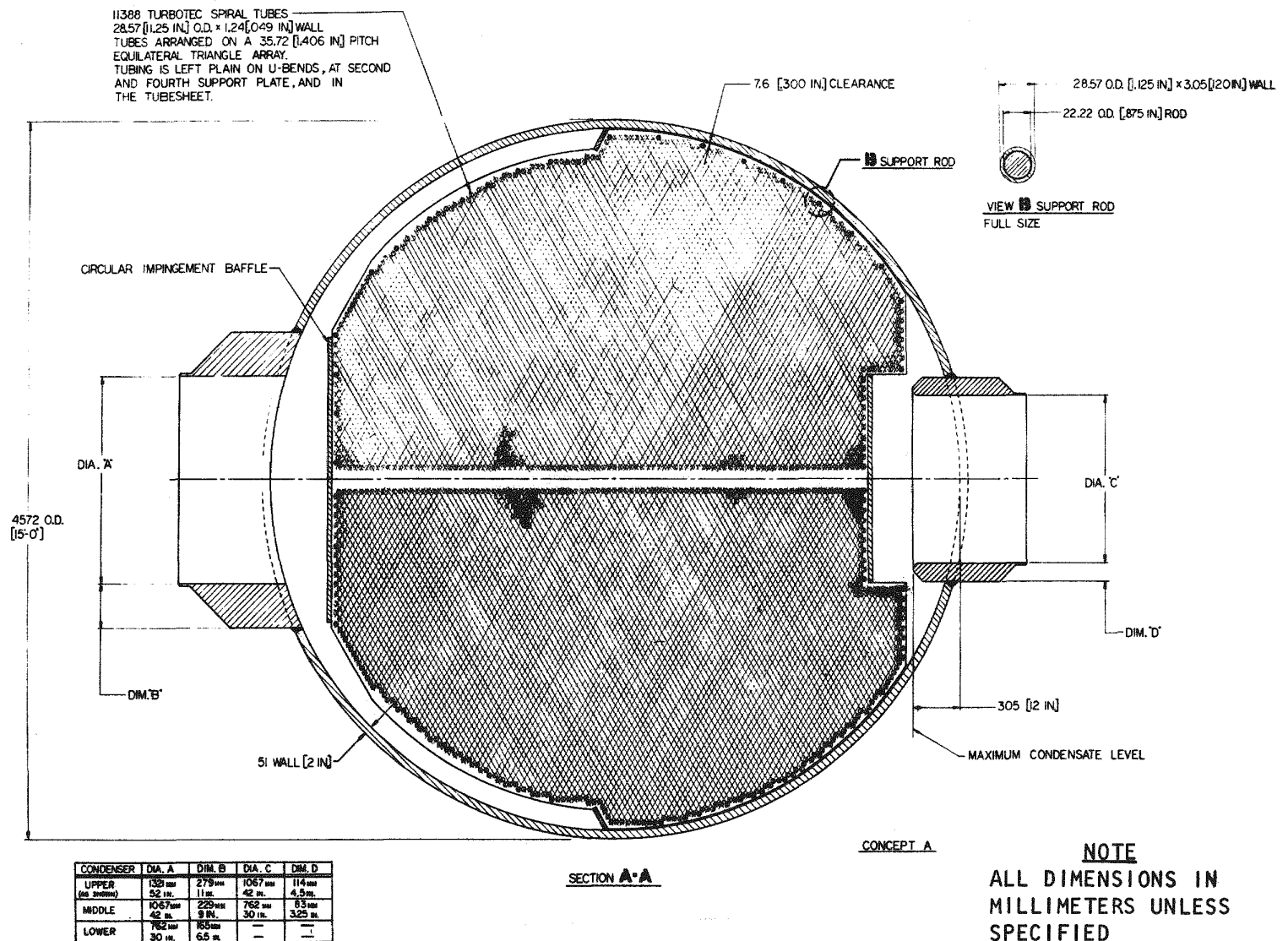


Fig. 7.11 Ammonia Condenser Tube Bundle Details

NOTE ALL DIMENSIONS ARE IN MILLIMETERS UNLESS OTHERWISE SPECIFIED.

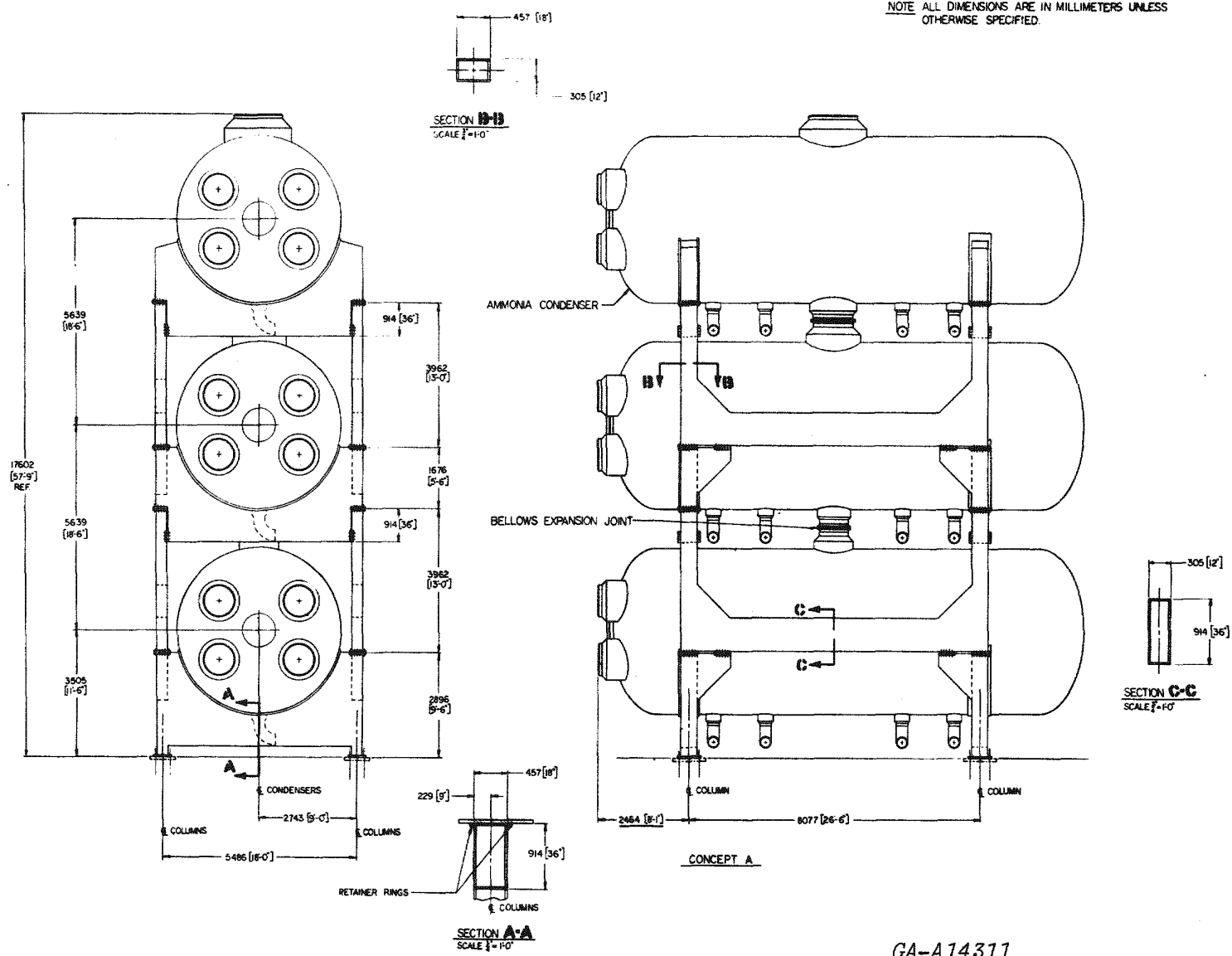


Fig. 7.12 Condenser Overall Arrangement

field from several directions so that bypass and pressure drop are minimized. The condensate collects at the bottom of each shell below the projection of the vapor outlet nozzle shown on Fig. 7.11.

7.4 Secondary Power Cycle Building Layout

The sizing of the major equipment items for the waste heat plant were done for the following reasons: (1) to establish feasibility; (2) to assist in balance-of-plant layouts; and (3) to enable cost data to be generated. A study was initiated to determine the sizes and geometries of the interconnecting ammonia pipe-work for the waste heat plant. The study consisted of component orientation layouts to establish the best equipment positions to satisfy criteria in the areas of: (1) minimum building size; (2) simple piping arrangement; and (3) component accessibility for maintenance and installation/replacement.

Fig. 7.13 shows a conceptual arrangement of the ammonia turbine building. The two turbines are shown positioned at an elevated location. Each turbine exit discharges the ammonia vapor (dry and saturated) vertically downwards to a bank of three condensers. From Fig. 7.13, it can be seen that the building is dominated by the bulk of the 24 condenser shells. The other major equipment items such as the surge tanks, pump-turbine package, and condenser hot well tanks are shown positioned inside the building. For the 920 MW(e) ammonia waste heat plant, the building length, width, and height are 241 ft. (73.5m), 121 ft. (37m), and 161 ft. (49m), respectively.

7.5 Summary of Secondary Power Cycle Design Studies

While extensive design and development programs are needed for the ammonia turbomachinery, existing technology from the power generating industry is generally applicable, and with specialized design attention, the conceptual turbine and pump designs presented above have the potential for satisfying the high-efficiency goals assumed for the cycle analysis. For the low-temperature secondary cycle, no materials technology advancements are necessary, and state-of-the-art design and fabrication methods are applicable. The overall configurations of the major components are very similar to power conversion systems being used in modern steam plants. Experience from the chemical and refrigeration industries in the areas of seals, maintenance, and the handling of ammonia components should be generally applicable.

243

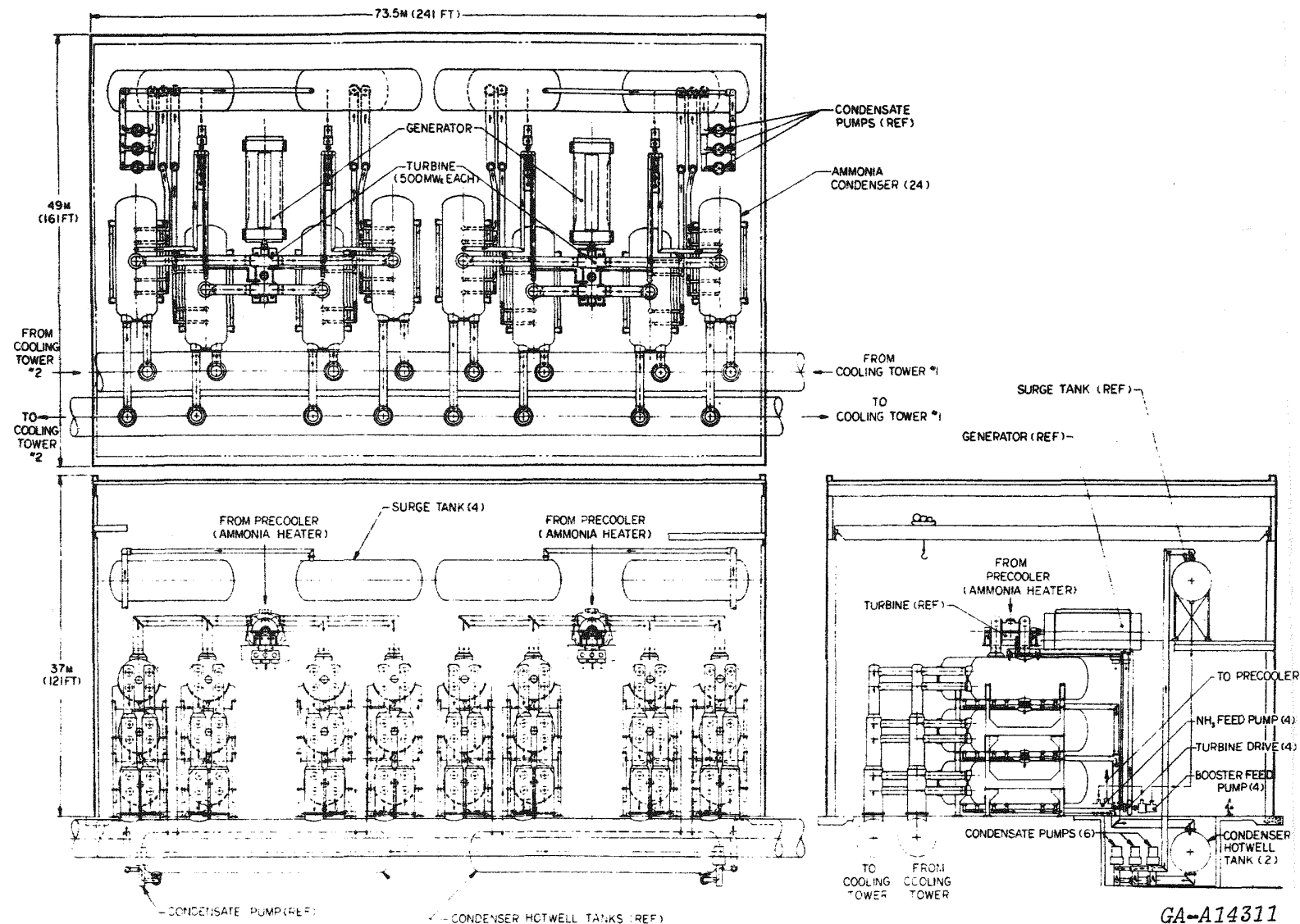


Fig. 7.13 Turbine Building Layout for GT-HTGR Waste Heat Power Plant

While the secondary power cycle work done at General Atomic has been directed towards a nuclear closed-cycle gas turbine, the heat source temperature of 482°F (250°C) is such that the component design work could be applied directly to other low-grade temperature systems such as geothermal, solar devices, and various industrial and marine heat engines and prime-movers.

References

- 7.1 Sager, P.H., "The HTGR Gas Turbine and Potential Beneficial Uses of its Reject Heat," Paper presented at the Symposium of Energy Production and Thermal Effects. Oak Brook, Illinois, Sept. 10, 1973.
- 7.2 Fortescue, P., "Nuclear Gas Turbines and Waste Heat Cycles," Paper presented at 10th IECEC Conference, Newark, Delaware, Aug. 17, 1975.
- 7.3 Schoene, T.W., J. M. Neill, and R. L. Cummings, "The Gas Turbine HTGR Plant with a Binary Cycle," Paper presented at Conference of the IEEE Power Engineering Society, Portland, Oregon, July 18, 1976.
- 7.4 Sager, P. H., and J. M. Krase, "Combined Nuclear Gas Turbine Power and Desalination Plant," Paper presented at 7th IECEC Conference, San Diego, California, September 25, 1972.
- 7.5 Escher, W. J. D., and T. D. Donakowski, "Competitively Prices Hydrogen Via High Efficiency Nuclear Electrolysis," Paper presented at 1st World Hydrogen Energy Conference, Miami Beach, Florida, March 1, 1976.
- 7.6 Weber, D., "Total Energy Applications for Closed-Cycle Gas Turbine," Paper presented at International Total Energy Congress, Copenhagen, Denmark, October 4, 1976.
- 7.7 Meyer, L. and J. W. Holland, "The Gas Turbine HTGR as a Thermal Energy Source for Desalination and District Heating," Ibid.
- 7.8 Vrable, D. L., and J. R. Schuster, "A Secondary Power Plant for Gas Turbine HTGR Waste Heat Utilization," ASME Paper No. 75-WA/HT-45.
- 7.9 Schuster, J. R., D. L. Vrable, and J. P. Huntsinger, "Binary Plant Cycle Studies for the GT-HTGR," ASME Paper No. 76-GT-39.

7.10 McDonald, C. F. , and D. L. Vrable, "Component Design Considerations for Gas Turbine HTGR Waste Heat Power Plant," Paper 769032 Presented at 11th IECEC Conference, Lake Tahoe, September 12, 1976.

7.11 Smith, S. F., "A Simple Correlation of Turbine Efficiency," Journal of Royal Aeronautical Society, 69, p 467 (1965).

7.12 Craig, H. R. M., and H. J. A. Cox, "Performance Estimation of Axial Flow Turbines," The Institution of Mechanical Engineers Proceedings, Vol. 185, 32/71, 1970.

7.13 Balje, O. E., "A Study on Design Criteria and Matching of Turbomachines, Part A-Similarity and Design Criteria of Turbines," ASME Paper No. 60-WA-230.

7.14 Reinhard, K. et al, "Experience with the World's Largest Steam Turbines," Brown Boveri Review, Vol. 63, No. 2, February 1976.

7.15 McDonald, C. F., and K. Vepa, "Ammonia Turbomachinery Design Considerations for the Direct Cycle Nuclear Gas Turbine Waste Heat Power Plant," ASME Paper No. 77-GT-75.

8.0 DEVELOPMENT AND TESTING ALTERNATIVES

While no major new technology or materials advancements are required for the nuclear closed-cycle gas turbine, an extensive program of design, development and testing is necessary to achieve the performance and structural integrity levels required for commercial power generation. Alternates for testing of the power conversion loop are briefly described below. They are not necessarily listed in order of preference, but rather are identified as viable development testing approaches.

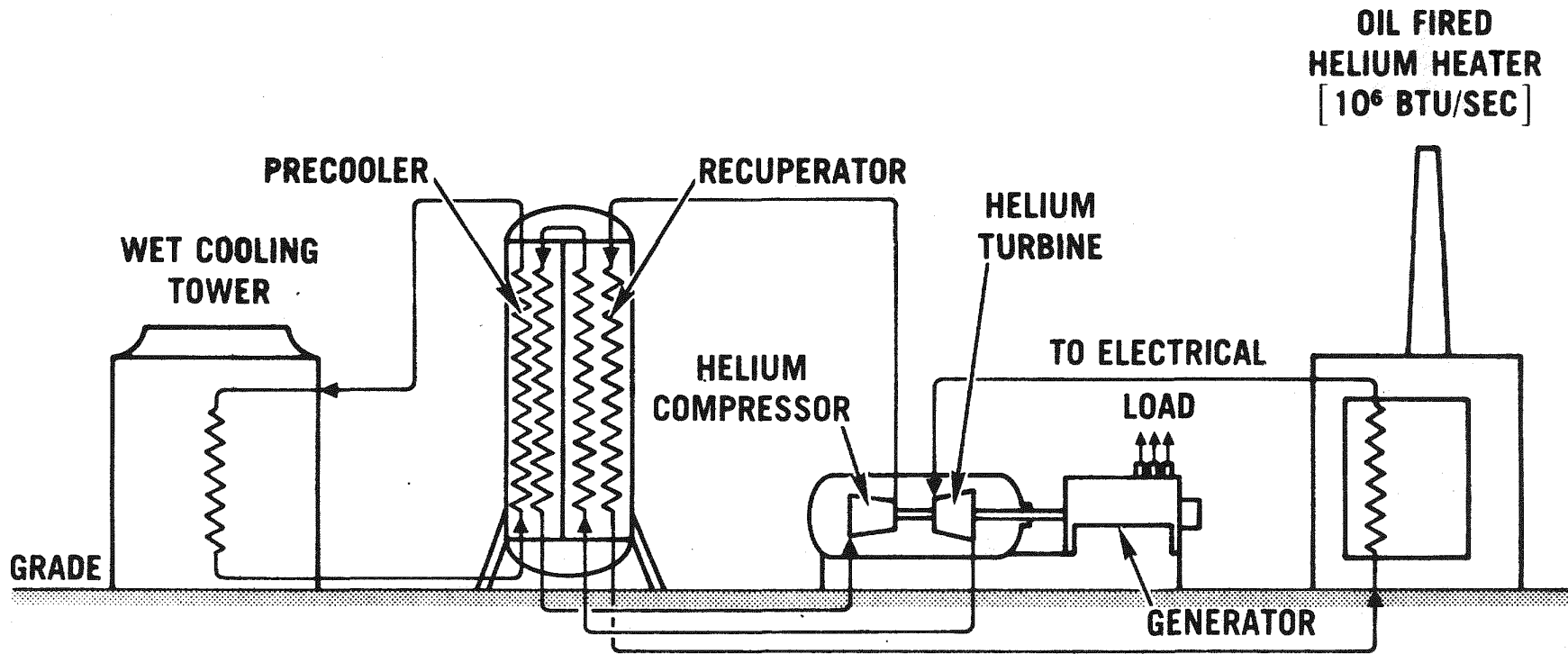
8.1 Helium Component Test Facility (HCTF)

This is a major facility for testing an entire power conversion loop at full power. The HCTF uses a fossil-fired heater to heat the helium, the heat simulating the nuclear reactor core. Conceptual details of the HCTF are shown on Figs. 8.1, 8.2, and 8.3. The power conversion equipment -- turbomachine, recuperator, precooler, valves, etc. -- are contained in steel pressure vessels, which are in turn arranged in a prototypical manner. The facility has been designed so that the helium flow will resemble in every respect the flow existing in one loop of a nuclear reactor. Hence, operation of the test facility will simulate steady-state, transient, and maintenance aspects of the nuclear plant. The HCTF preliminary design and cost estimate has been prepared in considerable detail by a major engineer/constructor firm, based upon requirements and interfaces defined by GA.

Construction of the nuclear demonstration plant would commence after completion of the initial phase of full-power testing in the HCTF. This program approach offers the lowest overall technical risk, and startup of the nuclear plant could be accelerated by about two years. Its disadvantage, however, is that it requires a large capital facility commitment and funding very early in the program.

8.2 Nuclear PCL Testing in a Demonstration Plant

In this alternative no fossil-fuel-fired test of a PCL is performed. Instead the reactor of the demonstration plant is used to test the full size power conversion system. An example of a single PCL integrated in a PCRV is shown on Figs. 8.4 and 8.5. A single loop arrangement of this type, in the 400 MWe - 600 MWe range, may indeed represent an economically viable plant from the utility power generating standpoint.



GA-A14311

Fig. 8.1 HCTF Schematic Diagram

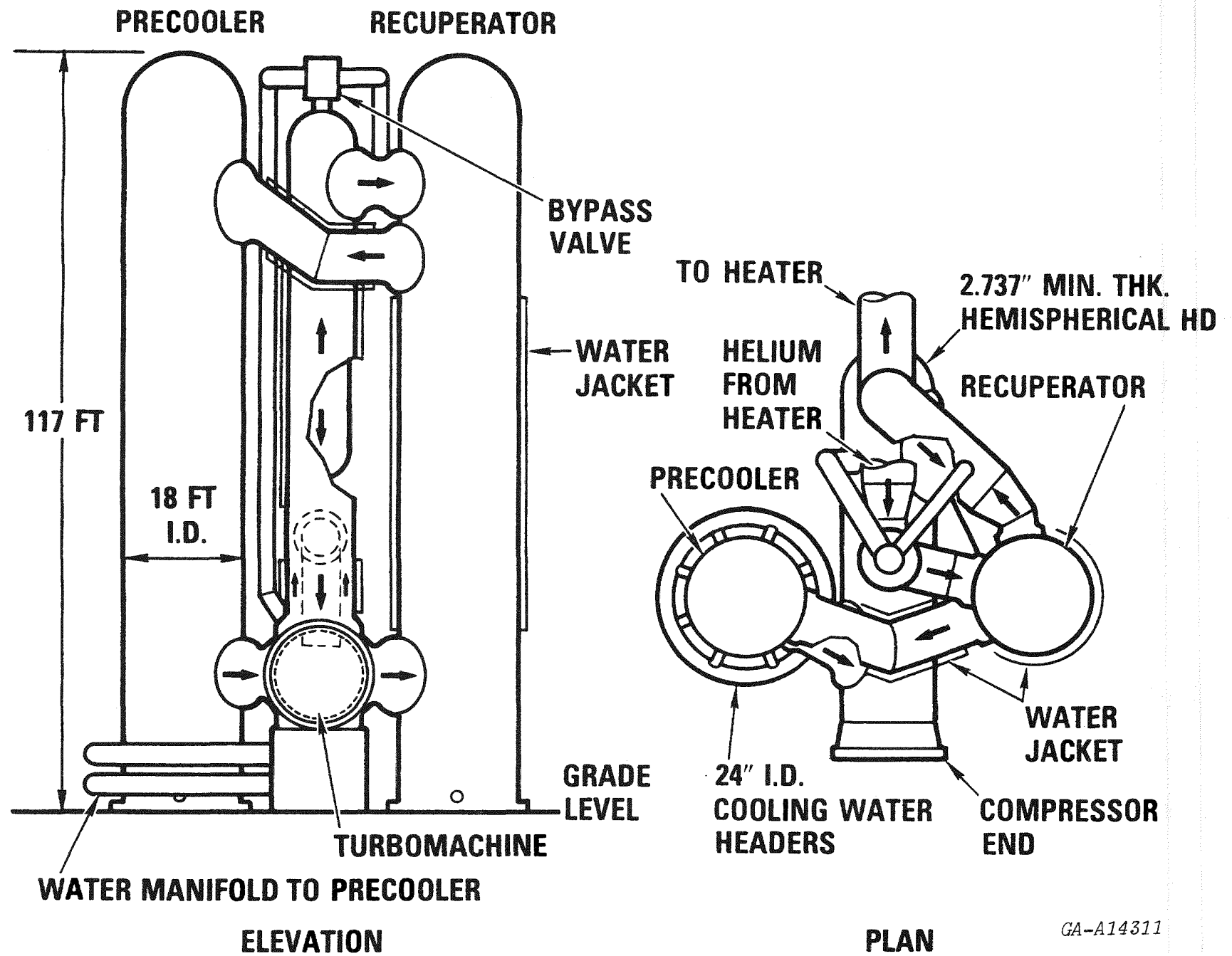


Fig. 8.2 Test Vessels and Helium Ducts Arrangement

GA-A14311

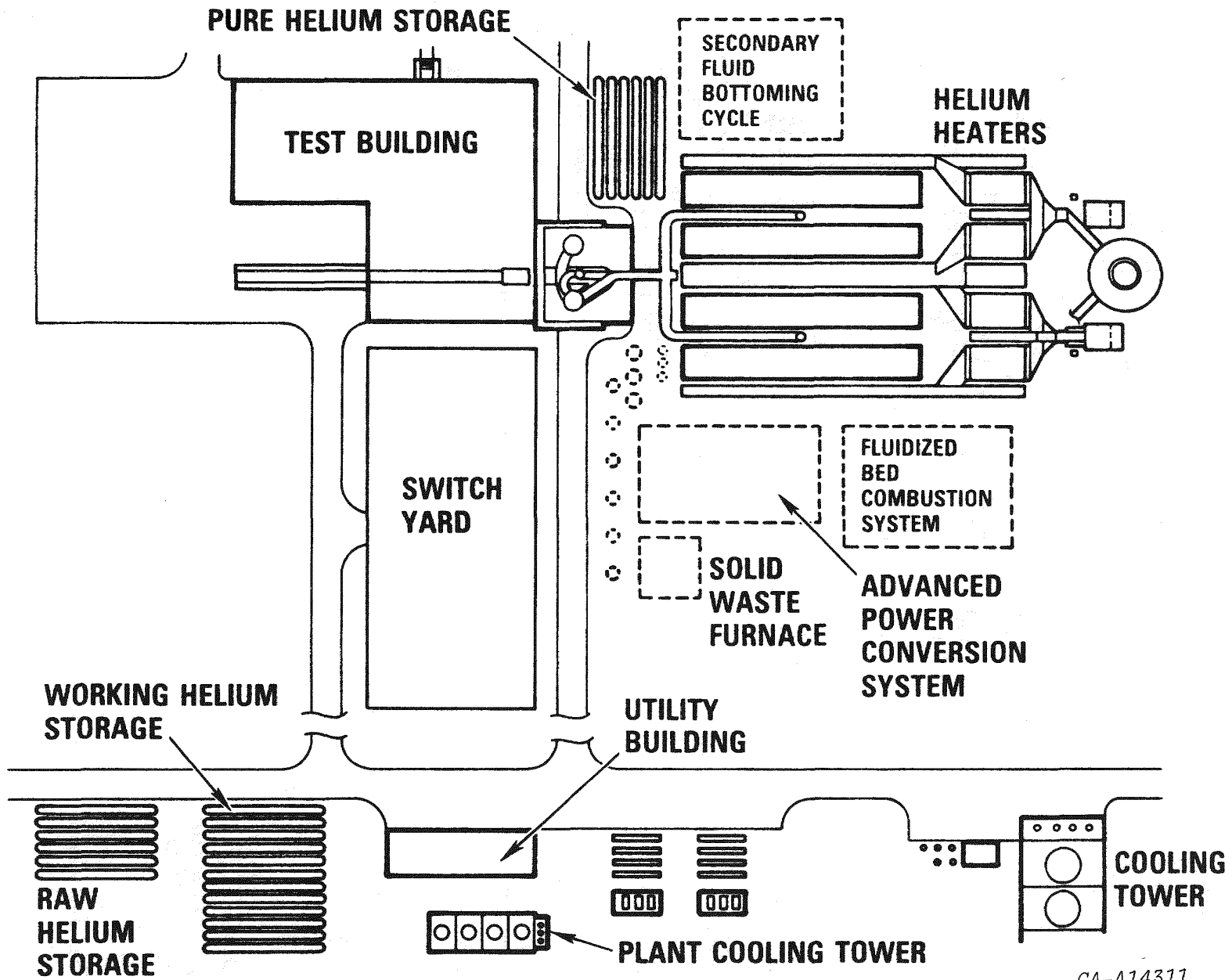
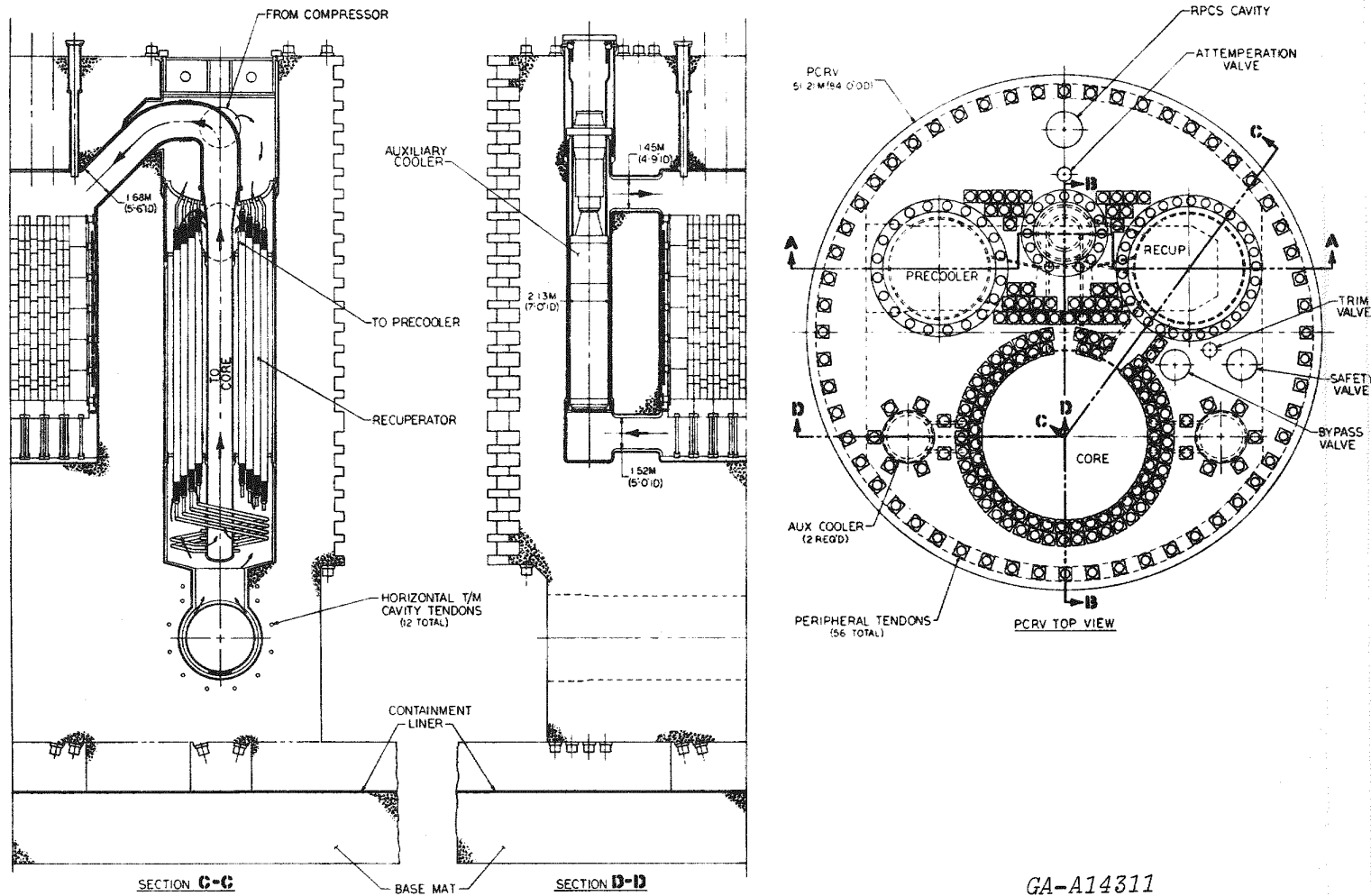


Fig. 8.3 HCTF Plot Plan

GA-A14311



GA-A14311

Fig. 8.4 Single-Loop GT-HTGR Arrangement

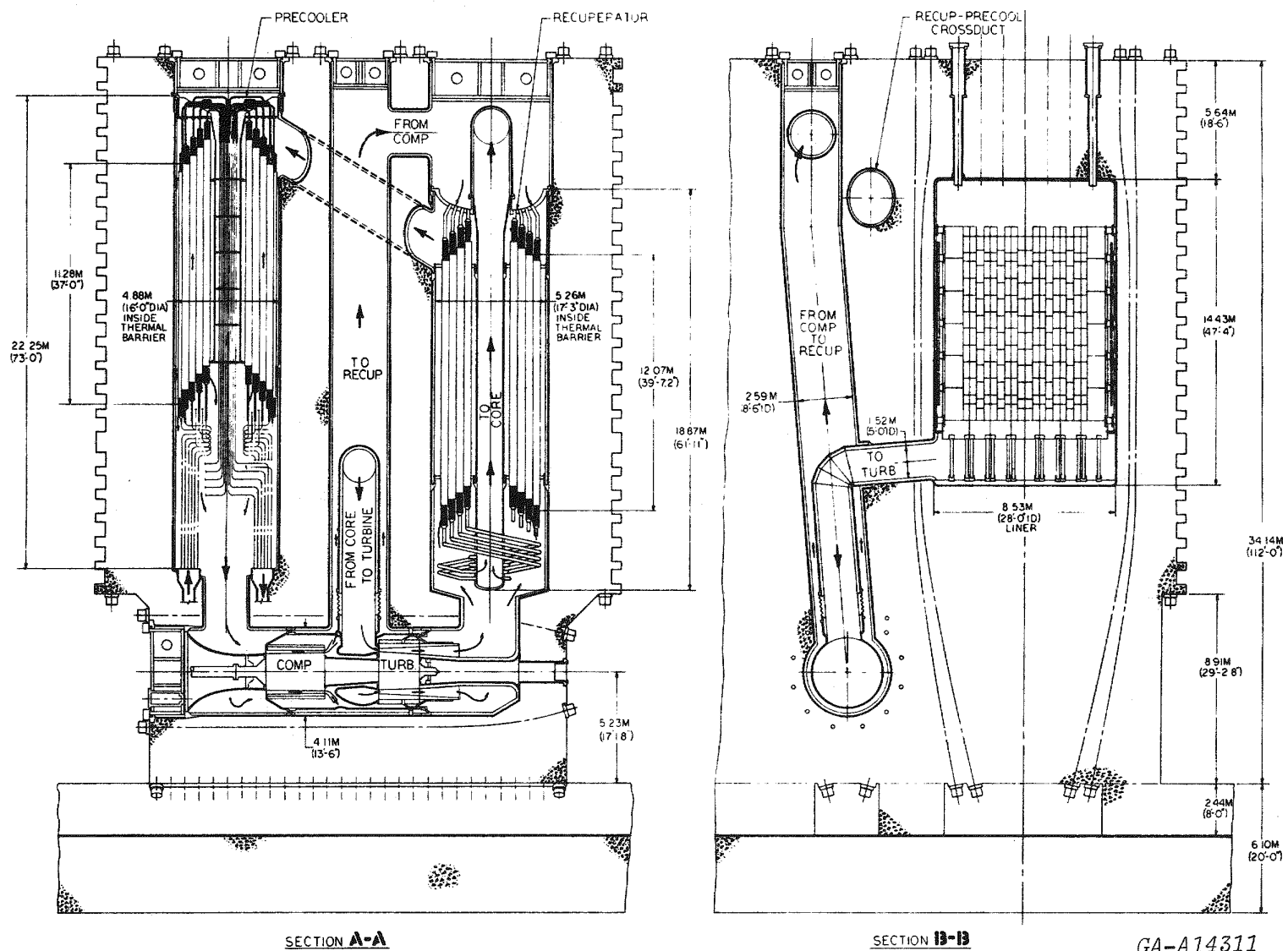


Fig. 8.5 PCL for Single-Loop GT-HTGR

The advantage of this alternative is there is no special test equipment, especially a separate heater. The potential problems with testing utilizing nuclear heat include:

- 1) Licensing
- 2) Handling of radioactive components during the initial test program which will increase the plant downtime.
- 3) Inspection of prototype components in place.
- 4) Instrumentation, installation, maintenance and removal in a contaminated environment.
- 5) Lack of flexibility in making changes to components since nuclear standards must be met.

8.3 Temporary Helium Heater Approach

This alternate aims at non-nuclear testing of the power conversion loop in the PCRV (of the type mentioned in 8.2) of the nuclear demonstration plant before nuclear fuel is loaded. Heat to the loop would be supplied using a two-stage, oil-fired and electric helium heater on the outside of the reactor containment building or an in-core electric heater. This approach requires significantly less early capital expenditure than the Helium Component Test Facility (outlined in 8.1). It provides a complete in-situ power conversion loop operation within the demonstration plant without the fission products contamination of the power conversion loop during shakedown operations. This system does, however, require that a temporary heater system of about 1000 MW(t) be constructed and installed at the reactor site and that appropriate primary circuit connections be provided. Additional construction and startup must be scheduled to install and remove the heater and to perform the power conversion loop tests before the plant operations.

8.4 Subcomponent Test Approach

This approach is based on testing of the subcomponents under simulated operating conditions without a pre-nuclear test of the entire loop. For this approach, full-scale subcomponents test articles, such as recuperator and precooler modules, and turbomachinery stages, would be tested. In addition, some complete assemblies such as hot gas ducting and bypass control valves would be tested. Nuclear plant startup could include warm flow startup tests by motoring the generator to rotate the turbomachines with

reduced helium pressure. Full-power demonstration operation of power conversion loop components will, thereafter, be first achieved with nuclear heat. The German/Swiss HHT Project has used this subcomponent testing approach as the basis for their planning and have expressed confidence in it. To support this development philosophy the HHT Project is building major facilities for subcomponent testing.

With the exception of the nuclear testing alternative, the above approaches are summarized on Table 8.1.

8.5 Development Needs Common to Fossil-Fired and Nuclear Closed-Cycle Gas Turbines

It has long been recognized that an advantage of the closed-cycle gas turbine is its adaptability to various heat sources, the two important ones being nuclear (HTGR) and fossil (coal in particular). With helium as the working fluid, the salient parameters can be selected to give power conversion loop commonality between nuclear (HTGR) and various modes of coal-fired inputs. While the specific layout of a closed-cycle gas turbine plant will be different for nuclear (as discussed in this paper) and fossil heat sources (such as the 50 MW(e) Oberhausen II helium turbine plant in Germany), there is a high degree of commonality as regards systems analysis, component design and development, and testing of the power conversion loop to verify performance and structural integrity. Fig. 8.6 was prepared to show some of the development needs common to fossil and nuclear closed-cycle gas turbines. An elaboration of the design and development commonality for each of the major areas identified is included. From the extensive range of related research, design, development, fabrication, and testing topics a coordinated program on closed-cycle gas turbines, particularly the power conversion loop, would minimize cost and development efforts for utility power generation.

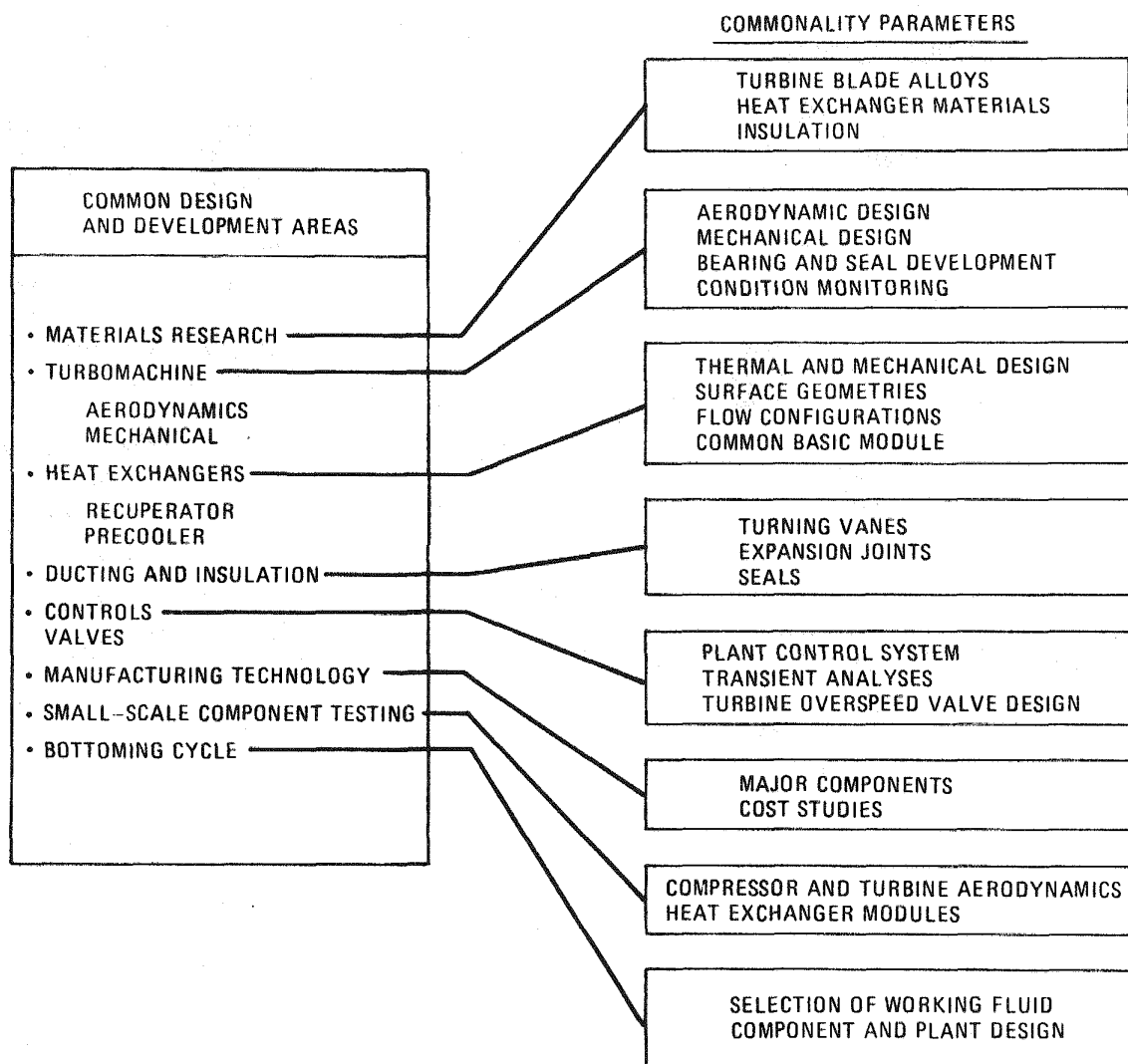
9.0 RELATED INTERNATIONAL NUCLEAR CLOSED-CYCLE GAS TURBINE PROGRAMS

In Europe an extensive effort is underway in the nuclear gas turbine field. The German/Swiss HHT Project (High Temperature Helium Turbine) consists of a partnership with participation by six industrial firms and two national research centers. This project is comprised of the following seven working areas: (1) design and planning, (2) component development, (3) fission

TABLE 8.1
GT-HTGR POWER CONVERSION LOOP TEST ALTERNATIVES

Helium Component Test Facility	Full-Scale, Fossil-Fired, Conceptual Design Study and Cost Estimate
Demonstration Helium Turbine Power Plant	Aimed at Development and Demonstration of Coal-Fired Heater for Closed-Cycle Gas Turbine Power Plants in Addition to PCL Test
Helium Heater in Nuclear Demonstration Plant	Operate PCL with Temporary In-Core Electric Heater, or External Oil-Fired and Electric Heater, Prior to Fuel Loading and Nuclear Operation
Subcomponent and Reduced Scale Component Tests, U.S. and Germany and Nuclear Demonstration Plant	Nuclear Plant Startup Includes Generator Motoring of Gas Turbines Before Nuclear Operation

GA-A14311



GA-A14311

Fig. 8.6 Projected Development Needs Common to Fossil-Fired and Nuclear Closed-Cycle Gas Turbines

product transport, (4) fuel element development, (5) materials development, (6) HHV test facility, and (7) EVO 50 MW closed-cycle helium gas turbine at Oberhausen.

In a previous cooperative design effort (in 1975), General Atomic and HHT jointly derived a common reactor-turbine system involving three power conversion loops integrated within the PCRV. In a recently announced statement, General Atomic Company and the above-mentioned eight German and Swiss organizations have signed an agreement to cooperate in the design of high efficiency, multipurpose nuclear power plants that would use hot helium gas to drive turbine-generators. Primary objectives of the cooperative program are: (1) to establish GT-HTGR conceptual plant designs offering major economic improvements compared to other present-day nuclear plants, (2) to jointly determine the significant design data and features of such plants, (3) exchange of technology concerning the planning, design and development of GT-HTGR plants, and (4) to reduce development costs.

10.0 SUMMARY

The work reported here is only one part of the international and widespread efforts on combining the gas turbine with nuclear power. The benefits of the nuclear gas turbine power plant appear so great that the worldwide efforts to bring it into use should increase rapidly since it can make a significant contribution to fuel conservation with a minimum impact on the environment.

It is worth reiterating the most significant advantages of the closed-cycle gas turbine, namely; (1) high potential efficiency, hence fuel conservation and minimum environmental impact, (2) adaptability to a wide range of heat inputs including fossil, nuclear (fission and fusion), and solar, (3) heat rejection characteristics well suited to either dry cooling, wet-dry cooling, district heating, utilization of a binary cycle, or LNG vaporization, (4) high availability, good reliability, and low maintenance, associated with the clean working fluid for the turbomachinery, (5) compact power conversion system giving lower capital cost, and (6) relatively short development period to get utility size machines into service.

The successful operation of the European closed-cycle gas turbines has been stressed to substantiate the viability of the closed-cycle concept. This, together with the helium component development efforts and plant

operating experience of the HTGR, forms the basis from which a successful GT-HTGR plant can be designed, developed, and introduced into utility service with a high degree of confidence that the performance, economic, safety, and reliability goals will be realized.

The plant description given in this article is of the General Atomic GT-HTGR design. A cooperation has been established between the U.S. GT-HTGR program and the European HHT program. Common positions have been established on many technical and design aspects, and the major issues under joint study relate to the size of the turbomachinery, the accommodation of 50 Hz generation for Europe and 60 Hz for the U.S., and to plant configuration.

ACKNOWLEDGEMENTS

Design studies and R & D work on the GT-HTGR have been supported by the U.S. Energy Research and Development Administration, a group of electric utilities, and by participating industrial firms. The current work is being accomplished by General Atomic, United Technologies Corporation (on the helium turbine generator) and United Engineers and Constructors (on balance-of-plant).

Appreciation is hereby expressed to USERDA and General Atomic Company for permission to publish this paper. Further thanks are expressed to Gutehoffnungshutte Sterkrade AG, Escher Wyss, and Brown Boveri Company, for supplying the many excellent photographs of the European closed-cycle gas turbine plants and related components.

The author further wishes to express his appreciation to the staff of the Advanced Concepts Division at General Atomic Company, and to acknowledge the work done by them over the last five years on the GT-HTGR plant.